Methanogenic hydrocarbon degradation

and methane oxidation

in benthic microbial communities

Zusammenfassung

Diese Arbeit untersucht das Schicksal von Kohlenstoff und Stickstoff während des mikrobiellen Kohlenwasserstoffabbaus (KW-Abbau) und der anschließenden Methanoxidation. Dies wurde erreicht durch die Erforschung mikrobieller Vergesellschaftungen welche höhere KW und Methan als Energiequellen metabolisieren. Da beide Abbauwege in marinen Systemen weit verbreitet sind, konzentriert sich diese Dissertation auf benthische mikrobielle Vergesellschaftungen.

In der Folge des Unfalls auf der Ölplattform "Deepwater Horizon" wurde Ölverschmutzungen in der Umwelt ein erhöhtes öffentliches Interesse zuteil. Da dieser Unfall durch eine aufsteigende Methanblase verursacht wurde, sollte auch der Abbau von höheren KW zu Methan besondere Beachtung finden. Wenngleich die offensichtlich nachteiligen Auswirkungen von Ölverunreinigungen nicht vernachlässigt werden dürfen, sind doch Öl und Gas die vorherrschenden Energieresourcen unserer Zeit.

Unsere Abhängig vom Öl erzwang die Erforschung neuer Strategien zur Ausbeutung von Energierostoffen, wie z.B. "Microbially Enhanced Oil Recovery" (MEOR). Während sich frühere Forschungsarbeiten auf die Ablösung des Öls vom Gestein konzentrierten, hat sich während der letzten zehn Jahre ein neuer Forschungszweig, der mikrobielle Abbau von Öl zu Methan, etabliert. Methanogener KW-Abbau wird auch als "mikrobielles Cracken" bezeichnet, da es sich um die mikrobielle Umwandlung höherer KW zum kleinsten KW Methan handelt.

Diese Arbeit zeigt, daß methanogener KW-Abbau durch die Zugabe von Elektronenakzeptoren zu mikrobiellen Vergesellschaftungen stimuliert werden kann. Verglichen mit anderen Methoden ist die Zugabe von Ferrihydrit kostengünstig und bietet zudem den Vorteil der Ausfällung von ungewünschtem Schwefelwasserstoff. Desweiteren konnte die Umwandlung eines polyaromatischen KWs (PAK) zu Methan gezeigt werden.

Beim methanogenen KW-Abbau ist es von Interesse, zu wissen, ob Methan in Öllagerstätten oder verschmutzten Standorten durch mikrobiellen Abbau entstanden ist. Folglich ist auch der Fortschritt des biologischen Abbaus von ökonomischem Interesse und die Bestimmung eines isotopischen "Fingerabdrucks" ist hierfür eine vielversprechende Methode. Diese Arbeit zeigt solch einen "Fingerabdruck" für Methan und CO_2 zum ersten Mal in zwei Dimensionen für Wasserstoff und Kohlenstoff. Dies kann zukünftig schnell einen mikrobiellen Anteil beim KW-Abbau anzeigen.

Wenn Methan beim methanogenen KW-Abbau freigesetzt wird, wird dieses wiederum durch methanotrophe Mikroorganismen oxidiert. In früheren Arbeiten wurde schon die mikrobiell katalysierte Methanoxidation durch verschiedene Elektronenakzeptoren gezeigt. Diese Arbeit bietet weitere Hinweise auf Metall-assoziierte Methanoxidation an einer neuen Methanaustrittsstelle vor Sumatra, dem "Simeulue Seep". Verglichen mit ölverschmutzten Standorten, waren die mikrobiellen Vergesellschaftungen am "Simeulue Seep" auf anaerobe Methanoxidation spezialisiert. Dies wird auch in der typischen Zusammensetzung der mikrobiellen Gemeinschaft deutlich, die Methan-oxidierende Archaeen und Sulfat-reduzierende Bakterien aufwies.

Außerdem konzentriert sich diese Arbeit auf Sulfat- und Nitrat-gekoppelte Methanoxidation. Sie zeigt, daß die anaerobe Oxidation von Methan (AOM) in mikrobiellen Matten aus dem Schwarzen Meer mit der Nitratreduktion über Sulfatreduktion verbunden ist. Stickstoff aus Nitrat und Ammonium wurde in die Biomasse, z.B. Proteine und besonders in die Methyl-Coenzym M Reduktase, eingebaut. Stickstofffixierung konnte vernachlässigt werden. Zusätzlich zu den schon bekannten AOM-Matten aus dem Schwarzen Meer, wurde ein neuer Mattentyp – Die Trolle – ca. 500 m tiefer, nahe der Methanhydrat-Bildungszone, entdeckt.

Aufgrund der Tatsache, daß aerobe und anaerobe Methanoxidation durch verschiedene Mikroorganismen, Enzyme und Reaktionen betrieben wird, ist es sinnvoll, anzunehmen, daß stabile Wasserstoff- und Kohlenstoffisotope auch unterschiedlich fraktioniert werden. Diese Arbeit zeigt, daß dies nicht der Fall war. Statt dessen kann mit Hilfe von Isotopenfraktionierungsexperimenten zwischen biotischer und abiotischer Methanoxidation unterschieden werden.

Abstract

This work aims to trace the fate of carbon and nitrogen during microbial methanogenic hydrocarbon degradation and subsequent methane oxidation, by investigating microbial communities utilising hydrocarbons and especially methane as energy source. Since both processes, microbial hydrocarbon degradation and methane oxidation, are widespread in marine environments, this work focuses on benthic microbial communities.

As a result of the recent accident on the drilling rig Deepwater Horizon the environmental impacts of spilled petroleum received a great deal of public attention. The accident was caused by an exploding methane bubble during the oilfield exploration, emphasising the importance of methanogenic hydrocarbon degradation. Although the apparent adverse effects of oil spills must not be neglected, petroleum and methane are still the predominant energy resources for mankind.

The dependence of our lifestyle on petroleum has led to new concepts of oilfield exploitation, including microbially enhanced oil recovery (MEOR). While previous research often focussed on the detachment of higher hydrocarbons from their mineral matrix, a relatively new branch – methanogenic hydrocarbon degradation – has emerged during the last decade. Methanogenic hydrocarbon degradation is also named "microbial cracking" because microorganisms convert higher hydrocarbons into the smallest hydrocarbon methane.

This work shows that methanogenic hydrocarbon degradation can be stimulated by adding electron acceptors to a hydrocarbon degrading microbial community. Compared with other methods, the addition of electron acceptors, like ferrihydrite, is inexpensive and has the advantage of scavenging unwanted sulfide. Moreover, the microbial conversion of a polyaromatic hydrocarbon (PAH) to methane was demonstrated.

It is interesting to know whether methane in oilfields or contaminated sites is of microbial origin. As a consequence, the stage of biodegradation is of economic and environmental interest. A promising tool is stable isotope fingerprinting of the degradation products methane and CO_2. For the first time, this work shows such fingerprints in the two dimension carbon and hydrogen. This allows the *in situ* identification of microbial involvement in methanogenic hydrocarbon degradation.

When methane is released from methanogenic hydrocarbon degradation, it is often oxidised by methanotrophic microorganisms. It has been demonstrated that, catalysed by methanotrophic consortia, several electron acceptors oxidise methane to CO_2. This work provides further hints for metal associated methane oxidation at a novel methane seep off Sumatra (Simeulue seep). Compared with other, hydrocarbon contaminated sites, the Simeulue seep's microbial community preferably oxidised methane anaerobically while methanogenic hydrocarbon degradation was negligible. This is reflected in a typical methane-seep community composition comprising anaerobic methane oxidising *Archaea* and sulfate reducing *Bacteria*.

Moreover, this work focuses on sulfate and nitrate coupled methane oxidation. It shows that anaerobic oxidation of methane (AOM) couples to nitrate reduction indirectly via sulfate reduction in micobial mats of the Black Sea. While nitrate and ammonium derived nitrogen was incorporated into biomass (proteins and especially methyl coenzyme M reductase), nitrogen fixation was negligible. In addition to the already known AOM performing microbial mats of the Black Sea, a novel type of mats – The Trolls – was discovered 500 m deeper, near the methane gas hydrate formation zone.

Due to the fact that aerobic and anaerobic methane oxidation involve different types of microorganisms, enzymes and reactions, it is plausible to assume that hydrogen and carbon stable isotopes are fractionated differently. However, this work shows that this is not the case. Instead, biotic and abiotic methane oxidation can be distinguished by isotope fractionation investigations.

Table of contents

Abbreviations

AAG	ancient archaeal group
ADP	adenosyl diphosphate
anammox	anaerobic ammonium oxidation
ANME	anaerobic methane oxidisers
AOM	anaerobic oxidation of methane
ATP	adenosyl triphosphate
CARD-FISH	catalysed reporter deposition – fluorescence in situ hybridisation
CMM	coal mine methane
cmbsf	centimetres below seafloor
CoA	coenzyme A
CoB	coenzyme B
DGGE	denaturing gradient gel electrophoresis
DNA	deoxyribonucleic acid
DNRA	dissimilatory nitrate reduction to ammonium
dsr	dissimilatory sulfite reductase gene
DSS	*Desulfococcus*/*Desulfosarcina* cluster
EA	elemental analyser
FA	fatty acid
FAME	fatty acid methyl ester
FPLC	fast protein liquid chromatrography
GC-(IR)MS	gas chromatography – (isotope ratio) mass spectrometry
MALDI-TOF	matrix assisted laser desorption / ionisation – time of flight
MBG	marine benthic group
MCG	miscellaneous crenarcheaotic group
MCR	methyl coenzyme M reductase
mcr	methyl coenzyme M reductase gene
MMO	methane monooxygenase
nanoSIMS	nanometer secondary ion mass spectrometry
nar	nitrate reductase gene
nif	nitrogenase gene
nir	nitrite reductase gene
nor	nitric oxide reductase
nos	nitrous oxide reductase gene
OP	obsedian Pool
OTU	operational taxonomic unit
PAH	polyaromatic hydrocarbon

PCR	polymerase chain reaction
PMI	2,6,10,15,19-pentamethylicosene
RNA	ribonucleic acid
SDS	sodium dodecyl sulfate
SIP	stable isotope probing
SMOW	Standard Mean Ocean Water
SR	sulfate reduction
SRB	sulfate reducing bacteria
SRR	sulfate reduction rate
THSG	terrestrial hot spring group
TRF	terminal restriction fragment
TRFLP	terminal restriction fragment length polymorphism
TM	Torf, mittlere Schicht
UPLC	ultra performance liquid chromatography
VPDB	Vienna Pee Dee Belemnite

Chapter 1

Introduction

1.   Introduction

1.1.   The role of hydrocarbons in the environment

Hydrocarbons are abundant substances in nature. They play an important role in the global carbon cycle because: (I) It is commonly agreed that carbon arrived as hydrocarbons on the young Earth. Therefore, they were an important factor in the evolution of life. (II) They are actively produced by microorganisms and plants as intrinsic cell compounds or by reduction of organic matter [1-3]. (III) They are of great economic interest.

Moreover, hydrocarbons represent the most reduced redox state of carbon (-IV). Oxidation of hydrocarbons results in substantial energy yields for life, which is the major reason for its value as energy resource for mankind. Increasing worldwide wealth will result in an increased global energy demand of 49% until 2035 [4]. The demand for energy from liquid hydrocarbons will increase from 1.9×10^{17} kJ (2010) to 2.3×10^{17} kJ y^{-1} (2035), from coal carbon from 1.4×10^{17} to 2.2×10^{17} kJ y^{-1} and from natural gas (methane) from 1.4×10^{17} to 1.7×10^{17} kJ y^{-1}, respectively [4]. Besides fuel supply, hydrocarbons are valuable resources for petrochemical products.

Chemically, hydrocarbons are molecules consisting exclusively of carbon and hydrogen. When a hydrocarbon counts more than one carbon atom (>C1) it is termed a higher hydrocarbon. Carbon atoms in higher hydrocarbons may be connected by σ- or π-bonds (alkanes or alkenes and alkines respectively). In case of σ-bonds, hydrocarbons are saturated with hydrogen (aliphatic) and π-bond carbon atoms are unsaturated. π-bond carbon atoms may exchange electrons with adjacent carbon atoms (electron shift). These so-called delocalised electrons are typical for aromatic hydrocarbons. Aromatic hydrocarbons may be circular with one or more rings. When other atoms than carbon participate in the aromatic system then one speaks of hetero-aromatic (or hetero-cyclic) systems. In this case, the molecule is not a hydrocarbon.

Production, transport and refining are prone to leakages and high concentrations of hydrocarbons in the environment may have adverse environmental effects. The Exxon Valdez (1989) and Deepwater Horizon (2010) oil spills are only two prominent examples of a number of accidental hydrocarbon spills [5-9]. Toxic effects to humans are documented for more than a half century [10, 11]. Consequently, clearing various contaminated sites like aquifers, soils and sediments has become a high priority public demand to constrain negative public health effects of hydrocarbons during the last three decades [12-19].

Although toxic to many eukaryotes in high amounts, hydrocarbons are a carrier of energy and are therefore of great economic interest. Due to the worlds increasing demand for en-

ergy, new reservoirs are constantly explored. These oil reservoirs harbour a broad diversity of different hydrocarbons. The great structural diversity of hydrocarbons is a result of petroleum generation processes. It is commonly agreed that carbon is assimilated by light-harvesting carbon dioxide fixation [20]. Biosynthetic products in cells are mainly carbohydrates, lipids, proteins and lignin which usually occur as polymers in cells. When this organic matter arrives on the seafloor, sediment particles block substrate fluxes and prevent electron acceptor transport to microorganisms [20]. In time, the environment becomes more reduced and ultimately, carbon biopolymers (humic substances) themselves are reduced [20]. This defunctionalisation leads to the formation of kerogen which is the precursor of petroleum. It is the most abundant form of organic carbon on Earth [20].

One should note that the formation of hydrocarbons is believed to be mostly abiotic although biological production of hydrocarbons under moderate conditions is possible in prokaryotes [2, 3] and eukaryotes [21, 22]. The reason is that high pressure, high temperature and low substrate fluxes are ideal conditions for mere chemical reduction of kerogen. On the other hand, it is widely agreed that in marine sediment environments, temperatures above 80°C inhibit microbial growth [23].

Temperatures well above 130-140°C are required for thermogenic petroleum formation [24]. Hence, hydrocarbons originating directly from living organisms are rarely found in source rocks, where higher temperatures prevail and hydrocarbons are formed. Such source rocks are formed as a sedimentary column increases, for example in forelands (*Figure 1*). As results of tectonic activity, cracks in the sediment release petroleum and natural gas from source rocks and serve as conduits for ascending hydrocarbon fluids and gases. Such reservoirs can be exploited by petroleum companies.

Since microbial hydrocarbon degradation is restricted to relatively low temperatures, it is usually observed in further upward migrating petroleum bubbles or oil spills at the surface [23, 25-27]. However, this is rarely the case at moderate temperatures and hydrocarbons can be degraded by microorganisms [23]. When electron acceptors like sulfate or nitrate are depleted in hydrocarbon rich sediments, anaerobic methanogenic microbial consortia use hydrocarbons as substrates to convert them into methane [23]. While microbial hydrocarbon degradation is the most important methanogenic process [23], thermal cracking of higher hydrocarbons also leads to methane formation. Thermal cracking of hydrocarbons is hydrocarbon pyrolysis. Hydrocarbon pyrolysis is a process in petroleum refining to obtain smaller molecules from large hydrocarbon molecules. It also occurs in deep sediments when temperatures and are sufficiently high. Methane is also formed by methanogenic microorganisms (methanogens) under anoxic conditions. When hydrocarbons are cleaved a methanogenic microbial community, this process is also called "microbial cracking". Microbial hydrocarbon

dependent methanogenesis is further discussed in Chapter 3. However, typical substrates for methanogens are methylated compounds like methanol, methylamines and acetate. Many methanogens also utilise hydrogen to reduce CO_2 [28]. Methanogenic substrates are degradation products of cell decay or hydrocarbon degradation. Hence, methanogensis is the last step in decay of complex organic matter.
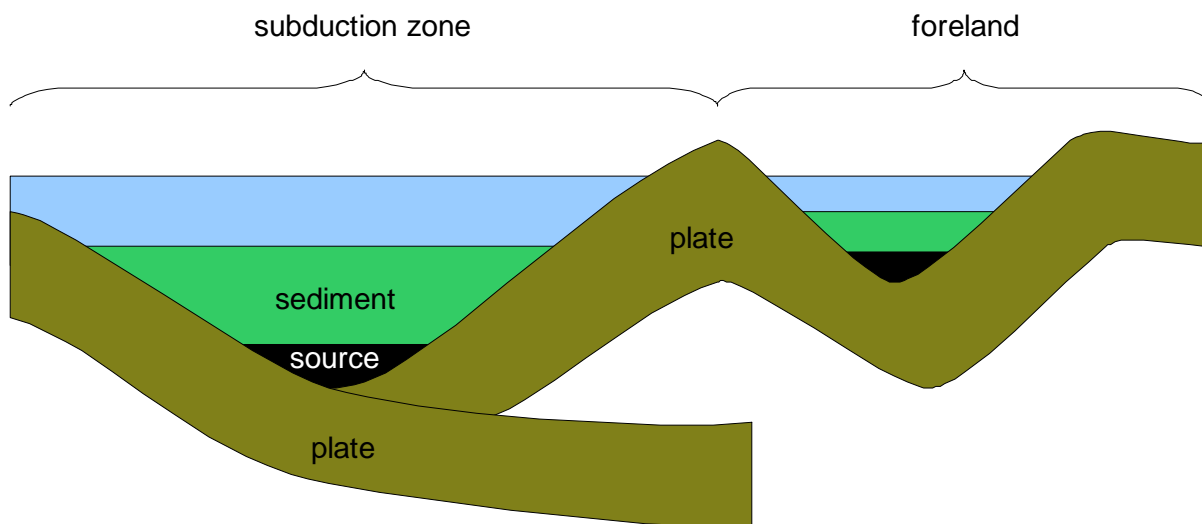
Figure 1: Schematic formation of a foreland up-folding adjacent to a subdation zone of two plates. "Source" indicates the source rock where petroleum or natural gas is formed.

Methane is the smallest hydrocarbon, and usually occurs as gas but also as deep-sea clathrate (gas hydrate) or liquid under high pressure and low temperatures. While methane is the prevailing component in conventional natural gas, methane hydrates are regarded as a potential future energy source for mankind [29]. Methane naturally occurs in the atmosphere in trace concentrations (ppb) and is a potent greenhouse gas [30]. While the highest global abundance of atmospheric methane during the last 650,000 years was detected in 2005, a release from deep gas hydrate depositions may self-accelerate the global warming [30]. That is, increasing temperatures of the oceans will possibly trigger spontaneous decomposition of methane hydrates and hence its release into the water column and, if not oxidised by methanotrophs, into the atmosphere. Therefore, an understanding methane biodegradation in the water column is essential to assess risks of the global warming.

1.2.   Oxidation of methane

During its passage through sediments, wetlands or permafrost soils methane passes zones of several redox states, i.e. the capability of a system to transfer electrons and enable chemical reduction and oxidation reactions. In the electron acceptor chain, oxygen is the most potent oxidant for hydrocarbons, succeeded by nitrate, manganese oxides, iron (hydr)oxides, sulfate and others [31].

Carbon in methane represents the highest state of reduction. In spite its high ionisation energy methane release is accompanied by its oxidation. Hence, estimations of methane oxidation rates are of importance for economic as well as greenhouse risk evaluations. Methane can be oxidised by various oxidants but oxygen and sulfate are globally significant [32]. Oxygen, sulfate, nitrate and nitrite are known soluble oxidants for methane while oxidised iron and manganese are insoluble compounds within the sediment [33-36]. If other oxidants are reduced by anaerobic methanotrophic microbial communities remains to be elucidated. Potential candidates are various heavy metals like uranium or chromium, but also oxidised arsenicals. Ultimately, abiotic hydroxylation in the troposphere and stratosphere removes remaining methane and accounts for 90% of global methane oxidation [30].

The energetically most favourable reaction is methane oxidation by molecular oxygen (dioxygen). This is reflected in increased rates of aerobic methane oxidation in sediments compared to anaerobic oxidation with sulfate but strongly depends on methane concentrations and the oxidation state of the investigated sediment [37]. However, rates and global estimates of aerobic methane oxidation are rarely available [38]. In sediments, volume related aerobic methane oxidation rates are higher by orders of magnitude (nmoles ml^{-1} d^{-1}) compared to open ocean (nmoles l^{-1} yr^{-1}; [37, 38]).

Reciprocal sulfate-methane profiles in marine sediments mislead previous investigators to the conclusion that microbial methanogenesis and sulfate reduction were mutually exclusive processes [39]. However, sulfate reduction coupled to the anaerobic oxidation of methane (AOM) was already suspected to account for the observed sulfate-methane profiles [39-41]. An early work suggested AOM by the sulfate reducer *Desulfovibrio desulfuricans* [42]. However, only little radioactive CO_2 was detected and this experiment has never been repeated. Since AOM was so controversial, it took another two decades until AOM coupled sulfate reduction became accepted in the scientific community [38]. Boetius *et al.* [43] were the first to show that AOM coupled sulfate reduction is a syntrophic process mediated by methane oxidising *Archaea* and sulfate reducing *Bacteria* (see Section 1.4. and *Formula 7*).

In 2006, Raghoebarsing *et al.* [36] provided evidence for AOM coupled to nitrate reduction. It seemed obvious that this reaction was catalysed by syntrophic anaerobic methane oxidisers (ANME *Archaea*) and nitrate reducers. However, in a recent publication it became clear, that two moles of nitric oxide (NO) were cleaved to produce one mole of N_2 and O_2 each by an enzyme named NO dismutase [34]. In fact, the authors could show that it was aerobic methane oxidation carried out by an anaerobic microorganism. This process was theoretically possible without a syntrophic partner, although the authors could not provide a pure culture of the responsible organism *Candidatus Methylomirabilis oxyfera*. By coupling methane oxidation to denitrification, this reaction links three essential elements of life – carbon, oxygen

and nitrogen – for energy conservation within the same organism. Nonetheless, it remains unclear if this pathway had played a role on early earth or if this pathway evolved after synthetic fertilisers were employed in industrialised agriculture [44].

While oxygen is often depleted in sediments, oxidised metals like iron or manganese are frequently present. Hence, it seems plausible to link AOM to metal reduction. However, not much is known about microbial methane oxidation coupled to metal reduction. A recent study could show that methane was oxidised when birnessite (manganese[IV] oxide) or ferrihydrite (iron[III] [hydr]oxide) were added to sulfate free sediment microcosms of the Eel River Basin [33]. This was an indirect evidence for coupling AOM to metal reduction. Moreover, Beal *et al.* [33] showed that a small proportion of a 16S rRNA gene clone library was related to ANME groups. Thus, another pathway of methane oxidation possibly mediated this process.

1.3. Degradation of higher hydrocarbons

An appreciable amount of scientific literature covering aerobic and anaerobic microbial hydrocarbon degradation has accumulated during several decades of hydrocarbon research (nearly complete reviews of the last three decades are references [3, 45, 46]). However, the huge structural diversity of higher hydrocarbons still makes research in this field necessary and challenging.

1.3.1. Aerobic hydrocarbon degradation

Aerobic hydrocarbon degradation requires molecular oxygen. It serves as electron acceptor and directly oxidises the hydrocarbon. This process can be ignited spontaneously but bacteria and fungi are able to degrade hydrocarbons aerobically as well. Microbial hydrocarbon degradation under aerobic conditions is known for more than a century now. Since oxygen is not simply an electron acceptor in this case, the biochemistry of aerobic hydrocarbon degradation is briefly introduced in Section 1.3.6. "Biological hydrocarbon activation". However, due to low oxygen solubility in water, organic rich sediments are usually oxygen depleted and anaerobic hydrocarbon degradation is mostly anoxic.

1.3.2. Hydrocarbon degradation coupled to nitrate reduction

Nitrate is abundant in the oceans. In the water column, it appears in global average concentrations of about 30 µM in the aphotic zone but decreases towards the water surface [47]. Nitrite, however, can be found near the euphotic zone in global average concentrations of 10 µM and sharply deceases with depth [47]. Average nitrate concentrations in the sediment are comparable to water column concentrations but are highly variable and dependent on the availability of organic carbon and other reductants in deeper sediments [48]. The steep de-

cline of nitrate concentrations in marine sediments makes it less important for benthic hydrocarbon degraders [48]. Nevertheless, nitrate is a well described electron acceptor for hydrocarbon degraders [49-51].

However, nitrate is a well known inhibitor of microbial sulfide release [52, 53]. Thus, the addition of nitrate may inhibit the release of corrosive sulfide, but may simultaneously accelerate the degradation of hydrocarbons. Moreover, nitrate is a potent inhibitor of methanogenesis [54]. This may impose problems when methane is the desired product of hydrocarbon degradation rather than carbon dioxide.

On the other hand, denitrification (N_2 and CO_2 release) causes an increase of pressure in oilfields which results in higher production yields and makes nitrate addition economically favourable. Also in case of bioremediation of oil spills, nitrate may serve as electron acceptor for hydrocarbon degraders as well as a source of nitrogen.

1.3.3. Hydrocarbon degradation coupled to sulfate reduction

Sulfate is an abundant compound in marine environments (up to 28 mM, [55]) but as an oxidant it is one of the least favourable compounds in nature. In spite the low energy gain from sulfate reduction, microorganisms frequently use sulfate in marine sediments which is reflected in a broad diversity and a high number of sulfate reducers commonly found therein [56-60].

The terminal product of sulfate reduction is sulfide. Sulfide is a relatively potent and hazardous reducing agent. Its reactivity makes it an important compound in geochemical process, e.g. as reductant or during precipitation of various iron sulfides [61]. As corrosive substance, it is responsible for substantial economic losses for the petroleum industry when hydrocarbon degradation is coupled to microbial sulfate reduction [53, 62]. Knowledge about sulfate reduction coupled to hydrocarbon degradation is therefore essential to control such undesired processes.

Like nitrate, sulfate is a well soluble electron acceptor and sulfate reducers are frequently found among anaerobic hydrocarbon degrading microbial communities. A famous culture became strain Hxd3 (non-official name: *Desulfococcus oleovorans* Hxd3) because it was described as the first pure and stable culture able to degrade hexadecane [63-65]. Alkane degradation under sulfate reducing conditions was known for almost a half century when strain Hxd3 was discovered [66]. As oil spills became a serious environmental problem [5-7, 9] and sulfide corrosion on production materials caused substantial economic losses [53, 62] sulfate reducing hydrocarbon degraders received increasing attention. Since the early reports, many

new insights in the biochemistry of hydrocarbon degradation were gained in recent years and many of these studies were conducted using sulfate reducing bacteria [3, 67].

1.3.4. Hydrocarbon degradation coupled to metal reduction

Much less is known about metal reduction coupled to hydrocarbon degradation. Environmentally important are trivalent iron and tetravalent manganese [67-70]. Iron and manganese were detected in considerable amounts in marine environments [71]. A full redox cycle of iron was shown when photosynthetic oxidation of bivalent iron was demonstrated [72]. Apparently, iron reduction coupled to hydrocarbon degradation is worth closer investigation [73, 74]. For example, it has been successfully attempted to add or chelate insoluble trivalent iron in order to stimulate benzene degradation [75]. Within the following ten years, *Geobacter grbiciae* was shown to oxidise toluene coupled to iron reduction. Another five years later Jahn *et al.* [76] were able to show degradation of ethylbenzene, toluene and *o*-xylene in an iron reducing enrichment culture. Two well known metal reducing hydrocarbon degraders, *Geobacter* and *Shewanella*, reduced the iron cyanide Prussic Blue [77]. Additionally, manganese(IV) reduction was demonstrated to couple to toluene degradation in enrichment cultures [78, 79]. However, only two heterotrophic manganese(IV) reducing strains from an oilfield could be isolated, which were unable to degrade hydrocarbons [80, 81].

1.3.5. Degradation of hydrocarbons to methane

Besides CO_2, methane is a terminal product of hydrocarbon degradation [82]. CO_2 can be reduced to methane as well by hydrogenotrophic carbon dioxide reduction. This is important to understand risks of man-made or natural oil spills [5-7, 9]. Since methane is a much more potent greenhouse gas than CO_2 and less soluble in water, the risk of methane release from microbiological hydrocarbon degradation potentially accelerates the greenhouse effect [30]. On the other hand, methane as terminal hydrocarbon degradation product may be desired when higher hydrocarbons inaccessibly remain in technically exhausted petroleum reservoirs (*Figure 2*; [83, 84]). The conversion of higher hydrocarbons to methane may be an elegant method for microbially enhanced hydrocarbon recovery (MEOR). This was demonstrated for organic matter from shale [85], coal [86] and petroleum [87]. Today, 1.1×10^9 m^3 yr^{-1} coal mine methane (CMM) are already recovered from abandoned coal mines in the USA [88]. Since financial investments are apparently lower for CMM recovery than for oilfield exploration, this seems to be an interesting option for further research to enhance methane recovery. In summary, the conversion of higher hydrocarbons to methane adds new opportunities to MEOR. While the classical approach attempts to enhance the recovery of higher hydrocarbons by detaching them from reservoir minerals, the conversion to methane could be a pragmatic option when energy is the only interest.
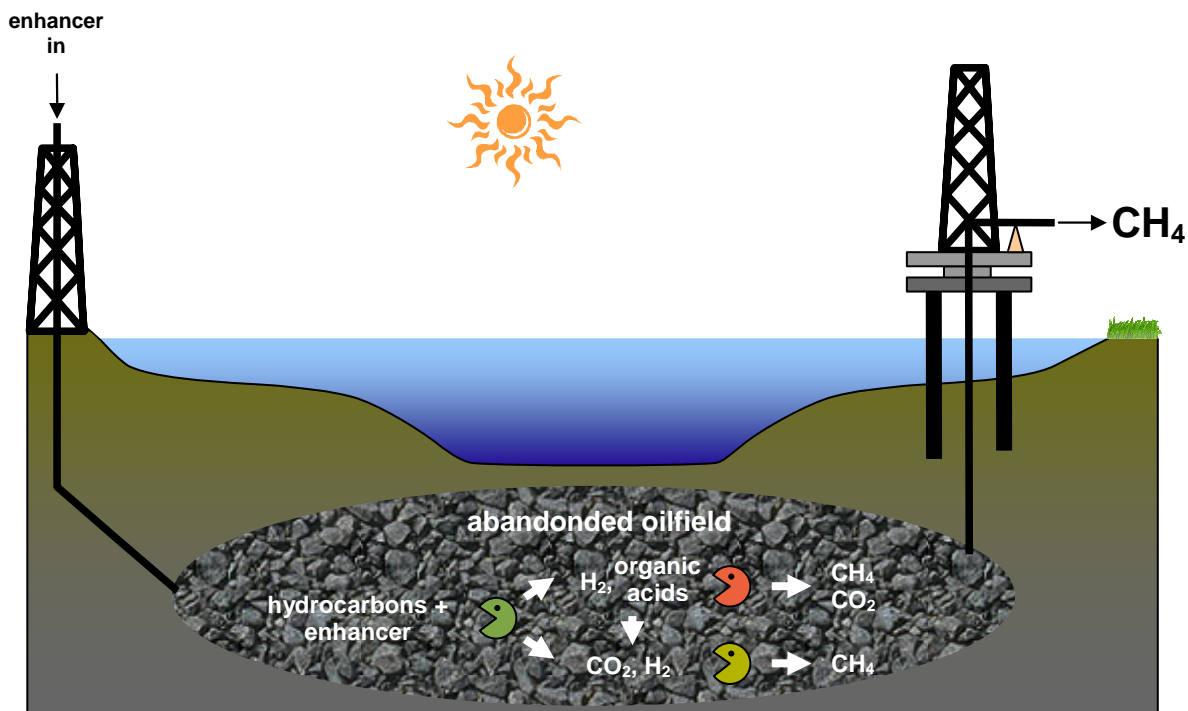
Figure 2: Principle of microbially enhanced oil recovery (MEOR) by converting complex hydrocarbons to methane. Enhancers are pumped with production fluids into an abandoned oilfield with residual oil. Such stimulation causes present microbial communities to convert complex hydrocarbons into small carbon compounds. Subsequently, these compounds are utilised by methanogens to produce volatile natural gas (methane).

1.3.6. Biological hydrocarbon activation

The activation of hydrocarbons is the first step in the degradation cascade terminating with CO_2 and methane. Since many different electron acceptors may drive hydrocarbon degradation and since hydrocarbons are structurally extremely diverse, many different activation mechanisms have been reported so far.

Oxygen is the only electron acceptor directly involved in hydrocarbon activation. Two different activation mechanisms have been reported for hydrocarbon activation by molecular oxygen. The first mechanism is initiated by a radical transfer and subsequent peroxidation (*Figure 3*) while the second type of mechanism involves oxygen addition to alkenes, alkines or aromatics (*Figure 3*; [89-95]). Enzymes involved are called monooxygenases or dioxygenases [89, 93]. Alcohols, aldehydes and fatty acids are products of hydrocarbon oxidation. Subsequent ß-oxidation provides acetyl-CoA for microbial metabolism. However, in hydrocarbon rich marine sediments, molecular oxygen is usually depleted and oxic hydrocarbon degradation occurs in the water column.

So far, two different processes were shown to oxidise methane. Enzymes involved in this reaction activate methane by an electron transfer from methane to an oxygen molecule. The formation of highly reactive methyl hydroperoxide is the first step (similar to *Figure 3A*). This methyl hydroperoxide is further oxidised to carbon dioxide [96]. The mediating enzyme is called methane monooxygenase (MMO; [97]). Two different types of MMO are known: a particulate, membrane bound, type (pMMO) and a soluble, cytoplasmatic, type (sMMO). Both forms of MMO are further described in Chapter 4. This is essentially the enzyme type which also catalysed methane oxidation in *Candidatus Methylomirabilis oxyfera* [34]. Therefore, AOM coupled nitrate reduction is actually aerobic methane oxidation.

Another reaction mechanism involving radical activation is fumarate addition (*Figure 4*; [67]). This was first was published for anaerobic toluene activation [98] and later on for alkanes as well [99, 100]. However, fumarate addition to methane has never been reported. Also carboxylation was shown to initiate polyaromatic hydrocarbon (PAH) degradation but knowledge about the enzymatic machinery is scarce [101-103]. Furthermore, methylation was proposed to be the initial step during the degradation of naphthalene (Chapter 3; [104]).

A special case of anaerobic hydrocarbon activation mechanisms is the activation of ethylbenzene. Ethylbenzene may be activated by α-hydroxylation [107, 108] or fumarate addition [109]. A reason may be hybrid nature of ethylbenzene [67]. While it is an alkane with a phenyl residue in α position it is also alkylated benzene. In case of hydroxylation, the molybdenum co-factor of the ethylbenzene dehydrogenase presumably hydroxylates ethylbenzene directly in α position [107, 108].

Another exception is AOM which is exclusively catalysed by a variant of the methyl coenzyme M reductase (MCR). This enzyme usually drives the synthesis of the Coenzyme M-Coenzyme B disulfide (CoM-S-S-CoB) in methanogens, transferring an electron and releasing methane. The reversal of this reaction cleaves CoM-S-S-CoB to CoM-S-CH$_3$ and HS-CoB, transferring activated methane [110]. Three different mechanisms for the initial attack are discussed [111]. However, Thauer and Shima [111] proposed a nucleophilic methylation of a putative Ni(III) core of the methyl thioether of the co-factor F$_{430}$ [110]. This modified co-factor was first discovered in high amounts in anaerobic methanotrophic mats of the Black Sea, indicating that it is the key catalyst in AOM [112].
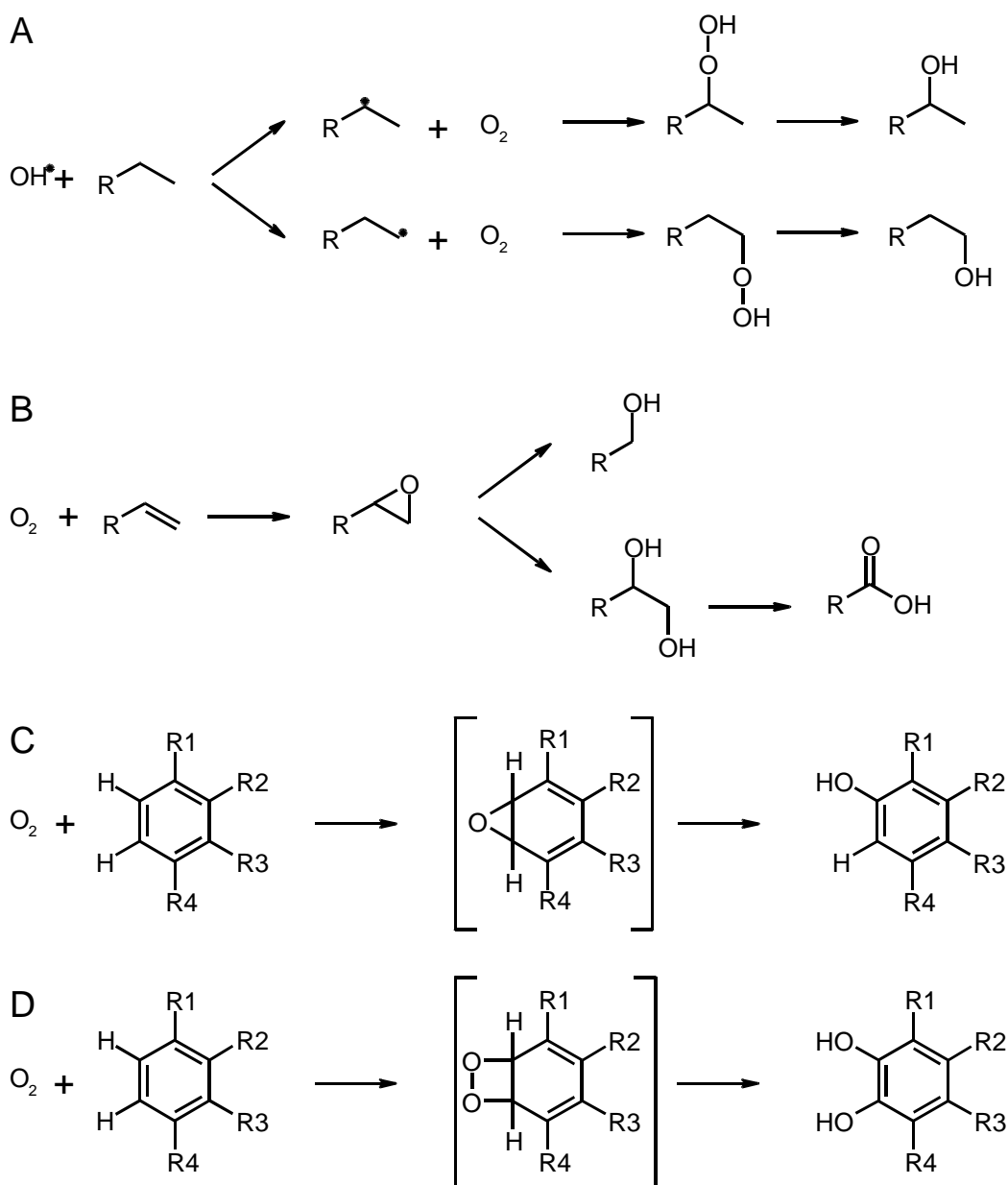
*Figure 3: Simplified activation mechanisms involving molecular oxygen. (**A**) Terminal and subterminal peroxidation of an alkane [93]. Products of the peroxides are either a secondary or primary alcohol. The radical starter is a hydroxyl radical. (**B**) Epoxidation of an alkene [93]. Reaction products are either the corresponding alcohol or carboxylic acid. (**C**) A special case of epoxidation is the epoxidation of aromatic rings [92]. The epoxide transition state is depicted in brackets. Like in (B) the di-hydroxy alcohol may be the result (not shown; [89]). (**D**) Dioxygenation of aromatic rings [94]. The dioxygenated transition state is shown in brackets.*
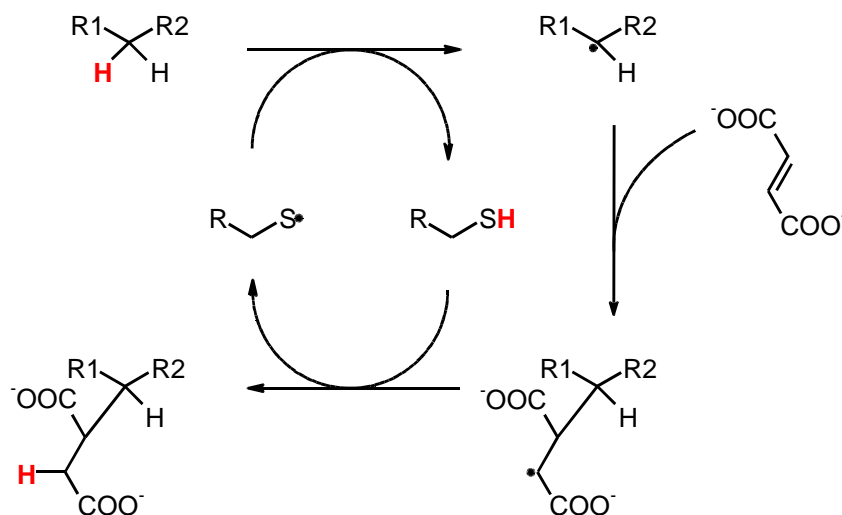
Figure 4: Simplified activation mechanism by fumarate addition [67, 105]. The recycled thiyl radical of a cystein residue is formed by radical transmission from a glycyl radical, analogous to Knappe et al. [106].

1.4. The role of nitrogen in marine sediments

Nitrogen is an essential element for life and hence also for hydrocarbon degraders. The concentration of reactive nitrogen varies in marine environments and is sometimes limiting [113]. Apparently, the use of nitrogen sources is dependent on the supply with other nutrients like phosphate or the availability of carbon. This has implications for bioremediation of contaminated sites [5, 14, 114, 115]. In consequence, a good measure for the nitrogen richness of an investigated environment is the nitrogen concentration relative to phosphorous or carbon or both (N:P, C:N or C:N:P). The preferential removal of nitrogen from decomposing organic matter is reflected in increasing C:N ratios with increasing shore distance [116] and increasing water depth [117, 118]. Concentrations of nitrogen in the marine water column are often up to 7 µM [119] near shore or 40 µM [120] in estuarine waters. Nitrogen may appear in various oxidation states and numerous organic variations (*Figure 5*). In its lowest oxidation state of -3, nitrogen occurs as ammonium. At the same time, ammonium is the only form of nitrogen that can be directly assimilated by a living cell. Ammonium concentrations in sediment porewater vary between e.g. 0.1-19.1 µM in the Black Sea [121], 3-60 µM in the North Sea [122], 2.1 mM in the Atlantic NW African Continental Margin [123] or 5.7 mM in foreland sediments of the Sunda Arc [124].
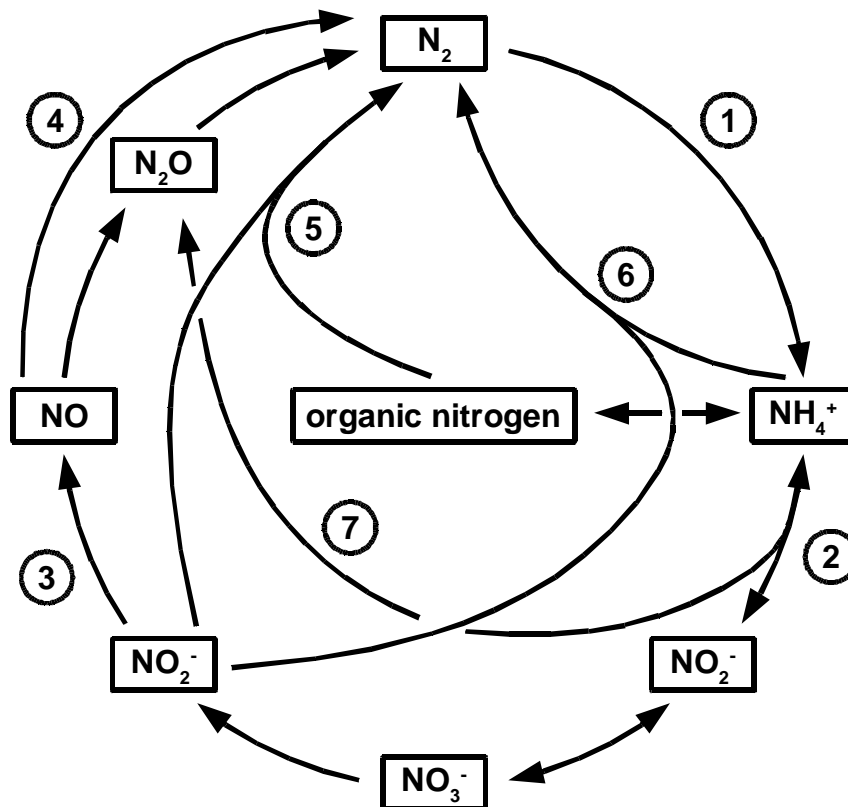
Figure 5: The nitrogen cycle (modified and updated after [34, 47, 125]). Only major extracellular nitrogen species are depicted. Clockwise: 1 diazotrophy; 2 nitrification to nitrate via nitrite and its reversal, nitrate reduction to ammonium (DNRA); 3 denitrification to dinitrogen via nitric and nitrous oxide; 4 reduction of nitric oxide to dinitrogen either via nitrous oxide or directly as reported recently by Ettwig et al. [34]; 5 co-denitrification [126]; 6 anaerobic ammonium oxidation (anammox); 7 spontaneous decomposition of nitrite during nitrification and nitrite does not accumulate

1.4.1. Ammonium oxidation

Ammonium concentrations are highly dependent on oxygen supply and deposition rates of organic matter [127]. While organic matter is decomposed, ammonium is excreted (*Figure 5*). Released ammonium can be further oxidised to nitrate via nitrite (*Figure 5*). These processes are nitrification *(Formula 1)* and subsequent denitrification (*Formula 2*):

1 $NH_4^+ + 2\,O_2 \qquad \rightarrow \qquad NO_3^- + 2\,H^+ + H_2O$

ΔG° = -348.80 kJ/mol NH_4^+

2 $5\,CH_2O + 4\,NO_3^- \qquad \rightarrow \qquad 5\,HCO_3^- + 2\,N_2 + H^+ + 2\,H_2O$

ΔG° = -470.07 kJ/mol carbon
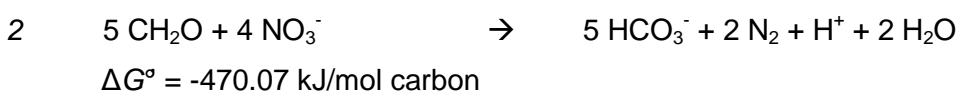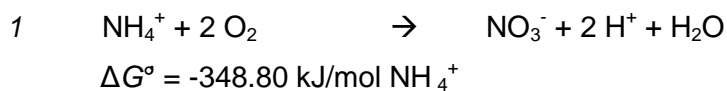
When oxygen is depleted or even absent, ammonium oxidation can be achieved by nitrate and subsequent by nitrite reduction, so called anaerobic ammonium oxidation (anammox; *Formula 3*; [128, 129]):

3 $5\ NH_4^+ + 3\ NO_3^- \quad \rightarrow \quad 4\ N_2 + 2\ H^+ + 9\ H_2O$

         $\Delta G^\sigma = -296.66\ kJ/mol\ NH_4^+$
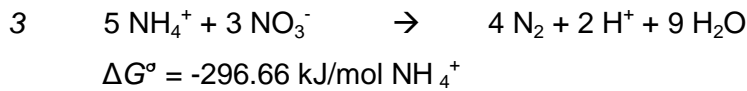
Apperantly, anammox usually occurs where nitrite and ammonium meet [130, 131]. The source for nitrite may be denitrification (*Formula 2*; [130, 131]) but nitrification seems possible when oxygen concentrations are low enough to allow anammox. However, since anammox is an anoxic process it can usually be found in sediments [132] but also in the water column [130, 131].

Anaerobic oxidation of ammonium by sulfate is energetically possible at standard conditions but has never been demonstrated (*Formula 4*; [133]):

4 $8\ NH_4^+ + 3\ SO_4^{2-} \quad \rightarrow \quad 4\ N_2 + 3\ HS^- + 5\ H^+ + 12\ H_2O$

         $\Delta G^\sigma = -17.54\ kJ/mol\ NH_4^+$
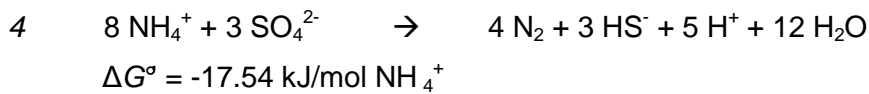
Apparently, sulfate coupled ammonium oxidation would likely occur in ammonium rich environments.

1.4.2. Nitrate reduction

Since all inorganic nitrogen is assimilated into cells as ammonium via amino acid and subsequently purine biosynthesis, all other forms of inorganic nitrogen must be converted to ammonium first. When nitrate is the nitrogen source, it is first reduced to ammonium (*Figure 5*; [134]). As feedback, ammonium has an inhibitory effect on assimilatory nitrate reduction [134]. Assimilatory nitrate reduction is in principle nitrate and nitrite reduction to ammonium (*Formula 5*; [135]):

5 $2\ CH_2O + NO_3^- + H_2O \quad \rightarrow \quad 2\ HCO_3^- + NH_4^+$

         $\Delta G^\sigma = -321.74\ kJ/mol\ carbon$
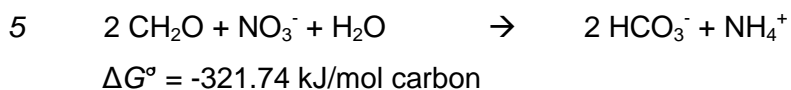
while denitrification is nitrate and nitrite reduction to dinitrogen (*Formula 2*).

Denitrification results in loss of nitrogen from denitrifying systems. When nitrate is utilised for ammonium production (dissimilative nitrate reduction to ammonium, DNRA), less energy than for denitrification is gained (*Formulas 5* and *2*; [136]). Both, denitrification and DNRA, are respiratory processes coupled to substrate phosphorylation but DNRA may be preferably used as electron sink [136, 137]. As electron sink, DNRA has advantages over denitrification in reduced anoxic environments where lacking electron acceptors are often a severe hurdle

for life. Such environments are organic rich deep sea environments where AOM usually occurs [32] and typically exhibit an excess of ammonium [127].

1.4.3. Diazotrophy (nitrogen fixation)

Denitrification and anammox lead to a loss of nitrogen from the benthos to the water column and ultimately to the atmosphere (*Figure 5*; [138]). A part of this dinitrogen is retained by microorganisms which feed on dissolved dinitrogen (*Figure 5*). This process is called nitrogen fixation or diazotrophy and the enzymatic complex was termed nitrogenase [139, 140]. Biochemically, diazotrophy hydrolyses as much as 16 ATP to convert one molecule dinitrogen to two molecules ammonium (*Formula 6*; [141]):

6 $N_2 + 8 [H] + 16 ATP$ $\rightarrow$ $2 NH_3 + H_2 + 16 ADP + 16 P_i$
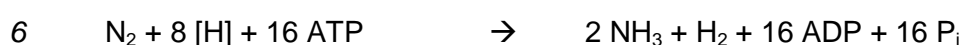
Consequently, diazotrophy only occurs when other ways of nitrogen uptake are impossible. In nitrogen replete environments, like organic rich marine sediments, diazotrophic activity may therefore represent only a small fraction of the overall nitrogen cycle [142].

1.5.   Hydrocarbon associated benthic microbial communities

1.5.1.   What is a microbial community?

Microbial ecology studies microbial populations. Microbial cells are compartments. Segmentation was essential for the evolution of life. The reason is that biochemical processes need special conditions under which they become feasible. While one reaction is feasible under certain conditions another one may not. An example is the accumulation of reaction products which prevents a reaction from proceeding. Reaction compartments overcome this problem. Living organisms contain compartments which enable specific chemical reactions. Multicellular organisms develop specialised cells for special chemical reactions (e.g. kidney cells, neurons etc.) while unicellular organisms apparently do not possess such capabilities. Hence, unicellular prokaryotes form microbial communities of different species to handle cascaded chemical reactions (food chains or food webs). Complexity increases when reaction conditions change and former active members of the microbial population become less active or dormant while others are activated and divide. Consequently, microbial communities become more diverse. Since natural communities rarely comprise a single species, diversity is apparently required for survival in complex environments. A relevant example for a specialised yet diverse microbial community is an AOM community in which ANME *Archaea* perform methane oxidation to carbonate and *Bacteria* of the *Desulfococcus*/*Desulfosarcina* cluster transfer released electrons to sulfate, thereby reducing it to sulfide (*Formula 7*; [32]):

7 $CH_4 + SO_4^{2-}$ → $HCO_3^- + HS^- + H_2O$

ΔG^o = -32.98 kJ/mol methane
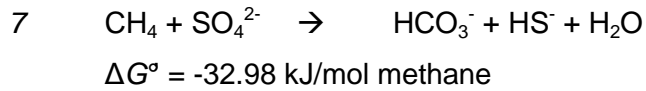
Hydrocarbon degrading communities are another example for aggregates of different microbial species [143-146].

1.5.2. The species concept in microbial ecology, briefly

For a microbiologist, the description of a microbially mediated substrate turnover process in an investigated environment usually comes along with the question for the participating microbial species. While this seems a natural approach, the definition of a microbial species is nothing but easy. For eukaryotic organisms, a species is defined as an interbreeding population. Unlike eukaryotes, prokaryotes do not sexually reproduce. Hence, the description of a microbial community starts with the problem of defining a species. This issue is subject of an ongoing controversial dispute [147]. Hence, microbiologists have chosen a pragmatic path and "define" a species by two different nucleic acid based criteria: less than 97% 16S rRNA sequence identity and less than 70% chromosome sequence identity to any other species [148]. Still, this imposes the problem of chromosomal sequencing in the environment which is difficult to implement with current DNA processing technology. For this reason, environmental microbiologists make use of the conserved nature of 16S rRNA [149] and describe clusters of similar 16S rRNA sequences obtained from the investigated environment. Such clusters have become necessary because an organism of the same or less than 3% different 16S rRNA genotype may exhibit – sometimes extremely – different phenotypes. For example, closely related 16S rRNA genotypes belong to distinct phenotypes of the phototroph *Prochlorococcus* [150]. Additionally, it is well known phenomenon that named species show a great metabolic variability [151] and carry different functional genes [152]. Instead of genotypes and species, Cohan [153, 154] suggested the use of ecotypes. Moreover, as long as there is no theoretical model for describing prokaryotic species, environmental microbiologists introduced the term "operational taxonomic units" (OTUs) for organisms sharing less than 97% identity of their ribotypes. In summary, one must keep in mind the limitations of the ribotype model before interpreting phylotypic relationships merely built on 16S rRNA sequence data (*Figure 6*).
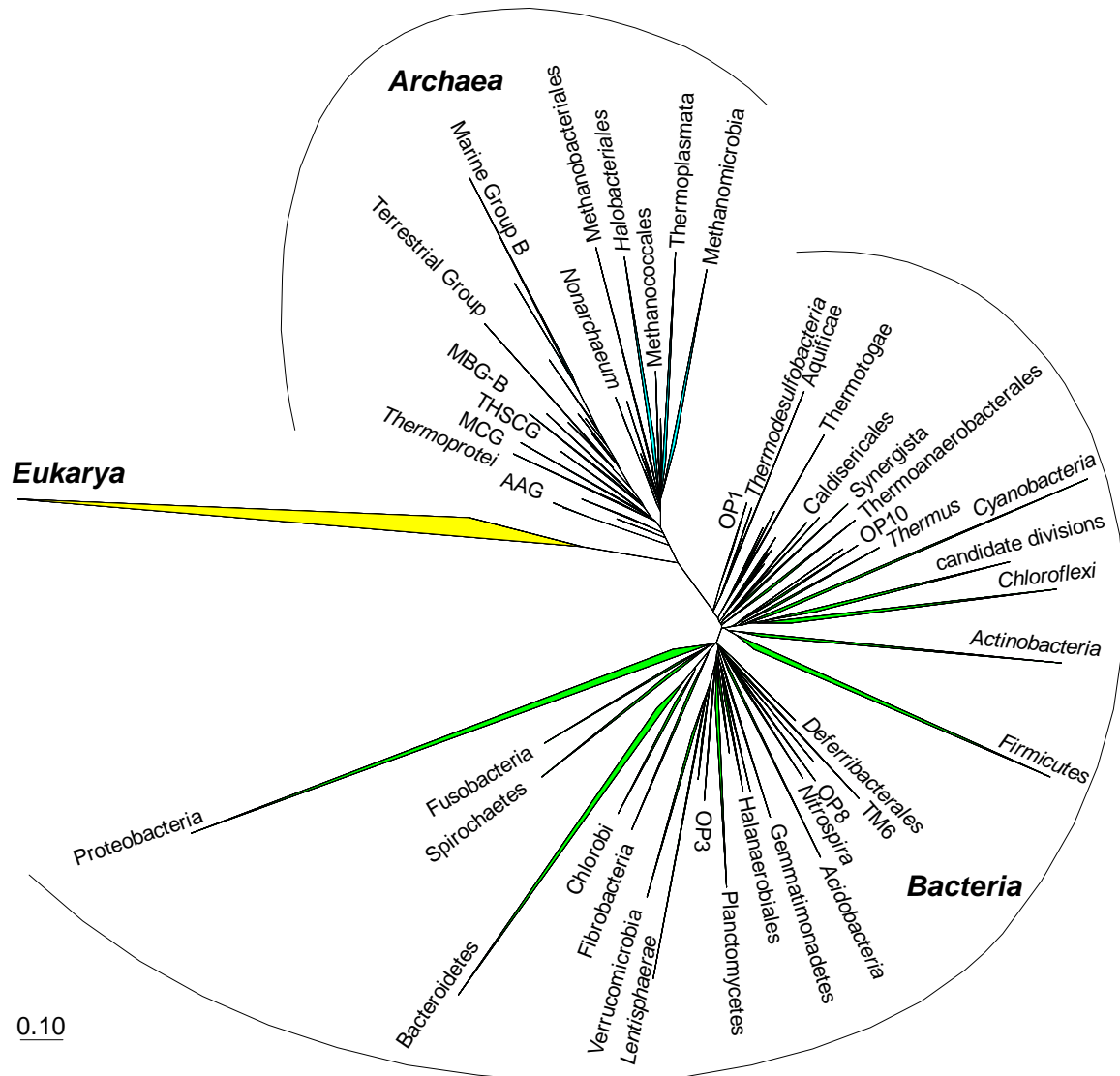
Figure 6: Phylogenetic tree showing the three domains of life: Archaea, Bacteria, Eukarya. This tree is a Parsimony tree version 102 REF (February 2010) basing on high quality 16S rRNA reference sequences and was created as part of the SILVA project [155]. Abbreviations indicate the ecosystem where first clones of a group were obtained from. They are, clockwise, starting with Archaea: AAG = ancient archaeal group, MCG = miscellaneous crenarcheaotic group, THSG = terrestrial hot spring group, MBG = marine benthic group, OP = Obsedian Pool [156], TM = Torf, mittlere Schicht [157]. "Candidate divisions" indicate a cluster of several such candidate divisions. The bar is calibrated to 0.1 nucleotide base pair variability per one nucleotide base pair.

Nevertheless, some phenotypic features are shared among microorganisms of rather distantly related ribotypes. Membrane lipids, light adaptation, extremophilic lifestyle or physiology are some phenotypic delineation criteria which are correlated to ribotype clusters. Examples for membrane lipids are ethers which are exclusively synthesised by *Archaea* while *Bacteria* and *Eukarya* assemble their cell membranes from phospholipid esters. Anammox *Bacteria* belong to the class *Planctomycetales* (*Figure 6*) and are the only *Bacteria* synthesising ladderanes [158, 159]. *Cyanobacteria* are an example for a genotypic cluster which exclu-

sively hosts Gram negative light harvesting *Bacteria*. Extremophiles belonging to the class *Halobacteria* (*Figure 6*) are *Archaea* known for their halophilic lifestyle while other halophiles are also found among *Bacteria* and *Eukarya* [160]. Members of the family *Halobacteriaceae* live exclusively in brines or salt saturated microenvironments [161]. A physiological feature that is usually found among *Archaea* is the capability of methane production although plants have been reported to release methane as well [1]. *Methanosarcina, Methanosaeta* (both *Methanomicrobia* in *Figure 6*) and *Methanococcus* (*Figure 6*) are typical methanogenic genera, to name only a few [162].

1.5.3. Hydrocarbon degrading microbial communities
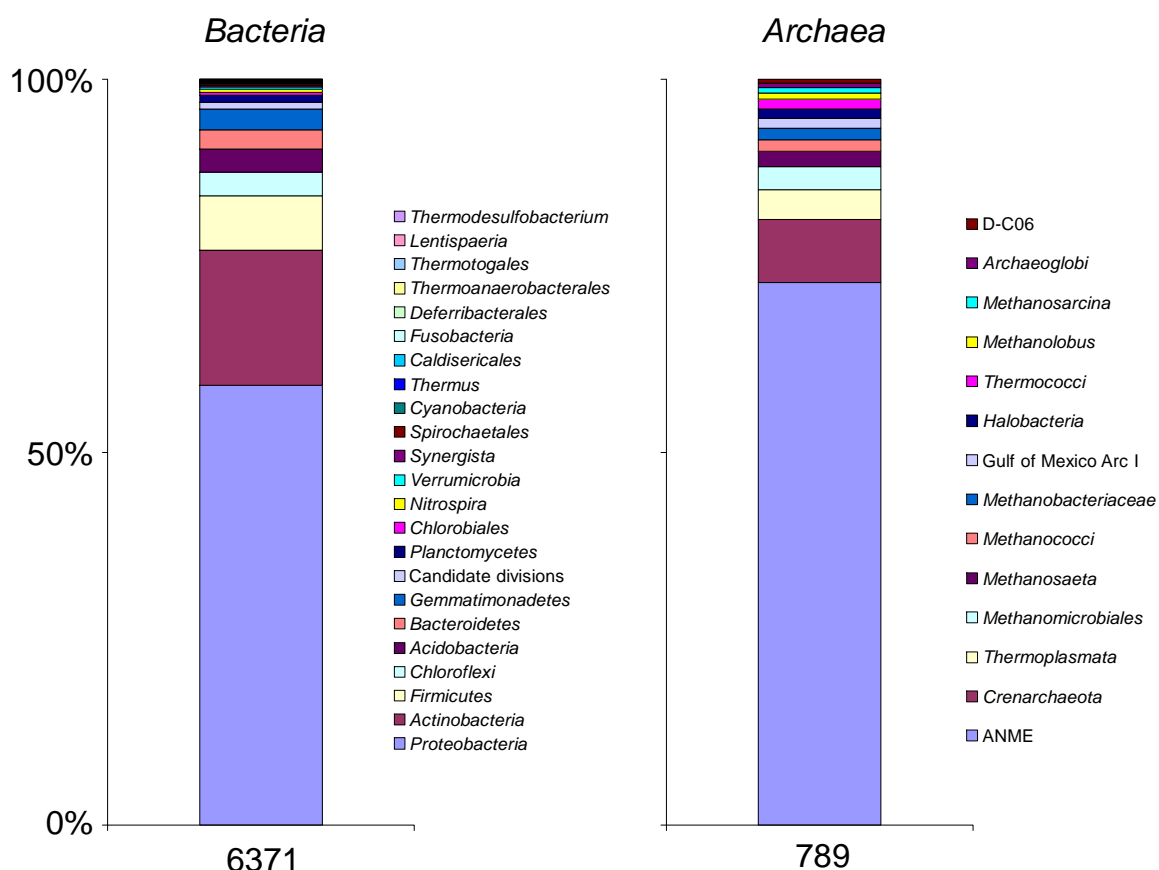
Figure 7: Prokaryotic OTUs that (potentially) degrade hydrocarbons. The SILVA database 102 REF was used to search for cultured and uncultured, confirmed and potential hydrocarbon degraders [155]. OTUs selected for depiction comprise environmental samples as well as cultured communities and isolates. The x-axis displays the number of OTUs of Bacteria (left) and Archaea (right). Eukaryotic yeasts and fungi often degrade hydrocarbons [89, 164] but were not screened for this figure.

Hydrocarbons comprise an uncounted number of diverse structural molecules. Therefore one may expect a similar diversity of degradation pathways and microorganisms involved in such pathways. Indeed, a broad diversity of hydrocarbon associated OTUs can be revealed from the SILVA ribosomal sequence database (*Figure 7*). This 16S rRNA database research is

supported by a study that unveiled a low numbered but potentially broad diverse microbial community in a deep marine oilfield by lipid biomarker analysis [163]. However, only a minute fraction of prokaryotic hydrocarbon degraders has been cultured so far [3, 89].

Typical aerobic hydrocarbon degraders are *Pseudomonads* and *Bacilli* [89]. Yeasts and fungi were also reported to degrade hydrocarbons aerobically [89, 164]. However, due to their cell size it seems unlikely that eukaryotic cells are able to penetrate deeper layers of marine sediments. Many pure cultures of anaerobic hydrocarbon degraders were assigned to *Proteobacteria* [3]. One example for a nitrate reducing strain is *Azoarcus* sp. EbN1 [50, 165] and for a sulfate reducing isolate *Desulfococcus oleaovorans* strain Hxd3 [63, 65].

1.5.4. Microbial communities in the nitrogen cycle

One might anticipate from the complexity of the nitrogen cycle (*Figure 5*) that a great diversity of prokaryotic microorganisms is involved. For example, genes encoding nitrite reductases (*nir* genes) are distributed over α-, ß-, γ- and ε-*Proteobacteria* [166, 167] as well as over *Bacteroidetes* and *Firmicutes* [166]. Among *Firmicutes*, *nar* genes encoding nitrate reductases were found in *Clostridia* and *Bacilli* [168]. A novel clade of nitrate reducing *Bacteria* was established by the isolation of the deep sea thermophile *Caldithrix abyssi* [169]. However, Jones *et al.*, [170] could show in a phylogenetic analyses of 68 complete genomes, 147 *nirK* and 101 *nirS* genotypes as well as 118 *nosZ* and 181 *norB* genotypes (nitrous oxide and nitric oxide reductase, respectively) that denitrification is largely dominated by *Proteobacteria* (88%). Interestingly, some *Archaea* (1%) are involved in denitrification as well [170]. Nitrogen uptake in *Cyanobacteria* is possible via nitrate and nitrite reduction as well as ammonium assimilation [171]. However, ammonium assimilation is the only way of nitrogen uptake that can be found in all living organisms.

Another wide spread nitrogen assimilation pathway is nitrogen assimilation or diazotrophy. Of this re-assimilated dinitrogen, one half is reduced to ammonia by mankind in the Haber-Bosch Process while the other half is fixed by diazotrophic microorganisms [113]. A recent study, however, suggests that microbial diazotrophy is globally underestimated by one order of magnitude [172, 173]. Hence, diazotrophic microorganisms may play a more important role in the nitrogen cycle than estimated so far. Consequently, diazotrophy is a wide spread feature among microorganisms and can be found among *Bacteria* and *Archaea* [141]. Beijerinck was the first to isolate the aerobic gram-negative diazotroph *Azotobacter chroococcum* [174] and later on Benecke and Keutner [175] speculated whether this process is carried out by anaerobic gram-positive *Clostridia* in a sediment culture obtained from Baltic Sea sediment. Today, we know that their early observations were correct and a number of prokaryotic isolates carrying *nif*-genes, encoding for subunits of nitrogenises, were described [141, 176].

Typical diazotrophic organisms belong to α-, γ- and δ- *Proteobacteria*, *Cyanobacteria*, *Chlorobi*, *Clostridia*, *Bacilli*, *Methanobacteria* as well as *Methanosarcinales* [141]. Phototrophic bacteria make up a large fraction of diazotrophs, apparently because their typical habitats are closer to their substrate, dinitrogen. However, *nif*-genes where discovered in a cold abyssal valley [177] and an adjacent deep hydrothermal vent [178]. AOM driven marine environments were reported to host *nif*-genes as well [179, 180]. Consequently, diazotrophic activity was demonstrated in $^{15}N_2$ labelling studies associated to AOM [181, 182].

1.6. Methods in microbial ecology

In general, scientific methodology applied in microbiology is culture dependent or culture independent. While the first approach investigates living systems, for culture independent techniques, extracts of the investigated system are prepared and cell molecules (so-called biomarkers) are analysed. Culture dependent techniques give the investigator a good certainty under which conditions an investigated metabolism is active. These techniques are based on incubating a sample obtained from the environment in bottles, flasks, tubes or plates. Samples should be homogenised and are either mixed with a liquid or viscous medium, or are plated on a solid medium. Incubation without a medium is possible as well. Incubation flasks may be closed or open but in either case, sterility must be ensured. Open systems have the advantage of a constant gas or medium input and are often preferred in aerobic incubations. They are called constant flow reactors because reaction conditions are kept constant. In closed systems, an exchange of the gas or liquid phase is impossible. Reaction conditions change during incubation because some nutrients are consumed while reaction products accumulate. These systems are called batch reactors. Since reaction products accumulate in batch reactors, they can be detected easily. Substrates and products can often be linked directly because the concentration of the latter increases along with a decrease of substrates. A number of different reactors were designed and sometimes serve highly specialised research objectives. Combinations of different approaches are possible. A technique which is frequently used in anaerobic cultivation is the so-called Hungate technique [183]. This incubation technique uses sealed roll-tubes, usually under oxygen exclusion. Another technique, used for aerobic cultivation, is plating samples on solid agar medium on a so-called agar Petri-dish.

However, a weak spot is that a natural system can not be perfectly mimicked in laboratory established microcosms, i.e. a bottled living culture obtained from the environment and incubated in a laboratory [184]. Hence, microcosm experiments give good results under laboratory conditions (*in vitro*) but only an estimate of natural (*in situ*) processes. The main reason for deceiving results *in vitro* is that the investigator establishes conditions, which he believes stimulates the investigated process. It is obvious that under these conditions the investigated

process is more likely to be active. However, if drawn conclusions can be expanded to *in situ* conditions remains unknown.

To overcome this problem, investigators developed culture independent techniques to extract biomarkers from *in situ* samples and compare the results with existing databases. Unfortunately, databases are never complete and information therein were collected and published by scientists investigating a certain study area. Consequently, their vision influences the interpretation of results that were obtained under different conditions. For example, 16S rRNA biomarkers of a pure hydrocarbon degrading culture are published in a database. To achieve this, 16S rRNA or 16S rRNA genes are extracted and amplified in polymerase chain reactions (PCR) for further investigation. These can involve sequencing of polynucleotide chains or so-called restriction analyses. While DNA sequencing results give direct information about genotypes by their nucleotide sequence, restriction analyses result in restriction fragments (RF) of a genotype specific length. Restriction analyses take advantage of the fact that DNA restriction enzymes are specific for a certain order of nucleotides in a DNA strain, so-called restriction sites [185]. Restriction sites are located at different – genotype specific – positions within a gene which results in distinguishable fragment lengths after restriction and chromatography. This difference in fragment morphology is called "restriction fragment length polymorphism" (RFLP). RFLP analyses are less specific and usually require cloning of PCR-amplified sequences from the investigated, e.g. hydrocarbon degrading, environment followed by sequencing. This is necessary because concluding that an identical RF length of another system than the investigated is a good indication for hydrocarbon biodegrading properties therein would neglect that: (i) an organism of even the same 16S rRNA sequence does not necessarily degrade hydrocarbons and (ii) this organism has other metabolic capabilities which were simply not investigated but are active under different conditions. This may be the case when, for example, an aerobe was not tested for an anaerobic lifestyle.

To avoid this pitfall, a combination of culture dependent und culture independent techniques is currently used. Stable isotope labelling techniques are a further development of this combination [186-189]. Briefly, added substrates of rare isotopes are metabolised by microorganisms in the same way as substrates of dominant isotopes. Mass spectrometry and density gradient centrifugation can be used to determine either metabolic products and intermediates or incorporation of unusual isotopes into cell molecules like DNA or RNA. Albeit promising in principle these techniques are still difficult to apply in environmental samples like soil or sediment microcosms. This is often owed to slow growth and resulting low label incorporation as well as insufficient visualisation techniques. Moreover, extracting DNA, RNA, lipids or proteins from environmental samples can be challenging sometimes.

1.6. Goals of this work

This work examines the fate of carbon and nitrogen during methanogenic hydrocarbon degradation and methane oxidation.

- (I)   It points out possibilities to stimulate methanogenic hydrocarbon degradation and attempts to shed light on microbial communities and their structural changes when hydrocarbon dependent methanogenesis is stimulated (Chapter 3).

- (II)   By measuring hydrogen and carbon isotopic effects during methanogenic hydrocarbon degradation this work may help to assess whether methane is hydrocarbon derived (Chapter 3).

- (III) It closes the circle from hydrocarbon degradation to methane and methane re-oxidation (Chapters 3 and 4).

- (IV)   It points out possible effects of sediment methane seepage on benthic communities of micro- and macro-biota by describing a novel methane seep of the Island Sumatra (Chapter 4).

- (V)   This work links anaerobic methane oxidation to the nitrogen cycle by investigating the behaviour of anaerobic mats of the Black Sea. Thereby, a novel protein-SIP technique is applied to demonstrate nitrogen incorporation into mat proteins (Chapter 4).

- (VI)   Novel microbial AOM mats at 720 m water depth in the Black Sea were discovered (Chapter 4)

- (VII) Ultimately, this work closes a gap in knowledge about carbon stable isotope fractionation during aerobic methane oxidation (Chapter 4).

1.7. References

1.   Keppler F, Hamilton JTG, Braß M & Röckmann T (2006) Methane emissions from terrestrial plants under aerobic conditions. *Nature* **439**: 187-191.

2.   McInerney MJ, Hoehler TM, Gunsalus RP & Schink B (2010) Introduction to Microbial Hydrocarbon Production: Bioenergetics. *Handbook of Hydrocarbon and Lipid Microbiology,* Vol. 1 (Timmis KN, ed.), pp. 321-335. Springer-Verlag, Berlin, Heidelberg.

3.   Widdel F & Rabus R (2001) Anaerobic biodegradation of saturated and aromatic hydrocarbons. *Curr Opin Biotechnol* **12**: 259-276.

4.   U.S. Energy Information Administration & U.S. Department of Energy (2010) International Energy Outlook. Office of Integrated Analysis and Forecasting, Washington, D.C.

5.   Hazen TC, Dubinsky EA, DeSantis TZ*, et al.* (2010) Deep-Sea Oil Plume Enriches Indigenous Oil-Degrading Bacteria. *Science* **330**: 204-208.

6.   Joye S & MacDonald I (2010) Offshore oceanic impacts from the BP oil spill. *Nature Geosci* **3**: 446-446.

7.   Li H & Boufadel MC (2010) Long-term persistence of oil from the *Exxon Valdez* spill in two-layer beaches. *Nature Geosci* **3**: 96-99.

8.   Peperzak L, Kienhuis P, Brussaard CPD & Huisman J (2010) Accidental and Deliberate Oil Spills in Europe: Detection, Sampling and Subsequent Analyses. *Handbook of Hydrocarbon and Lipid Microbiology,* Vol. 5 (Timmis KN, ed.), pp. 3471-3489. Springer, Berlin, Heidelberg.

9.   Valentine DL (2010) Measure methane to quantify the oil spill. *Nature* **465**: 421.

10. Gerurde NW (1960) *Toxicology and Biochemistry of Aromatic Hydrocarbons.* Elsevier Publishing, Amsterdam, London, New York, Princeton.

11. Henson EV (1959) Toxicology of Some of the Aliphatic and Alicylic Hydrocabons. *J Occup Med* **1**: 105-112.

12. Anderson RT & Lovley DR (1999) Naphthalene and benzene degradation under Fe(III)-reducing conditions in petroleum-contaminated aquifers. *Bioremediat J* **3**: 121-135.

13. Anderson RT & Lovley DR (2000) Anaerobic bioremediation of benzene under sulfate-reducing conditions in a petroleum-contaminated aquifer. *Environ Sci Technol* **34**: 2261-2266.

14. Hazen TC (2010) In Situ: Groundwater Bioremediation. *Handbook of Hydrocarbon and Lipid Microbiology,* Vol. 4 (Timmis KN, ed.), pp. 2583-2596. Springer, Berlin, Heidelberg.

15. Hinchee RE, Alleman BC, Hoeppel RE & Miller RN (1994) *Hydrocarbon Bioremediation.* Lewis Publishers, Boca Raton.

16. Margesin R & Schinner F (2001) Biodegradation and bioremediation of hydrocarbons in extreme environments. *Appl Microbiol Biotechnol* **56**: 650-663.

17. Prince RC (2010) Bioremediation of Marine Oil Spills. *Handbook of Hydrocarbon and Lipid Microbiology,* Vol. 4 (Timmis KN, ed.), pp. 2617-2630. Springer, Berlin, Heidelberg.

18. Ron E & Rosenberg E (2010) Bioremediation/Biomitigation: Introduction. *Handbook of Hydrocarbon and Lipid Microbiology,* Vol. 4 (Timmis KN, ed.), pp. 2459-2463. Springer, Berlin Heidelberg.

19. Al-Mailem D, Sorkhoh N, Al-Awadhi H, Eliyas M & Radwan S (2010) Biodegradation of crude oil and pure hydrocarbons by extreme halophilic archaea from hypersaline coasts of the Arabian Gulf. *Extremophiles* **14**: 321-328.

20. Tissot BP & Welte HD (1984) *Petroleum Formation and Occurrence.* Springer-Verlag Berlin Heidelberg New York Tokyo.

21. Calvin M (1980) Hydrocarbons from plants: Analytical methods and observations. *Naturwissenschaften* **67**: 525-533.

22. Strobel GA, Knighton B, Kluck K*, et al.* (2008) The production of myco-diesel hydrocarbons and their derivatives by the endophytic fungus *Gliocladium roseum* (NRRL 50072). *Microbiology* **154**: 3319-3328.

23. Head IM, Jones DM & Larter SR (2003) Biological activity in the deep subsurface and the origin of heavy oil. *Nature* **426**: 344-352.

24. Philp RP (1995) Petroleum and Coal. Source Rocks. *Anal Chem* **67**: 343-348.

25. Kniemeyer O, Musat F, Sievert SM*, et al.* (2007) Anaerobic oxidation of short-chain hydrocarbons by marine sulphate-reducing bacteria. *Nature* **449**: 898-901.

26. MacDonald IR, Bohrmann G, Escobar E*, et al.* (2004) Asphalt Volcanism and Chemosynthetic Life in the Campeche Knolls, Gulf of Mexico. *Science* **304**: 999-1002.

27. Muyzer G & van der Kraan GM (2008) Bacteria from hydrocarbon seep areas growing on short-chain alkanes. *Trends Microbiol* **16**: 138-141.

28. Madigan MT, Martinko J, Brock TD & Dunlap P (2009) *Brock biology of microorganisms*. Pearson/Benjamin Cummings.

29. Kvenvolden KA (1999) Potential effects of gas hydrate on human welfare. *Proc Natl Acad Sci U S A* **96**: 3420-3426.

30. International Panel on Climate Change (2007) IPCC Fourth Assessment Report: Climate Change 2007 (AR4). Vol. 1 (Solomon S, Qin D, Manning M*, et al.*, eds.), pp. 130-234. International Panel on Climate Change, Cambridge, New York.

31. Froelich PN, Klinkhammer GP, Bender ML*, et al.* (1979) Early oxidation of organic matter in pelagic sediments of the eastern equatorial Atlantic: suboxic diagenesis. *Geochim Cosmochim Acta* **43**: 1075-1090.

32. Knittel K & Boetius A (2009) Anaerobic Oxidation of Methane: Progress with an Unknown Process. *Annu Rev Microbiol* **63**: 311-334.

33. Beal EJ, House CH & Orphan VJ (2009) Manganese- and Iron-dependent marine methane oxidation. *Science* **325**: 184-187.

34. Ettwig KF, Butler MK, Le Paslier D*, et al.* (2010) Nitrite-driven anaerobic methane oxidation by oxygenic bacteria. *Nature* **464**: 543-548.

35. Ettwig KF, Shima S, van de Pas-Schoonen KT*, et al.* (2008) Denitrifying bacteria anaerobically oxidize methane in the absence of *Archaea. Environ Microbiol* **10**: 3164-3173.

36. Raghoebarsing AA, Arjan Pol A, van de Pas-Schoonen KT*, et al.* (2006) A microbial consortium couples anaerobic methane oxidation to denitrification. *Nature* **440**: 918-921.

37. Krüger M, Treude T, Wolters H, Nauhaus K & Boetius A (2005) Microbial methane turnover in different marine habitats. *Palaeogeogr Palaeoclimatol Palaeoecol* **227**: 6-17.

38.   Reeburgh WS (2007) Oceanic Methane Biogeochemistry. *Chem Rev* **107**: 486-513.

39.   Martens CS & Berner RA (1974) Methane Production in the Interstitial Waters of Sulfate-Depleted Marine Sediments. *Science* **185**: 1167-1169.

40.   Barnes RO & Goldberg ED (1976) Methane production and consumption in anoxic marine sediments. *Geology* **4**: 297-300.

41.   Reeburgh WS (1976) Methane consumption in Cariaco Trench waters and sediments. *Earth Planet Sci Lett* **28**: 337-344.

42.   Davis JB & Yarbrough HF (1966) Anaerobic oxidation of hydrocarbons by *Desulfovibrio desulfuricans*. *Chem Geol* **1**: 137-144.

43.   Boetius A, Ravenschlag K, Schubert CJ*, et al.* (2000) A marine microbial consortium apparently mediating anaerobic oxidation of methane. *Nature* **407**: 423-426.

44.   Oremland RS (2010) NO connection with methane. *Nature* **464**: 500-501.

45.   Ollivier B & Magot M (2005) *Petroleum Microbiology*. ASM Press, Washington, D.C.

46.   Timmis KN (2009) *Handbook of Hydrocarbon and Lipid Microbiology*. Springer Verlag, Berlin, Heidelberg.

47.   Gruber N (2008) The Marine Nitrogen Cycle: Overview and Challenges. *Nitrogen in the Marine Environment,* (Capone DG, Bronk DA, Mulholland MR & Carpenter EJ, eds.), pp. 1-50. Academic Press, London.

48.   Thamdrup B & Dalsgaard T (2008) Nitrogen cycling in sediments. *Microbial Ecology of the Oceans,* (Kirchman DL, ed.), pp. 527-568. John Wiley & Sons, Hoboken.

49.   Bregnard TPA, Höhener P, Häner A & Zeyer J (1996) Degradation of weathered diesel fuel by microorganisms from a contaminated aquifer in aerobic and anaerobic microcosms. *Environ Toxicol Chem* **15**: 299-307.

50.   Rabus R & Widdel F (1995) Anaerobic degradation of ethylbenzene and other aromatic hydrocarbons by new denitrifying bacteria. *Arch Microbiol* **163**: 96-103.

51.   Traxler RW & Bernard JM (1969) The utilization of n-alkanes by *P. aeruginosa* under conditions of anaerobiosis. I. Preliminary observations. *International Biodeterioration Bulletin* **5**: 21-25.

52.   Gittel A, Sorensen KB, Skovhus TL, Ingvorsen K & Schramm A (2009) Prokaryotic Community Structure and Sulfate Reducer Activity in Water from High-Temperature Oil Reservoirs with and without Nitrate Treatment. *Appl Environ Microbiol* **75**: 7086-7096.

53.   Vance I & Thrasher DR (2005) Reservoir souring: mechanisms and prevention. *Petroleum Microbiology,*(Ollivier B & Magot M, eds.), pp. 123-142. ASM Press, Washington, D.C.

54.   Klüber HD & Conrad R (1998) Effects of nitrate, nitrite, NO and N_2O on methanogenesis and other redox processes in anoxic rice field soil. *FEMS Microbiol Ecol* **25**: 301-319.

55.   Jørgensen BB & Kasten S (2006) Sulfur cycling and methane oxidation. *Marine geochemistry,* Vol. 2 (Schulz HD & Zabel M, eds.), pp. 271-310. Springer, Berlin, Heidelberg, New York.

56.   Blumenberg M, Krüger M, Nauhaus K*, et al.* (2006) Biosynthesis of hopanoids by sulfate-reducing bacteria (genus Desulfovibrio). *Environ Microbiol* **8**: 1220-1227.

57. Karr EA, Sattley WM, Rice MR, Jung DO, Madigan MT & Achenbach LA (2005) Diversity and Distribution of Sulfate-Reducing Bacteria in Permanently Frozen Lake Fryxell, McMurdo Dry Valleys, Antarctica. *Appl Environ Microbiol* **71**: 6353-6359.

58. Leloup J, Fossing H, Kohls K, Holmkvist L, Borowski C & Jørgensen BB (2009) Sulfate-reducing bacteria in marine sediment (Aarhus Bay, Denmark): abundance and diversity related to geochemical zonation. *Environ Microbiol* **11**: 1278-1291.

59. Leloup J, Loy A, Knab NJ, Borowski C, Wagner M & Jørgensen BB (2007) Diversity and abundance of sulfate-reducing microorganisms in the sulfate and methane zones of a marine sediment, Black Sea. *Environ Microbiol* **9**: 131–142.

60. Minz D, Flax JL, Green SJ*, et al.* (1999) Diversity of Sulfate-Reducing Bacteria in Oxic and Anoxic Regions of a Microbial Mat Characterized by Comparative Analysis of Dissimilatory Sulfite Reductase Genes. *Appl Environ Microbiol* **65**: 4666-4671.

61. Jørgensen BB & Nelson DC (2004) Sulfide oxidation in marine sediments: Geochemistry meets microbiology. *Geological Society of America Special Paper* **379**: 63-81.

62. Sunde E & Torsvik T (2005) Microbial control of hydrogen sulfide production in oil reservoirs. *Petroleum Microbiology,*(Ollivier B & Magot M, eds.), pp. 201-213. ASM Press, Washington, D.C.

63. Aeckersberg F, Bak F & Widdel F (1991) Anaerobic oxidation of saturated hydrocarbons to CO_2 by a new type of sulfate-reducing bacterium. *Arch Microbiol* **156**: 5-14.

64. Aeckersberg F, Rainey FA & Widdel F (1998) Growth, natural relationships, cellular fatty acids and metabolic adaptation of sulfate-reducing bacteria that utilize long-chain alkanes under anoxic conditions. *Arch Microbiol* **170**: 361-369.

65. So CM, Phelps CD & Young LY (2003) Anaerobic Transformation of Alkanes to Fatty Acids by a Sulfate-Reducing Bacterium, Strain Hxd3. *Appl Environ Microbiol* **69**: 3892-3900.

66. Novelli GD & ZoBell CE (1944) Assimilation of petroleum hydrocarbons by sulfate-reducing bacteria. *J Bacteriol* **47**: 447-448.

67. Rabus R (2005) Biodegradation of hydrocarbons under anoxic conditions. *Petroleum Microbiology,* (Ollivier B & Magot M, eds.), pp. 277-299. ASM Press, Washington D.C.

68. Lovley DR (2000) Anaerobic benzene degradation. *Biodegradation* **11**: 107-116.

69. Lovley DR & Phillips EJP (1986) Organic Matter Mineralization with Reduction of Ferric Iron in Anaerobic Sediments. *Appl Environ Microbiol* **51**: 683-689.

70. Ollivier B & Cayol JL (2005) Fermentative, iron-reducing, am nitrate-reducing microorganisms. *Petroleum Microbiology,* (Ollivier B & Magot M, eds.), pp. 71-88. ASM Press, Washington D.C.

71. Lovley DR (2000) Fe(III) and Mn(IV) Reduction in Environmental Metal–Microbe Interactions. (Lovley DR, ed.), ASM Press, Washington, D.C.

72. Widdel F, Schnell, S., Heising, S., Ehrenreich, A., Assmus, B., Schink, B. (1993) Ferrous iron oxidation by anoxygenic phototrophic bacteria. *Nature* **362**: 834-836.

73. Lovley DR, Baedecker MJ, Lonergan DJ, Cozzarelli IM, Phillips EJP & Siegel DI (1989) Oxidation of aromatic contaminants coupled to microbial iron reduction. *Nature* **339**: 297-300.

74. Lovley DR & Lonergan DJ (1990) Anaerobic Oxidation of Toluene, Phenol, and p-Cresol by the Dissimilatory Iron-Reducing Organism, GS-15. *Appl Environ Microbiol* **56**: 1858-1864.

75. Lovley DR, Woodward JC & Chapelle FH (1996) Rapid Anaerobic Benzene Oxidation with a Variety of Chelated Fe(III) Forms. *Appl Environ Microbiol* **62**: 288-291.

76. Jahn MK, Haderlein SB & Meckenstock RU (2005) Anaerobic Degradation of Benzene, Toluene, Ethylbenzene, and o-Xylene in Sediment-Free Iron-Reducing Enrichment Cultures. *Appl Environ Microbiol* **71**: 3355-3358.

77. Jahn MK, Haderlein SB & Meckenstock RU (2006) Reduction of Prussian Blue by the two iron-reducing microorganisms *Geobacter metallireducens* and *Shewanella alga*. *Environ Microbiol* **8**: 362-367.

78. Langenhoff AA, Brouwers-Ceiler DL, Engelberting JH, Quist JJ, Wolkenfelt JG, Zehnder AJ & Schraa G (1997) Microbial reduction of manganese coupled to toluene oxidation. *FEMS Microbiol Ecol* **22**: 119-127.

79. Langenhoff AA, Nijenhuis I, Tan NC, Briglia M, Zehnder AJ & Schraa G (1997) Characterisation of a manganese-reducing, toluene-degrading enrichment culture. *FEMS Microbiol Ecol* **24**: 113-125.

80. Greene AC, Patel BKC & Sheehy AJ (1997) *Deferribacter thermophilus* gen. nov., sp. nov., a Novel Thermophilic Manganese- and Iron-Reducing Bacterium Isolated from a Petroleum Reservoir. *Int J Syst Bacteriol* **47**: 505-509.

81. Greene AC, Patel BKC & Yacob S (2009) *Geoalkalibacter subterraneus* sp. nov., an anaerobic Fe(III)- and Mn(IV)-reducing bacterium from a petroleum reservoir, and emended descriptions of the family *Desulfuromonadaceae* and the genus *Geoalkalibacter*. *Int J Syst Evol Microbiol* **59**: 781-785.

82. Zengler K, Richnow HH, Rossello-Mora R, Michaelis W & Widdel F (1999) Methane formation from long-chain alkanes by anaerobic microorganisms. *Nature* **401**: 266-269.

83. Anderson RT & Lovley DR (2000) Hexadecane decay by methanogenesis. *Nature* **404**: 722-723.

84. Callaghan AV, Gieg LM, Kropp KG, Suflita JM & Young LY (2006) Comparison of Mechanisms of Alkane Metabolism under Sulfate-Reducing Conditions among Two Bacterial Isolates and a Bacterial Consortium. *Appl Environ Microbiol* **72**: 4274-4282.

85. Petsch ST, Edwards KJ & Eglinton TI (2005) Microbial transformations of organic matter in black shales and implications for global biogeochemical cycles. *Palaeogeogr Palaeoclimatol Palaeoecol* **219**: 157-170.

86. Krüger M, Beckmann S, Engelen B, Thielemann T, Cramer B, Schippers A & Cypionka H (2008) Microbial Methane Formation from Hard Coal and Timber in an Abandoned Coal Mine. *Geomicrobiol J* **25**: 315–321.

87. Gieg LM, Duncan KE & Suflita JM (2008) Bioenergy Production via Microbial Conversion of Residual Oil to Natural Gas. *Appl Environ Microbiol* **74**: 3022-3029.

88. U.S. Environmental Protection Agency (2005) Identifying Opportunities for Methane Recovery at U.S. Coal Mines: Profiles of Selected Gassy Underground Coal Mines 1999-2003.

89. Fritsche W & Hofrichter M (2004) Aerobic Degradation by Microorganisms. *Environmental Biotechnology,* (Jördening HJ & Winter J, eds.), pp. 145-155. Wiley-VCH Verlag GmbH & Co KGaA, Weinheim.

90. Maeng JH, Sakai Y, Ishige T, Tani Y & Kato N (1996) Diversity of dioxygenases that catalyze the first step of oxidation of long-chain n-alkanes in Acinetobacter sp. M-1. *FEMS Microbiol Lett* **141**: 177-182.

91. May SW, Katopodis AG & Mary EL (1990) Hydrocarbon monooxygenase system of *Pseudomonas oleovorans. Methods Enzymol* **188**: 3-9.

92. Mitchell KH, Rogge CE, Gierahn T & Fox BG (2003) Insight into the mechanism of aromatic hydroxylation by toluene 4-monooxygenase by use of specifically deuterated toluene and *p*-xylene. *Proc Natl Acad Sci U S A* **100**: 3784-3789.

93. Rehm H & Reiff I (1981) Mechanisms and occurrence of microbial oxidation of long-chain alkanes. *Reactors and Reactions,* Vol. 19, pp. 175-215. Springer Berlin / Heidelberg.

94. Smith MR (1990) The biodegradation of aromatic hydrocarbons by bacteria. *Biodegradation* **1**: 191-206.

95. van Beilen JB, Wubbolts MG & Witholt B (1994) Genetics of alkane oxidation by *Pseudomonas oleovorans. Biodegradation* **5**: 161-174.

96. Trotsenko YA & Murrell JC (2008) Metabolic aspects of aerobic obligate methanotrophy. *Adv Appl Microbiol* **63**: 183-229.

97. Lidstrom ME (2006) Aerobic Methylotrophic Prokaryotes. *The Prokaryotes,* Vol. 2 (Dworkin M, Falkow S, Rosenberg E, Schleifer K-H & Stackebrandt E, eds.), pp. 618-634. Springer Science+Business Media, New York.

98. Beller HR, Reinhard M & Grbić-Galić D (1992) Metabolic by-products of anaerobic toluene degradation by sulfate-reducing enrichment cultures. *Appl Environ Microbiol* **58**: 3192-3195.

99. Davidova IA, Gieg LM, Nanny M, Kropp KG & Suflita JM (2005) Stable isotopic studies of n-alkane metabolism by a sulfate-reducing bacterial enrichment culture. *Appl Environ Microbiol* **71**: 8174-8182.

100. Kropp KG, Davidova IA & Suflita JM (2000) Anaerobic oxidation of *n*-dodecane by an addition reaction in a sulfate-reducing bacterial enrichment culture. *Appl Environ Microbiol* **66**: 5393-5398.

101. Davidova IA, Gieg LM, Duncan KE & Suflita JM (2007) Anaerobic phenanthrene mineralization by a carboxylating sulfate-reducing bacterial enrichment. *ISME J* **1**: 436-442.

102. Zhang X, Sullivan ER & Young LY (2000) Evidence for aromatic ring reduction in the biodegradation pathway of carboxylated naphthalene by a sulfate reducing consortium. *Biodegradation* **11**: 117-124.

103. Zhang X & Young LY (1997) Carboxylation as an initial reaction in the anaerobic metabolism of naphthalene and phenanthrene by sulfidogenic consortia. *Appl Environ Microbiol* **63**: 4759-4764.

104. Safinowski M & Meckenstock RU (2005) Methylation is the initial reaction in anaerobic naphthalene degradation by a sulfate-reducing enrichment culture. *Environ Microbiol* **8**: 347-352.

105. Li L & Marsh ENG (2006) Deuterium Isotope Effects in the Unusual Addition of Toluene to Fumarate Catalyzed by Benzylsuccinate Synthase. *Biochemistry (Mosc)* **45**: 13932-13938.

106. Knappe J, Neugebauer FA, Blaschkowski HP & Gänzler M (1984) Post-translational activation introduces a free radical into pyruvate formate lyase. *Proc Natl Acad Sci U S A* **81**: 1332-1335.

107. Hagel C (2006) Struktur und Funktion der Ethylbenzol-Dehydrogenase, einer anaeroben Kohlenwasserstoff-Hydroxylase. Thesis, Tecnische Hochschule Darmstadt, Darmstadt.

108. Kloer DP, Hagel C, Heider J & Schulz GE (2006) Crystal Structure of Ethylbenzene Dehydrogenase from Aromatoleum aromaticum. *Structure (London, England : 1993)* **14**: 1377-1388.

109. Kniemeyer O, Fischer T, Wilkes H, Glockner FO & Widdel F (2003) Anaerobic Degradation of Ethylbenzene by a New Type of Marine Sulfate-Reducing Bacterium. *Appl Environ Microbiol* **69**: 760-768.

110. Scheller S, Goenrich M, Boecher R, Thauer RK & Jaun B (2010) The key nickel enzyme of methanogenesis catalyses the anaerobic oxidation of methane. *Nature* **465**: 606-608.

111. Thauer RK & Shima S (2008) Methane as Fuel for Anaerobic Microorganisms. *Ann N Y Acad Sci* **1125**: 158-170.

112. Krüger M, Meyerdierks A, Glöckner FO*, et al.* (2003) A conspicuous nickel protein in microbial mats that oxidize methane anaerobically. *Nature* **426**: 878-818.

113. Galloway JN, Dentener FJ, Capone DG*, et al.* (2004) Nitrogen Cycles: Past, Present, and Future. *Biogeochemistry* **70**: 153-226.

114. Ebuehi OAT, Abibo IB, Shekwolo PD, Sigismund KI, Adoki A & Okoro IC (2005) Remediation of Crude Oil Contaminated Soil by Enhanced Natural Attenuation Technique. *J Appl Sci Environ Manag* **9**: 103-106.

115. Schrauf TW, Sheehan PJ & Pennington LH (1993) Alternative method of groundwater sparging for petroleum hydrocarbon remediation. *Remed J* **4**: 93-114.

116. Martens CS (1978) Some of the chemical consequences of microbially mediated degradation of organic materials in estuarine sediments. *Biogeochemistry of estuarine sediments: proceedings of a Unesco/SCOR workshop held in Melreux, Belgium, 29 November to 3 December, 1976,* (Scientific Committee on Oceanic Research, ed.), pp. 266-278. UNESCO, Paris.

117. Knauer GA, Martin JH & Bruland KW (1979) Fluxes of particulate carbon, nitrogen, and phosphorus in the upper water column of the northeast Pacific. *Deep Sea Research Part A. Oceanographic Research Papers* **26**: 97-108.

118. Lee C & Cronin C (1982) The vertical fluxes of particulate organic nitrogen in the sea: Decomposition of amino acids in the Peru upwelling area and the equatorial Atlantic. *J Mar Res* **40**: 227-251.

119. Zehr JP & Ward BB (2002) Nitrogen Cycling in the Ocean: New Perspectives on Processes and Paradigms. *Appl Environ Microbiol* **68**: 1015-1024.

120. Sharp JH (1983) The distribution of inorganic nitrogen and dissolved and particulate organic nitrogen in the sea. *Nitrogen in the Marine Environment,* (Carpenter EJ & Capone DG, eds.), pp. 1-36. Academic Press Inc., New York, London.

121. Friedl G, Dinkel C & Wehrli B (1998) Benthic fluxes of nutrients in the northwestern Black Sea. *Mar Chem* **62**: 77-88.

122. van Duyl FC, van Raaphorst W & Kop AJ (1993) Benthic bacterial production and nutrient sediment-water exchange in sandy North Sea sediments. *Mar Ecol Prog Ser* **100**: 85-95.

123. Hartmann M, Müller PJ, Suess E & van der Weiden CH (1976) Chemistry of the late quaternary sediments and their interstitial waters from the NW African continental margin. *Meteor*

Forschungsergebnisse, Reihe C 24, (Seibold E & Closs H, eds.), Deutsche Forschungsge-meinschaft, Berlin, Stuttgart.

124. Schippers A, Köweker G, Höft C & Teichert BMA (2010) Quantification of microbial communi-ties in three forearc sediment basins off Sumatra. *Geomicrobiol J* 1-13.

125. Hayatsu M, Tago K & Saito M (2008) Various players in the nitrogen cycle: Diversity and func-tions of the microorganisms involved in nitrification and denitrification. *Soil Sci Plant Nutr* **54**: 33-45.

126. Tanimoto T, Hatano Ki, Kim Dh, Uchiyama H & Shoun H (1992) Co-denitrification by the deni-trifying system of the fungus Fusarium oxysporum. *FEMS Microbiol Lett* **93**: 177-180.

127. Klump JV & Martens CS (1983) Benthic Nitrogen Regeneration. *Nitrogen in the Marine Envi-ronment,*(Carpenter EJ & Capone DG, eds.), pp. 411-457. Academic Press Inc., New York, London.

128. Strous M, Fuerst JA, Kramer EHM*, et al.* (1999) Missing lithotroph identified as new plancto-mycete. *Nature* **400**: 446-449.

129. van de Graaf AA, Mulder A, de Bruijn P, Jetten MS, Robertson LA & Kuenen JG (1995) An-aerobic oxidation of ammonium is a biologically mediated process. *Appl Environ Microbiol* **61**: 1246-1251.

130. Kuypers MMM, Lavik G, Woebken D*, et al.* (2005) Massive nitrogen loss from the Benguela upwelling system through anaerobic ammonium oxidation. *Proc Natl Acad Sci U S A* **102**: 6478-6483.

131. Kuypers MMM, Sliekers AO, Lavik G*, et al.* (2003) Anaerobic ammonium oxidation by anam-mox bacteria in the Black Sea. *Nature* **422**: 608-611.

132. Schmid MC, Risgaard-Petersen N, Van De Vossenberg J*, et al.* (2007) Anaerobic ammonium-oxidizing bacteria in marine environments: widespread occurrence but low diversity. *Environ Microbiol* **9**: 1476-1484.

133. Schrum HN, Spivack AJ, Kastner M & D'Hondt S (2009) Sulfate-reducing ammonium oxida-tion: A thermodynamically feasible metabolic pathway in subseafloor sediment. *Geology* **37**: 939-942.

134. Rice CW & Tiedje JM (1989) Regulation of nitrate assimilation by ammonium in soils and in isolated soil microorganisms. *Soil Biol Biochem* **21**: 597-602.

135. Tiedje JM (1988) Ecology of denitrification and dissimilatory nitrate reduction to ammonium. *Biology of Anaerobic Microorganisms,* (Zehnder AJB, ed.), pp. 179-245. John Wiley and Sons, New York.

136. Kimura M (2000) Dissimilatory Nitrate Reduction to Ammonium (DNRA). *Soil Biochemistry,* Vol. 10 (Bollag J-M & Stotzky G, eds.), pp. 61-62. Marcel Dekker Inc., New York.

137. Simon J (2002) Enzymology and bioenergetics of respiratory nitrite ammonification. *FEMS Microbiol Rev* **26**: 285-309.

138. Dalsgaard T & Thamdrup B (2002) Factors Controlling Anaerobic Ammonium Oxidation with Nitrite in Marine Sediments. *Appl Environ Microbiol* **68**: 3802-3808.

139. Eady RR & Postgate JR (1974) Nitrogenase. *Nature* **249**: 805-810.

140. Postgate JR (1970) Biological Nitrogen Fixation. *Nature* **226**: 25-27.

141. Zehr JP & Pearl HW (2008) Molecular ecological aspects of nitrogen fixation in the marine environment. *Microbial Ecology of the Oceans,* (Kirchman DL, ed.), pp. 481-525. John Wiley & Sons, Hoboken.

142. Gruber N & Galloway JN (2008) An Earth-system perspective of the global nitrogen cycle. *Nature* **451**: 293-296.

143. Gallagher E, McGuinness L, Phelps C, Young LY & Kerkhof LJ (2005) ^{13}C-Carrier DNA Shortens the Incubation Time Needed To Detect Benzoate-Utilizing Denitrifying Bacteria by Stable-Isotope Probing. *Appl Environ Microbiol* **71**: 5192-5196.

144. Kunapuli U, Lueders T & Meckenstock RU (2007) The use of stable isotope probing to identify key iron-reducing microorganisms involved in anaerobic benzene degradation. *ISME J* **1**: 643-653.

145. Redmond MC, Valentine DL & Sessions AL (2010) Identification of Novel Methane-, Ethane-, and Propane-Oxidizing Bacteria at Marine Hydrocarbon Seeps by Stable Isotope Probing. *Appl Environ Microbiol* **76**: 6412-6422.

146. Winderl C, Penning H, Netzer Fv, Meckenstock RU & Lueders T (2010) DNA-SIP identifies sulfate-reducing Clostridia as important toluene degraders in tar-oil-contaminated aquifer sediment. *ISME J* **4**: 1314-1325.

147. Rosselló-Mora R & Amann R (2001) The species concept for prokaryotes. *FEMS Microbiol Rev* **25**: 39-67.

148. Stackebrandt E & Goebel BM (1994) Taxonomic Note: A Place for DNA-DNA Reassociation and 16S rRNA Sequence Analysis in the Present Species Definition in Bacteriology. *Int J Syst Bacteriol* **44**: 846-849.

149. Woese CR, Fox GE, Zablen L*, et al.* (1975) Conservation of primary structure in 16S ribosomal RNA. *Nature* **254**: 83-86.

150. West NJ, Schonhuber WA, Fuller NJ, Amann RI, Rippka R, Post AF & Scanlan DJ (2001) Closely related *Prochlorococcus* genotypes show remarkably different depth distributions in two oceanic regions as revealed by in situ hybridization using 16S rRNA-targeted oligonucleotides. *Microbiology* **147**: 1731-1744.

151. Logan NA & Berkeley RCW (1984) Identification of *Bacillus* Strains Using the API System. *J Gen Microbiol* **130**: 1871-1882.

152. Alm RA, Ling L-SL, Moir DT*, et al.* (1999) Genomic-sequence comparison of two unrelated isolates of the human gastric pathogen *Helicobacter pylori*. *Nature* **397**: 176-180.

153. Cohan FM (2001) Bacterial Species and Speciation. *Syst Biol* **50**: 513-524.

154. Cohan FM (2002) What are bacterial species? *Annu Rev Microbiol* **56**: 457-487.

155. Pruesse E, Quast C, Knittel K, Fuchs B, Ludwig W, Peplies J & Glöckner FO (2007) SILVA: a comprehensive online resource for quality checked and aligned ribosomal RNA sequence data compatible with ARB. *Nucleic Acids Res* **35**: 7188-7196.

156. Hugenholtz P, Pitulle C, Hershberger KL & Pace NR (1998) Novel Division Level Bacterial Diversity in a Yellowstone Hot Spring. *J Bacteriol* **180**: 366-376.

157. Rheims H, Rainey FA & Stackebrandt E (1996) A molecular approach to search for diversity among bacteria in the environment. *J Ind Microbiol Biotechnol* **17**: 159-169.

158. Boumann HA, Hopmans EC, Van De Leemput I*, et al.* (2006) Ladderane phospholipids in anammox bacteria comprise phosphocholine and phosphoethanolamine headgroups. *FEMS Microbiol Lett* **258**: 297-304.

159. Rattray J, van de Vossenberg J, Hopmans E*, et al.* (2008) Ladderane lipid distribution in four genera of anammox bacteria. *Arch Microbiol* **190**: 51-66.

160. Oren A (2002) Taxonomy of Halophilic Microorganisms: *Archaea*, *Bacteria*, and *Eucarya*. *Halophilic Microorganisms and their Environments,* Vol. 5. pp. 23-68. Springer Netherlands.

161. Oren A, Arahal DR & Ventosa A (2009) Emended descriptions of genera of the family *Halobacteriaceae*. *Int J Syst Evol Microbiol* **59**: 637-642.

162. Thauer RK, Kaster A-K, Seedorf H, Buckel W & Hedderich R (2008) Methanogenic archaea: ecologically relevant differences in energy conservation. *Nat Rev Micro* **6**: 579-591.

163. Hallmann C, Schwark L & Grice K (2008) Community dynamics of anaerobic bacteria in deep petroleum reservoirs. *Nature Geosci* **1**: 588 - 591.

164. Harayama S, Kishira H, Kasai Y & Shutsubo K (1999) Petroleum Biodegradation in Marine Environments. *J Mol Microbiol Biotechnol* **1**: 63-70.

165. Kniemeyer O & Heider J (2001) Ethylbenzene Dehydrogenase, a Novel Hydrocarbon-oxidizing Molybdenum/Iron-Sulfur/Heme Enzyme. *J Biol Chem* **276**: 21381-21386.

166. Heylen K, Gevers D, Vanparys B, Wittebolle L, Geets J, Boon N & De Vos P (2006) The incidence of nirS and nirK and their genetic heterogeneity in cultivated denitrifiers. *Environ Microbiol* **8**: 2012-2021.

167. Tiquia SM, Masson SA & Devol A (2006) Vertical distribution of nitrite reductase genes (nir S) in continental margin sediments of the Gulf of Mexico. *FEMS Microbiol Ecol* **58**: 464-475.

168. Fujinaga K, Taniguchi Y, Sun Y, Katayama S, Minami J, Matsushita O & Okabe A (1999) Analysis of genes involved in nitrate reduction in Clostridium perfringens. *Microbiology* **145**: 3377-3387.

169. Miroshnichenko ML, Kostrikina NA, Chernyh NA*, et al.* (2003) *Caldithrix abyssi* gen. nov., sp. nov., a nitrate-reducing, thermophilic, anaerobic bacterium isolated from a Mid-Atlantic Ridge hydrothermal vent, represents a novel bacterial lineage. *Int J Syst Evol Microbiol* **53**: 323-329.

170. Jones CM, Stres B, Rosenquist M & Hallin S (2008) Phylogenetic Analysis of Nitrite, Nitric Oxide, and Nitrous Oxide Respiratory Enzymes Reveal a Complex Evolutionary History for Denitrification. *Mol Biol Evol* **25**: 1955-1966.

171. Flores E & Herrero A (2005) Nitrogen assimilation and nitrogen control in cyanobacteria. *Biochem Soc Trans* **33**: 164-167.

172. Mahaffey C, Michaels AF & Capone DG (2005) The conundrum of marine N_2 fixation. *Am J Sci* **305**: 546-595.

173. Mohr W, Großkopf T, Wallace DWR & LaRoche J (2010) Methodological Underestimation of Oceanic Nitrogen Fixation Rates. *PLoS ONE* **5**: e12583.

174. Beijerinck MW (1901) Über oligonitrophile Mikroben. *Centralblatt für Bakteriologie, Parasitenkunde, Infektionskrankheiten und Hygiene, Abteilung II* **7**: 561-582.

175. Benecke W & Keutner J (1903) Über stickstoffbindende Bakterien aus der Ostsee. *Berichte der Deutschen Botanischen Gesellschaft* **21**: 333-346.

176.   Postgate JR (1998) *Nitrogen Fixation*. Cambridge University Press, Cambridge.

177.   Mehta MP, Huber JA & Baross JA (2005) Incidence of novel and potentially archaeal nitro-genase genes in the deep Northeast Pacific Ocean. *Environ Microbiol* **7**: 1525-1534.

178.   Mehta MP, Butterfield DA & Baross JA (2003) Phylogenetic Diversity of Nitrogenase (*nifH*) Genes in Deep-Sea and Hydrothermal Vent Environments of the Juan de Fuca Ridge. *Appl Environ Microbiol* **69**: 960-970.

179.   Meyerdierks A, Kube M, Kostadinov I, Teeling H, Glöckner FO, Reinhardt R & Amann R (2010) Metagenome and mRNA expression analyses of anaerobic methanotrophic archaea of the ANME-1 group. *Environ Microbiol* **12**: 422-439.

180.   Pernthaler A, Dekas AE, Brown CT, Goffredi SK, Embaye T & Orphan VJ (2008) Diverse syn-trophic partnerships from deep-sea methane vents revealed by direct cell capture and me-tagenomics. *Proc Natl Acad Sci U S A* **105**: 7052-7057.

181.   Dekas AE, Poretsky RS & Orphan VJ (2009) Deep-Sea Archaea Fix and Share Nitrogen in Methane-Consuming Microbial Consortia. *Science* **326**: 422-426.

182.   Orphan VJ, Turk KA, Green AM & House CH (2009) Patterns of ^{15}N assimilation and growth of methanotrophic ANME-2 archaea and sulfate-reducing bacteria within structured syntrophic consortia revealed by FISH-SIMS. *Environ Microbiol* **11**: 1777-1791.

183.   Hungate RE (1969) A roll tube method for cultivation of strict anaerobes. *Methods Microbiol,* Vol. 3B (Norris R & Ribbons DW, eds.), pp. 117-132. Academic Press Inc.

184.   Amann R, Ludwig W & Schleifer K-H (1995) Phylogenetic Identification and In Situ Detection of Individual Microbial Cells without Cultivation. *Microbiol Rev* **59**: 143-169.

185.   Liu W-T, Marsh TL, Cheng H & Forney LJ (1997) Characterization of Microbial Diversity by Determining Terminal Restriction Fragment Length Polymorphisms of Genes Encoding 16S rRNA. *Appl Environ Microbiol* **63**: 6452–6456.

186.   Jehmlich N, Schmidt F, von Bergen M, Richnow HH & Vogt C (2008) Protein-based stable isotope probing (Protein-SIP) reveals active species within anoxic mixed cultures. *ISME J* **2**: 1122-1133.

187.   Musat N, Halm H, Winterholler B*, et al.* (2008) A single-cell view on the ecophysiology of an-aerobic phototrophic bacteria. *Proc Natl Acad Sci U S A* **105**: 17861-17866.

188.   Neufeld JD, Vohra J, Dumont MG, Lueders T, Manefield M, Friedrich MW & Murrell JC (2007) DNA stable-isotope probing. *Nat. Protocols* **2**: 860-866.

189.   Wegener G, Niemann H, Elvert M, Hinrichs K-U & Boetius A (2008) Assimilation of methane and inorganic carbon by microbial communities mediating the anaerobic oxidation of methane. *Environ Microbiol* **10**: 2287-2298.

Chapter 2

Results and discussion

2. Results and discussion

This chapter summarises the results of this work (Chapters 3-4). It is a brief discussion and it sometimes adds results and new aspects which were out of focus in Chapters 3-4.

This work links methanogenic hydrocarbon degradation as a possible process in the deep subsurface to successive AOM at the seafloor. By using culturing and SIP techniques, it demonstrates that methanogenic hydrocarbon degradation can be stimulated and how released methane affects the benthos.

2.1. Methanogenic hydrocarbon degradation (Chapter 3)

Figure 8: Hydrocarbon contaminated sludge in the sea port of Zeebrugge at low tide.

Microbial communities are able to cleave complex hydrocarbons under anaerobic conditions to methane (Chapter 3; [1-3]). Factors to stimulate hydrocarbon dependent methanogenesis were investigated. Anaerobic hydrocarbon degradation can be stimulated by the addition of inexpensive electron acceptors like trivalent iron [4, 5], manganese dioxide [6], nitrate [7] and sulfate [4, 8] thus providing an increased supply of substrates to methanogens. Consequently, the effect of these four different electron acceptors on methanogenesis was examined. Two aliphatic hydrocarbons (butane and hexadecane) and two aromatic hydrocarbons (ethylbenzene and naphthalene) were employed as model substrates of microcosms obtained from three different locations. Two contaminated sites (Zeebrugge, Belgium and Gölzau-Weißandt, Germany) and one pristine location (Eckernförde Bay) were investigated (the Zeebrugge site in *Figure 8*).

2.1.1. Acceleration of hydrocarbon dependent methanogenesis by electron acceptor addition
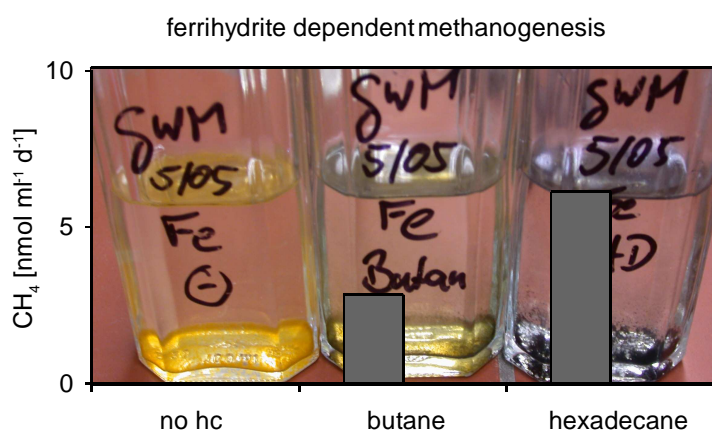
Figure 9: Hydrocarbon dependent methanogenesis in microcosms obtained from a contaminated aquifer in Weißandt-Gölzau (Germany). Note that trivalent ferrihydrite changes its colour to green and black, presumably caused by iron and/or sulfate reducing microorganisms. At the same time, rates of methanogenesis increase depending on the type of added hydrocarbon. When no electron acceptor or 20 mM sulfate were added methanogenesis was not observed. no hc = no hydrocarbon added

Ferrihydrite had a stimulating effect on hydrocarbon dependent methanogenesis in case of butane (*Figure 9*) and hexadecane compared with sulfate (Chapter 3). Manganese dioxide was neither stimulating nor inhibiting hydrocarbon dependent methanogenesis from hexadecane, and ethylbenzene. Butane and naphthalene degradation were not investigated with manganese dioxide as electron acceptor. Nitrate was inhibitory in case of hexadecane and ethylbenzene but not naphthalene. However, the concentration of nitrate was important when hexadecane was converted to methane. More than 1 mM nitrate inhibited hexadecane-dependent methanogenesis. The addition of 1 mM of 2 mM sulfate counter-acted the nitrate induced inhibition of hexadecane-dependent methanogenesis in microcosms from a pristine environment. In general, hexadecane-dependent methanogenesis was correlated to sulfate concentrations in the microcosms. While 2 mM sulfate hat a stimulating effect on hexadecane-dependent methanogenesis compared to microcosms without sulfate, concentrations higher than 5 mM sulfate were inhibitory.

Apparently, when an aliphatic hydrocarbon is converted to methane, electron acceptor addition can accelerate this process. This is of potential relevance for MEOR and bioremediation. In case methane is the desired terminal product of hydrocarbon degradation, the addition of ferrihydrite seems to be a viable option. Bivalent iron can be applied as siderite ($FeCO_3$) to re-injected production water in oilfields in order to scavenge hydrogen sulfide [9, 10]. Hence, applying ferrihydrite may be an option when alkanes are to be converted to methane.

On the other hand, methane's radiative efficiency is 23 times higher compared with CO_2 [11]. Therefore, methane, as a degradation product of higher hydrocarbons, may not be desired.

In this case (e.g. bioremediation) the addition of nitrate would inhibit the formation of sulfide [10, 12] as well as methane (Chapter 3).

2.1.2. Methanogenic naphthalene degradation

Naphthalene was converted to methane and CO_2 in microcosms of contaminated harbour mud of Zeebrugge. Degradation of naphthalene to methane was investigated previously [13, 14] but this is the first time that satisfactory evidence for the conversion of a PAH to methane is presented (Chapter 3).

The evolution of naphthalene derived methane was delayed compared with CO_2 while hexadecane and ethylbenzene induced the release of both gases at the same time. One reason for this discrepancy could be the utilisation of different intermediates, like acetate or carbonate, for methanogenesis. For example, when acetate was the primary methanogenic substrate produced by hexadecane or ethylbenzene degradation but not naphthalene degradation, then a delay seems possible. This might be because in substrate competition for hydrogen, lithotrophs dominated over carbonate reducing methanogens. Possibly, acetate was better available to methanogens compared with carbonate and hydrogen. In conclusion, hexadecane or ethylbenzene degradation products could have been better available to methanogens because they were possibly able to degrade these hydrocarbons themselves and never released the potential intermediate acetate. However, this remains speculative although acetate was shown to be the major intermediate in hydrocarbon dependent methanogenesis (Chapter 3; [15-17]. A pure methanogenic strain capable of hydrocarbon degradation was not isolated so far.

Another reason could be that naphthalene was merely detoxified by members of the Zeebrugge community and not used as carbon or energy source. If this was the case in the hydrocarbon contaminated harbour mud of Zeebrugge seems unlikely because contamination with PAHs was reported previously [18]. Consequently the microbial community was presumably adapted to PAHs.

2.1.3. Carbon and hydrogen isotope fractionation during methanogenic hydrocarbon degradation

Isotope fractionation was often observed in biotic and abiotic substrate turnover and can be employed to assess progressing decontamination of polluted sites [19, 20]. Knowledge about isotope enrichment factors, i.e. isotopic discrimination between substrate and product, is required for such assessments. So far, nothing was known about isotopic enrichment or depletion of methanogenic hydrocarbon degradation. In a contaminated aquifer of Weißandt-

Gölzau (Germany), a depletion of ^{13}C in methane was observed along with an enrichment of ^{13}C in CO_2 (Chapter 3). While this pattern is consistent with other sites of this study, it shows that CO_2 is used as methanogenic substrate besides acetate (Chapter 3; [2, 15, 17]).

2.1.4. Methanogenic hydrocarbon degradation and anaerobic methanotrophy

Methane laden sediments are usually inhabited by methanotrophic microorganisms [21, 22]. In sediments, however, oxygen is often depleted and AOM prevails. Methanogenic activity as well as *mcrA* genes were observed in Zeebrugge sediments. Hence, it is not surprising that these sediments hosted AOM performing microorganisms of the ANME-1 and -2 clades (Chapter 3). Additionally, AOM activity was observed in Zeebrugge sediment microcosms under iron, manganese, nitrate and sulfate reducing conditions. This is in good agreement with AOM studies which previously reported such activities at other sites [21, 23, 24].

Possibly, AOM removed some of the produced methane, as the increase of the AOM community in hexadecane amended microcosms indicated (Chapter 3). However, Thauer and Shima [25] calculated a specific AOM rate of 10 nmol methane min^{-1} g^{-1} (dry weight) at a methane partial pressure of 1.4×10^6 Pa. After 178 days of incubation, the concentration of methane in ferrihydrite/hexadecane cultures was 3.5% at atmospheric pressure. Assuming a decline of the AOM rate depending on methane partial pressure (slope = 1), the theoretical AOM oxidation rate in ferrihydrite/hexadecane microcosms was 14 nmol methane cm^{-3} d^{-1}. In other words, theoretically, no more than 12% methane was lost to AOM.

The observed methane consumption rates for incubations with metal or sulfate were similar. Since ferrihydrite or manganese dioxide can be reduced abiotically by sulfide, it is difficult to make a distinction. The community, however, shared some features with the one described in a recent study about AOM coupled to metal reduction (Chapter 3; [23]). Furthermore, substrate competition for sulfate between methane and higher hydrocarbon oxidisers has to be taken into account. Possibly, besides removing methane produced by the hydrocarbon degrading community, AOM also slowed down hydrocarbon oxidation by scavenging sulfate and thus choking the initial hydrocarbon attack. One the other hand, experiments employing different sulfate concentrations demonstrated the reciprocal correlation of fast AOM at higher sulfate concentrations and corresponding slow hydrocarbon dependent methanogenesis (Chapter 3). This suggests that sulfate limitation was more important for the AOM community than for the hydrocarbon degrading community. Apparently, AOM did not out-compete hydrocarbon degraders for sulfate reduction.

2.2.   AOM communities at a novel methane seep off Sumatra (Chapter 4)

Geological hydrocarbon reservoirs are often formed in foreland basins [3, 26]. A primary example for a foreland basin is the Sunda Arc (Sunda forearc). It is flanked in the North-West by the Sumatra island and in the South-East by the Sunda islands [27]. As a consequence of tectonic activity, cracks in the sediment give rise to petroleum fluids and natural gas (methane). On their passage to the sediment surface, temperature decreases and nutrients become available. As a result of microbial activity hydrocarbons are bio-degraded to methane [3, 28]. Ultimately, methane escapes into the water column. These so-called methane seeps supply the benthos with organic carbon [29-34].
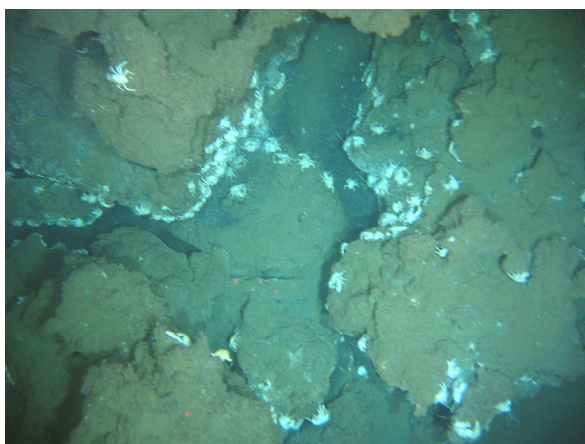
Figure 10: White crabs populated carbonate rocks in the centre of the seep area.

A typical seep community, comprising ANME-1 and -2 *Archaea*, sulfate reducers, potential sulfide oxidisers, potential heterotrophs and marine *Crenarchaeota* as well as crabs (*Figure 10*), bivalves and tubeworms was discovered at a natural methane seep in the basin between the islands Sumatra and Simeulue (Chapter 4). This is the first report of a natural marine methane seep in the Indian Ocean. The discovered community was driven by methane as carbon and energy source. Evidence for this finding were carbon isotopic signatures, indicating ^{13}C depletion *in situ* and microcosm experiments showing AOM activity *in vitro*. In labelling experiments, ^{13}C-labelled methane was converted to $^{13}CO_2$. Moreover, hexadecane and ethylbenzene were used as model substrates to demonstrate their conversion to methane. Indeed, sediment microcosms exhibiting sustained hydrocarbon dependent methanogensis were obtained in subcultures.

2.3. Linking methane oxidation to the nitrogen and sulfur cycles in microbial mats of the Black Sea (Chapter 4)
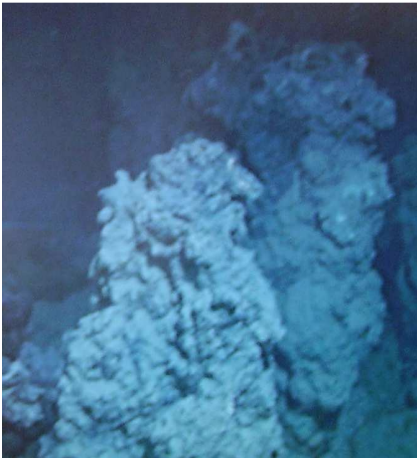
Figure 11: Anaerobic methane oxidising mats in the Black Sea at approximately 230 m water depth (GHOSTDABS site)

When methane breaches into the sediment surface, electron acceptors like oxygen, sulfate or nitrate become available at the sediment surface and in the water column. Electron transport processes from methane to these electron acceptors result in an increased energy yield which fuels a sometimes rich microbial community [33, 35, 36]. However, in the stratified Black Sea water column a steep decrease of electron acceptors other than sulfate was reported below 70-100 m in cyclonic gyres (western and eastern) or below 120-200 m in peripheral areas [37]. On the other hand, spatial and temporal variations in nitrate-phosphate ratios were observed in north-western shelf regions during the last two decades [38]. Hence, it seems possible that the mats experienced different redox states in their natural environment over geological time. Methanotrophic mats inhabit the larger Black Sea area at least since the Eocene and their concretions near the Bulgarian coast are the most prominent example for methanotrophy as an ancient lifestyle (*Figure 12*; [39, 40]). This and the finding of the nitrate reducing genus *Caldithrix* [41] in anaerobic methanotrophic mats of the Black Sea (*Figure 11*; [35]) are indicators for a possible coupling of anaerobic methane oxidation to nitrate reduction. Moreover, *nif* genes in these mats [42] presumably enable the microbial community of diazotrophic nitrogen assimilation.

Figure 12: Concretions of methanotrophic mats near Varna, Bulgaria. Foto: Eva De Boever

2.3.1. The nitrogen cycle in the Black Sea mats

In ^{15}N isotope tracing experiments, diazotrophy, denitrification and DNRA were discovered in the anaerobic mathenotrophic mats (Chapter 4). Additionally, all these processes were dependent on AOM coupled to sulfate reduction. Therefore, this is evidence for an indirect coupling of AOM to nitrate reduction which occurred in significantly higher rates when sulfate was added. Possibly, AOM coupled nitrate reduction is rather dependent on sulfate reduction as suggested by Bowles and Joye [43] than on dismutation of NO [44].

An incorporation of the three nitrogen species nitrate, dinitrogen and ammonium into the mat's biomass was observed. Also, this biomass incorporation was dependent on AOM. Assimilation of nitrogen was tracked into proteins as well. Nitrogen from ammonium and nitrate was incorporated into MCR proteins in unexpected low rates. Dinitrogen incorporation into proteins was not observed, indicating that diazotrophy was rather unimportant for the nitrogen cycle of the mats. This is surprising because other studies demonstrated high dinitrogen incorporation into AOM consortia of Eel River basin [45, 46].

2.3.2. Carbon turnover in the Black Sea mats

The microbial community composition of the Black Sea mats [35] reflected the anaerobic lifestyle adapted to methane. Consequently, *Archaea* comprised mainly ANME-1 and ANME-2 clades (Chapter 4) while the bacterial diversity was higher. Besides the nitrate reducer *Caldithrix* [47], δ- and γ-*Proteobacteria* were discovered in the pink and black mats [41]. Members of *Clostridia* and *Bacteroidetes* were discovered as well, reflecting the anaerobic lifestyle of the indigenous community. Additionally, pink and black mats incorporated ^{13}C-labelled methane in experiments, demonstrating the use of methane as carbon source (data not shown).

[13]C-labelled substrates were used to trace the fate of carbon in pink and black mats in a similar fashion compared to the nitrogen labelling experiments (Chapter 4). To elucidate the variability of methanogenesis rates, two experiments were conducted. The concentrations of ^{13}C-substrates were 3 mM acetate, 6 mM carbonate (+100%$_{v/v}$ H$_2$ and 31 mM ^{12}C-carbonate) and 4 mM methanol in both experiments. Rates were normalised vs. 10%$_{w/v}$ formaldehyde killed controls. In experiment 2 (*Figure 13B-D*), H$_2$ was not added in ^{13}C-carbonate microcosms.

[13]C-labelled methane was detected in incubations of black and pink mats when ^{13}C-labelled acetate, carbonate and methanol were added (*Figure 13*). However, methane formation was missing in pink mats incubated under acetoclastic conditions with methane in the headspace (*Figure 13*A). To investigate the acetoclastic nature of methanogenesis in the mats, CH$_3$F was used as specific inhibitor in acetate incubations [48]. In black mats, methanogenesis,

methanotrophy and sulfate reduction were inhibited by CH$_3$F in the presence of acetate (*Figure 13B*). In contrast, methyl fluoride inhibited methanogenesis and methanotrophy in pink mats, but not sulfate reduction (*Figure 13C* and *D*). Conclusively, it seems possible that pink and also black mats depend on acetate when assimilating methane derived carbon or perform methanotrophy as reverse acetoclastic methanogenesis. In summary, acetate seems to play a significant role in the complex mat ecosystem. The highest rates of methanogenesis were observed when methanol was added (*Figure 13A* and *B*). This is not surprising because methanol serves as substrate in all methanogenic pathways directly preceding the next reduction state methane.

Notably, there is more methane synthesised in incubations with 100% methane atmosphere under hydrogenotrophic conditions in pink and black mats (*Figure 13A*). Moreover, the methanogenic rates were higher with methane in the headspace in pink mats with methanol as substrate. Apparently, methane induced methanogenesis possibly because it activated the AOM performing parts of the community. Since different types of MCR enzymes are responsible for methanogenesis and methanotrophy within the same community [49-51], triggering activity of this community may be a possible explanation.

In carbonate set-ups, the methanogenesis rates were the same for pink and black mats when H$_2$ was absent (*Figure 13B*). Compared to acetate incubations without CH$_3$F inhibition, no significant change of methane formation rates was observed in this case. Taking the possible acetate dependence into account, carbonate could be assimilated to form acetate by homoacetogens. This is plausible because CO$_2$ fixation was shown to be the major route of carbon uptake in the Black Sea mats [52]. The higher abundance of *Clostridia* (homoacetogens are *Clostridia*) in pink mats than in black mats supports this hypothesis [41]. Hence, the pink mats may be prone to CH$_3$F inhibition rather than the black mats when acetate formed by acetogenesis is the methanogenic substrate. Testing the medium for labelled acetate in carbonate incubations, with simultaneous inhibition of methanogenesis to allow accumulation of intermediates, will clarify this hypothesis. On the other hand, CH$_3$F inhibited AOM dependent sulfate reduction in the black mats to the level of sulfate reduction of the pink mats (*Figure 13D*). Since sulfate reduction mostly occurs in black mats, CH$_3$F is possibly toxic to sulfate reducers in addition to methanogens. However, this effect was not investigated so far.
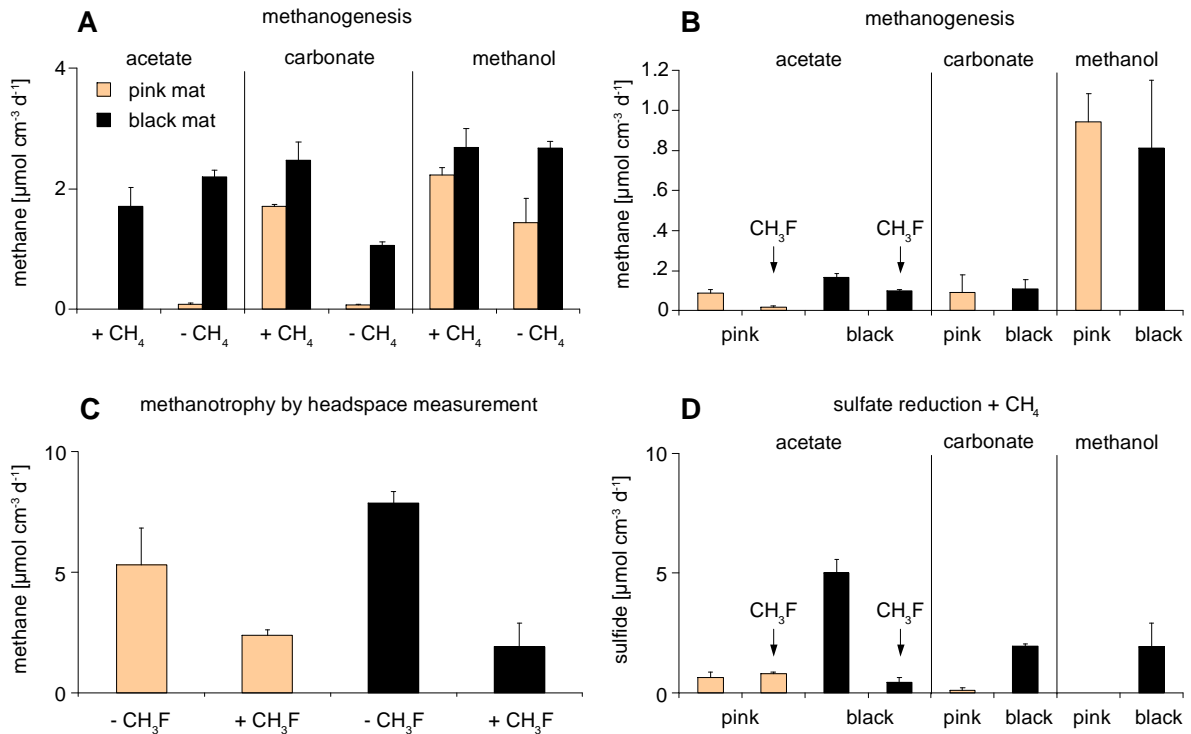
*Figure 13: Comparison of methanogenesis and AOM in ^{13}C-labelling experiments. (**A**) <u>Experiment 1:</u> ^{13}C-methane evolution in presence of methane in the headspace (+ CH$_4$) and the release of methane measured by GC-FID when no additional methane was present (- CH$_4$). Note that the rates of methanogenesis are higher from pink mats when carbonate or methanol were the substrates. (**B-D**) <u>Experiment 2</u>: (**B**) Methanogenesis rates were determined when no methane was added. CH$_3$F was added as specific inhibitor for acetoclastic methanogenesis (1%$_{v/v}$) to acetate containing microcosms. (**C**) The impact of CH$_3$F on methanotrophy, as measured by headspace measurements. (**D**) Sulfate reduction with methane in the headspace (AOM coupled sulfate reduction) and ^{13}C-labelled substrates acetate, carbonate and methanol. For acetate, the inhibitory effect of CH$_3$F on AOM coupled sulfate reduction was examined as well.*

Methanol rapidly induced methanogenesis in pink and black mats with little difference (*Figure 13A* and *B*). Whether methanol is utilised for methanogenesis rather than for biomass production will be shown in future biomass and lipid analyses. Sulfate reduction rates were not affected by methanol, which confirms the hypothesis that methanol is not an electron shuttle from methanotrophs to sulfate reducers.

2.4. The Troll field – novel ANME-2 dominated microbial mats in the Black Sea (Chapter 4)
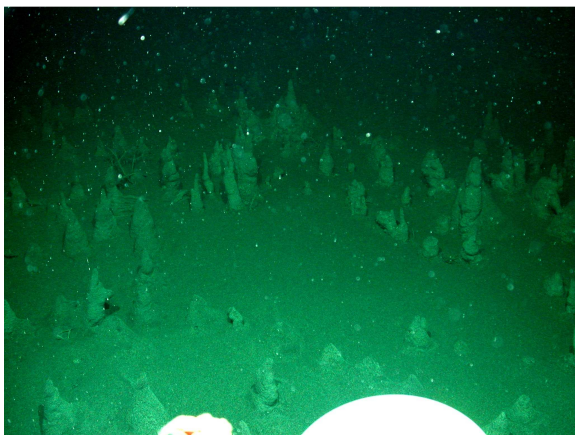
Figure 14: Novel microbial build-ups in the Black Sea at 720 m water depth, near the methane hydrate formation zone. The mats erect approx. 20 cm from the sediment into the water column. This Photo is copyright and shown with permission of the marum institute in Bremen, Germany. Picture was taken using the submersible Quest on the R/V Meteor cruise M72-1.

Novel AOM performing microbial mats were discovered near the methane hydrate formation zone of the Black Sea, at 720 m water depth (*Figure 14* and Chapter 4). Their appearance was different compared to the one of the so-called GHOSTDABS mats at 230 m [35]. Surprisingly, the community composition of the Trolls and their AOM turnover rates resembled those of the previously reported mats. The archaeal population was exclusively dominated by ANME-2 while the bacterial population was more diverse. Barophilic incubations of mat material demonstrated a better pressure adaptation compared to the mats of 230 m water depth. This discovery indicates that AOM performing microbial communities are in principle able to form mats in the proximity of solid methane hydrate.

2.5. Carbon isotope fractionation during aerobic methane oxidation (Chapter 4)

Isotope fractionation experiments were carried out to obtain fractionation factors for ^{2}H and ^{13}C fractionation during aerobic methane oxidation (Chapter 4). Isotope fractionation factors may provide a tool distinguish different (bio-) chemical reaction pathways. The reason is that different bond energies differ depending on the element and the kind of chemical bond (σ- or π-bond). Hence, incubation experiments were conducted to measure isotope fractionation factors of pMMO and sMMO enzymes in living pure cultures. The experiments could demonstrate that the use of fractionation factors

(I)   can not predict whether or not pMMO or sMMO were responsible for methane oxidation

(II)   possibly can not predict whether or not AOM or aerobic methane oxidation were the biological processes

(III)   can distinguish between biological or chemical methane oxidation.

While a recent study reported fraction factors for AOM similar to those of aerobic methane oxidation, the authors did not take intrinsic methanogenesis into account [53]. Therefore, natural methanogenesis of the investigated systems (e.g. AOM performing mats of the Black Sea) might have obscured the real carbon isotope fractionation during AOM. Further studies by either inhibiting intrinsic methanogensis or by examining pure AOM performing strains may provide hints whether methanogenesis affects the detected AOM isotope effects.

2.5. Conclusions

Due to worldwide increasing energy demand, new energy resources are required. Methane has the potential to satisfy the need for energy in industrialised nations. Since its oxidation products are only water and CO_2, it can be considered as a clean burning fuel. Moreover, methane can be obtained by the microbial cleavage of higher hydrocarbons ("microbial cracking"). As a gaseous compound it could easily escape from abandoned oilfields to be recovered as natural gas. This work demonstrates how this process can be stimulated by adding inexpensive electron acceptors. While some electron acceptors can stimulate hydrocarbon dependent methanogensis, others – like nitrate – could inhibit methanogensis. Inhibition of methanogensis could be desired in bioremediation of hydrocarbon contaminated sites. The reason is the 23 times higher radiative efficiency which makes methane a much more potent greenhouse gas than CO_2.

When hydrocarbons are converted to methane, stable isotope fractionation of hydrogen and carbon occurs. To distinguish abiotic from biotic methane release in petroleum reservoirs or contaminated sites, isotopic patterns are required. For the first time, this work systematically analyses such isotopic fingerprints of methane and CO_2. These isotopic fingerprints are suggestive of CO_2 reduction besides actetoclastic methanogenesis. However, the observed isotopic fingerprints of methane are not clear and further studies will show if they can be used to distinguish abiotic from biotic methane in hydrocarbon reservoirs.

As methane – may it be of biotic or abiotic origin – rises from a hydrocarbon reservoir, it becomes available for methane oxidising microbial consortia. These consortia oxidise methane anaerobically or – when oxygen is available – aerobically. This research presents for the first time anaerobic methane oxidising microbial communities in the Indian Ocean. The microbial community was typical compared to other communities at marine methane seeps and fuels a vital benthos in the Sumatra forearc basin. Methane oxidation was coupled to sulfate reduction but indications for alternative electron acceptors were found.

A relevant alternative electron acceptor may nitrate. To elucidate the role of nitrate in particular and other nitrogen sources in general, a well studied AOM system of the Black Sea was

examined. Here, data are presented to demonstrate that nitrate was reduced by sulfide, the reaction product of AOM coupled sulfate reduction. Moreover, incorporation of nitrate, ammonium and dinitrogen was largely dependent on methane supply. The incorporation of nitrogen sources indicated growth and consequently protein biosynthesis of the Black Sea mats. Additionally, nitrogen incorporation into a specific enzyme – the MCR – was demonstrated by using a novel and inexpensive experimental setup. The *de novo* synthesis of this enzyme was relatively slow, indicating a long life time in the anaerobic mats of the Black Sea.

After methane escapes from the sediment, it may be oxidised aerobically at the sediment-water interface or in the water column. To distinguish aerobic from anaerobic methane oxidation, isotopic signatures of methane and CO_2 could be a useful tool. However, this work demonstrates, that isotopic signatures during aerobic and anaerobic microbial methane oxidation are too similar to make a distinction. Nevertheless, it provides useful clues to distinguish abiotic from biotic aerobic methane oxidation.

In summary, this work demonstrates that a stimulation of hydrocarbon dependent methanogensis in deep subsurface hydrocarbon reservoirs or contaminated sites affects benthic communities and the associated element cycles.

2.6.   Summary of publications and author contributions

Chapter 3

3.1.   Accelerated methanogenesis from aliphatic and aromatic hydrocarbons under iron and sulfate reducing conditions

Michael Siegert, Danuta Cichocka, Steffi Herrmann, Friederike Gründger, Stefan Feisthauer, Hans-Hermann Richnow, Dirk Springael, Martin Krüger

FEMS Microbiology Letters 315 (2011) 6–16

Author contributions: **M. Siegert** designed the experimental set-up, conducted the experiments except the naphthalene experiment as well as parts of the cloning and wrote the manuscript. D. Chichocka and S. Herrmann conducted the naphthalene experiment. S. Herrmann, S. Feisthauer contributed to the preparation of the manuscript. S. Feisthauer contributed data to an early version of the manuscript. F. Gründger contributed to the preparation of the clone libraries. H.-H. Richnow and D. Springael contributed to the design of the naphthalene experiment and the manuscript. M. Krüger contributed Eckernförde data and reviewed the manuscript.

3.2. Isotopic Fingerprinting of Methane and CO₂ Formation from Aliphatic and Aromatic Hydrocarbons

Stefan Feisthauer, Michael Siegert, Martin Seidel, Hans Hermann Richnow, Karsten Zengler, Friederike Gründger, Martin Krüger

Organic Geochemistry 41 (2010) 482–490

Author contributions: S. Feisthauer prepared the manuscript and was in charge of the field sampling and isotope measurements of the field samples. M. Seidel performed the isotope measurements. K. Zengler and M. Krüger performed the enrichment cultures and contributed to the preparation of the manuscript. **M. Siegert** and H.H. Richnow contributed to data interpretation and manuscript preparation. H.-H. Richnow reviewed the manuscript.

Chapter 4

4.1. Anaerobic oxidation of methane dominates hydrocarbon degradation at a marine methane seep in a forearc basin off Sumatra, Indian Ocean

Michael Siegert, Martin Krüger, Barbara M.A. Teichert, Michael Wiedicke, Axel Schippers

Manuscript in preparation

Author contributions: **M. Siegert** carried out the incubation and molecular experiments except the cell counts and wrote the manuscript. M. Krüger and A. Schippers planned the incubation and molecular experiments and reviewed the manuscript. B. Teichert and A. Schippers conducted the geochemical analyses and M. Wiedicke was the chief scientist on the cruise and responsible for the preparation of maps.

4.2. Linking carbon, sulfur and nitrogen cycles in anaerobic methanotrophic mats of a marine cold vent in the Black Sea by stable isotope probing

Michael Siegert, Martin Taubert, Felipe Bastida, Mirko Basen, Martin von Bergen, Matthias Gehre, Hans-Hermann Richnow, Jana Seifert, Martin Krüger

Manuscript in preparation

Author contributions: **M. Siegert** designed and conducted the N-cycle experiments, analyses (incubation, protein extraction, isotope analyses) and wrote the manuscript. H.-H. Richnow and M. Krüger planned the protein-SIP experiments. M. Taubert and F. Bastida conducted the protein-SIP experiments. F. Bastida, J. Seifert and M. von Bergen contributed to the

preparation of the manuscript. M. Basen established the protein extraction and M. Krüger reviewed the manuscript.

4.3.   The Trolls – novel anaerobic methanotrophic microbial mats near the methane gas hydrate stability zone of the Black Sea

Richard Seifert, Michael Siegert, Martin Blumenberg, Birte Oppermann, Michael Friedrich, Martin Krüger

Manuscript in preparation

Author contributions: **M. Siegert** conducted the incubation and molecular experiments, selected the samples aboard and wrote the respective parts of the manuscript. R. Seifert discovered the Troll field as chief scientist on cruise M72-1 and reviewed the manuscript. M. Krüger designed the incubation and molecular experiments, wrote parts of the manuscript and reviewed it. B. Oppermann and M. Blumenberg conducted the lipid analyses and M. Blumenberg wrote the respective part of the manuscript.

4.4.   Different types of methane monooxygenases produce similar carbon and hydrogen isotope fractionation patterns during methane oxidation

Stefan Feisthauer, Carsten Vogt, Jakub Modrzynski, Maurycy Szlenkier, Martin Krüger,   Michael Siegert, Hans-Hermann Richnow

Geochimica et Cosmochimica Acta, 75 (2011), 1173-1184

Author contributions: J. Modrzynski and M. Szlenkier performed the cultivation experiments and the isotope measurements under the supervision of S. Feisthauer. S. Feisthauer prepared the manuscript. **M. Siegert**, M. Krüger, C. Vogt and H.-H. Richnow contributed to interpretation and manuscript preparation.

2.7.   References

1. Gieg LM, Duncan KE & Suflita JM (2008) Bioenergy Production via Microbial Conversion of Residual Oil to Natural Gas. *Appl Environ Microbiol* **74**: 3022-3029.

2. Zengler K, Richnow HH, Rossello-Mora R, Michaelis W & Widdel F (1999) Methane formation from long-chain alkanes by anaerobic microorganisms. *Nature* **401**: 266-269.

3. Head IM, Jones DM & Larter SR (2003) Biological activity in the deep subsurface and the origin of heavy oil. *Nature* **426**: 344-352.

4. Coates JD, Anderson RT, Woodward JC, Phillips EJP & Lovley DR (1996) Anaerobic Hydrocarbon Degradation in Petroleum-Contaminated Harbor Sediments under Sulfate-Reducing and Artificially Imposed Iron-Reducing Conditions. *Environ Sci Technol* **30**: 2784-2789.

5. Lovley DR, Woodward JC & Chapelle FH (1996) Rapid Anaerobic Benzene Oxidation with a Variety of Chelated Fe(III) Forms. *Appl Environ Microbiol* **62**: 288-291.

6. Langenhoff AA, Brouwers-Ceiler DL, Engelberting JH, Quist JJ, Wolkenfelt JG, Zehnder AJ & Schraa G (1997) Microbial reduction of manganese coupled to toluene oxidation. *FEMS Microbiol Ecol* **22**: 119-127.

7. Powell SM, Ferguson SH, Snape I & Siciliano SD (2006) Fertilization Stimulates Anaerobic Fuel Degradation of Antarctic Soils by Denitrifying Microorganisms. *Environ Sci Technol* **40**: 2011-2017.

8. Coates JD, Anderson RT & Lovley DR (1996) Oxidation of Polycyclic Aromatic Hydrocarbons under Sulfate-Reducing Conditions. *Appl Environ Microbiol* **62**: 1099-1101.

9. Eden B, Laycock PJ & Fielder M (1993) *Oilfield Reservoir Souring.* HSE Books.

10. Vance I & Thrasher DR (2005) Reservoir souring: mechanisms and prevention. *Petroleum Microbiology,* (Ollivier B & Magot M, eds.), pp. 123-142. ASM Press, Washington, D.C.

11. International Panel on Climate Change (2007) IPCC Fourth Assessment Report: Climate Change 2007 (AR4). Vol. 1 (Solomon S, Qin D, Manning M*, et al.*, eds.), pp. 130-234. International Panel on Climate Change, Cambridge, New York.

12. Gittel A, Sorensen KB, Skovhus TL, Ingvorsen K & Schramm A (2009) Prokaryotic Community Structure and Sulfate Reducer Activity in Water from High-Temperature Oil Reservoirs with and without Nitrate Treatment. *Appl Environ Microbiol* **75**: 7086-7096.

13. Chang W, Um Y & Holoman TR (2006) Polycyclic aromatic hydrocarbon (PAH) degradation coupled to methanogenesis. *Biotechnol Lett* **28**: 425-430.

14. Sharak Genthner BR, Townsend GT, Lantz SE & Mueller JG (1997) Persistence of Polycyclic Aromatic Hydrocarbon Components of Creosote Under Anaerobic Enrichment Conditions. *Arch Environ Contam Toxicol* **32**: 99-105.

15. Dolfing J, Larter SR & Head IM (2007) Thermodynamic constraints on methanogenic crude oil biodegradation. *ISME J* **2**: 442-452.

16. Herrmann S, Kleinsteuber S, Chatzinotas A, Kuppardt S, Lueders T, Richnow HH & Vogt C (2010) Functional characterization of an anaerobic benzene-degrading enrichment culture by DNA stable isotope probing. *Environ Microbiol* **12**: 401-411.

17.   Krüger M, Beckmann S, Engelen B, Thielemann T, Cramer B, Schippers A & Cypionka H (2008) Microbial Methane Formation from Hard Coal and Timber in an Abandoned Coal Mine. *Geomicrobiol J* **25**: 315–321.

18.   Ministerie van de Vlaamse Gemeenschap AWK (2002) Uitvoeren van een waterbodemonder-zook in het Albert I dok, het Tijdok an toegang Visartsluis te Zeebrugge: bijkomende studie. (De Vos M & Bogaert G, eds.), pp. 12-19. ABO n.v., Gent.

19.   Elsner M, Zwank L, Hunkeler D & Schwarzenbach RP (2005) A New Concept Linking Observable Stable Isotope Fractionation to Transformation Pathways of Organic Pollutants. *Environ Sci Technol* **39**: 6896-6916.

20.   Meckenstock RU, Morasch B, Griebler C & Richnow HH (2004) Stable isotope fractionation analysis as a tool to monitor biodegradation in contaminated acquifers. *J Contam Hydrol* **75**: 215-255.

21.   Knittel K & Boetius A (2009) Anaerobic Oxidation of Methane: Progress with an Unknown Process. *Annu Rev Microbiol* **63**: 311-334.

22.   Lidstrom ME (2006) Aerobic Methylotrophic Prokaryotes. *The Prokaryotes,* Vol. 2 (Dworkin M, Falkow S, Rosenberg E, Schleifer K-H & Stackebrandt E, eds.), pp. 618-634. Springer Science+Business Media, New York.

23.   Beal EJ, House CH & Orphan VJ (2009) Manganese- and Iron-dependent marine methane oxidation. *Science* **325**: 184-187.

24.   Raghoebarsing AA, Arjan Pol A, van de Pas-Schoonen KT*, et al.* (2006) A microbial consortium couples anaerobic methane oxidation to denitrification. *Nature* **440**: 918-921.

25.   Thauer RK & Shima S (2008) Methane as Fuel for Anaerobic Microorganisms. *Ann N Y Acad Sci* **1125**: 158-170.

26.   Tissot BP & Welte HD (1984) *Petroleum Formation and Occurrence.* Springer-Verlag Berlin Heidelberg New York Tokyo.

27.   Izart A, Kemal BM & Malod JA (1994) Seismic stratigraphy and subsidence evolution of the northwest Sumatra fore-arc basin. *Mar Geol* **122**: 109-124.

28.   Jones DM, Head IM, Gray ND*, et al.* (2008) Crude-oil biodegradation via methanogenesis in subsurface petroleum reservoirs. *Nature* **451**: 176-180.

29.   Heijs SK, Sinninghe Damsté JS & Forney LJ (2005) Characterization of a deep-sea microbial mat from an active cold seep at the Milano mud volcano in the Eastern Mediterranean Sea. *FEMS Microbiol Ecol* **54**: 47-56.

30.   Inagaki F, Nunoura T, Nakagawa S*, et al.* (2006) Biogeographical distribution and diversity of microbes in methane hydrate-bearing deep marine sediments on the Pacific Ocean Margin. *Proc Natl Acad Sci U S A* **104**: 2815–2820.

31.   Knittel K, Lösekann T, Boetius A, Kort R & Amann R (2005) Diversity and Distribution of Methanotrophic Archaea at Cold Seeps. *Appl Environ Microbiol* **71**: 467–479.

32.   Niemann H, Elvert M, Hovland M*, et al.* (2005) Methane emission and consumption at a North Sea gas seep (Tommeliten area). *Biogeosciences* **2**: 335-351.

33.   Niemann H, Losekann T, de Beer D*, et al.* (2006) Novel microbial communities of the Haakon Mosby mud volcano and their role as a methane sink. *Nature* **443**: 854-858.

34. Childress JJ, Fisher CR, Brooks JM, Kennicutt MC, Bidigare R & Anderson AE (1986) A Methanotrophic Marine Molluscan (Bivalvia, Mytilidae) Symbiosis: Mussels Fueled by Gas. *Science* **233**: 1306-1308.

35. Michaelis W, Seifert R, Nauhaus K*, et al.* (2002) Microbial Reefs in the Black Sea Fueled by Anaerobic Oxidation of Methane. *Science* **297**: 1013-1015.

36. Redmond MC, Valentine DL & Sessions AL (2010) Identification of Novel Methane-, Ethane-, and Propane-Oxidizing Bacteria at Marine Hydrocarbon Seeps by Stable Isotope Probing. *Appl Environ Microbiol* **76**: 6412-6422.

37. Yakushev EV, Chasovnikov VK, Murray JW, Pakhomova SV, Podymov OI & Stunzhas PA (2008) Vertical Hydrochemical Structure of the Black Sea. *The Handbook of Environmental Chemistry: The Black Sea Environment: Part 5Q,* Vol. 5 (Kostianoy AG & Kosarev AN, eds.), Springer Verlag, Berlin, Heidelberg.

38. Yilmaz A, Çoban-Yildlz Y, Telli-Karakoç F & Bologa A (2006) Surface and mid-water sources of organic carbon by photoautotrophic and chemoautotrophic production in the Black Sea. *Deep Sea Research Part II: Topical Studies in Oceanography* **53**: 1988-2004.

39. De Boever E, Swennen R & Dimitrov L (2006) Lower Eocene carbonate cemented chimneys (Varna, NE Bulgaria): Formation mechanisms and the (a)biological mediation of chimney growth? *Sediment Geol* **185**: 159-173.

40. De Boever E, Swennen R & Dimitrov L (2006) Lower Eocene carbonate-cemented "chimney" structures (Varna, Bulgaria) -- Control of seepage rates on their formation and stable isotopic signature. *J Geochem Explor* **89**: 78-82.

41. Friedrich MW, Pommerenke B, Seifert R & Krüger M (2007) Unexpected Microbial Diversity in Anaerobically Methane-oxidizing Mats of the Black Sea. San Francisco.

42. Meyerdierks A, Kube M, Kostadinov I, Teeling H, Glöckner FO, Reinhardt R & Amann R (2010) Metagenome and mRNA expression analyses of anaerobic methanotrophic archaea of the ANME-1 group. *Environ Microbiol* **12**: 422-439.

43. Bowles M & Joye S (2010) High rates of denitrification and nitrate removal in cold seep sediments. *ISME J.*

44. Ettwig KF, Butler MK, Le Paslier D*, et al.* (2010) Nitrite-driven anaerobic methane oxidation by oxygenic bacteria. *Nature* **464**: 543-548.

45. Dekas AE, Poretsky RS & Orphan VJ (2009) Deep-Sea Archaea Fix and Share Nitrogen in Methane-Consuming Microbial Consortia. *Science* **326**: 422-426.

46. Orphan VJ, Turk KA, Green AM & House CH (2009) Patterns of ^{15}N assimilation and growth of methanotrophic ANME-2 archaea and sulfate-reducing bacteria within structured syntrophic consortia revealed by FISH-SIMS. *Environ Microbiol* **11**: 1777-1791.

47. Miroshnichenko ML, Kostrikina NA, Chernyh NA*, et al.* (2003) *Caldithrix abyssi* gen. nov., sp. nov., a nitrate-reducing, thermophilic, anaerobic bacterium isolated from a Mid-Atlantic Ridge hydrothermal vent, represents a novel bacterial lineage. *Int J Syst Evol Microbiol* **53**: 323-329.

48. Penning H & Conrad R (2006) Effect of Inhibition of Acetoclastic Methanogenesis on Growth of Archaeal Populations in an Anoxic Model Environment. *Appl Environ Microbiol* **72**: 178-184.

49.   Hallam SJ, Putnam N, Preston CM, Detter JC, Rokhsar D, Richardson PM & DeLong EF (2004) Reverse Methanogenesis: Testing the Hypothesis with Environmental Genomics. *Science* **305**: 1457-1462.

50.   Krüger M, Meyerdierks A, Glöckner FO*, et al.* (2003) A conspicuous nickel protein in microbial mats that oxidize methane anaerobically. *Nature* **426**: 878-818.

51.   Scheller S, Goenrich M, Boecher R, Thauer RK & Jaun B (2010) The key nickel enzyme of methanogenesis catalyses the anaerobic oxidation of methane. *Nature* **465**: 606-608.

52.   Wegener G, Niemann H, Elvert M, Hinrichs K-U & Boetius A (2008) Assimilation of methane and inorganic carbon by microbial communities mediating the anaerobic oxidation of methane. *Environ Microbiol* **10**: 2287-2298.

53.   Holler T, Wegener G, Knittel K, Boetius A, Brunner B, Kuypers MMM & Widdel F (2009) Substantial ^{13}C/^{12}C and D/H fractionation during anaerobic oxidation of methane by marine consortia enriched *in vitro. Environ Microbiol Rep* **1**: 370-376.

Chapter 3

Methanogenic hydrocarbon degradation

3.1. Accelerated methanogenesis from aliphatic and aromatic hydrocarbons under iron and sulfate reducing conditions

Michael Siegert*[1], Danuta Cichocka[2], Steffi Herrmann[2], Friederike Gründger[1], Stefan Feisthauer[3], Hans-Hermann Richnow[3], Dirk Springael[2], Martin Krüger[1]

[1]Bundesanstalt für Geowissenschaften und Rohstoffe, Stilleweg 2, 30655 Hannover, Germany

[2]Katholieke Universiteit Leuven, Afdeling Bodem- en Waterbeheer, Kasteelpark Arenberg 20 - bus 2459, 3001 Heverlee, Belgium

[3]Helmholtzzentrum für Umweltforschung – UFZ, Permoserstr. 15, 04318 Leipzig, Germany

Running title: Methanogenic hydrocarbon degradation

Key words: methanogenic hydrocarbon degradation, MEOR, metal reduction, bioremediation, *Geobacter*, anaerobic oxidation of methane

*Corresponding author: Michael Siegert, Bundesanstalt für Geowissenschaften und Rohstoffe, Stilleweg 2, 30655 Hannover, Germany, email: michael@siegert.org

Abstract

The impact of four electron acceptors on hydrocarbon induced methanogenesis was studied. Methanogenesis from residual hydrocarbons may enhance exploitation of oil reservoirs and may improve bioremediation. The conditions to drive the rate-limiting first hydrocarbon oxidising steps for conversion of hydrocarbons into methanogenic substrates are crucial. Thus, the electron acceptors ferrihydrite, manganese dioxide, nitrate or sulfate, were added to sediment microcosms acquired from two brackish water locations. Hexadecane, ethylbenzene or 1-^{13}C-naphthalene were used as model hydrocarbons. Methane was released most rapidly from incubations amended with ferrihydrite and hexadecane. Ferrihydrite enhanced only hexadecane-dependent methanogensis. Rates of methanogenesis were negatively affected by sulfate and nitrate at concentrations of more than 5 mM and 1 mM, respectively. Metal-reducing *Geobacteraceae* and potential sulfate reducers as well as *Methanosarcina* were present *in situ* and *in vitro*. Ferrihydrite addition triggered growth of *Methanosarcina* related methanogens. Additionally, methane was removed concomitantly by anaerobic methanotrophy. ANME-1 and 2 methyl coenzyme M reductase genes were detected, indicating anaerobic methanotrophy as an accompanying process. The experiments presented here demonstrate the feasibility of enhancing methanogenic alkane degradation by ferrihydrite or sulfate addition in different geological settings.

3.1.1. Introduction

Roughly, one third of oil in reservoirs remains inaccessible [1]. Since Zengler *et al.* [2] reported the conversion of hexadecane to methane, it has been suggested that remaining energy can be recovered as methane gas [3, 4]. Moreover, the conversion of hydrocarbons to CO_2 or methane represents a useful tool for bioremediation of oil impacted ecosystems. The overall reaction kinetics of hydrocarbon biodegradation are controlled by the initial attack on hydrocarbons, where hydrocarbon biodegradation with oxygen as an electron acceptor is the energetically most favourable process. However, microbial methanogenesis usually requires anoxic conditions and methanogenesis including conversion of hexadecane to methane is a slow process [2, 5].
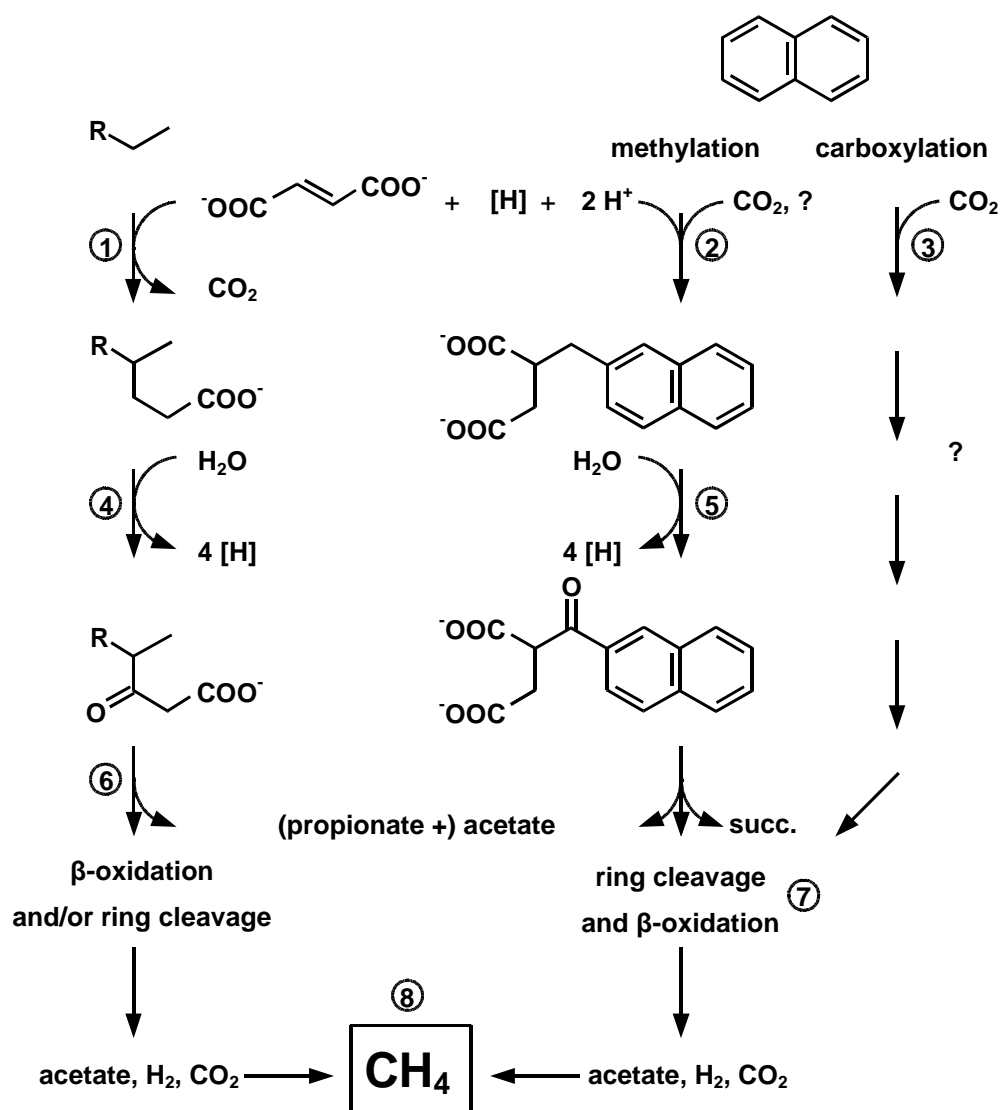
Figure 15: Conceptual figure depicting proposed pathways of anaerobic hydrocarbon degradation. A removal of electrons [H] by adding electron acceptors like Fe(III), Mn(IV), nitrate or sulfate may accelerate overall reactions to yield substrates for methanogens. This may accelerate all ß-oxidation reactions, e.g. at numbers 4-7. R may be an aliphatic or aromatic residue. Note that besides fumarate addition, hydroxylation was shown for R = phenyl [24]. 1: fumarate addition to the hydrocarbon (e.g. hexadecane [6, 7] or ethylbenzene [9]). 2: fumarate addition to methylnaphthalene after methylation [25, 26]. This may possibly be achieved by CO_2 reduction/acylation in a reversed CO-dehydrogenase pathway [26]. Intermediate succinate adducts and carbon skeleton rearrangements [6] are not shown because they may be indirectly driven by electron acceptor addition. 3: Carboxylation and further ring reduction [27]. 4 and 5: Proposed ß-oxidation yielding four electrons [6, 25]. 6: ß-oxidation yielding acetate. Propionate would only be released when R = aliphatic. 7: ring cleavage would precede further ß-oxidation to yield acetate and CO_2 analogous to a proposed ring cleavage of toluene [28]. Steps 4-7 and all subsequent ß-oxidations may be accelerated by electron acceptor addition. 8: The substrates acetate and CO_2/H_2 are finally converted to methane by methanogenic Archaea. Question marks indicate not yet elucidated pathways [26, 29]. succ. = succinate

The initial anaerobic activation of hexadecane may be irreversible and a removal of reaction products is unlikely to accelerate the initial steps or the overall degradation (*Figure 4*; [6, 7]). However, β-oxidation and the release of electrons are essential steps in hydrocarbon biodegradation pathways (*Figure 15*; [6, 8, 9]). It is commonly accepted that the removal of reducing power from the reaction system drives β-oxidation. Examples for this are fermentative hydrogen releasing microorganisms, which require low hydrogen partial pressure to effectively unload electrons from the system. One can deduce that electron acceptors are required to accelerate oxidation of hydrocarbons and their intermediate reaction products to transform them into substrates for methanogens, e.g. acetate, CO_2 and H_2 (*Figure 2* and *Figure 15*; [10]). For activation and processing biological hydrocarbon degradation, the presence of oxidants is not necessary [2]. However, it is plausible to indirectly stimulate the activity of the methanogenic community by providing oxidants other than oxygen to hydrocarbon degrading microorganisms [2, 10].

Sulfate reduction is well described in oil spills and oil field souring where the latter can result in substantial economic losses [11]. Research on trivalent iron reduction by hydrocarbon oxidation emerged during the last twenty years [8, 12, 13] but was not studied in detail in conjunction with hydrocarbon induced methanogenesis. Hydrocarbon associated manganese reduction was described in only few reports so far [14-17]. Alkane biodegradation to methane is well documented and some reports for methanogenesis from aromatics and polyaromatics are available [2, 5, 18-23]. However, detailed research on the impact of electron acceptors on hydrocarbon dependent methanogenesis remains elusive. Our central hypothesis is that electron acceptors can accelerate hydrocarbon dependent methanogenesis. Thus, we tested their stimulating effect on rates of hydrocarbon dependent methanogenesis in different sediments.

3.1.2. Materials and methods

<u>Site descriptions and sampling</u>

Sediment samples were obtained from two different sites. One sampling site was contaminated by hydrocarbons (Zeebrugge) and the other site was pristine (Eckernförde Bay, Supporting Information, Appendix S1).

The sea port of Zeebrugge (Belgium; NW: 51°19'59 N 3°11'57 E, SE: 51°19'55 N 3°12'12 E, approx. 0.1 km^2) comprised several sediment sections with anoxic conditions and was contaminated with hydrocarbons and heavy metals [30]. The water depth was 3 m during ebb. Constant freshwater influx was maintained by the irrigation system of Brugge. In September 2008, samples were obtained from three locations within the harbour basin using a manual

sediment grabber. Sample bottles were filled completely and closed using butyl rubber stoppers and screw caps. Surface water samples were also collected.

Chemical analyses were performed by SGS, Mol, Belgium. Typical contaminants in the harbour mud originated from protective boat paints and fuel leakages. Besides metals like nickel, zinc, lead, copper, mercury and chromium, concentrations of mineral oil ranged from 5 to 400 µg cm^{-3} sediment. Iron, manganese and sulfate were detected in concentrations of up to 85 µmol cm^{-3}, 0.1 µmol cm^{-3} or 2 µmol cm^{-3}, respectively. The pH was between 8.0 and 8.5 and the *in situ* water temperature 14°C.

Preparation of microcosms

For incubations established from the Zeebrugge samples, filter-sterilised harbour water (using 0.2 µm membrane filters) served as medium to mimic *in situ* conditions. However, the harbour water naturally contained 2 mM sulfate and sediment microcosms without electron acceptors were therefore impossible to prepare. Basal salts were not added. Dissolved oxygen was removed by nitrogen gassing of 1 l filtered water. All additional manipulations were performed in an anaerobic glove box. To homogenise the sediment sample, a 1/1 mix of sediment and medium was stirred. The slurry was sampled for DNA extraction and 20 ml were used to inoculate 40 ml medium in 120 ml serum bottles. These were sealed with butyl rubber stoppers and aluminium crimp caps. Triplicate microcosms were incubated under nitrogen headspace at atmospheric pressure at 25°C.

Before inoculation, 2.5 mM ferrihydrite, 1.25 mM manganese dioxide, 1 mM potassium nitrate or 20 mM sodium sulfate were added to the medium. Ferrihydrite was precipitated by neutralisation of a $FeCl_3$ solution [31] and manganese dioxide was obtained by oxidation of a $MnCl_2$ solution with $KMnO_4$ [32]. To determine indigenous methanogenesis, controls without additional hydrocarbons and electron acceptors were prepared. Controls without hydrocarbons but with electron acceptors were set up as single incubations.

Final hexadecane or ethylbenzene concentrations were 0.1%$_{v/v}$ in 60 ml total liquid volume. To test PAH degradation, 1.6 mg 1-^{13}C-naphthalene or ^{12}C-naphthalene were added to 100 ml medium containing 20 ml sediment in 120 ml serum bottles sealed with butyl rubber stoppers and aluminium crimp caps. Manganese dioxide was not used in case of naphthalene. To examine the activity of anaerobic methanotrophs, the headspace of separate microcosms was flushed with a 1/1 methane-nitrogen mix without additional higher hydrocarbons.

Methane and CO$_2$ measurements

Methane and CO$_2$ in headspace samples were analysed using a GC-FID (+ nickel catalyst methaniser, SRI 8610C, SRI Instruments, USA) equipped with a 6 foot Hayesep D column (SRI Instruments, USA) running continuously at 60°C . Methane and CO$_2$ formation from ^{12}C- and 1-^{13}C-naphthalene was also measured using a Thermo Fisher MAT252 GC-IRMS [23]. Rates were calculated based upon the formation of ^{13}CH$_4$ measured in the headspace and subtracted from the $\delta^{13}C_{CH4}$ of indigenously produced methane. δ^{13}C values are expressed as ‰ vs. Vienna Pee Dee Belemnite (VPDB)

Rates in not amended control experiments, hexadecane, ethylbenzene and methane incubations were calculated for a timeframe of 178 days with an intermediate measurement at day 155. For naphthalene incubations, rates were calculated in a timeframe of 435 days without an intermediate measurement.

DNA analytical methods

Sediment DNA was extracted using a FastDNA for Soil DNA extraction kit (MP Biomedicals, USA). Genes of interest were quantified using an Applied Biosystems StepOne thermocycler. 16S rRNA gene copy numbers of *Archaea* and *Bacteria* were determined as described previously [33, 34]. Concentrations of *mcrA* or *dsrA* genes were investigated according to Nunoura *et al.* [35] or Schippers and Nerretin [36], respectively. Members of the *Geobacteraceae* were quantified using the method described by Holmes *et al.* [37]. Copy numbers are expressed as copies cm^{-3} sediment.

Members of the microbial community in the Zeebrugge sediment were identified by incorporation of 16S rRNA gene sequence fragments of a clone library into an existing Maximum-Parsimony tree (version 102) provided by [38]. Fragments of 16S rRNA genes were obtained using the modified primer sets Ar109f (5'-ACKGCTCAGTAACACGT) and Ar912r (5'-CTCCCCCGCCAATTCCTTTA) for *Archaea* and 27f (5'-AGAGTTTGATCCTGGCTCAG) and 907r (5'-CCATCAATTCCTTTRAGTTT) for *Bacteria* [39]. Subsequently, cloning was performed using the pGEM-T vector system according to the manufacturer's instructions (Promega, USA). All sequencing was conducted at Seqlab Göttingen (Germany). Sequences were deposited at the GenBank online database under accession numbers HM598465 to HM598629.

3.1.3. Results

Aliphatic hydrocarbon dependent methanogenesis and CO_2 release

Methanogenesis was observed in all Zeebrugge microcosms after 178 days. Without added hydrocarbons, methanogenesis rates were 2.9, 0.8, 0.6, 0.3 or 0.8 nmol methane cm^{-3} d^{-1} for ferrihydrite, manganese dioxide, nitrate, 2 or 22 mM sulfate amended microcosms, respectively. Respective CO_2 release rates in these controls ranged from 35.5 nmol CO_2 cm^{-3} d^{-1} for ferrihydrite to 73.8 nmol CO_2 cm^{-3} d^{-1} for nitrate.
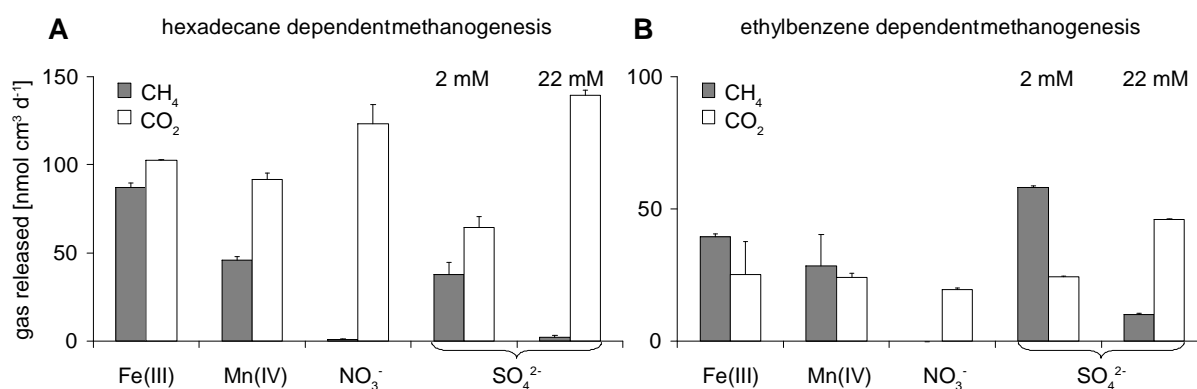
Figure 16: **A** *and* **B**: *Effect of the type of electron acceptor on hydrocarbon dependent methanogenesis in Zeebrugge sediments. Hexadecane (**A**) and ethylbenzene (**B**) were used as substrates. 95% confidence intervals of the triplicate regression slopes against time were calculated. Standard errors within this confidence limit are shown.*

In microcosms containing Zeebrugge sediment with hexadecane, a significant increase of methanogenesis was observed compared to control experiments without hexadecane (Figure 2A). Moreover, hexadecane-dependent methanogenesis rates were significantly different between microcosms with and without added electron acceptor (*Figure 16A*). Most prominently, ferrihydrite accelerated hexadecane-dependent methanogenesis to 87.3±2.3 nmol methane cm^{-3} d^{-1} compared to 37.8±6.6 nmol methane cm^{-3} d^{-1} in 2 mM sulfate incubations (natural harbour water). The increase of methanogenesis in manganese dioxide incubations to 45.9±1.9 nmol methane cm^{-3} d^{-1} was insignificant compared to 2 mM sulfate incubations (*Figure 16A*). Adding 20 mM sulfate decreased methanogenesis to 2.1±1.1 nmol methane cm^{-3} d^{-1}. Nitrate completely inhibited methanogenesis. However, the addition of hexadecane triggered CO_2 release from the microcosms (*Figure 16A*). CO_2 release rates ranged from 64.6±5.8 nmol CO_2 cm^{-3} d^{-1} for 2 mM sulfate to 139.6±3.0 nmol CO_2 cm^{-3} d^{-1} for 22 mM sulfate.

The addition of 1 mM nitrate or 10 mM sulfate almost completely inhibited methanogenesis in Eckernförde Bay microcosms (*Figure 17*A). Hexadecane-dependent methanogenesis

(46.5±3.5 nmol methane cm^{-3} d^{-1}) was higher than naturally occurring methanogenesis without hexadecane of no more than 10 nmol methane cm^{-3} d^{-1} in the sediment layer of the highest methanogenesis (*Figure 17*A; [40]). While hexadecane-dependent methanogenesis occurred without additional electron acceptors in a rate of 24.5±1.7 nmol methane cm^{-3} d^{-1}, the process was significantly slower than in incubations with 2 mM sulfate concentrations 46.5±3.5 nmol methane cm^{-3} d^{-1} (*Figure 17B*).

Aromatic hydrocarbon dependent methanogenesis and CO_2 release
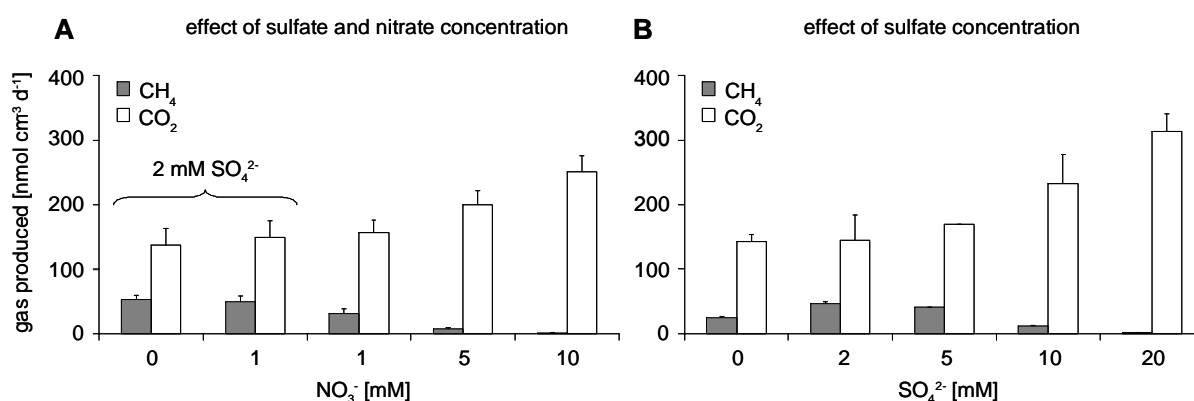
*Figure 17: **A** and **B**: Shift from methane production towards CO_2 upon hexadecane addition in dependence on increased sulfate and/or nitrate concentrations in Eckernförde Bay microcosms. Error bars indicate standard errors of three incubations. **A**: nitrate concentrations from 1 to 10 mM are displayed on the x-axis. Additionally, 0 mM and 1 mM nitrate were tested with 2 mM sulfate present (left). All other microcosms were incubated without nitrate. **B**: sulfate concentrations are displayed on the x-axis. Nitrate was not added.*

Also the addition of ethylbenzene significantly increased methanogenesis in microcosms containing Zeebrugge sediment (*Figure 16B*). Compared to 2 mM sulfate, the addition of ferrihydrite or manganese dioxide reduced methanogenesis from 58.1±0.6 to 39.6±0.9 or 28.2±12.1 nmol methane cm^{-3} d^{-1}, respectively (*Figure 16B*). Like in hexadecane incubations, an increase of sulfate concentrations to 22 mM decreased the methanogenesis rate to 10.0±0.5 nmol methane cm^{-3} d^{-1}. Nitrate completely inhibited methanogenesis. The addition of ethylbenzene inhibited CO_2 release (*Figure 16B*) compared to unamended controls. The lowest CO_2 production rate was detected with nitrate (19.5±0.6 nmol CO_2 cm^{-3} d^{-1}), while 22 mM sulfate increased CO_2 release to 45.9±0.3 nmol CO_2 cm^{-3} d^{-1}.

Methanogenesis depending on 1-^{13}C-naphthalene commenced between days 124 and 235 in 2 mM sulfate incubations with maximum rates of 12.5±0.3 pmol methane cm^{-3} d^{-1} (*Table 1*). At the same time, the $\delta^{13}C_{CH4}$ was -37.1±1.6‰ (unamended control: $\delta^{13}C_{CH4}$ = -43.2±1.1‰; *Figure 18D*). At day 435, 1-^{13}C-naphthalene derived $^{13}CH_4$ formation was also detected as indicated by the elevated $\delta^{13}C_{CH4}$ values compared to unamended controls. Methanogenesis

rates were, however, within the same order of magnitude in all microcosms (*Table 1*). Furthermore, a strong enrichment in $^{13}CO_2$ was observed already after 42 days of incubation in all set-ups amended with 1-^{13}C-naphthalene (*Figure 18E-H*). The $\delta^{13}C_{CO2}$ values ranged from +34.9±2.6‰ (nitrate addition) to +68.4±23.5‰ (iron addition) which was significantly different to the $\delta^{13}C_{CO2}$ values produced in microcosms amended with unlabelled naphthalene (total mean -26.6±0.2‰). In the 1-^{13}C-naphthalene degrading cultures, $\delta^{13}C_{CO2}$ values further increased to a maximum at day 235 (total mean $\delta^{13}C_{CO2}$ +419±21‰; *Figure 18E-H*). CO_2 release rates were at least 200 times higher than methane formation rates (*Table 1*). Ferrihydrite addition resulted in relatively low CO_2 formation rates from 1-^{13}C-naphthalene of 236.7±3.4 pmol CO_2 cm^{-3} d^{-1} while the highest rate was observed with nitrate (499.4±0.5 pmol CO_2 cm^{-3} d^{-1}).

Table 1: Change of $\delta^{13}C_{CH4}$ and $\delta^{13}C_{CO2}$ values during 435 days of incubation with 1-^{13}C-naphthalene, ^{12}C-naphthalene or without naphthalene. Errors are standard deviations from the mean of samples within 95% confidence intervals. Methane formation rates (MFR) and CO_2 formation rates (CFR) were calculated based on the difference between the isotopic ratios of day 0 and day 435 based on the total amount of methane in the headspace. Of the two $\delta^{13}C_{CH4}$ errors (day 0 and 435), the greater error was selected for calculation of rate errors. n/a = not available

electron acceptor	$\delta^{13}C_{CH4}$ [‰ VPDB]							MFR [pmol cm^{-3} d^{-1}]	
	day 0		day 435						
	1-^{13}C-naphthalene		1-^{13}C-naphthalene		^{12}C-naphthalene		without naphthalene		
	mean	error	Mean	error	mean	error		mean	error
ferrihydrite	-48.4	±1.5	-35.5	±0.1	-52.4	±2.1	-52.1	8.3	±1.0
nitrate	-48.6	±0.4	-30.7	±0.4	-50.1	±1.0	-53.5	11.8	±0.3
2 mM sulfate	-48.7	±0.5	-30.0	±0.1	-58.5	±4.0	-53.6	12.5	±0.3
22 mM sulfate	-48.7	±0.1	-30.5	±0.4	-50.2	n/a	-55.3	12.4	±0.3
	$\delta^{13}C_{CO2}$ [‰ VPDB]							CFR	
ferrihydrite	-24.8	±0.3	374.5	±5.8	-30.3	±0.0	-27.7	236.7	±3.4
nitrate	-24.8	±0.1	363.4	n/a	-28.9	±0.1	-26.6	499.4	±0.5
2 mM sulfate	-24.5	±0.2	336.9	±3.6	-29.4	±0.3	-27.2	285.0	±2.9
22 mM sulfate	-24.3	±0.5	317.3	n/a	-28.7	±0.0	-27.8	338.6	±0.1

Anaerobic methanotrophy

In parallel experiments, anaerobic oxidation of methane was observed in Zeebrugge microcosms. Incubations with 22 mM sulfate showed the highest AOM rates (1216.0±135.3 nmol methane cm^{-3} d^{-1}), while cultures with ferrihydrite or manganese dioxide displayed slightly lower rates (1117.3±0.2 or 1070.9±37.8 nmol methane cm^{-3} d^{-1}, respectively). AOM rates were lower with nitrate (881.3±0.7 nmol methane cm^{-3} d^{-1}) or with 2 mM sulfate, (479.0±6.4 0.0 nmol methane cm^{-3} d^{-1}).
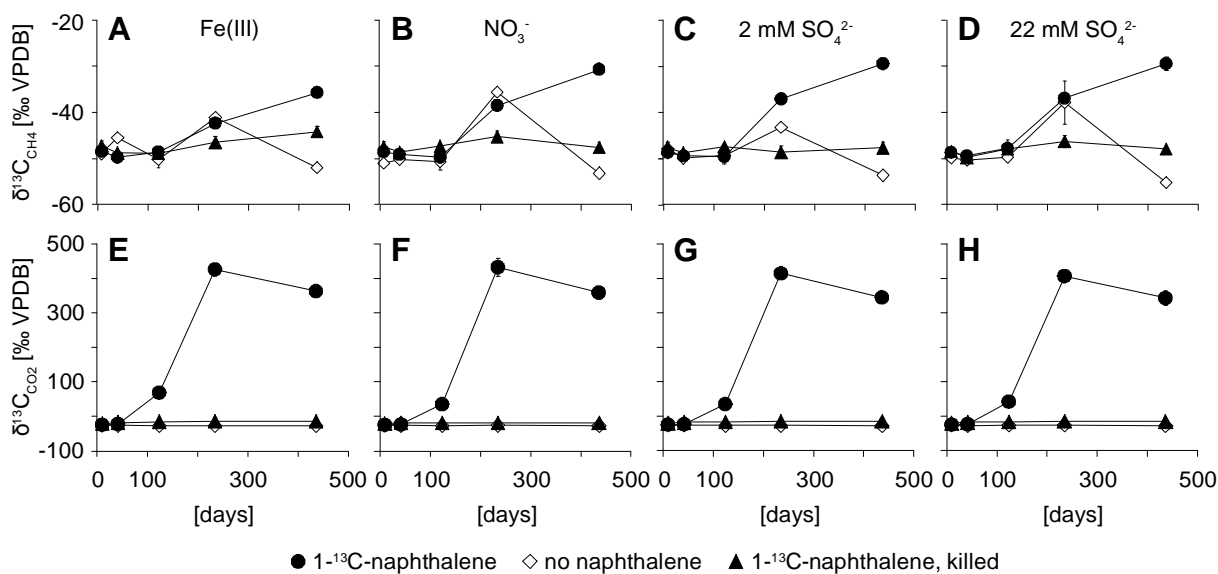
Figure 18: Time course of $^{13}CH_4$ (top) and $^{13}CO_2$ (bottom) formation upon 1-^{13}C-naphthalene addition to microcosms prepared from contaminated Zeebrugge harbour mud. ● 1-^{13}C-naphthalene, ▲ 1-^{13}C-naphthalene, killed, ◊ without naphthalene. Error bars are standard deviations from the mean of three parallel microcosms. Error bars of control experiments (no naphthalene, dead controls) are standard deviations from the mean of two parallel microcosms. Dead controls were killed with 8% formaldehyde final concentration.

Hydrocarbon degrading microbial community

The original Zeebrugge sediment contained 16S rRNA gene copy numbers of 2.6×10^9 copies cm^{-3} for *Bacteria* and 3.1×10^8 copies cm^{-3} for *Archaea* (Supporting Information, *Figure S1*). Compared to the sediment used as inoculum, a significant increase of the methanogenic (*Methanosarcina mcrA*) and the methanotrophic (ANME-1 and 2 *mcrA*) populations was observed in microcosms with ferrihydrite and hexadecane (*Figure 19*). With sulfate and methane, only the number of ANME-2 copies increased. The growth of *Geobacteraceae* – although present in significant numbers – was not initiated by addition of hexadecane or electron acceptors compared to the inoculum (*Figure 19*). In contrast, the addition of sulfate and/or ferrihydrite stimulated growth of the sulfate reducing community in the microcosms. Experiments with ethylbenzene, naphthalene, nitrate or manganese were not monitored by real-time PCR.
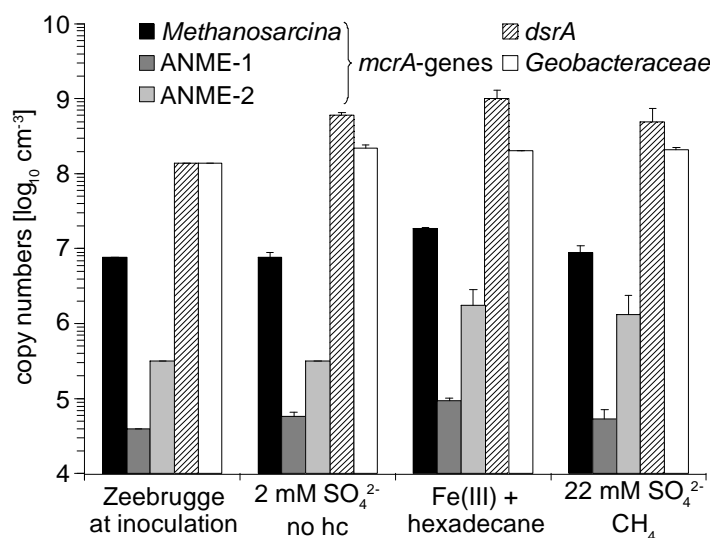
Figure 19: Logarithmic plots of community composition in microcosms of contaminated harbour mud of Zeebrugge. DNA was extracted from the sediment microcosms after 178 days of incubation with 2 mM sulfate without any additional hydrocarbon (hc), ferrihydrite and hexadecane or methane and 22 mM sulfate. ANME-1, ANME-2 and Methanosarcina specific mcrA genes were quantified. Sulfate reducers were detected targeting their dsrA gene and Geobacteraceae were quantified by amplification of their 16S rRNA genes. When given, error bars were calculated from standard deviations of the mean of two extracted incubations, each determined in three parallel PCR reactions.

16S rRNA gene clone libraries of *Bacteria* (n=82) and *Archaea* (n=93) of the Zeebrugge sediment revealed a broad microbial diversity (Supporting Information, *Figure S3 & Figure S4*). Among *Bacteria*, *α-, γ-* and *δ-Proteobacteria* 16S rRNA gene sequences were recovered as well as sequences associated with *Campylobacterales, Planctomycetes, Clostridia, Actinobacteria* and *Chloroflexi.* 16S rRNA gene sequences associated with potential pathogens, like *Neisseria* and *Coxiella*, were also found as well as sequences associated with *Geobacteraceae*. Seven potential aerobic iron oxidisers of the family *Acidithiobacillaceae* and another seven of the *Acidimicrobinea* could be identified. Some clones were closely related to sequences recovered in other potentially hydrocarbon influenced environments like the Victoria Harbour in Hongkong, China [41], the Belgian coast off Zeebrugge [42], the Milano mud volcano [43] as well as the Gullfaks and Tommeliten oilfields of the North Sea [44] (Supporting Information, *Figure S3*). The phylogenetic diversity of *Archaea* comprised *Crenarchaeota* and *Euryarchaeota*. In the latter, members of the *Methanosarcina* prevailed.

3.1.4. Discussion

Electron acceptors may accelerate hydrocarbon degradation, thus providing an increased substrate supply for methanogenesis. In this work we evaluate the hypothesis that the addition of electron acceptors leads to accelerated hydrocarbon dependent methanogenesis. This process may be useful to stimulate the recovery of oil related carbon as methane from reservoirs, or for bioremediation of contaminated sites. Our aim was to stimulate the initial steps in hydrocarbon degradation and thus the formation of methanogenic substrates like acetate, CO_2 and H_2. Four different electron acceptors were added to sediment microcosms.

Two different ecosystems – contaminated harbour mud and pristine marine sediment – were investigated to show that this approach is generally applicable.

Hydrocarbon dependent methanogenesis

Methane evolved upon hexadecane, ethylbenzene or naphthalene addition in different sediment microcosms (*Figure 16*; *Table 1*). In most cases, conversion of hexadecane to methane was faster compared to aromatic hydrocarbons (*Figure 16*; *Table 1*). Exceptions were ethylbenzene microcosms with 2 mM sulfate, in which the conversion to methane was faster (58.1 ± 0.6 nmol methane $cm^{-3} d^{-1}$) than in the respective hexadecane incubation (37.8 ± 6.6 nmol methane $cm^{-3} d^{-1}$). The observed rates are approximately one order of magnitude lower than those reported in a study of an inoculated oilfield sediment core [45]. Apparently, inoculation using an enriched consortium was more efficient than stimulation of indigenous hydrocarbon degraders. In another study of a sediment free methanogenic hexadecane degrading enrichment culture, hexadecane-dependent methanogenesis was lower (13 nmol methane $ml^{-1} d^{-1}$) than the rates observed in our experiments [5]. Presumably, a sediment free enrichment culture never reaches cell densities of sediments (approximately 10^9 cells cm^{-3} sediment, Supporting Information *Figure S1*), resulting in lower volume related rates.

Methanogenesis from naphthalene was in a picomolar range while other hydrocarbons induced methane release in nanomolar ranges (*Figure 16*; *Table 1*). The time-lag between $^{13}CO_2$ and $^{13}CH_4$ evolution as well as the significant difference in $\delta^{13}C$-signature shifts (*Figure 18*) indicate that methanogenesis played a minor role in naphthalene degrading cultures. Primarily, naphthalene seems to have been mineralised to CO_2. Anaerobic oxidation of naphthalene and subsequent formation of CO_2 was demonstrated under nitrate (Bregnard 1996) and sulfate reducing conditions [46-49]. Nevertheless, methanogenesis occurred in our naphthalene degrading microcosms, a process which was suggested [19, 50] but hitherto never confirmed.

Sharak Genthner *et al.* [50] observed an inhibition of methanogenesis after naphthalene addition and concluded that naphthalene may be toxic to methanogens. In our microcosms this seems unlikely because they were naturally exposed to various mineral oil compounds found in the sediments [30]. Regardless of naphthalene toxicity, methanogens possibly had better access to degradation products of hexadecane and ethylbenzene than to those of naphthalene. We therefore postulate that methanogens themselves were directly involved in the degradation chain of hexadecane and ethylbenzene but not of naphthalene degradation. The observed increase of the methanogenic population and the finding of a rich methanogenic

community in 16S rRNA gene clone libraries support this assumption (*Figure 19*; Supporting Information, *Figure S4* and *Figure S5*).

Impact of electron acceptors on hydrocarbon dependent methanogenesis

We studied the impact of ferrihydrite, manganese dioxide, nitrate and sulfate on hydrocarbon dependent methanogenesis. Ferrihydrite accelerated hexadecane-dependent methanogenesis compared to sulfate or nitrate. Nitrate almost completely inhibited methanogenesis from hexadecane and ethylbenzene (*Figure 16* and *Figure 17A*). This is not surprising because nitrate is a well known inhibitor of methanogenesis [51]. Furthermore, nitrate and high sulfate concentrations negatively influenced conversion rates of hexadecane to methane (*Figure 16* and *Figure 17A*). However, in presence of 2 mM sulfate, nitrate was not inhibitory (*Figure 17A*) indicating that a sulfate reducing hexadecane degrading community prevailed.

Adding sulfate in concentrations up to 5 mM to the sediment microcosms of Eckernförde Bay resulted in a significant increase of hexadecane-dependent methanogenesis (*Figure 17B*). In contrast, concentrations higher than 5 mM strongly inhibited hexadecane-dependent methanogenesis. Possibly, sulfate addition stimulated growth of new or other sulfate reducers, dominating substrate competition for intermediates with methanogens. In contrast, a previous study reported no inhibition of methanogenesis by sulfate of up to 10 mM [45]. The inhibitory effect of 22 mM sulfate on ethylbenzene-dependent methanogenesis was less pronounced compared to hexadecane. For naphthalene, neither inhibition nor stimulation of methanogenesis was found with either electron acceptor (*Figure 18*; *Table 1*). This agrees with a recent study of contaminated sediments where no stimulating effect of Fe(III) on PAH degradation was observed [52].

The impact of electron acceptors on hydrocarbon dependent methanogenesis demonstrates that (i) the concentration of the added electron acceptor is crucial for hexadecane fed methanogenesis and (ii) the solubility of the electron acceptor appears to be important. Indeed, insoluble electron acceptors like ferrihydrite or manganese dioxide had a stimulating effect on hexadecane-dependent methanogenesis (*Figure 16A*). However, these electron acceptors are only locally bioavailable, which may result in microscale compartment formation. In contrast, theoretically possible products of hexadecane degradation, like carbonate, acetate and hydrogen, can freely diffuse and become available for methanogens in niches where other electron acceptors are depleted.

In Zeebrugge microcosms, the observed increase of the total archaeal community and *mcrA* gene copies suggests that especially *Methanosarcina* species account for iron reduction as demonstrated by [53] (*Figure 19*; Supporting Information). Moreover, neither ferrihydrite or

sulfate nor hexadecane or methane addition triggered growth of *Geobacteraceae*. In conclusion, members of this family are probably less important for the respective processes (*Figure 19*). This is not surprising because *Geobacteraceae* are known for their aromatic metabolism while alkane degradation has not been reported. Instead, other members of the *Proteobacteria*, known for hosting many known hydrocarbon degraders [54] were identified (Supporting Information, *Figure S3*). One sequence was closely related to a clone identified at the Gullfaks and Tommeliten oilfield methane seeps of the North Sea [55].

Methanogenesis versus AOM

AOM rates were determined to assess potential methane losses during incubation time. These rates were in good agreement with those typically observed in methane fed environments [56]. However, methane seepage was apparently not the major energy source of Zeebrugge sediments. Therefore, *in situ* AOM possibly depended on hydrocarbon derived methane, as indicated by the growth of the AOM community in hexadecane amended microcosms (*Figure 19*). Based on the methane partial pressure dependent and cell specific AOM rate constant reported by Thauer and Shima [57], we calculated a loss of no more than 12% of the produced methane in hydrocarbon amended microcosms.

Conclusions and possible practical implications

To fully exploit exhausted oil reservoirs, the conversion of residual oil to methane seems a viable technique to recover energy which would otherwise be lost. As a possible contribution for this application, our experiments demonstrated that additional sulfate or trivalent iron accelerated methanogenesis in aliphatic and aromatic hydrocarbon (e.g. BTEX) degrading communities. In contrast, the inhibitory effect of nitrate, commonly used to suppress sulfate reducers in oil fields, most likely prohibits its application for oil recovery as methane. Additionally, we present convincing evidence for the conversion of a PAH to methane.

Consequently, our results also provide novel insights for bioremediation, where the conversion of hydrocarbon contaminants to volatile methane seems an elegant option. Nevertheless, methane is a much more potent greenhouse gas than CO_2. Therefore, the addition of high amounts of nitrate or sulfate may be preferred to stimulate biodegradation when methanogenesis is unwanted and oxygen treatment is impossible.

Acknowledgements

Innovation Platform (MIP, project "In situ conditioning of dredged and mineral sludge"). We thank Dr. Axel Schippers for fruitful discussions and improving the manuscript.

3.1.5. Supporting information

Appendix S1

Eckernförde Bay:

Samples of Eckernförde Bay were taken to demonstrate that hydrocarbon dependent methanogensis accelerated by electron acceptor addition is not restricted to the Zeebrugge site.

Materials and methods

Site description:

The Eckernförde Bay is located at the German coast of the western Baltic Sea. Its pristine sediment was methane rich and was sampled in autumn 2001 [40]. This site and sampling procedures were described in detail by Treude *et al.* [40]. Briefly, this marine site was characterised by the absence of tides, a stratified water column and a resulting thermocline and halocline. Sediment samples were derived from the sediment surface at 28 m water depth. Sulfate concentrations ranged from 16 mM to 21 mM at the sediment-water interface.

Sampling:

After sampling, sediment microcosms of Eckernförde Bay were maintained by several transfers in sulfate containing artificial sea water medium amended with hexadecane as described previously [5, 40, 58]. 1/10 transfers were prepared after methane evolved from the previous incubation. To study the effect of nitrate and sulfate concentrations on hexadecane-dependent methanogenesis, nitrate concentrations ranged from 0-10 mM KNO_3 and sulfate concentrations from 0-20 mM $MgSO_4$. In case of 1 mM nitrate, the stimulating effect of sulfate was compared to microcosms without sulfate by adding 2 mM $MgSO_4$. All Eckernförde Bay microcosms were incubated for 70 days at room temperature.

Gas chromatography:

Methane and carbon dioxide in Eckernförde Bay microcosms were determined in weekly intervals. Methane and CO_2 were detected by GC-FID (+ nickel catalyst methaniser) headspace measurements (SRI 8610C, SRI Instruments, USA) equipped with a 6 foot

Appendix S2:
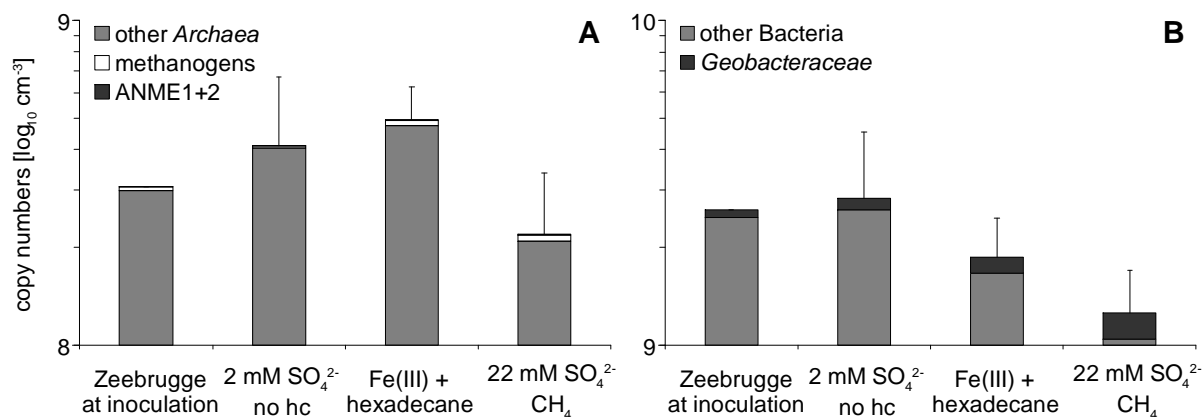
Figure S1: Archaeal (**A**) and bacterial (**B**) 16S rDNA copy numbers of Zeebrugge harbour mud in situ (sampling event) and after incubation of 178 days. Error bars represent the error of two parallel incubations. Each incubation was determined in three parallel PCR reactions. Only error bars of the domains (Archaea, Bacteria) are displayed.
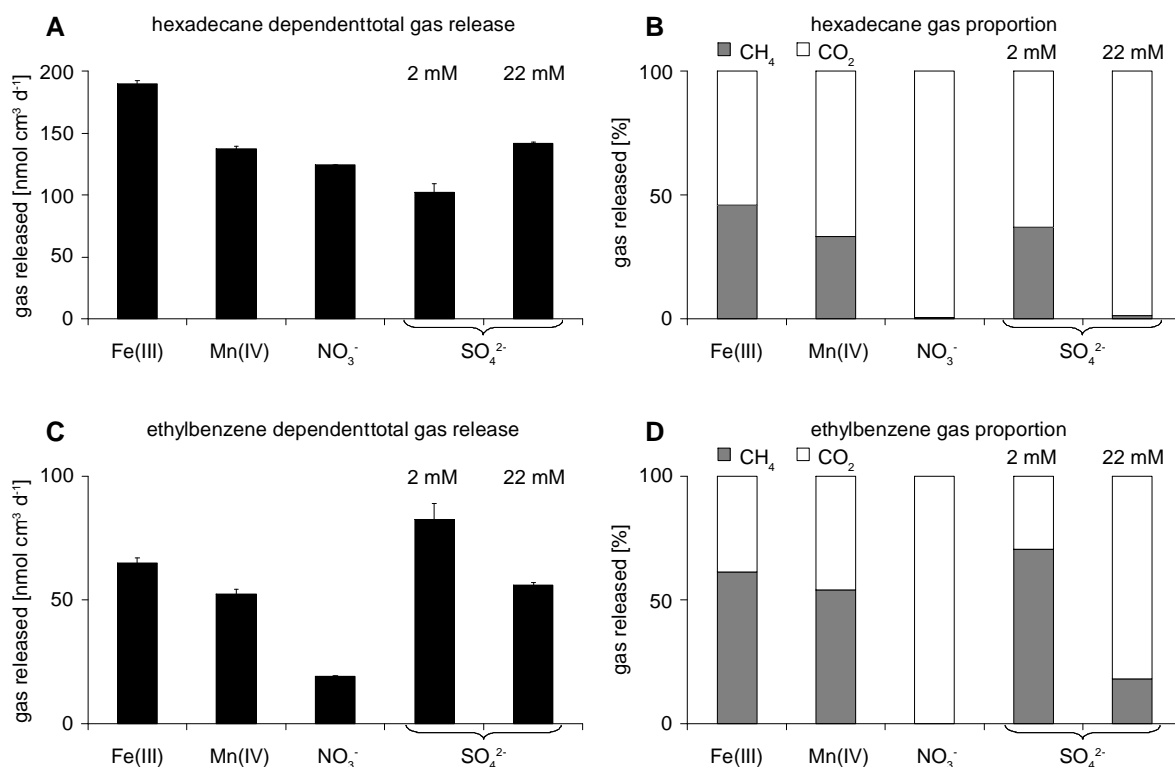
Figure S2: Zeebrugge microcosms: **A**: Total gas release (CO_2 + CH_4) upon hexadecane addition **B**: Proportions of CO_2 + CH_4 **C**: Total gas release upon ethylbenzene addtions **D**: Proportions of CO_2 + CH_4 after ethylbenzene addition.

number of OTUs

◆ Archaea
■ Bacteria

100

50

0

0   50   100

clones

Anderseniella 1

Filomicrobium 1

Rhodobium 4

AB476277, from *Shinkaia crosnieri* setae

Zeebrugge B85

Ahrensia 1

Oceanicola pacificus

Rhodobacter 2

Zeebrugge B57

Phyllobacteriaceae

Rhodobacteraceae

α-Protobacteria

Neisseriaceae 1

Zeebrugge B16

Zeebrugge B33

Thioalkalivibrio 2

HOC36 1

Coxiella 1

Acidithiobacillaceae 7

marine benthic group 6

Thiohalophilus thiocyanatoxyda

JTB148 1

Granulosicoccus antarcticus

FJ264655, Beal *et al.*, 2009 AOM metal reducers, Eel River Basin, USA [1]

Zeebrugge B42

Sulfovorum 1

γ-Protobacteria

Campylobacterales

Desulforhopulus 1

Desulfobulbus 1

FJ516990, Tablas de Daimiel, Spain

Zeebrugge B61

FJ416128, Northern Bering Sea sediment

Zeebrugge B83

EU440668, agricultural soil

Zeebrugge B63

Desulfomonile 1

Geobacter metallireducens

Geoalkalibacter ferrihydriticu

Geopsychrobacter electrodiphilus

AY771969, Mussmann *et al.*, 2005 Wadden Sea, Germany [2]

Zeebrugge B50

GQ357030, AOM metal reducers, Eel River Basin, USA

DQ394990, Zhang *et al.*, 2008 Victoria Harbour, China [3]

Zeebrugge B89

Desulfobacula 1

Desulfofrigus 1

Desulfonema magnum

AB294969, Hirayama *et al.*, 2007 marine hot spring, Taketomi island, Japan [4]

Zeebrugge B74

DQ351775, Gillan & Pernet, 2007, Belgian Plate sediments North Sea [5]

Zeebrugge B22

AB250561, Grotta Azzura of Palinuro Cape, Italy

Zeebrugge B73

Zeaxanthinibacter 1

Aestuariicola saemankumensis

Tenacibaculum 2

Desulfobaceae

Geobacteraceae

Desulfobacteraceae

Flavobacteriaceae

δ-Protobacteria

Bacteroidetes

Acidobacteraceae

FM179875, Wegener *et al.*, 2008 Gullfaks and Tommeliten methane seeps, North Sea [6]

Zeebrugge B62

GQ246340, Northern Yellow Sea sediments

Zeebrugge B88

candidate devision WS3

Planctomycetes

candidatus *Kuenenia stuttgartiensis*

MSB-3A7 sediment group 1

AY592419, Amsterdam mud volcano, Mediterranean Sea

Zeebrugge B84

Blastopirellula 1

to *Archaea*

Veillonellaceae 1

Shuttleworthia 2

Clostridium 1   2

Clostridium 2   1

Rubrobacteridae 2

Frankia 1

uncultured *Acidimicrobineae* 1

uncultured *Acidimicrobineae* 1

Ilumatobacter 1

uncultured *Acidimicrobiaceae* 4

Clostridiales

Acidimicrobinea

Firmicutes

Actinobacteria

EU488018, siliciclastic sediment Dog Island, FL, USA

Zeebrugge B58

FJ873275, Okhotsk Sea sediment

Zeebrugge B48

Zeebrugge B65

Anaerolineaceae 3

Chloroflexi

0.10

Figure S3: Parsimony tree assembled for Bacteria from a 16S rDNA clone library (n=87) of Zeebrugge harbour mud according to Pruesse et al. (2007). Duplicate sequences of 100% identity were removed before constructing the final tree. The SILVA database version 102 was used. Numbers in boxes indicate the number of clones which could be affiliated to the respective group. Numbers in clusters indicate numbers of Zeebrugge 16S rRNA gene sequences which were assigned to the respective cluster. References are   1 = [59], 2 = [60], 3 = [41], 4 = [61], 5 = [42] and 6 = [44]. Insert: Rarefaction curve using a 97% identity cutoff. The Mothur software package was used for calculation [62].
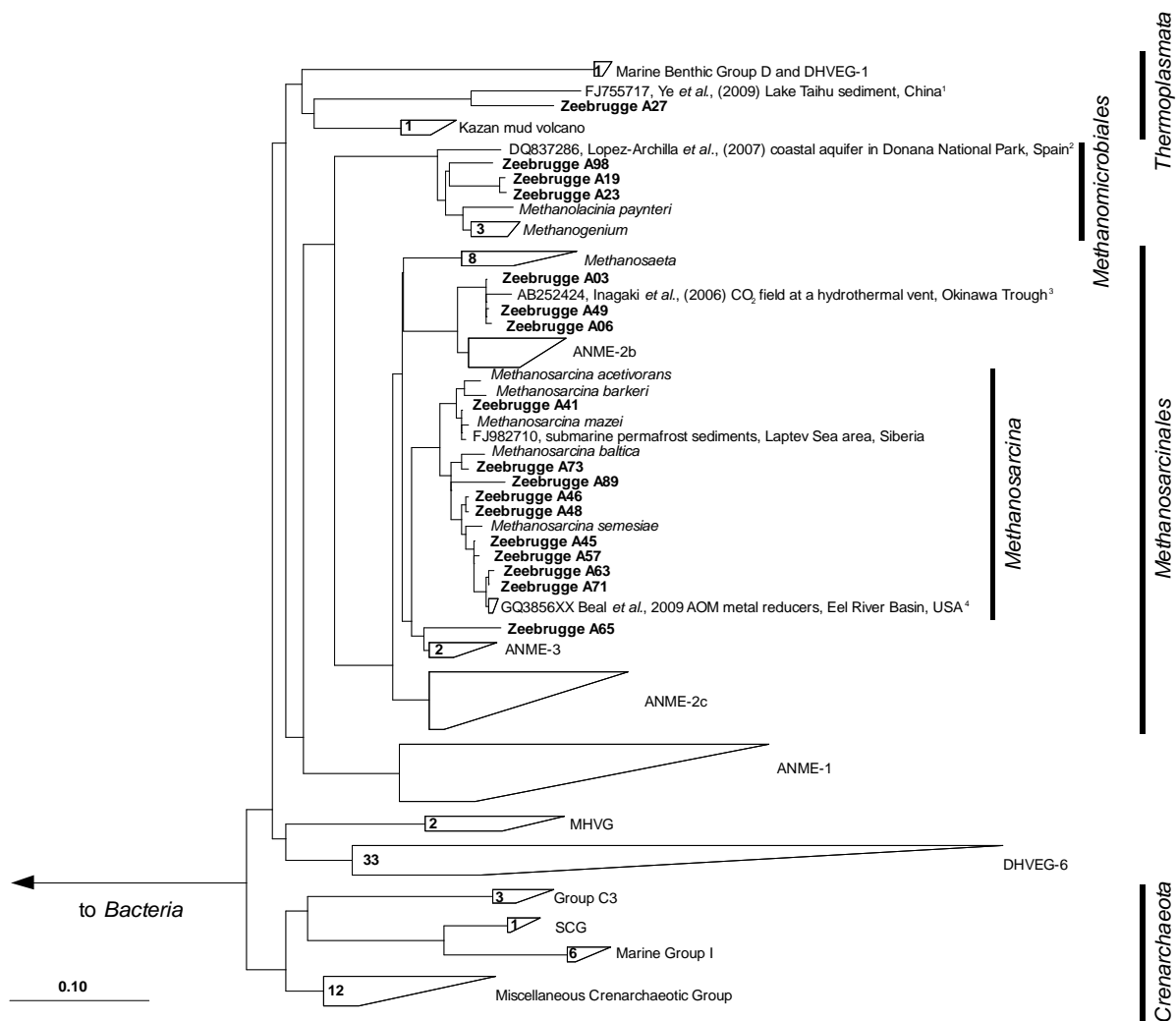
Figure S4: Parsimony tree assembled for Archaea from a 16S rDNA clone library (n=98) of Zeebrugge harbour mud according to Pruesse et al. (2007). Duplicate sequences of 100% identity were removed before constructing the final tree. The SILVA database version 102 was used. Numbers in boxes indicate the number of clones which could be affiliated to the respective group. Numbers in clusters indicate numbers of Zeebrugge 16S rRNA gene sequences which were assigned to the respective cluster. uReferences are 1 = [63], 2 = [64], 3 = [65] and 4 = [59]
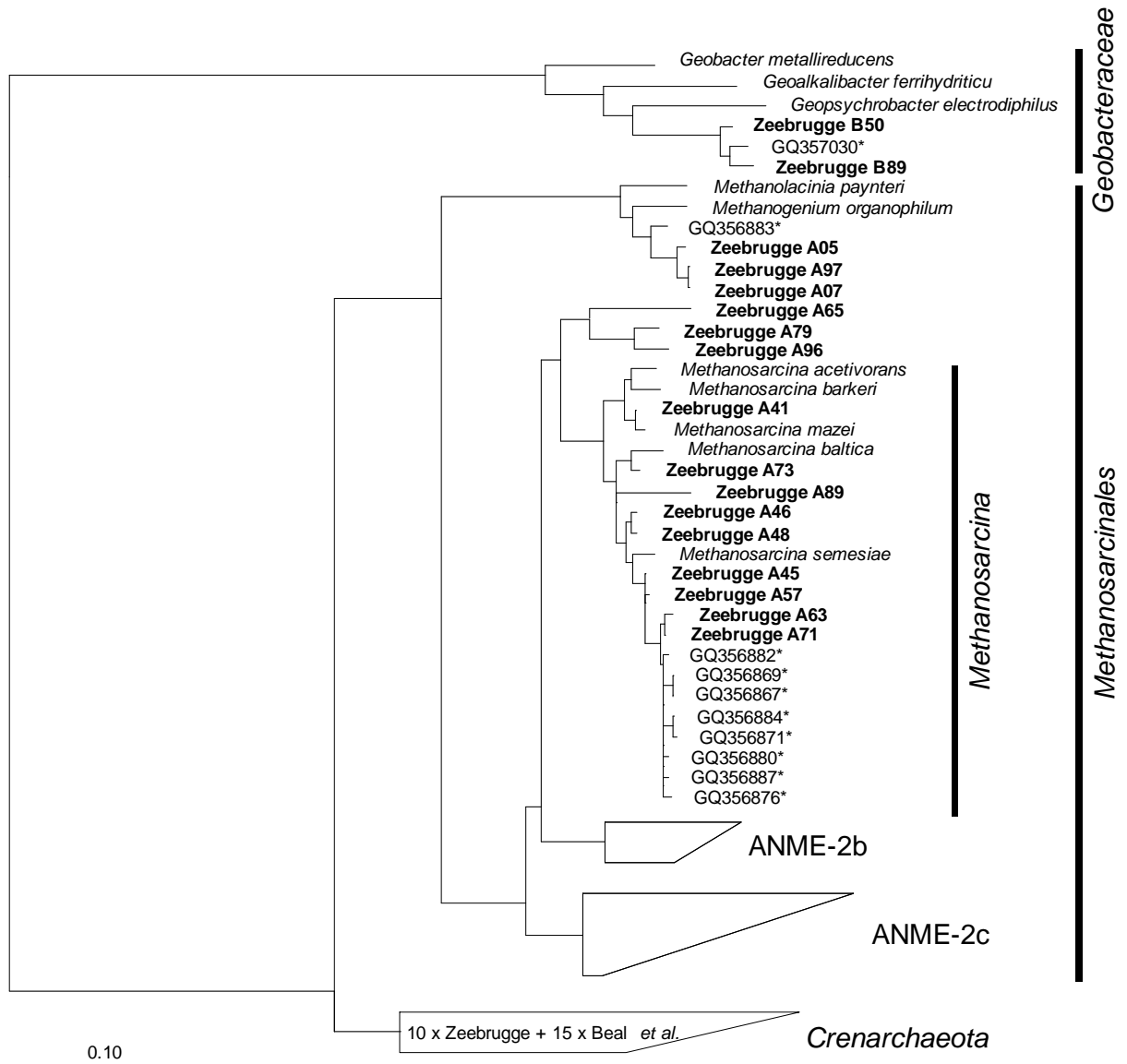
Figure S5: 16S rRNA gene Parsimony tree excerpted from the SILVA database 102. The excerpt contains sequences of a proposed metal reducing AOM community sampled in the Eel River basin [59]. OTUs of at least 80% distance matrix identity with clones obtained from Zeebrugge sediment are displayed in the tree. Reference species are italic*, Zeebrugge clones* **bold** *and Eel River clones are asterisk (*) marked.*
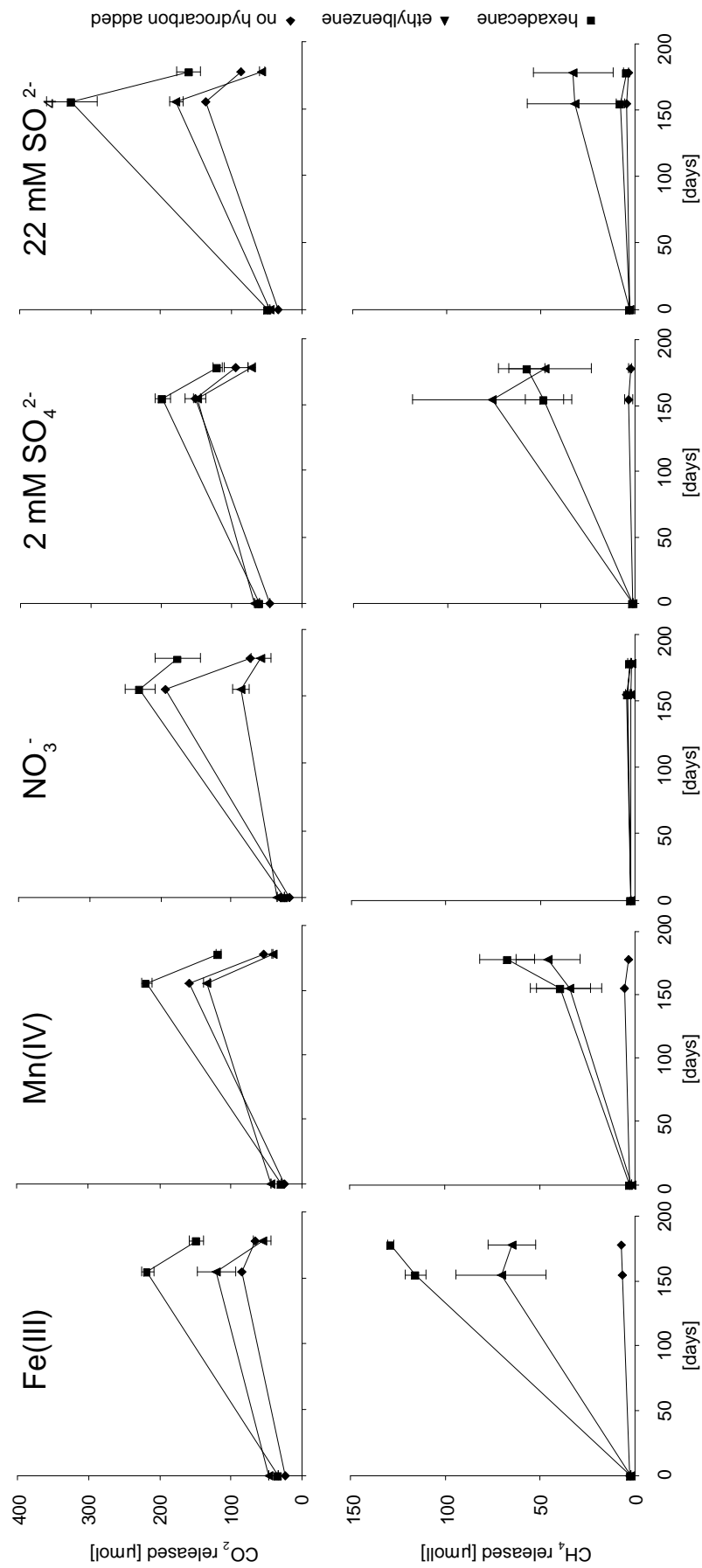
Figure S6: Absolute gas release in Zeebrugge microcosms. Upper row: evolution of CO_2 versus time [days] when ■ hexadecane or ▲ ethylbenzene were added. ● Controls without additional hydrocarbons. Bottom row: corresponding methane release.

3.2. Isotopic fingerprinting of methane and CO_2 formation from aliphatic and aromatic hydrocarbons

Stefan Feisthauer[1], Michael Siegert[2], Martin Seidel[1], Hans H. Richnow[1]*, Karsten Zengler[3], Friederike Gründger[2], Martin Krüger[2]

[1]Helmholtzzentrum für Umweltforschung – UFZ, Department Isotopen-biogeochemie, Permoserstr. 15, 04318 Leipzig, Germany

[2]Bundesanstalt für Geowissenschaften und Rohstoffe, Stilleweg 2, 30655 Hannover, Germany

[3]Department of Bioengineering, University of California, San Diego, 9500 Gilman Drive, La Jolla, CA 92093-0412, USA

*Corresponding author; Tel.: +49 341 2351212; fax: +49 341 2351443, email: hans.richnow@ufz.de (H. H. Richnow).

Abstract

We investigated the stable carbon and hydrogen isotopic signature of methane, CO_2 and water during microbial formation of methane from mineral oil related compounds in order to determine the variability of methane carbon and hydrogen isotopic signatures. The isotopic discrimination for carbon and hydrogen between substrate and methane was calculated and resulted in $\varepsilon C_{DIC-CH4}$ 26 to 60‰, $\varepsilon C_{substrate-CH4}$ 16 to 33‰, $\varepsilon H_{H2O-CH4}$ 257 to 336‰, and $\varepsilon H_{substrate-CH4}$ 174 to 318‰, respectively. These carbon and hydrogen isotope signatures fell in a relatively narrow range, suggesting a coupling of fermentation with acetoclastic and CO_2 reducing methanogenesis. In order to characterise the microbial consortia involved in the methanogenic degradation of hexadecane, a methanogenic enrichment culture was incubated with 1-^{13}C-hexadecane and its biomass was analysed for the pattern and isotopic signature of carboxylic acids. The highest labelling was detected in *n*-C17 fatty acid with methyl groups at carbon atom 4, presumably indicative of *Syntrophus* sp. To determine if the isotope composition of methane can be used as an indicator for methanogenesis during growth with oil related compounds in field studies, we analysed the isotope composition of methane in a confined mineral oil contaminated aquifer. The variability of carbon and hydrogen isotope composition was almost identical to the values obtained from enrichment cultures, thereby providing a tool for screening for microbial methane formation during hydrocarbon exploration.

3.2.1. Introduction

Methanogenesis is the terminal electron accepting process for degradation of organic matter after the depletion of other organic and inorganic electron acceptors in a closed environmental system. This unique metabolic pathway may explain the frequently observed hydrocarbon biodegradation in petroleum reservoirs, e.g. [4, 18, 45, 66-68]. Except for CO_2, which is formed stoichiometrically with methane, no external electron acceptors are required to sustain the degradation process over long-term periods. Thus, only water and essential nutrients may be required for methanogenesis in oil reservoirs. Methane formation from oil related compounds in petroleum reservoirs may provide an opportunity for enhanced recovery of fossil fuels from previously exploited oil reservoirs and coal bed strata [45, 68, 69]. Even in times of intense exploration for alternative energy sources, the worldwide demand for hydrocarbons, the most readily available energy and carbon source, persists and may even grow as a result of the increase in world population. At the same time, easily accessible petroleum reserves are declining. Roughly 40% of existing crude oil can be recovered using conventional technologies, resulting in large amounts of inaccessible oil remaining within the world's oil deposits [1]. Around 50 to 98% of typical crude oil consists of hydrocarbons such as alkanes, cycloalkanes, and alkylated aromatic compounds [22]. Different constituents within

the hydrocarbon fraction have been shown to be biodegradable under anoxic conditions with various electron acceptors, e.g. [70, 71]. For example, *n*-alkanes comprise a major fraction of most crude oils and have been found to be biodegradable under methanogenic conditions both as pure substrates, e.g. *n*-hexadecane, [2, 72] and as crude oils [18, 22, 45, 73]. Converting at least a portion of currently unrecoverable oil biotechnologically into methane may provide an opportunity to increase the recovery of energy from oil reservoirs. This represents and emerging research area for biotechnology and fuel production. Gieg *et al.* [45] estimated an additional methane production potential in the USA of up to 2.8×10^{10} m^3 per year from exploited oil reservoirs. This would mean that up to 16% of the annual gas consumption in the USA could be offset by enhanced methanogenesis [74]. In addition, natural gas is a cleaner-burning alternative to gasoline and reduces CO_2 emissions by 25% [75].

Zengler *et al.* [2] showed that methane can be produced from hexadecane by methanogenic microorganisms in a syntrophic consortium with acetogenic *Bacteria*. Acetate, CO_2 and H_2 are intermediates in the process of methanogenic alkane degradation. Acetate is cleaved by methanogenic *Archaea* to form methane and carbon dioxide. Furthermore, CO_2-reducing methanogenic *Archaea* maintain a low hydrogen partial pressure, a thermodynamic prerequisite to make the overall reaction energetically favorable. The transformation of hexadecane to methane occurs via the following net reaction [2], showing that about 77% of the carbon can be transformed to methane when neglecting biomass formation and energy demands of the cell:

(8) $4\ C_{16}H_{34} + 30\ H_2O \rightarrow 49\ CH_4 + 15\ CO_2$
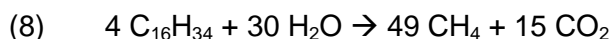
The carbon and hydrogen stable isotopic signatures of methane provide clues for characterizing the origin of methane and may allow for a better description of methanogenic processes in the field [76, 77]. In order to describe the level of conversion of alkane-derived carbon to methane, Jones *et al.* [18] linked the stable carbon isotopic composition of CO_2 to biogenic methane from a degraded oil reservoir.

The objective of our study was to elucidate the processes involved in microbial gas generation during growth on oil related compounds. To analyse the isotopic fractionation processes during methane production from *n*-alkanes, we incubated several enrichment cultures of anaerobic oil degraders from methanogenic environments with *n*-hexadecane as a model aliphatic hydrocarbon. Also, we described the structure of the syntrophic consortium involved in methane production by tracking a carbon isotope label from 1-^{13}C-hexadecane into microbial biomarkers such as the carboxylic acid fraction. Finally, to characterise the origin of methane in situ and in vitro, we investigated the isotopic composition (^{13}C/^{12}C; D/H) of gases (CH_4 and CO_2) and water at a contaminated aquifer field site. The comparison of in vitro and in situ re-

sults confirmed that the variability in carbon and hydrogen isotope enrichment factors between the CO_2 and methane, as well as between water and methane, respectively, may be used to monitor biogenic methane formation from crude oil-related compounds in situ. This tool may contribute to a better understanding of methanogenic processes in the field that result in altered oil phases and methane and CO_2 production in petroliferous formations.

3.2.2. Materials and methods

Reagent grade solvents were obtained from Merck (Darmstadt, Germany). Hexadecane was acquired from Sigma Aldrich. 1-^{13}C-hexadecane and U-^{13}C–hexadecane were synthesised from 1-^{13}C-hexadecanoic and U-^{13}C–hexadecanoic acid, both obtained from Campro Scientific (Berlin, Germany). The hexadecanoic acids were (i) converted to the methyl ester (with dimethyl sulfate), (ii) reduced to hexadecanol (with $NaAlH_4$) and (iii) converted to the *p*-tosylate ester and further reduced to hydrocarbons (with $NaAlH_4$; [2]). The purity was confirmed using gas chromatography-mass spectrometry (GC-MS).

<u>Experimental setup and growth conditions</u>

For the investigation of microbial growth with labelled and unlabelled hexadecane, the substrate was immobilised onto the surface of Teflon filters (pore sise 0.45 µm). The microbial enrichment cultures obtained from Kuhgraben (Bremen, Germany) were cultivated in anoxic mineral medium buffered at pH 7 with bicarbonate (30 mM) plus CO_2 and reduced with sulfide (1 mM; [58]). Cultures were incubated at 28°C. Further culture conditions and handling protocols are described elsewhere [2]. The unlabelled hexadecane (50 µl equating to 0.17 mmol) had a carbon isotope signature of -32.4‰. For the experiments with labelled hexadecane, either fully labelled U-^{13}C–hexadecane (100 µl equating to 0.32 mmol) or 1-^{13}C-hexadecane (50 µl equating 0.17 mmol) with an isotope composition of 5960‰ vs. VPDB (Vienna Pee Dee Belemnite) was added.

Table 2: Overview of sampling sites for sediments used in enrichment cultures. Ref. = reference

Site	Code	Short description	Ref.
Lake Plußsee	LakeP	Eutrophic lake with stable anoxic hypolimnion. Sample from 28 m depth. In situ temperature ca. 12°C.	[78]
Kuhgraben	Kug	Freshwater ditch close to Bremen. Sample from 2 m depth. *In situ* temperature during sampling, 25°C.	Similar to Zengler *et al.* [2]
Eckernförde Bay	E-Bay	Baltic Sea, with brackish water, samples from 28 m water depth. *In situ* temperature during sampling, 16°C.	[40, 79]
Gulf of Mexico	GoM	Sample from natural gas and oil seeps. Depth 560 m. *In situ* temperature 8-12°C.	[80]
Mangroves	Man	Sample from brackish water Mangroves (Brazil, 2005). Intertidal sediments, with *in situ* temperature during sampling,29°C	this work
Romanian mud volcanoes	Rov	Terrestrial mud volcano field with naturally occurring oil seepage. *In situ* temperature during sampling, 25°C	[81]
Weißandt-Gölzau	Göl	Gas samples from a groundwater aquifer contaminated with crude oil Saxony-Anhalt, Germany. *In situ* temperature 12°C.	this work

For the two dimensional isotopic analysis of methane, several microcosms from different methanogenic environments were set up anoxically using inocula obtained from different methanogenic field sites. Sediment samples for enrichment cultures were obtained from a range of habitats, including freshwater (Lake Plußsee, Kuhgraben), marine (Gulf of Mexico; Eckernförde Bay, Mangroves) and terrestrial (Romanian mud volcanoes) environments. Kuhgraben, a non-contaminated creek in Bremen, Germany, was described by Zengler *et al.* [2]. Plussee is a eutrophic lake in Northern Germany with relatively stable stratification and significant methane production in the sediments [78]. Eckernförde Bay is a marine site on the Baltic Sea side of Schleswig-Holstein (Germany) and is characterised by methane production in the sediment [40, 79]. Weißandt-Gölzau (Saxony-Anhalt, Germany) represents a mineral oil contaminated aquifer with high rates of microbial methane production within the contamination source zone. The oil phase in the source zone consists mainly of aliphatic hydrocarbons similar to those in diesel fuel with a low contribution from gasoline-related compounds (benzene, toluene, ethylbenzene, and xylenes). Details and acronyms used are provided in *Table 2*. The set up and transfer of the enrichment cultures was carried out as described by Zengler *et al.* [2]. Mineral medium was prepared according to Widdel and Bak [58] and the salinity was adjusted to the respective in situ conditions with NaCl. Hexadecane was added immobilised on Teflon filters (0.5 ml / 100 ml medium; [2]), methylnaphthalene was dissolved in 5 to 7 ml of the inert carrier HMN (2,2,4,4,6,8,8-heptamethylnonane,

10 mg methylnaphthalene ml^{-1} HMN) as described elsewhere [49]. Incubation of the enrichments was done in the dark at in situ temperatures (*Table 2*). CH$_4$ and CO$_2$ were analysed quantitatively in headspace samples using gas chromatography-flame ionisation (GC-FID; [82]). Samples for stable isotope analysis were stored on saturated NaCl. Contaminated ground water (30 ml) was added to a 50 ml flat glass bottle and sealed gas tight using butyl rubber stoppers and Al screw caps. Hexadecane was added at a final concentration of 0.03%$_{v/v}$. All microcosms were incubated horizontally without shaking. Gas samples from a methanogenic site in Weißandt-Gölzau were taken for the isotopic analysis of methane and CO$_2$.

Isotope analysis

An isotope ratio mass spectrometry system (Finnigan MAT 253, Thermofinnigan Bremen) was used. The system was coupled to a gas chromatograph (HP 6890 Series, Agilent Technology, USA) either via a combustion device (for carbon analysis) or via a pyrolyis unit (for hydrogen analysis; [83, 84]). For the GC separation of CH$_4$ and CO$_2$, headspace samples (from 50 to 500 µl) were injected into the GC instrument equipped with a CP-Porabond Q column (50 m x 0.32 mm x 0.5 µm, Varian) held at a constant temperature of 40℃ and a constant flow of He (2 ml min^{-1} for carbon and 1.6 ml min^{-1} for hydrogen).

For the isotope analysis of CO$_2$ in liquid samples, the culture samples were acidified to a pH below 2 to avoid fractionation via the carbonate system. For carbon isotope measurement, each sample was analysed at least two times and the statistical standard deviation of the measurements was always better than 0.5‰ STD (1□). For analysis of the hydrogen isotope composition at least three measurements for each sample were conducted and the STD (1□) was reported.

The carbon isotope signature of all substrates (unlabelled hexadecane, methylnaphthalene and toluene) were analysed with an elemental analyser (Euro EA, HEKAtech GmbH, Wegberg) coupled to an isotope ratio mass spectrometry system (Finnigan MAT 253, Thermo Finnigan Bremen). The same system was used for hydrogen isotope analysis. In addition, the hydrogen isotope composition of water from the field site (Weißandt-Gölzau), as well as water used for incubation experiments, was analysed [85]. This analysis required the addition of activated carbon to liquid samples in order to adsorb dissolved organic matter from the aqueous phase.

Analysis of carboxylic acid fraction

The microbial carboxylic acid fraction was isolated and methylated according to Bligh and Dyer [86] and Morrison and Smith [87], respectively. The fatty acid methyl esters (FAMEs)

were separated on a BPX-5 column (30 m x 0.32 mm x 0.25 µm, SGE Griesheim, Germany) using a HP 6890 gas chromatograph coupled to a HP 5973 quadrupole mass spectrometer (Hewlett Packard, Wilmington, USA). The temperature program for GC-MS was: 120°C (held 4 min) to 250°C at 4°C min $^{-1}$, to 300°C (held 10 min) at 20°C min $^{-1}$. The injector was set to 280°C and 1 µl of sample was injected splitless. Th e transfer line was held at 250°C and the He flow was set to 2 ml min^{-1}. The isotopic composition of individual FAMEs was determined using gas chromatography-combustion-isotope ratio mass spectrometry (GC-C-IRMS; Finni-gan MAT 253 ThermoFinnigan, Bremen, Germany). The isotopic values of the fatty acids have been corrected for the methyl groups introduced by methylation. The FAMEs were separated on a BPX-5 column (50 m x 0.32 mm x 0.25 µm, SGE, Darmstadt, Germany) us-ing an HP 6890 gas chromatograph with the following temperature program: 70°C (1 min to 120°C at 20°C min $^{-1}$, then to 265°C at 2°C min $^{-1}$ and then to 300°C (held 2 min). Samples (2 µl) were injected with a split ratio of 1:1. The injector temperature was 250°C. The He-flow was 2 ml min^{-1}. Vienna Pee Dee Belemnite [VPDB, $^{13}C/^{12}C = (11237.2\pm2.9) \times 10^{-6}$] was the standard for calibration of carbon isotope signatures [88] and Vienna Standard Mean Ocean Water [VSMOW, $^{2}H/^{1}H = (155.76\pm0.05) \times 10^{-6}$] was the standard for calibration of hydrogen isotope ratio values.

3.2.3. Results

Long term incubation with labelled hexadecane

In a long term incubation experiment (ca. 500 days) with enrichment cultures obtained from Kuhgraben sediment, methane and CO_2 formed during the degradation of U-^{13}C-labelled n-hexadecane (100 µl corresponding to 0.32 mmol, in 100 ml of 30 mM carbonate buffer of natural isotopic composition) were monitored to elucidate the active methanogenic pathway in the system. During the first 158 days, only low amounts of labelled methane were formed, indicating a lag phase with low methane production. After the initiation of methane production
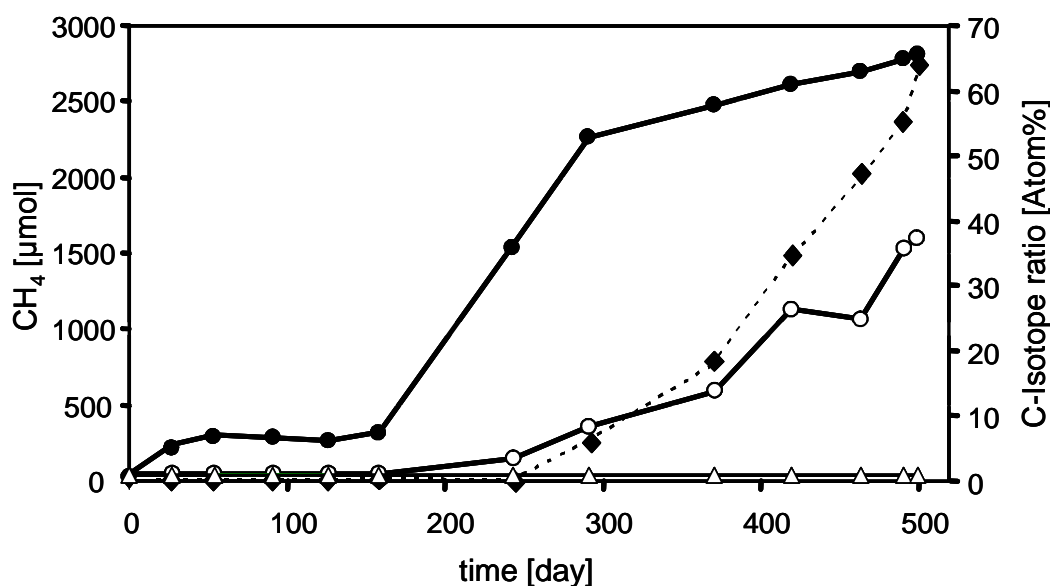
Figure 20: Carbon isotope ratio of CH₄ and CO₂ in an oil degrading enrichment culture obtained from Kuhgraben (Bremen, Germany) incubated with ^{13}C labelled n-hexadecane (100 atom%). ●, carbon isotope ratio of methane; o, carbon isotope ratio of CO_2; ♦, amount of methane produced; Δ, amount of methane in the sterile control.

at day 158, up to 2.7 mmol were produced until day 499. Simultaneously, the carbon isotope composition of methane and CO_2 rose to about 66 and 37 atom% ^{13}C, respectively, at day 499 demonstrating the conversion of labelled substrate into methane and CO_2 (*Figure 20*). The formation of 2.7 mmol CH_4 was consistent with a yield of about 70%, in relation to a stoichiometric transformation of 5.1 mmol of the *n*-hexadecane carbon into a maximum of 3.9 mmol of methane. A sterile control incubated under the same conditions did not show labelling of CO_2 or methane.

Carbon flux in the microbial community

A similar batch experiment with enrichment cultures obtained from Kuhgraben amended with 1-^{13}C-hexadecane as the sole source for carbon and energy was conducted to analyse the flux of carbon through the microbial community. The incorporation of an isotopic label into biomarkers such as carboxylic acids might provide evidence of direct usage of the labelled substrate as a carbon source. Such labelled acids might provide information about the structure of the methanogenic microbial community. The same enrichment culture as described above was cultivated using 1-^{13}C-hexadecane (5960‰) and unlabelled hexadecane (-32.4‰) as a carbon substrate and the pattern and isotopic composition of carboxylic acids was analysed. The isotopic composition of carboxylic acid carbon allowed us to identify three groups of different labelling intensity (*Figure 21*). The non-specific carboxylic acids *n*-C_{16} and *n*-C_{18} had an isotope value ranging from 50 to 500‰. Values from 2100 to 2700‰ combined

n-C$_{15}$ and *i,a*-C$_{15}$ to a second group. Their isotopic composition indicates that about 50% of the carbon used for the biosynthesis of these FAs was derived from 1-^{13}C-hexadecane. The highest labelling intensities, ranging from 4700 to 5800‰, were observed in the *n*-C17 and all 4-methyl fatty acids. The very extensive label showed that the parent organisms almost exclusively used the 1-^{13}C-hexadecane (5960‰) as a carbon source for the biosynthesis of the *n*-C$_{17}$ and all of the 4-methyl FAs. In contrast to this labelling experiment, the isotopic values of FAs synthesised with unlabelled hexadecane (-32.4‰) ranged from -30 to -37‰.
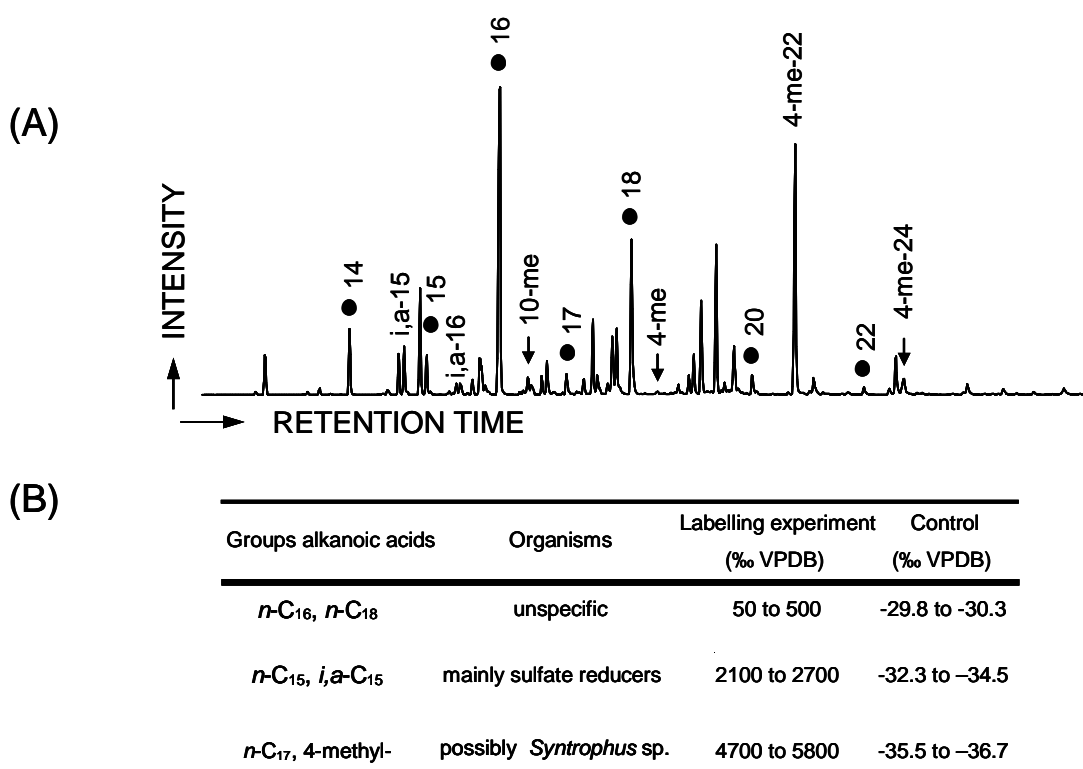
*Figure 21: (**A**) Carboxylic acid fraction as biomarkers for a methanogenic consortium grown on ^{13}C labelled n-hexadecane (5960‰ vs. VPDB; ●, n-alkanoic acids; 4-me, 4-methyl alkanoic acids; i,a , iso- and anteiso-alkanoic; 15, etc., carbon numbers). (**B**) Classification of microbial carboxylic acids according to carbon isotope ratio and biomarker function.*

Groups alkanoic acids	Organisms	Labelling experiment (‰ VPDB)	Control (‰ VPDB)
n-C$_{16}$, *n*-C$_{18}$	unspecific	50 to 500	-29.8 to -30.3
n-C$_{15}$, *i,a*-C$_{15}$	mainly sulfate reducers	2100 to 2700	-32.3 to –34.5
n-C$_{17}$, 4-methyl-	possibly *Syntrophus* sp.	4700 to 5800	-35.5 to –36.7

Isotope fractionation during methanogenic hydrocarbon degradation

In order to study the isotopic fractionation during methanogenic growth, the stable carbon isotopic composition of methane and CO$_2$ was monitored over time in an enrichment culture obtained from Kuhgraben sediments incubated with hexadecane of natural carbon isotope composition (-32.4‰; *Figure 22*). After a lag phase of ca. 240 days of low methane formation, the methane production strongly increased during the following 200 days to more than 1000 µmol (equivalent to the transformation of 36.8% of the added hexadecane carbon into methane). For the remaining 400 days of the experiment, the methane formation rate de-

creased slightly but resulting in an overall methane production of more than 1300 µmol after 850 days of incubation. This equates to a transformation of 47.8% of the hexadecane

Figure 22: Carbon isotope signature of CH₄ and CO₂ and methane production in an oil degrad-ing enrichment culture obtained from Kuhgraben (Bremen, Germany) incubated with n-hexadecane (δ¹³C, -32.4‰ vs. VPDB; ●, carbon isotope ratio of methane; o, carbon isotope ra-tio of CO₂; ♦, amount of methane produced.

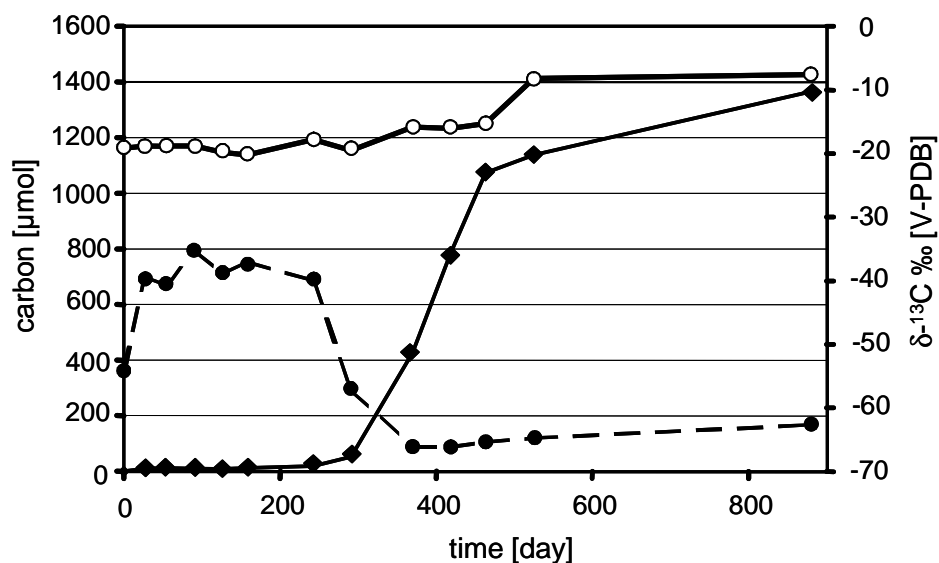carbon into methane. During the lag phase, methane with a carbon isotopic composition of about -40‰ was formed. The isotopic signal of methane during the first 50 days was influ-enced by isotopically light methane (-60‰) introduced with the inoculum, and the freshly produced methane (-40‰). The influence of the inoculum on the isotope signature of meth-ane disappeared after about 80 days. During the main phase of methane formation (days 240 to 440), the carbon isotopic composition of methane decreased to -65‰, while the CO_2 signature increased to -16‰, leading to an isotope discrimination of about 33 and 49‰ com-pared to hexadecane and CO_2, respectively. In the later phase of methane formation, the carbon isotope value of both methane and CO_2 slightly increased, maintaining discrimination of about 54‰ at the end of the experiment (850 days). This may be the result of strong iso-topic fractionation during CO_2 reduction.

Environmental variability of isotope enrichment factors

In order to examine the variability of carbon and hydrogen isotope enrichment factors for methane, we investigated the isotopic signature of methane, CO_2, and water during microbial formation of methane from mineral oil-related compounds. The investigation included 41 samples from oil degrading enrichment cultures from diverse methanogenic environments amended with different carbon sources, as well as six gas samples from different monitoring wells within a methane-producing, contaminated field site (*Table 2*). Slurry samples from

freshwater (Kug, LakeP), marine (Man, GoM, E-Bay) and terrestrial (Rov) sites were used. The carbon and hydrogen isotope values of the biologically produced methane in all enrichment cultures were clustered closely together. The variability ranged from -40 to -66‰ for carbon and from -317 to -390‰ for hydrogen, respectively (*Table 3*). The corresponding carbon isotope values for carbon dioxide exhibited a range from -18 to -1‰. Apart from these ranges, gas samples from a contaminated fieldsite ranged from -57 to -70‰ for carbon and from -329 to -373‰ for hydrogen, respectively.

In order to calculate the isotope enrichment factors $\varepsilon_{DIC-CH4}$, $\varepsilon_{substrate-CH4}$ and $\varepsilon_{H2O-CH4}$ for carbon and hydrogen, we determined the carbon isotope value for the applied carbonate buffer (-13.4±0.1‰ vs. VPDB), hexadecane (-23.2±0.1‰ vs. VPDB; -99.5±1.9‰ vs. SMOW), toluene (-26.1±0.5‰ vs. VPDB; -88±1.0‰ vs. SMOW) and methylnaphthalene (-25.3±0.1‰ vs. VPDB; -57.5±0.7‰ vs. SMOW) as well as the hydrogen isotope value of the water (-59.0±3.3‰ vs. SMOW). The calculated enrichment factors ranged from 26 to 60‰ and from 257 to 336‰ for carbon and hydrogen, respectively (*Table 3*). The enrichment factor representing the substrates ranged from 16 to 33‰ for carbon and from 174 to 318‰ for hydrogen. In order to asses the dependency of enrichment factors on the methanogenic environment the samples originated from, both carbon and hydrogen enrichment factors were plotted in a box-and-whisker-plot (*Figure 24*). The overall variability indicated by the whiskers for all habitats together ranged from 26 to 53‰ ($\varepsilon C_{CO2-CH4}$), 257 to 336‰ ($\varepsilon H_{H2O-CH4}$), 16 to 30‰ ($\varepsilon C_{C16-CH4}$), and 228 to 280‰ ($\varepsilon H_{C16-CH4}$).

Table 3 (next page): Variability in carbon and hydrogen enrichment factors during methanogenic growth with crude oil. The standard deviation of carbon isotope signatures was always better then the analytical accuracy of 0.5‰. The samples for hydrogen analysis were measured at least in triplicate. (nd, not detected; cooling, single injection with cryo focussing at -160 °C with liquid N_2; C_{16}, hexadecane; Me-Naph, methylnaphthalene; oil contam., crude oil contamination).

Code	Substrate	Methane $^{13}C/^{12}C$ [‰ VPDB]		Methane $^2H/^1H$ [‰ SMOW]		CO_2 $^{13}C/^{12}C$ [‰ VPDB]		Water $^2H/^1H$ [‰ SMOW]		εC DIC-CH_4	εC sub-CH_4	εH H_2O-CH_4	εH sub-CH_4
Kug1	C_{16}	-53.3	±0.5	-364.0	±5.8	-13.4	±0.1	-59.0	±3.3	39.9	30.1	305	264
Kug2	C_{16}	-52.3	±0.5	-353.1	±17.4	-13.4	±0.1	-59.0	±3.3	38.9	29.1	294	254
Kug3	C_{16}	-50.7	±0.5	-365.1	±18.2	-13.4	±0.1	-59.0	±3.3	37.3	27.5	306	266
Kug4	C_{16}	-49.6	±0.5	-377.2	±9.2	-13.4	±0.1	-59.0	±3.3	36.2	26.4	318	278
Kug5	C_{16}	-54.3	±0.5	-316.9	±3.2	-5.4	±0.5	-59.2	±2.6	48.9	21.9	258	174
Kug6	C_{16}	-57.9	±1.2	-389.7	±17.3	-5.4	±0.5	-53.9	±1.3	52.5	25.5	336	247
Kug7	C_{16}	-65.6	±0.7	-389.7	±10.6	-5.4	±0.5	-53.9	±1.3	60.2	33.2	336	247
Kug8	Toluene	-52.4	±0.6	-374.5	±3.0	-5.4	±0.5	-53.9	±1.3	47.0	26.3	321	287
LakeP1	C_{16}	-47.2	±0.1	-365.7	±11.3	-4.6	±0.1	-65.7	±1.1	42.7	24.0	300	266
LakeP2	C_{16}	-44.0	±0.5	-369.4	±7.0	-13.4	±0.1	-59.0	±3.3	30.6	20.8	310	270
LakeP3	C_{16}	-43.9	±0.5	-377.4	±2.7	-13.4	±0.1	-59.0	±3.3	30.5	20.7	318	278
LakeP4	C_{16}	-43.6	±0.5	-355.6	±3.8	-13.4	±0.1	-59.0	±3.3	30.2	20.4	297	256
LakeP5	Me-Naph	-49.3	±0.5	-375.3	±6.1	-13.4	±0.1	-59.0	±3.3	35.9	24.0	316	318
LakeP6	Me-Naph	-47.5	±0.5	-374.7	±7.2	-13.4	±0.1	-59.0	±3.3	34.1	22.2	316	317
Göl1	oil contam.	-59.1	±0.1	-343.1	±6.5	-19.2	±0.3	-71.8	±2.1	39.9	n.d.	271	n.d.
Göl2	oil contam.	-56.9	±0.1	-328.5	cooling	-17.8	±0.1	-71.2	±3.3	39.1	n.d.	257	n.d.
Göl3	oil contam.	-69.8	±0.1	-359.8	cooling	-21.1	±0.2	-69.1	±1.6	48.7	n.d.	291	n.d.
Göl4	oil contam.	-57.1	±0.0	-373.3	cooling	-15.3	±0.3	-75.7	±1.5	41.8	n.d.	298	n.d.
Göl5	oil contam.	-66.3	±0.2	-340.1	cooling	-20.3	±0.0	-72.8	±1.6	46.0	n.d.	267	n.d.
Göl6	oil contam.	-62.9	±0.0	-346.3	cooling	-11.0	±0.2	-71.3	±6.4	51.9	n.d.	275	n.d.
Man01	C_{16}	-42.0	±0.5	-374.4	±6.1	-13.4	±0.1	-59.0	±3.3	28.6	18.8	315	275
Man02	C_{16}	-42.5	±0.5	-371.0	±7.4	-13.4	±0.1	-59.0	±3.3	29.1	19.3	312	272
Man03	C_{16}	-48.6	±0.5	-359.1	±19.3	-13.4	±0.1	-59.0	±3.3	35.2	25.4	300	260
Man04	C_{16}	-44.5	±0.5	-330.3	±10.5	-13.4	±0.1	-59.0	±3.3	31.1	21.3	271	231
Man05	C_{16}	-50.0	±0.5	-382.0	±9.6	-13.4	±0.1	-59.0	±3.3	36.6	26.8	323	283
Man06	C_{16}	-45.8	±0.5	-359.7	±1.8	-13.4	±0.1	-59.0	±3.3	32.4	22.6	301	260
Man07	C_{16}	-42.9	±0.5	-325.5	±14.8	-13.4	±0.1	-59.0	±3.3	29.5	19.7	267	226
Man08	C_{16}	-48.9	±0.1	-345.2	±8.1	-2.4	±0.4	-67.0	±0.8	46.5	25.7	278	246
Man09	C_{16}	-48.6	±0.5	-354.1	±5.6	-13.4	±0.1	-59.0	±3.3	35.2	25.4	295	255
Man10	C_{16}	-44.2	±0.5	-331.6	±12.4	-13.4	±0.1	-59.0	±3.3	30.8	21.0	273	232
Man11	C_{16}	-46.9	±0.5	-343.9	±14.2	-13.4	±0.1	-59.0	±3.3	33.5	23.7	285	244
Man12	C_{16}	-39.8	±0.5	-369.6	±14.6	-13.4	±0.1	-59.0	±3.3	26.4	16.6	311	270
Man13	C_{16}	-46.5	±0.5	-363.3	±15.4	-13.4	±0.1	-59.0	±3.3	33.1	23.3	304	264
Man14	C_{16}	-39.6	±0.5	-360.5	±7.5	-13.4	±0.1	-59.0	±3.3	26.2	16.4	302	261
Man15	C_{16}	-45.7	±0.5	-361.5	±14.9	-13.4	±0.1	-59.0	±3.3	32.3	22.5	302	262
Man16	C_{16}	-42.1	±0.5	-372.7	±6.2	-13.4	±0.1	-59.0	±3.3	28.7	18.9	314	273
Man17	C_{16}	-45.4	±0.5	-343.3	±10.7	-13.4	±0.1	-59.0	±3.3	32.0	22.2	284	244
Man18	C_{16}	-48.3	±0.1	-367.8	±0.3	-0.8	±0.2	-65.0	±1.1	47.5	25.1	303	268
Man19	Me-Naph	-46.0	±0.5	-354.5	±6.4	-13.4	±0.1	-59.0	±3.3	32.6	20.7	295	297
Man20	Me-Naph	-44.8	±0.5	-346.1	±18.6	-13.4	±0.1	-59.0	±3.3	31.4	19.5	287	289
Man21	Me-Naph	-46.1	±0.5	-359.9	±12.5	-13.4	±0.1	-59.0	±3.3	32.7	20.8	301	302
GoM1	C_{16}	-56.1	±0.5	-348.5	±2.0	-13.4	±0.1	-59.0	±3.3	42.7	32.9	290	249
E-Bay1	C_{16}	-51.5	±0.5	-354.5	±11.5	-13.4	±0.1	-59.0	±3.3	38.1	28.3	296	255
Rov1	C_{16}	-48.8	±0.1	-364.6	±4.3	-6.7	±0.3	-67.3	±3.6	42.1	25.6	297	265
Rov2	C_{16}	-49.9	±0.6	-356.0	±7.2	-6.8	±0.3	-75.3	±0.6	43.1	26.7	281	256
Rov3	C_{16}	-42.2	±0.1	-355.0	±5.3	-7.4	±0.3	-79.5	±2.2	34.8	19.0	275	255
Rov4	C_{16}	-47.3	±0.1	-345.9	±16.7	-6.1	±0.1	-70.6	±1.5	41.2	24.1	275	246

3.2.4. Discussion

We conducted a series of experiments designed to investigate methane generation during hydrocarbon degradation. First, we conducted experiments with ^{13}C-labelled hexadecane to elucidate the degradation pathway and to characterise the methanogenic community. In a parallel experiment with unlabelled hexadecane, the carbon isotopic discrimination pattern over time was investigated. In a third set of experiments, we investigated the carbon and hydrogen discrimination pattern in order to characterise the biodegradation of different hydrocarbons in a variety of enrichment cultures from various ecosystems by means of isotopic analysis of methane, CO_2, water and the carbon source.

Metabolism of ^{13}C-labelled hexadecane

In our experiment with fully labelled ^{13}C-hexadecane, the ^{13}C label in methane and CO_2 demonstrates the transformation of hexadecane to methane and CO_2 by a consortium consisting of fermenting *Bacteria* and acetoclastic and CO_2 reducing *Archaea*, as described previously [2]. A stoichiometric calculation performed according to Zengler *et al.* [2] would result in a production of 3.9 mmol CH_4, if 0.32 mmol of hexadecane were provided. Thus, a final methane production of 2.7 mmol after 499 days of incubation implies a yield of about 70%. The fact that the isotopic composition of the methane did not show a complete labelling (100 atom%) suggests that a fraction of the methane was formed by the reduction of CO_2. This process lowers the isotope composition of the methane due to the unlabelled carbonate buffer (3 mmol) being used as the main source for CO_2. On one hand, methane formed by CO_2 reduction should therefore exhibit an isotopic signature similar to that of the buffer. On the other hand, the buffer represents a carbon reservoir that becomes enriched in ^{13}C as a result of CO_2 formation during methanogenesis from intermediates, such as acetate formed during the oxidation of labelled hexadecane.

In order to assess the extent to which [13]CO_2 derived from acetoclastic methanogenesis influences the isotopic label of the carbonate buffer, we assumed that unlabelled [12]CO_2 (0.9 mmol) from the carbonate buffer is used to form unlabelled methane (0.9 mmol) via CO_2 reduction. This reduces the residual carbonate buffer to 2.1 mmol. Based on a 70% yield, a maximum of 1.8 mmol of labelled [13]CO_2 would be added to the 2.1 mmol of unlabelled carbonate buffer (cf. *Equation (1* in [2]). According to the following simple dilution equation (*Equation (1)*), this would result in an isotopic value for the carbonate buffer of 47 atomic %.

Equation (1): $aR_{CO_2} = bR_{cb} + cR_{ac}$

Where R_{CO2}, R_{cb}, and R_{ac} are the isotope ratio values [atom%] of the measured carbon dioxide, carbonate buffer, and acetoclastically derived carbon dioxide, respectively, and $a = b + c$, where a, b, and c are the amounts [mmol] of the corresponding CO_2 pools.

The difference between the calculated isotope value for the carbonate buffer of 47 atom% and the actually determined isotope value of 37 atom% may be explained by the fact that carbon dioxide reduction may not exclusively consume unlabelled $^{12}CO_2$ from the carbonate buffer, but may also the acetate-derived $^{13}CO_2$, thus resulting in a ^{13}C-depleted isotopic value for the carbonate buffer in comparison to the theoretical calculated value. Assuming that the $^{12}CO_2$ reduction dominates the reduction of $^{13}CO_2$, the isotopic signature of methane (66 atom%) reflects the stoichiometric calculations of 65% and 35% for acetoclastic methanogenesis and CO_2 reduction quite well, respectively. This supports the author's assumptions that a cooperative community of fermentative *Bacteria* and methanogenic *Archaea* is responsible for the methane formation from hexadecane [2].

Microbial consortia involved in hexadecane degradation

In order to characterise the microbial consortia involved in methanogenic degradation of hexadecane, the above enrichment culture was incubated with 1-^{13}C-hexadecane and the biomass was analysed for the pattern and isotopic signature of carboxylic acids. Their isotope composition demonstrates the extent to which the microbial community used the carbon from the 1-^{13}C-hexadecane for the biosynthesis of lipids. Membrane lipids of *Archaea* consist of isoprenoids ether-linked to glycerol or other carbohydrates rather than ester bonded carboxylic acids [89-91]. These are not detected by the method used. The carboxylic acids could be divided into three different groups on the basis of isotope signatures. The lowest extent of label, 50 to 500‰, was seen in the *n*-C_{16} and *n*-C_{18} FAs, suggesting that the parent organisms of these relatively unspecific taxonomic biomarkers did not use the amended hexadecane as a major carbon source. These organisms were possibly transferred by the inoculation and may grow on dead cells or other unlabelled carbon sources. Microbes using detritus from dead cells as a carbon substrate will become labelled in a later phase of the experiment compared organisms using the 1-^{13}C-hexadecane directly. Since *n*-C_{16} and *n*-C_{18} FAs represent abundant species, despite a relatively low labelling, a significant part of the ^{13}C is bound to this FA fraction. For an estimation of the absolute carbon flux by means of the ^{13}C-label someone has to consider the concentration and the ^{13}C label in the respective FA. The low labelling thus may be interpreted as a result of relatively low usage of the 1-^{13}C-hexadecane by organisms synthesizing these compounds.

A second group with more extensive carbon labelling ranging from 2100 to 2700‰ consisted of *n*-C_{15} and *i,a*-C_{15} FAs. These acids may be characteristic for sulfate reducers like *Desul-*

fovibrio spp., *Desulfococcus* spp. or *Desulfosarcina* spp. [92]. These findings support the results obtained by Zengler *et al.* [2]. In a similar degradation experiment, the 16S rRNA gene sequences of the sulfate reducers affiliated with the delta subclass of *Proteobacteria* such as *Desulfovibrio desulfuricans*, *Desulfobacter postgatei*, *Syntrophobacter wolnii*, and *Desulfobulbus elongatus* have been detected [2].

The most extensive label was measured in the *n*-C_{17} FA or FAs with methyl groups at carbon atom 4 (from 4700 to 5800‰). In the investigation by Zengler *et al.* [2], some synthrophic *Bacteria* of the genus *Syntrophus* were detected by 16S ribosomal RNA gene sequences. In addition, Jones *et al.* [18] found *Synthrophus* sp. by means of 16S rRNA sequences. These organisms are commonly recovered in methanogenic alkane degrading systems, whereas controls without oil amendment also lacked detectable levels of *Synthrophus* sp. [18]. These *Bacteria* likely perform the degradation of hexadecane to acetate and hydrogen. In further steps, the acetate can then be used by acetoclastic *Archaea* for methanogenesis. The extensive incorporation of a ^{13}C-label into the carboxylic acid fraction clearly demonstrates a substantial usage of the labelled hexadecane as carbon source. Methylated branched fatty acids at carbon atom 2, 4 or 6 have been indentified as metabolites during growth of sulfate reducing *Bacteria* with alkanes of different chain lengths [29, 93, 94]. However, the highly labelled 4-methyl FAs detected in our investigation had chain lengths of more than 18 carbon atoms and can not be considered as intermediates of the degradation of hexadecane. In addition to the cellular fatty acid composition of *Synthrophus aciditrophicus* revealed by Jackson and colleagues [95], the highly labelled 4-methyl and *n*-C_{17} FAs might be suggested as tentative biomarkers for the alkane consuming synthrophic partners in an oil degrading methanogenic consortium, such as *Syntrophus* sp.

Isotope fractionation during methanogenic growth with hexadecane

To further characterise the isotopic fractionation during methanogenic growth with hexadecane, we cultivated an enrichment culture obtained from Kuhgraben with unlabelled hexadecane (-32.4‰). The carbon isotope signature for methane of -62‰ after 850 days clearly demonstrate the gas arises from microbial origins [76]. The isotope value for CO_2 increased in two steps. The first increase (from --8 to -16‰) coincided with the start of methane production after 240 days. The second (from -16 to -8‰) then signalled the initiation of CO_2 reduction (after 450 days) as a complimentary methane production to acetoclastic methanogenesis that predominantly occurred from day 240 to day 450. During the first 240 days, an enrichment factor of 22‰ between CO_2 and methane was calculated. This value falls within the range of enrichment factors reported as indicative of acetoclastic methanogenesis [76, 77, 96]. Thereby, it is assumed that the isotope fractionation between organic carbon and fermentatively produced acetate (methyl group) is negligible [97, 98]. With increasing methane

production, the influence of CO_2 reduction became more distinct, increasing the enrichment factor to 54‰. The discrimination of more than 40‰ between CO_2 and methane may be indicative of CO_2 reduction and supports the thermodynamic assumptions and molecular biological conclusions made by Zengler *et al.* [2] that methane was formed by acetoclastic and CO_2 reducing processes simultaneously. These two methanogenic pathways are considered to be associated with two different groups of *Archaea*. Members of the genus *Methanosaeta* have been found to be involved in the cleavage of acetate to CO_2 and methane. The second archeal genera, *Methanospirillum* and *Methanoculleus*, respectively, reduce the CO_2 to methane [2]. The same authors suggested that the acetate for methane generation is provided by *Bacteria* of the *Deltaproteobacterial* genus *Syntrophus* breaking the hydrocarbon chain of hexadecane down to acetate. The carbon enrichment factor ε between CO_2 and methane of 54‰ lies within a range that suggests that both methanogenic pathways influence the isotopic signal of microbially derived methane in our system. In contrast, a clear dominance of CO_2 reduction in methanogenic enrichment cultures from gas field formation waters has recently been shown [67]. The authors reported that methanogenic growth with acetate as a sole carbon source did not occur. The enrichment factor in our enrichment culture between hexadecane and methane resulted in a value of 30‰.

Enrichment factors in the environment

These enrichment factors might be influenced not only by the two different major methanogenic pathways, but also by the abiotic conditions of different environments such as substrate concentration, e.g. in Goevert and Conrad, [99], or energy status [100]. In order to examine the variability in carbon and hydrogen isotope enrichment factors during microbial formation of methane from crude oil-related compounds, the isotope signatures of methane, CO_2 and water were determined in 41 samples from different oil degrading methanogenic environments grown on several substrates (hexadecane, toluene and methylnaphthalene). The observed two dimensional isotope signature fell in a narrow range for both hydrogen and carbon isotopes (*Figure 23*). The relative CO_2 carbon isotope signatures were enriched in ^{13}C with regard to the carbon sources (*Table 3*). During aerobic degradation of jet fuels, organic contaminations or oil spills in ground water, CO_2 carbon isotope values close to those of the carbon source have been reported [101-104]. With decreasing redox potential, CO_2 became enriched in ^{13}C due to CO_2 reduction during methanogenesis [102].
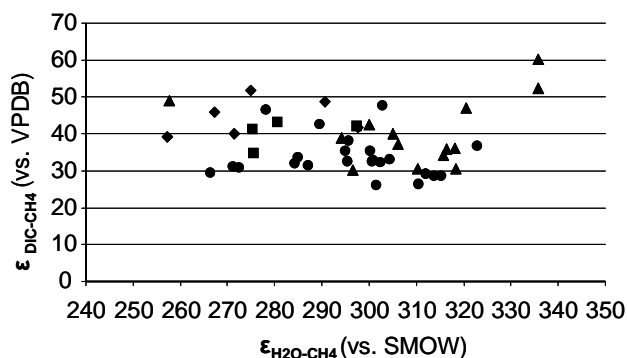
Figure 23: Carbon isotope enrichment factor $\varepsilon_{DIC\text{-}CH4}$ and hydrogen isotope enrichment factor $\varepsilon_{H2O\text{-}CH4}$ of 41 oil degrading enrichment cultures from different methanogenic environments and 6 gas samples from a contaminated methanogenic field site (Weißandt-Gölzau, Germany; ●, marine enrichments; ■, terrestrial enrichments;▲, freshwater enrichments; ♦, gas samples).

At sites where methanogenesis occurred, carbon isotope signatures in dissolved inorganic carbon were reported to range from -30 up to +12‰ [105, 106]. The model introduced by Jones *et al.* [18] predicts a stable carbon isotopic composition for carbon dioxide of about -16 and 21‰ for acetoclastic or hydrogenotrophic methanogenesis, respectively. However, the large range of carbon isotope values for carbon dioxide during methanogenesis lends difficulties to the characterisation of the degradation process.

In order to distinguish between the two major methanogenic pathways related to freshwater and marine environments, Whiticar *et al.* [77] reported carbon and hydrogen signatures for CO_2, methane, and water. In freshwater sediments, CH_4 production from acetate is the major methanogenic process with a contribution of 30-70% [107-109]. In marine sediments, it has been assumed that CH_4 is predominantly produced from CO_2 and H_2 [77]. According to this data set, the isotopic signatures of methane observed in our incubation exhibit a range typical for acetoclastic methanogenesis in freshwater systems. However, the results from our enrichment culture incubated with fully labelled hexadecane lead to the assumption that the isotopic signature of methane is influenced not only by acetoclastic methanogenesis but also by CO_2 reducing methanogenesis occurring simultaneously. This assumption should be considered for the observed enrichment factor ε for CO_2 and CH_4 ranging between 26 and 60‰ in our incubation. Based on Whiticar's [76] data set, fractionation factors $\varepsilon_{DIC\text{-}CH4}$ for acetoclastic methanogenesis and CO_2 reduction can be separated and exhibit a typical range from 40 to 55‰ and from 49 to 100‰, respectively. The range of ε_H between H_2O and methane from 257 to 336‰ is slightly larger than one would expect using regression curves obtained for acetoclastic methanogenesis and CO_2 reduction, e.g. in Sugimoto and Wada [110], as well as for cultures from landfill material with both methanogenic pathways occurring simultaneously at unknown relative proportions, e.g. Waldron *et al.* [111]. However, one has to consider a considerable impact of the hydrogen isotope signature for the environmental water and the partial pressure of hydrogen on the stable hydrogen composition of methane, e.g. in Burke Jr. [112]. Additionally, one has to take into account that the approximation of the isotopic fractionation fac-

tor is feasible for $\Delta\varepsilon < 100‰$ (Fry, 2003). Thus, the larger ε for hydrogen found here may imply some uncertainty.
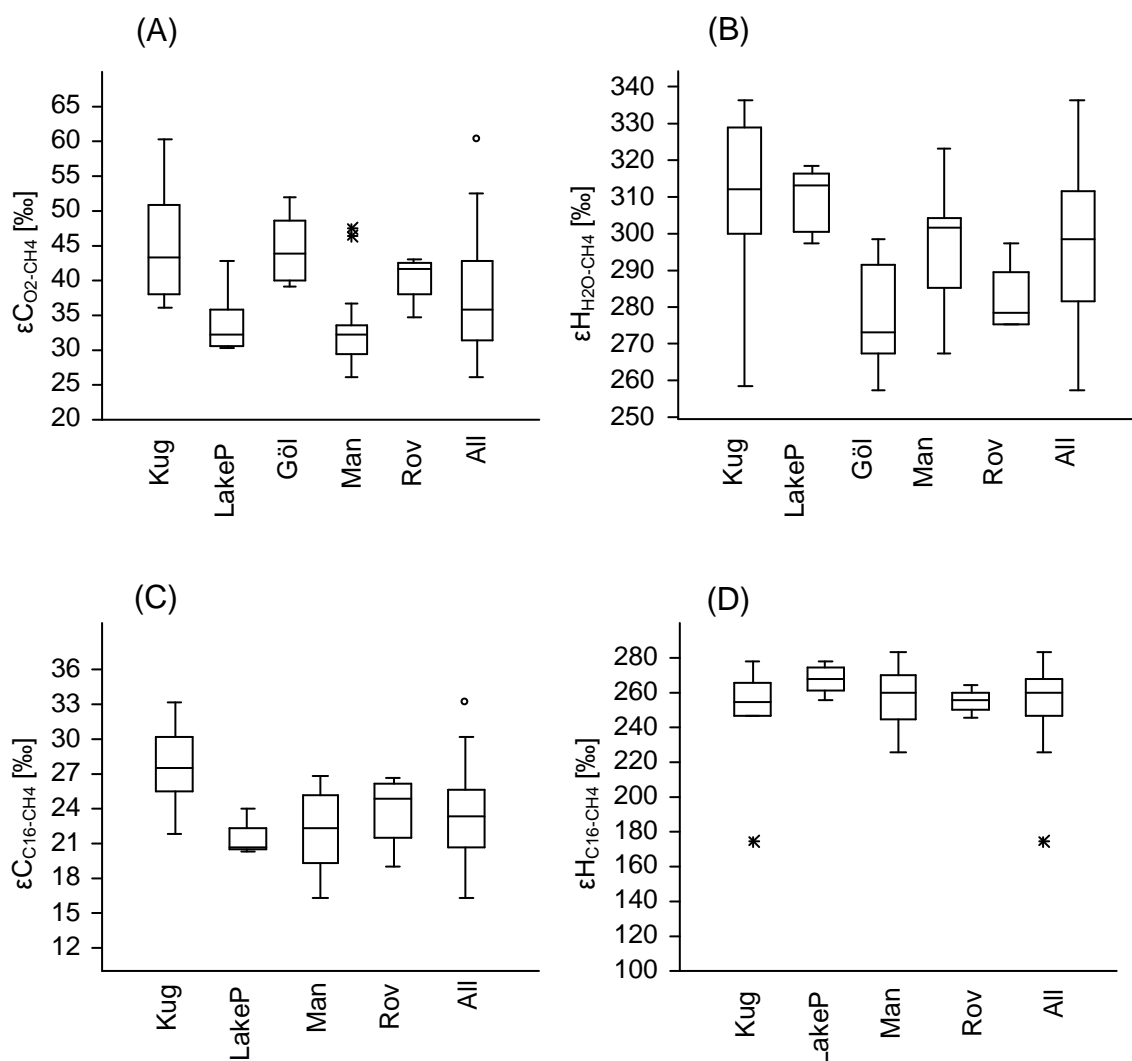

*Figure 24: Enrichment factors sorted by methanogenic environments: $\varepsilon C_{CO2\text{-}CH4}$ (**A**), $\varepsilon H_{H2O\text{-}CH4}$ (**B**), $\varepsilon C_{C16\text{-}CH4}$ (**C**), and $\varepsilon H_{C16\text{-}CH4}$ (**D**). The 25 and 75% quartiles are drawn using a box. The median is shown with a horizontal line inside the box. The whiskers are drawn from the top of the box up to the largest data point less than 1.5 times the box height from the box, and similarly below the box. ○, values outside the inner fence; ∗, values further than 3 times the box height from the box considered as outliers.*

In order to test the influence of different methanogenic communities on the ε values, we plotted the calculated values in a box-whisker-plot sorted by locations of the enrichment cultures (*Figure 24*). In addition to the enrichment factors between CO_2 and CH_4, and between H_2O and CH_4, respectively, this also includes the enrichment factors between hexadecane and CH_4. By comparing the variability of enrichment factors to each other, any influence of the methanogenic environment was apparent. Since a cooperation of fermenting *Bacteria* and methane producing *Archaea* was shown by Zengler *et al.* [2] and supported by our findings, it

can be assumed that similar oil degrading pathways are taking place and result in similar enrichment factors independent of the methanogenic environment. In conclusion, these ε values might be used to characterise hydrocarbon-driven methanogenesis during exploration in oil, coal, and gas reservoirs, shales, and contaminated aquifers, and may enable researchers to gain a better understanding of methanogenic microbial processes *in situ*.

The microbial conversion of crude oil to methane in mature oil reservoirs may enable us to recover an additional fraction of the large energy pool left behind by conventional recovery techniques. It has also been shown recently by Gieg *et al.* [45] that heavy crude oils stranded in mature reservoirs can be converted into methane by hydrocarbon degrading methanogenic consortia. This microbially enhanced oil recovery provides a novel biotechnological perspective for enhancing the recovery of hydrocarbons. The data provided here may contribute to a better characterisation of methanogenic processes in oil fields and help to develop further tools for tracing methanogenesis in situ.

Acknowledgements

3.3. References

1.   U.S. Department of Energy (2006) Undeveloped domestic oil resources. U.S. Department of Energy, Washington D.C.

2.   Zengler K, Richnow HH, Rossello-Mora R, Michaelis W & Widdel F (1999) Methane formation from long-chain alkanes by anaerobic microorganisms. *Nature* **401**: 266-269.

3.   Anderson RT & Lovley DR (2000) Hexadecane decay by methanogenesis. *Nature* **404**: 722-723.

4.   Head IM, Jones DM & Larter SR (2003) Biological activity in the deep subsurface and the origin of heavy oil. *Nature* **426**: 344-352.

5.   Feisthauer S, Siegert M, Seidel M, Richnow HH, Zengler K, Gründger F & Krüger M (2010) Isotopic fingerprinting of methane and CO_2 formation from aliphatic and aromatic hydrocarbons *Org Geochem* **41**: 482-490.

6.   Callaghan AV, Gieg LM, Kropp KG, Suflita JM & Young LY (2006) Comparison of Mechanisms of Alkane Metabolism under Sulfate-Reducing Conditions among Two Bacterial Isolates and a Bacterial Consortium. *Appl Environ Microbiol* **72**: 4274-4282.

7.   Cravo-Laureau C, Grossi V, Raphel D, Matheron R & Hirschler-Rea A (2005) Anaerobic *n*-Alkane Metabolism by a Sulfate-Reducing Bacterium, *Desulfatibacillum aliphaticivorans* Strain CV2803T. *Appl Environ Microbiol* **71**: 3458-3467.

8.   Rabus R (2005) Biodegradation of hydrocarbons under anoxic conditions. *Petroleum Microbiology,* (Ollivier B & Magot M, eds.), pp. 277-299. ASM Press, Washington D.C.

9.   Kniemeyer O, Fischer T, Wilkes H, Glockner FO & Widdel F (2003) Anaerobic Degradation of Ethylbenzene by a New Type of Marine Sulfate-Reducing Bacterium. *Appl Environ Microbiol* **69**: 760-768.

10.   Zhang T, Gannon SM, Nevin KP, Franks AE & Lovley DR (2010) Stimulating the anaerobic degradation of aromatic hydrocarbons in contaminated sediments by providing an electrode as the electron acceptor. *Environ Microbiol* **12**: 1011-1020.

11.   Vance I & Thrasher DR (2005) Reservoir souring: mechanisms and prevention. *Petroleum Microbiology,* (Ollivier B & Magot M, eds.), pp. 123-142. ASM Press, Washington, D.C.

12.   Lovley DR (2000) Anaerobic benzene degradation. *Biodegradation* **11**: 107-116.

13.   Kunapuli U, Lueders T & Meckenstock RU (2007) The use of stable isotope probing to identify key iron-reducing microorganisms involved in anaerobic benzene degradation. *ISME J* **1**: 643-653.

14.   Greene AC, Patel BKC & Sheehy AJ (1997) *Deferribacter thermophilus* gen. nov., sp. nov., a Novel Thermophilic Manganese- and Iron-Reducing Bacterium Isolated from a Petroleum Reservoir. *Int J Syst Bacteriol* **47**: 505-509.

15.   Greene AC, Patel BKC & Yacob S (2009) *Geoalkalibacter subterraneus* sp. nov., an anaerobic Fe(III)- and Mn(IV)-reducing bacterium from a petroleum reservoir, and emended descriptions of the family *Desulfuromonadaceae* and the genus *Geoalkalibacter*. *Int J Syst Evol Microbiol* **59**: 781-785.

16. Langenhoff AA, Brouwers-Ceiler DL, Engelberting JH, Quist JJ, Wolkenfelt JG, Zehnder AJ & Schraa G (1997) Microbial reduction of manganese coupled to toluene oxidation. *FEMS Microbiol Ecol* **22**: 119-127.

17. Langenhoff AA, Nijenhuis I, Tan NC, Briglia M, Zehnder AJ & Schraa G (1997) Characterisation of a manganese-reducing, toluene-degrading enrichment culture. *FEMS Microbiol Ecol* **24**: 113-125.

18. Jones DM, Head IM, Gray ND*, et al.* (2008) Crude-oil biodegradation via methanogenesis in subsurface petroleum reservoirs. *Nature* **451**: 176-180.

19. Chang W, Um Y & Holoman TR (2006) Polycyclic aromatic hydrocarbon (PAH) degradation coupled to methanogenesis. *Biotechnol Lett* **28**: 425-430.

20. Grbić-Galić D & Vogel TM (1987) Transformation of toluene and benzene by mixed methanogenic cultures. *Appl Environ Microbiol* **53**: 254-260.

21. Kazumi J, Caldwell ME, Suflita JM, Lovley DR & Young LY (1997) Anaerobic degradation of benzene in diverse environments. *Environ Sci Technol* **31**: 813-818.

22. Townsend GT, Prince RC & Suflita JM (2003) Anaerobic Oxidation of Crude Oil Hydrocarbons by the Resident Microorganisms of a Contaminated Anoxic Aquifer. *Environ Sci Technol* **37**: 5213-5218.

23. Herrmann S, Kleinsteuber S, Chatzinotas A, Kuppardt S, Lueders T, Richnow HH & Vogt C (2010) Functional characterization of an anaerobic benzene-degrading enrichment culture by DNA stable isotope probing. *Environ Microbiol* **12**: 401-411.

24. Kniemeyer O & Heider J (2001) Ethylbenzene Dehydrogenase, a Novel Hydrocarbon-oxidizing Molybdenum/Iron-Sulfur/Heme Enzyme. *J Biol Chem* **276**: 21381-21386.

25. Annweiler E, Materna A, Safinowski M, Kappler A, Richnow HH, Michaelis W & Meckenstock RU (2000) Anaerobic Degradation of 2-Methylnaphthalene by a Sulfate-Reducing Enrichment Culture. *Appl Environ Microbiol* **66**: 5329-5333.

26. Safinowski M & Meckenstock RU (2005) Methylation is the initial reaction in anaerobic naphthalene degradation by a sulfate-reducing enrichment culture. *Environ Microbiol* **8**: 347-352.

27. Zhang X & Young LY (1997) Carboxylation as an initial reaction in the anaerobic metabolism of naphthalene and phenanthrene by sulfidogenic consortia. *Appl Environ Microbiol* **63**: 4759-4764.

28. Boll M & Fuchs G (1995) Benzoyl-Coenzyme A Reductase (Dearomatizing), a Key Enzyme of Anaerobic Aromatic Metabolism. *Eur J Biochem* **234**: 921-933.

29. Grossi V, Cravo-Laureau C, Guyoneaud R, Ranchou-Peyruse A & Hirschler-Réa A (2008) Metabolism of n-alkanes and n-alkenes by anaerobic bacteria: A summary. *Org Geochem* **39**: 1197-1203.

30. Ministerie van de Vlaamse Gemeenschap AWK (2002) Uitvoeren van een waterbodemonderzook in het Albert I dok, het Tijdok an toegang Visartsluis te Zeebrugge: bijkomende studie. (De Vos M & Bogaert G, eds.), pp. 12-19. ABO n.v., Gent.

31. Lovley DR & Phillips EJP (1986) Organic Matter Mineralization with Reduction of Ferric Iron in Anaerobic Sediments. *Appl Environ Microbiol* **51**: 683-689.

32.   Lovley DR & Phillips EJP (1988) Novel Mode of Microbial Energy Metabolism: Organic Carbon Oxidation Coupled to Dissimilatory Reduction of Iron or Manganese. *Appl Environ Microbiol* **54**: 1472-1480.

33.   Nadkarni MA, Martin FE, Jacques NA & Hunter N (2002) Determination of bacterial load by real-time PCR using a broad-range (universal) probe and primers set. *Microbiology* **148**: 257–266.

34.   Takai K & Horikoshi K (2000) Rapid Detection and Quantification of Members of the Archaeal Community by Quantitative PCR Using Fluorogenic Probes. *Appl Environ Microbiol* **6**: 5066–5072.

35.   Nunoura T, Oida H, Toki T, Ashi J, Takai K & Horikoshi K (2006) Quantification of *mcrA* by quantitative fluorescent PCR in sediments from methane seep of the Nankai Trough. *FEMS Microbiol Ecol* **57**: 149-157.

36.   Schippers A & Nerretin LN (2006) Quantification of microbial communities in near-surface and deeply buried marine sediments on the Peru continental margin using real-time PCR. *Environ Microbiol* **8**: 1251–1260.

37.   Holmes DE, Finneran KT, O'Neil RA & Lovley DR (2002) Enrichment of Members of the Family *Geobacteraceae* Associated with Stimulation of Dissimilatory Metal Reduction in Uranium-Contaminated Aquifer Sediments. *Appl Environ Microbiol* **68**: 2300–2306.

38.   Pruesse E, Quast C, Knittel K, Fuchs B, Ludwig W, Peplies J & Glöckner FO (2007) SILVA: a comprehensive online resource for quality checked and aligned ribosomal RNA sequence data compatible with ARB. *Nucleic Acids Res* **35**: 7188-7196.

39.   Liesack W & Dunfield PF (2004) T-RFLP Analysis: A Rapid Fingerprinting Method for Studying Diversity, Structure, and Dynamics of Microbial Communities. *Environmental Microbiology: Methods and Protocols,* Vol. 16 (Walker JM, Spencer JFT & Ragout de Spencer AL, eds.), pp. 23-37. Humana Press.

40.   Treude T, Krüger M, Boetius A & Jørgensen BB (2005) Environmental control on anaerobic oxidation of methane in the gassy sediments of Eckernförde Bay (German Baltic). *Limnol Oceanogr* **50**: 1771-1786.

41.   Zhang W, Ki JS & Qian PY (2008) Microbial diversity in polluted harbor sediments I: bacterial community assessment based on four clone libraries of 16S rDNA. *Estuar Coast Shelf Sci* **76**: 668-681.

42.   Gillan D & Pernet P (2007) Adherent bacteria in heavy metal contaminated marine sediments. *Biofouling* **23**: 1-13.

43.   Heijs SK, Sinninghe Damsté JS & Forney LJ (2005) Characterization of a deep-sea microbial mat from an active cold seep at the Milano mud volcano in the Eastern Mediterranean Sea. *FEMS Microbiol Ecol* **54**: 47-56.

44.   Wegener G, Shovitri M, Knittel K, Niemann H, Hovland M & Boetius A (2008) Biogeochemical processes and microbial diversity of the Gullfaks and Tommeliten methane seeps (Northern North Sea). *Biogeosciences* **5**: 1127-1144.

45.   Gieg LM, Duncan KE & Suflita JM (2008) Bioenergy Production via Microbial Conversion of Residual Oil to Natural Gas. *Appl Environ Microbiol* **74**: 3022-3029.

46. Coates JD, Anderson RT & Lovley DR (1996) Oxidation of Polycyclic Aromatic Hydrocarbons under Sulfate-Reducing Conditions. *Appl Environ Microbiol* **62**: 1099-1101.

47. Hayes LA, Nevin KP & Lovley DR (1999) Role of prior exposure on anaerobic degradation of naphthalene and phenanthrene in marine harbor sediments. *Org Geochem* **30**: 937-945.

48. Langenhoff AAM, Zehnder AJB & Schraa G (1989) Behaviour of toluene, benzene and naphthalene under anaerobic conditions in sediment columns. *Biodegradation* **7**: 267-274.

49. Musat F, Galushko A, Jacob J*, et al.* (2009) Anaerobic degradation of naphthalene and 2-methylnaphthalene by strains of marine sulfate-reducing bacteria. *Environ Microbiol* **11**: 209-219.

50. Sharak Genthner BR, Townsend GT, Lantz SE & Mueller JG (1997) Persistence of Polycyclic Aromatic Hydrocarbon Components of Creosote Under Anaerobic Enrichment Conditions. *Arch Environ Contam Toxicol* **32**: 99-105.

51. Klüber HD & Conrad R (1998) Effects of nitrate, nitrite, NO and N2O on methanogenesis and other redox processes in anoxic rice field soil. *FEMS Microbiol Ecol* **25**: 301-319.

52. Li C-H, Wong Y-S & Tam NF-Y (2010) Anaerobic biodegradation of polycyclic aromatic hydrocarbons with amendment of iron(III) in mangrove sediment slurry. *Bioresour Technol* **101**: 8083-8092.

53. van Bodegom P, M., Scholten JCM & Stams AJM (2004) Direct inhibition of methanogenesis by ferric iron. *FEMS Microbiol Ecol* **49**: 261-268.

54. Widdel F & Rabus R (2001) Anaerobic biodegradation of saturated and aromatic hydrocarbons. *Curr Opin Biotechnol* **12**: 259-276.

55. Wegener G, Niemann H, Elvert M, Hinrichs K-U & Boetius A (2008) Assimilation of methane and inorganic carbon by microbial communities mediating the anaerobic oxidation of methane. *Environ Microbiol* **10**: 2287-2298.

56. Knittel K & Boetius A (2009) Anaerobic Oxidation of Methane: Progress with an Unknown Process. *Annu Rev Microbiol* **63**: 311-334.

57. Thauer RK & Shima S (2008) Methane as Fuel for Anaerobic Microorganisms. *Ann N Y Acad Sci* **1125**: 158-170.

58. Widdel F & Bak F (1992) Gram-negative mesophilic sulfate-reducing bacteria. *The Prokaryotes,* Vol. 4 (Dworkin M, ed.), pp. 3352-3372. Springer, New York.

59. Beal EJ, House CH & Orphan VJ (2009) Manganese- and Iron-dependent marine methane oxidation. *Science* **325**: 184-187.

60. Mussmann M, Ishii K, Rabus R & Amann R (2005) Diversity and vertical distribution of cultured and uncultured Deltaproteobacteria in an intertidal mud flat of the Wadden Sea. *Environ Microbiol* **7**: 405-418.

61. Hirayama H, Sunamura M, Takai K*, et al.* (2007) Culture-Dependent and -Independent Characterization of Microbial Communities Associated with a Shallow Submarine Hydrothermal System Occurring within a Coral Reef off Taketomi Island, Japan. *Appl Environ Microbiol* **73**: 7642-7656.

62. Schloss PD, Westcott SL, Ryabin T*, et al.* (2009) Introducing mothur: Open-Source, Platform-Independent, Community-Supported Software for Describing and Comparing Microbial Communities. *Appl Environ Microbiol* **75**: 7537-7541.

63. Ye W, Liu X, Lin S, Tan J, Pan J, Li D & Yang H (2009) The vertical distribution of bacterial and archaeal communities in the water and sediment of Lake Taihu. *FEMS Microbiol Ecol* **70**: 263-276.

64. Lopez-Archilla AI, Moreira D, Velasco S & P. L-G (2007) Archaeal and bacterial community composition of a pristine coastal aquifer in Donana National Park, Spain. 2007. *Aquat Microb Ecol* **47**: 123-139.

65. Inagaki F, Kuypers MMM, Tsunogai U*, et al.* (2006) Microbial community in a sediment-hosted CO_2 lake of the southern Okinawa Trough hydrothermal system. *Proc Natl Acad Sci U S A* **103**: 14164-14169.

66. Dolfing J, Larter SR & Head IM (2007) Thermodynamic constraints on methanogenic crude oil biodegradation. *ISME J* **2**: 442-452.

67. Gray N, Sherry A, Larter S*, et al.* (2009) Biogenic methane production in formation waters from a large gas field in the North Sea. *Extremophiles* **13**: 511-519.

68. Grigoryan A & Voordouw G (2008) Microbiology to Help Solve Our Energy Needs. *Ann N Y Acad Sci* **1125**: 345-352.

69. Finkelstein M, DeBruyn RP, Weber JL & Dodson JB (2005) Buried hydrocarbons: A resource for biogenic methane generation. *World Oil* **226**: 61-67.

70. Wilkes H, Boreham C, Harms G, Zengler K & Rabus R (2000) Anaerobic degradation and carbon isotopic fractionation of alkylbenzenes in crude oil by sulphate-reducing bacteria. *Org Geochem* **31**: 101-115.

71. Wilkes H, Kühner S, Bolm C, Fischer T, Classen A, Widdel F & Rabus R (2003) Formation of *n*-alkane- and cycloalkane-derived organic acids during anaerobic growth of a denitrifying bacterium with crude oil. *Org Geochem* **34**: 1313-1323.

72. Anderson RT & Lovley DR (1999) Naphthalene and benzene degradation under Fe(III)-reducing conditions in petroleum-contaminated aquifers. *Bioremediat J* **3**: 121-135.

73. Siddique T, Fedorak PM & Foght JM (2006) Biodegradation of Short-Chain n-Alkanes in Oil Sands Tailings under Methanogenic Conditions. *Environ Sci Technol* **40**: 5459-5464.

74. U.S. Energy Information Administration & U.S. Department of Energy (2007) International Energy Outlook. Office of Integrated Analysis and Forecasting, Washington, D.C.

75. DeLuchi MA (1991) Emissions of Greenhouse Gases from the Use of Transportation Fuels and Electricity. Vol. 1, Argonne National Laboratory, Argonne, IL.

76. Whiticar MJ (1999) Carbon and hydrogen isotope systematics of bacterial formation and oxidation of methane. *Chem Geol* **161**: 291-314.

77. Whiticar MJ, Faber E & Schoell M (1986) Biogenic methane formation in marine and freshwater environments: CO_2 reduction vs. acetate fermentation--Isotope evidence. *Geochim Cosmochim Acta* **50**: 693-709.

78. Eller G, Känel L & Krüger M (2005) Cooccurrence of Aerobic and Anaerobic Methane Oxidation in the Water Column of Lake Plußsee. *Appl Environ Microbiol* **71**: 8925–8928.

79. Whiticar MJ (2002) Diagenetic relationships of methanogenesis, nutrients, acoustic turbidity, pockmarks and freshwater seepages in Eckernförde Bay. *Mar Geol* **182**: 29-53.

80. Joye SB, Boetius A, Orcutt BN, Montoya JP, Schulz HN, Erickson MJ & Lugo SK (2004) The anaerobic oxidation of methane and sulfate reduction in sediments from Gulf of Mexico cold seeps. *Chem Geol* **205**: 219-238.

81. Alain K, Holler T, Musat F, Elvert M, Treude T & Krüger M (2006) Microbiological investigation of methane- and hydrocarbon-discharging mud volcanoes in the Carpathian Mountains, Romania. *Environ Microbiol* **8**: 574-590.

82. Krüger M, Frenzel P & Conrad R (2001) Microbial processes influencing methane emission from rice fields. *Global Change Biology* **7**: 49-63.

83. Fischer A, Theuerkorn K, Stelzer N, Gehre M, Thullner M & Richnow HH (2007) Applicability of Stable Isotope Fractionation Analysis for the Characterization of Benzene Biodegradation in a BTEX-contaminated Aquifer. *Environ Sci Technol* **41**: 3689-3696.

84. Richnow HH, Meckenstock RU, Ask Reitzel L, Baun A, Ledin A & Christensen TH (2003) In situ biodegradation determined by carbon isotope fractionation of aromatic hydrocarbons in an anaerobic landfill leachate plume (Vejen, Denmark). *J Contam Hydrol* **64**: 59-72.

85. Gehre M, Geilmann H, Richter J, Werner RA & Brand WA (2004) Continuous flow ^{2}H/^{1}H and ^{18}O/^{16}O analysis of water samples with dual inlet precision. *Rapid Commun Mass Spectrom* **18**: 2650-2660.

86. Bligh EG & Dyer WJ (1959) A rapid method for total lipid extraction and purification. *Can J Biochem Physiol* **37**: 911-917.

87. Morrison WR & Smith LM (1964) Preparation of fatty acid methyl esters and dimethylacetals from lipids with boron fluoride-methanol. *J Lipid Res* **5**: 600-608.

88. Coplen TB, Brand WA, Gehre M, Gröning M, Meijer HAJ, Toman B & Verkouteren RM (2006) After two decades a second anchor for the VPDB δ^{13}C scale. *Rapid Commun Mass Spectrom* **20**: 3165-3166.

89. De Rosa M & Gambacorta A (1988) The lipids of archaebacteria. *Prog Lipid Res* **27**: 153-175.

90. Jones WJ, Nagle DP, Jr. & Whitman WB (1987) Methanogens and the diversity of archaebacteria. *Microbiol Mol Biol Rev* **51**: 135-177.

91. Langworthy TA (1985) Lipids of archaebacteria. *The bacteria,* (Woese CR & Wolfe RS, eds.), pp. 459-497. Academic Press, New York.

92. Kohring LL, Ringelberg DB, Devereux R, Stahl DA, Mittelman MW & White DC (1994) Comparison of phylogenetic relationships based on phospholipid fatty acid profiles and ribosomal RNA sequence similarities among dissimilatory sulfate-reducing bacteria. *FEMS Microbiol Lett* **119**: 303-308.

93. So CM, Phelps CD & Young LY (2003) Anaerobic Transformation of Alkanes to Fatty Acids by a Sulfate-Reducing Bacterium, Strain Hxd3. *Appl Environ Microbiol* **69**: 3892-3900.

94. So CM & Young LY (1999) Initial Reactions in Anaerobic Alkane Degradation by a Sulfate Reducer, Strain AK-01. *Appl Environ Microbiol* **65**: 5532-5540.

95.   Jackson BE, Bhupathiraju VK, Tanner RS, Woese CR & McInerney MJ (1999) *Syntrophus aciditrophicus* sp. nov., a new anaerobic bacterium that degrades fatty acids and benzoate in syntrophic association with hydrogen-using microorganisms. *Arch Microbiol* **171**: 107-114.

96.   Conrad R (2005) Quantification of methanogenic pathways using stable carbon isotopic signatures: a review and a proposal. *Org Geochem* **36**: 739-752.

97.   Blair N, Leu A, Munoz E, Olsen J, Kwong E & Des Marais D (1985) Carbon isotopic fractionation in heterotrophic microbial metabolism. *Appl Environ Microbiol* **50**: 996-1001.

98.   Blair NE & Carter Jr WD (1992) The carbon isotope biogeochemistry of acetate from a methanogenic marine sediment. *Geochim Cosmochim Acta* **56**: 1247-1258.

99.   Goevert D & Conrad R (2009) Effect of Substrate Concentration on Carbon Isotope Fractionation during Acetoclastic Methanogenesis by Methanosarcina barkeri and M. acetivorans and in Rice Field Soil. *Appl Environ Microbiol* **75**: 2605-2612.

100.   Penning H, Plugge CM, Galand PE & Conrad R (2005) Variation of carbon isotope fractionation in hydrogenotrophic methanogenic microbial cultures and environmental samples at different energy status. *Global Change Biology* **11**: 2103-2113.

101.   Aggarwal PK & Hinchee RE (1991) Monitoring in situ biodegradation of hydrocarbons by using stable carbon isotopes. *Environ Sci Technol* **25**: 1178-1180.

102.   Baedecker MJ, Cozzarelli IM, Eganhouse RP, Siegel DI & Bennett PC (1993) Crude oil in a shallow sand and gravel aquifer--III. Biogeochemical reactions and mass balance modeling in anoxic groundwater. *Appl Geochem* **8**: 569-586.

103.   Suchomel KH, Kreamer DK & Long A (1990) Production and transport of carbon dioxide in a contaminated vadose zone: a stable and radioactive carbon isotope study. *Environ Sci Technol* **24**: 1824-1831.

104.   van de Velde KD, Marley MC, Studer J & Wagner DM (1995) Stable carbon isotope analysis to verify bioremediation and bioattenuation. *Monitoring and verification of bioremediation,* (Hinchee RE, Douglas GS & Ong SK, eds.), pp. 241-257. Battelle Press, Columbus.

105.   Conrad ME, Daley PF, Fischer ML, Buchanan BB, Leighton T & Kashgarian M (1997) Combined ^{14}C and δ^{13}C Monitoring of *in Situ* Biodegradation of Petroleum Hydrocarbons. *Environ Sci Technol* **31**: 1463-1469.

106.   Landmeyer JE, Vroblesky DA & Chapelle FH (1996) Stable Carbon Isotope Evidence of Biodegradation Zonation in a Shallow Jet-Fuel Contaminated Aquifer. *Environ Sci Technol* **30**: 1120-1128.

107.   Koyama T (1955) Gaseous metabolism in lake mud and paddy soils. *Journal of Earth Sciences, Nagoya University* **3**: 68-76.

108.   Schütz H, Seiler W & Conrad R (1989) Processes involved in formation and emission of methane in rice paddies. *Biogeochemistry* **7**: 33-53.

109.   Takai Y (1970) The mechanism of methane fermentation in flooded paddy soil. *Soil Sci Plant Nutr* **16**: 238-244.

110.   Sugimoto A & Wada E (1995) Hydrogen isotopic composition of bacterial methane: CO2/H2 reduction and acetate fermentation. *Geochim Cosmochim Acta* **59**: 1329-1337.

111. Waldron S, Watson-Craik IA, Hall AJ & Fallick AE (1998) The carbon and hydrogen stable isotope composition of bacteriogenic methane: A laboratory study using a landfill inoculum. *Geomicrobiol J* **15**: 157 - 169.

112. Burke Jr RA Possible influence of hydrogen concentration on microbial methane stable hydrogen isotopic composition. *Chemosphere* **26**: 55-67.

Chapter 4

Methane oxidation

4.1. Anaerobic oxidation of methane dominates hydrocarbon degradation at a marine methane seep in a forearc basin off Sumatra, Indian Ocean

Michael Siegert, Martin Krüger*, Barbara M.A. Teichert[1], Michael Wiedicke, Axel Schippers

Bundesanstalt für Geowissenschaften und Rohstoffe (BGR), Stilleweg 2, 30655 Hannover, Germany

[1]Present address: Institut für Geologie und Paläontologie, Universität Münster, Corrensstr. 24, 48149 Münster, Germany

Manuscript in preparation

Key words: DGGE, quantitative PCR, CARD-FISH, methane seep, stable isotopes, AOM, hydrocarbon dependent methanogenesis

Running title: AOM in the Sumatra forearc

*Corresponding author: Dr. Martin Krüger phone: +495116433102, fax: +495116433664, Email: martin.krueger@bgr.de

Abstract

Anaerobic oxidation of methane (AOM) is an important process to remove the greenhouse gas methane from marine environments. It receives worldwide attention with intensive research activities. A cold methane-seep was discovered in a forearc basin off the island Sumatra, exhibiting a typical methane-seep adapted microbial community. The relevance of AOM was reflected by ^{13}C depleted isotopic signatures of dissolved inorganic carbon (DIC). The anaerobic conversion of methane to CO_2 was confirmed in a ^{13}C labelling experiment. Methane fuelled a vital microbial and invertebrate community which was reflected in cell numbers of up to 4×10^9 cells cm^{-3} sediment and ^{13}C depleted guts of crabs populating the seep area. The microbial community was analysed by total cell counting, catalysed reporter deposition – fluorescence in situ hybridisation (CARD-FISH), quantitative real-time PCR (qPCR) and denaturing gradient gel electrophoresis (DGGE). The archaeal community comprised largely members of ANME-1 and ANME-2, while δ-*Proteobacteria*, the OP9 cluster and *Anaerolineaceae* dominated the *Bacteria*. Active hydrocarbon-dependent methanogenic microcosms were obtained – despite the absence of seepage of higher hydrocarbons in the sediments. In conclusion, the majority of the microbial community at the seep consisted of AOM related microorganisms while the relevance of higher hydrocarbons as microbial substrates was negligible.

4.1.1. Introduction

Anaerobic oxidation of methane (AOM) has been described for decades, but became accepted as an important key process in anaerobic carbon cycling only during the last decade [1-5]. It was observed in numerous marine environments, e.g. in microbial reefs of the Black Sea [6], in the Black Sea water column [7], mud volcanoes [8, 9], at methane hydrates [10], sediment sulfate-methane transition zones (SMTZ) of the eastern and western Baltic Sea [11], the North Sea [12], the Chilean continental margin [13] and deep subsurface sediments [14, 15]. However, also limnic systems host AOM performing microbial consortia [16].

In deep marine sediments, electron acceptors are depleted and methane is relatively stable against microbial degradation, while at the sediment surface more electron acceptors as oxidants are available [17]. Parts of the oxidised methane precipitate as carbonates of various morphologies in and on top of the sediments. This was reported e.g. for the Black Sea [6], the Mediterranean Sea [18], the Hydrate Ridge [19] and the Gulf of Mexico [20]. Nonetheless, carbonate is also a reaction product of most organic matter degradation processes, and hence the reverse conclusion that carbonates exclusively indicate AOM is untrue. In the initial reports, methanogenesis and sulfate reduction were believed to be mutually exclusive

processes [21]. However, AOM coincides with methanogenesis [8, 22], and was therefore proposed to be reverse methanogenesis [23, 24].

So far, microbial sulfate and nitrite reduction have been reported to couple to AOM as a joint process of specialised methane-oxidising (ANME, <u>an</u>aerobic <u>me</u>thanotrophic *Archaea*) and sulfate- or nitrite-reducing bacterial microorganisms [25, 26].

AOM can potentially occur in marine sediments of various geological structures. In consequence of tectonic activity, faults alter overlying sediments of petroleum and natural gas reservoirs. On the seafloor, conduits give rise to gas seeps, gas hydrates, and mud volcanoes [27]. Since the forearc sediment basins off Sumatra frequently experience tectonic activity, they are optimal locations for studying AOM as well as microbial hydrocarbon degradation to methane [28]. Microbial degradation of higher hydrocarbons to methane has been demonstrated in several laboratory studies (Chapter 3; [29-31]) but the relevance in nature is not yet clear. However, it is possible that microbial hydrocarbon degradation and subsequent methane release have a greater impact on benthic communities than currently recognised. As free or dissolved gas, methane and the oxidised carbonate product may serve as indicators for deep hydrocarbon reservoirs and subsurface microbial oil degradation [20, 31, 32], methane gas hydrates [19, 33] or both [34, 35].

The Sumatra forearc is spatially remote from previous study sites. Continental margins and their forelands were examined in numerous biogeochemical studies [19, 36-38] and AOM as well as microbial hydrocarbon degradation was associated mainly to gas seeps as well as mud volcanoes [8, 10, 18, 39-42]. Previous studies often did not investigate other hydrocarbons than methane. Our main objectives on the R/V Sonne cruise SO189-2 into the Sumatra forearc basins were to identify and characterise seeps of methane and higher hydrocarbons, and to clarify the role of methanotrophs compared to other hydrocarbon degrading microorganisms in anaerobic marine environments. Thus, we used different biogeochemical proxies for AOM and anaerobic hydrocarbon degradation combined with micro- and molecular biological tools to determine potential microbial activities and the involved populations.

4.1.2. Materials and Methods

<u>Site description and sampling</u>

General features of the Simeulue and the Nias Basin in the Sumatra forearc are described by Sieh & Natawitjaja [43] and Schippers, *et al.* [44]. An area without seismic reflections ("seismic blanking") was discovered in the SE of the Simeulue basin, indicating free gases in the sediment (*Figure 25* and *Figure 26*). Free gas measurements of samples taken from the water column confirmed a possible gas seep in this area. Additionally, pictures and samples

from the seafloor revealed a typical seep fauna comprising mainly bivalves and white crabs [45], colonising outcropping carbonate precipitations and the surrounding sediments.

Table 4: Sampled stations in forearc sediment basins off Sumatra. cmbsf = centimetres below seafloor

		Temperature [°C]	Sampling depth [cmbsf]	Water depth [m]	Ship position		Station
Referred as	Basin				Longitude	Latitute	
					Seep stations (Simeulue)		
station 1	Simeulue	6	16	1130	96°45.424E	2°33.780N	128TV
station 2	Simeulue	6	6	1134	96°45.404E	2°33.770N	137TV
station 3	Simeulue	6	28	1135	96°45.410E	2°33.800N	98MC
station 4	Simeulue	6	333	1134	96°45.429E	2°33.781N	131SL
station 5	Simeulue	6	surface	1135	96°45.410E	2°33.800N	127TV
station 6	Simeulue	6	133	1134	96°45.410E	2°33.830N	70SL
station 7	Simeulue	6	surface	1134	96°45.397E	2°33.818N	134TV
					Nias		
station 8	Nias	22	40	90	98°02,415E	0°59,610N	52MC
station 9	Nias	23	40	70	97°47,426E	0°59,571N	64MC

During the R/V Sonne cruise SO189-2 in 2006, 9 sediment stations of the Simeulue basin and the Nias basin were sampled to different depth as summarized in *Table 4*. The sediment

was sampled using a 6 m long gravity corer (SL), a 0.5 m long multicorer (MC) and a TV camera guided 0.9 x 0.9 m grab (TV). The TV grab instrument was towed above the seafloor and it was positioned on the seafloor as the area of interest was visible on the TV camera picture. Then the closure of the grab was initiated. After closure of the grab and shipboard recovery, the sediment in the grab was further sampled using hand-held small pushcores. A station list including core ID is displayed in *Table 4*.
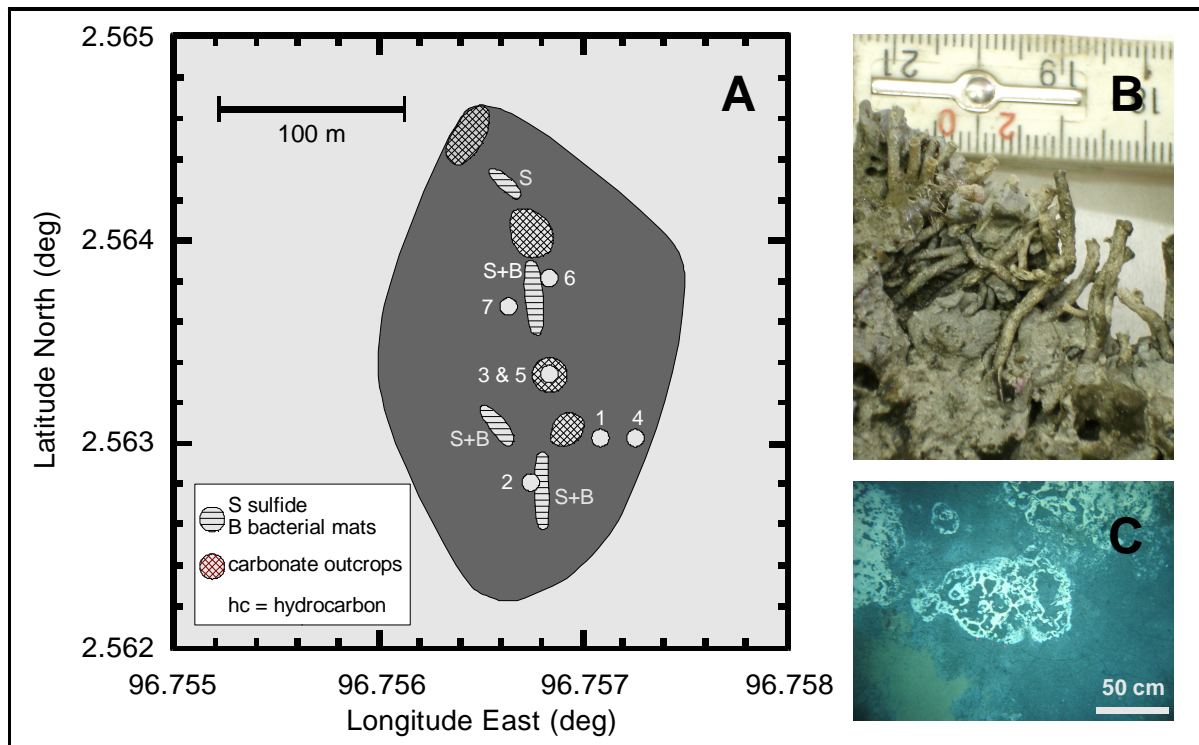

*Figure 25: (**A**) Map of the methane seep in the Simeulue basin off Sumatra. The area without seismic reflections in the sediment is shaded in dark gray. Circles indicate sampling stations according to the ship's position. Wire mesh areas depict carbonate outcrops and horizontal lines sulfide-rich surfaces "S" with microbial mats "B". (**B**) Unclassified tubeworms found at the carbonate outcrops. (**C**) White bacterial mats near the sediment surface of the station 2.*

<u>Biological samples</u>

Immediately after porewater sampling (described below), approx. 300-400 ml sediment samples of multicorer or 20-100 ml sediment of gravity cores were collected in glass bottles. Bottles were sealed with butyl rubber stoppers and plastic screw caps. The headspace was flushed with nitrogen gas. These "live" samples for sediment microcosm were stored and transported at 4°C until further on-shore processin g. For qPCR and DGGE community analysis, parallel samples were frozen onboard at -20°C. For fluorescence microscopic methods, samples were treated as described below.
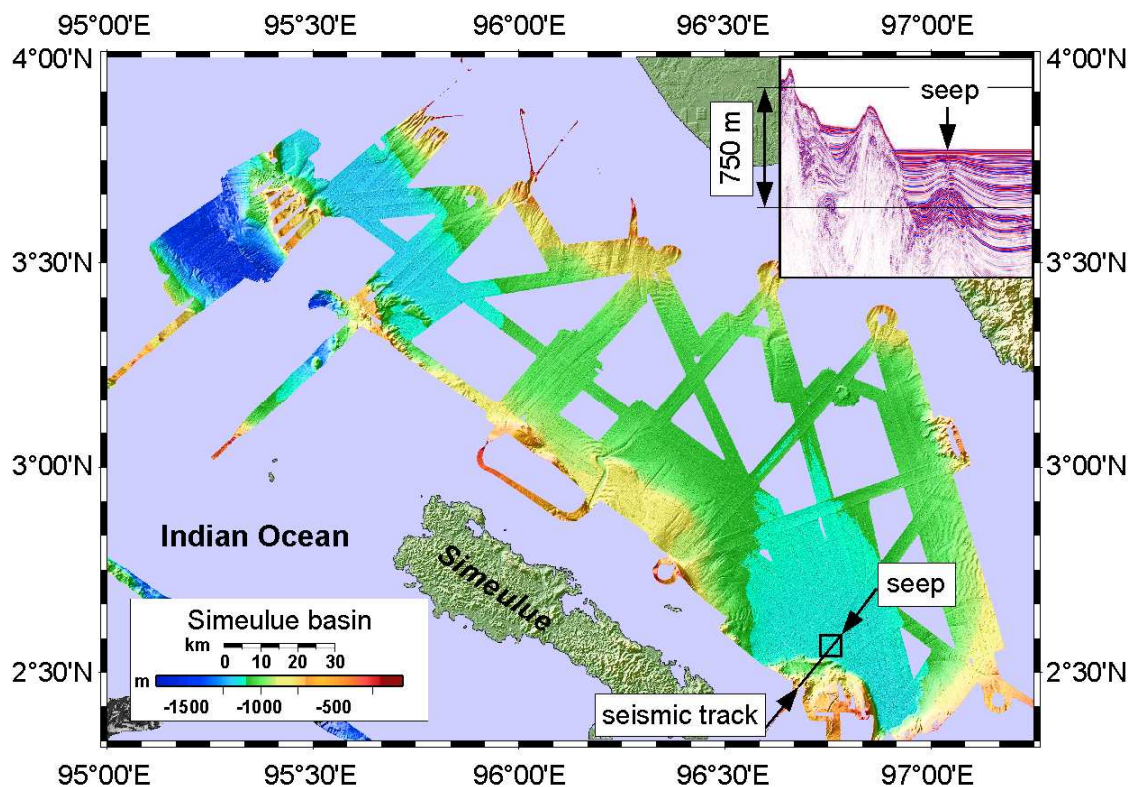
Figure 26: Bathymetric map of the Simeulue basin with the seep area in the SE. The insert (covering the island Sumatra) shows a seismic profile of the track drawn in the SE. 750 m is an approximate value.

Determination of microbial activity in sediment microcosms

General slurry preparation and microcosm inoculation

To prepare slurries for inoculation, sediment samples were mixed 1:1 with artificial seawater medium [46]. Subsequently, 10 ml of sediment slurry were added to 20 ml of medium, resulting in 5 ml sediment per bottle. Serum bottles of 60 ml volume were used. All manipulations were carried out under dinitrogen atmosphere in an anoxic glove box at room temperature. The headspace of the incubation tubes consisted of either methane (100%) or N_2/CO_2 (90%/10%$_{v/v}$). Microcosms were incubated horizontally in the dark without shaking at in situ temperature which was either 6 or 23°C (*Table 4*).

Monitoring of AOM microcosms and determination of sulfate reduction rates

Potential rates of AOM were measured in vitro by methane-dependent sulfate reduction [22, 47, 48]. Sulfide concentrations were determined spectrophotometrically by the formation of copper sulfide [49]. Sulfide concentrations of methane amended microcosms were subtracted from sulfide concentrations of controls without methane. Rates are given in

$\mu mol \ cm^{-3} \ d^{-1}$ wet sediment and deviations are expressed as 95% confidence intervals unless stated otherwise.

AOM labelling experiment with ^{13}C-methane

For further verification of AOM activity, ^{13}C-labelled methane ($17\%_{v/v}$) was added to first transfer microcosms (stations 1 and 2). After up to 14 months of incubation of the transferred microcosms a 10 ml headspace sample was precipitated in 1 ml concentrated BaOH solution. The obtained $BaCO_3$ suspension was transferred to a helium flushed vial and acidified with 100 µl concentrated HCl. To determine the $\delta^{13}C$ value, a nearly methane-free headspace sample was injected into a MAT 252 GC-IRMS. Mean $\delta^{13}C$ values were obtained from three individual batch cultures.

Tests for hydrocarbon dependent methanogenesis and methanogenic controls

Potential rates of methane production were determined in microcosms without substrates, and with addition of typical marine substrates trimethylamine (TMA) and methanol or selected hydrocarbons. Final concentrations in the microcosms for TMA and methanol were 1 mM and 2.4 mM respectively. To demonstrate hydrocarbon dependent methanogenesis, anaerobic microcosms with butane, hexadecane, and ethylbenzene were prepared. Butane was added by replacing the microcosm headspace completely by gaseous butane. Hexadecane or ethylbenzene were added directly to the medium in concentrations of $0.1\%_{v/v}$. Methane was measured using a GC-FID equipped with a silica gel column (SRI 8610 C, SRI Instruments, USA).

Most active hydrocarbon dependent methanogenic microcosms, i.e. with rates significantly higher than in the controls, were selected for further examinations. First transfers of hydrocarbon dependent methanogenic microcosms were incubated for 31 months (*Table 5*) [31]. Rates are given in $\mu mol \ cm^{-3} \ d^{-1}$. To simulate marine in situ conditions, all initial setups contained sulfate (28 mM) as electron acceptor. Additional electron acceptors to sulfate were nitrate (1 mM), ferrihydrite (2.5 mM) or manganese dioxide (1.2 mM). Negative controls without added carbon substrates were set up using the same electron acceptors as for hydrocarbon incubations.

When active microcosms were transferred for further enrichment, sulfate was replaced by an equimolar amount of chloride in case electron acceptors other than sulfate were added. Stock solutions of the metal oxides were prepared as follows: ferrihydrite was precipitated by neutralisation of a $FeCl_3$ solution [50]. Manganese dioxide was prepared by oxidation of a $MnCl_2$ solution with $KMnO_4$ [51]. Hydrocarbon degradation was not measured directly. Methanogenesis served as proxy for anaerobic hydrocarbon degradation [31].

Table 5: Incubation of initial microcosm set-ups and of subsequent transfers. Trimethylamine (TMA) or methanol were not used as substrates at station 6 and 7. n/a = not analysed.

Station	Substrate	Incubation time [months] initial set-up	1st transfer
station 1	Methane	17	14
station 2	Methane	17	14
station 1	TMA or methanol	2	n/a
station 2	TMA or methanol	2	n/a
station 6	butane, hexadecane or ethylbenzene	7	31
station 7	butane, hexadecane or ethylbenzene	7	31
station 8	butane, hexadecane or ethylbenzene	7	31
station 9	butane, hexadecane or ethylbenzene	7	31
station 8	TMA or methanol	2	n/a
station 9	TMA or methanol	2	n/a

Determination of cell numbers by SYBR green® and CARD-FISH

For SYBR green® total cell counts and CARD-FISH, fixations were carried out immediately after sampling. Two fixatives, formaldehyde (FA) or ethanol, were applied. A volume of 1 cm^3 wet sediment was treated for 10-15 hours at 4°C wit h 1 ml fixative solution (4%$_{w/v}$ FA in phosphate buffered saline [PBS]), removed in two centrifugation steps by washing with 1 ml PBS and stored at -20°C in 50%$_{v/v}$ ethanol/PBS. For total cell counts, in each sample 800-1000 cells were counted after SYBR green® staining according to Weinbauer *et al.* [52]. CARD-FISH counts were conducted after Pernthaler *et al.* [53] and Schippers *et al.* [54].

Gene quantification by qPCR

DNA extraction was carried out using a Fast DNA for Soil Kit (Fast DNA Spin Kit for soil, BIO 101, MP Biomedicals, Germany). To block sedimentary nucleic acid binding capacities, 10 µl of a 1% polyadenylic acid solution were added in the initial step [55]. Directly before PCR, 125 µl 0.3% bovine serum albumine (BSA) in ultra pure water were added as blocking agent to the Taqman master mix (Applied Biosystems, Germany) or the SYBR green® master mix (Eurogenetec, Germany). A real-time PCR instrument (ABI Prism 7000, Applied Biosystems) was employed to determine the 16S rRNA gene copy numbers of *Archaea* [56] and *Bacteria* [57]. Eukaryotic 18S rRNA genes were quantified according to the manual's instructions of the kit [58]. The functional genes *dsrA* and *mcrA* were investigated according to Schippers and Nerretin [59] as well as Nunoura *at al.* [60] respectively. Specific functional *mcrA* genes from anaerobic methanotrophic *Archaea* ANME-1 and ANME-2 were quantified using an as-say of Nunoura *et al.* [60]. Values are expressed in copy numbers per cm^3 wet sediment.

Denaturing gradient gel electrophoresis (DGGE)

For DGGE, 16S rRNA genes of *Bacteria* were amplified using the primer set 533F (5'-TTACCGCGGCTGCTGGCAC-3') / 907R (5'-AATTCCTTTGAGTTT-3') with a GC-clamp (5'-CGCCCGCCGCGCCCCGCGCCCGGCCCGCCGCCCCCGCCCC-3') attached to the reverse primer 907R at the 5'-end [61, 62]. Archaeal 16S rRNA genes were amplified with the primer set 340F (5'-CCCTACGGGGYGCASCAG-3') and 915R (5'-GTGCTCCCCGCCAATTCCT-3') [63, 64], a GC-clamped (as for 907R) 340F forward primer. A total of 2 µg of amplified and purified DNA (QIA quick PCR Purification Kit, Qiagen, Germany) was applied to each pocket of the gel and separated in a DCode System (BioRad, Germany) for 20 h at 60°C. Denaturing gradients of urea/formamide were 30-70%$_{w/v}$ (20-80%$_{w/v}$ for *Archaea*) and the acrylamide concentration was 6.5%$_{w/v}$. As many bands as possible were excised, vacuum-dried at 60°C for 3 hours (Eppendorf Concentrator 5301, Eppendorf, Germany), extracted with 30 µl PCR grade water (4°C, over night), re-amplified without GC-clamps and purified as described above. Sequencing reactions were conducted at Seqlab GmbH (Göttingen, Germany). Sequencing primers were 533F, 550F (5'-CGGAATTATTGGGCGTAAAG-3') and 906R (5'-CCCCAATTCCTTTGAGTTTC-3') for bacterial 16S rRNA genes and 340F and 915R for archaeal 16S rRNA genes. The obtained DNA sequences were aligned by ARB-SILVA (http://www.arb-silva.de) and assembled in an existing Parsimony tree of a recent reference database (SSURef 102, February 2010) according to Ludwig *et al.* [65] and Pruesse *et al.* [66]. All sequence data were submitted to the GenBank database (http://www.ncbi.nlm.nih.gov) under accession numbers HQ231693 to HQ231746.

Bathymetry and parasound

A Kongsberg SMRAD EM 120 multibeam echo sounder was operated continuously 24 h during the cruise. The device enabled mapping at ocean depth and was used as a low frequency sediment echosounder at 18.0 and 21.5 kHz to map seismic profiles of basin sediments. The transparent character of the seafloor (seismic blanking) was used to define the extent of sediments affected by methane seepage and authigenic carbonate precipitation (*Figure 26*) [67]. Often, seismic blanking may also be indicative for high density gas hydrates overlaying low density free gas, shown by a Bottom Simulating Reflector (BSR; [68, 69]).

Geochemical analyses

TOC in sediment samples was measured with the instrument LECO CS 200 (LECO Corporation, USA). Porewater was squeezed from sediment slices of up to 125 cm^3 using a porewater press at atmospheric pressure. Between 20 to 40 ml of porewater were obtained and fil-

tered through a 0.45 µm cellulose nitrate filter (Sartorius, Germany) and directly collected in polypropylene-vials. Polypropylene-vials were acid prewashed and dried to remove possible traces of carbonate from the vial surface. To remove particles and microorganisms, the collected porewater was filtered again through 0.2 µm polyethersulfone filters (Sartorius, Germany). For metal ion and sulfate concentrations, 5 ml porewater were acidified with 50 µl HNO_3 and measured using an ICP-MS instrument (Perkin Elmer Sciex Elan 5000, USA) as published by Dekov *et al*. [70]. After preservation of the sediment samples with $ZnCl_2$, porewater sulfide was determined spectrophotometrically as described by Cline [71].

To determine carbon stable isotopes of DIC, 2 ml of porewater, treated with 10 µl saturated $HgCl_2$ solution on board, were analysed in a Finnigan MAT 252 (Thermo Electron, USA) connected to a Finnigan Kiel III (Thermo Electron) carbonate preparation device [72]. Free gases were measured using 5 ml fresh sediment immediately transferred into 10 ml 2 M NaOH in a 56 ml serum bottle. The bottle was sealed with a butyl rubber stopper, the sediment suspended by shaking the flask, and 5 ml headspace were removed and stored in 20 ml injection vials over saturated NaCl solution for on-shore measurement. This procedure allowed a separation of free from adsorbed gases but some adsorbed gas may have evaporated as well [73]. $\delta^{13}C$ values for free gases were obtained by injection into a Finnigan MAT 253 (Thermo Electron, USA) connected to a gas chromatograph (GC 6890, Agilent, USA).

To determine the carbon stable isotopic composition of the macro fauna, the soft tissue of bivalves and crabs was freeze dried, milled, weighed into tin capsules and stored in a desiccator until measurement. For TOC carbon isotope ratios, dried sediment was stored in acid washed tin capsules, and the isotope ratios were determined by a coupled system of an elemental analyser and a MAT 252 isotope ratio mass spectrometer (Thermo Electron, USA) via a Finnigan ConFlo III open split interface. Concentrations and isotopic data are given as the arithmetic mean of at least two measurements. Isotopic carbon values are expressed in ‰ relative to Vienna PeeDeeBelemnite (VPDB). Concentrations are relative to one cm^3 of fresh (wet) sediment.

4.1.3. Results

Nine stations were investigated in the Simeulue and Nias basin with focus on demonstrating (i) AOM as major biogeochemical process and (ii) the potential role of higher hydrocarbons as energy source for the microbial community. All Simeulue stations were located in an area of high methane flux while stations in the Nias basin served as control sites (*Figure 25* and *Figure 26*).

Seafloor observations

Areas covered with white-coloured microbial mats were discovered and sampled in the Simeulue seep area using a TV-guided grab (*Figure 25*). The higher seafloor biota comprised tubeworms, bivalves and crabs. The latter settled on carbonate outcrops and could be identified as members of the species *Shinkaia crosnieri* (Enrique Macpherson, personal communication). Their soft tissue stable carbon isotopic signature ranged from -38‰ to -45‰. Soft tissue of one mytilid bivalve individual had a $\delta^{13}C$ of -31‰.

Anaerobic oxidation of methane

Results obtained from on-shore experiments with microcosms do often not perfectly reflect the in situ situation but provide a good estimate for potential microbial activities [22, 48]. Potential sulfate reduction rates in Simeulue seep sediment microcosms were higher with methane as electron donor than in controls without methane. The observed differences can be explained by AOM (*Table 6*). To confirm this, the conversion of methane into carbon dioxide was tested in 1:10 diluted subcultures, incubated with $17\%_{v/v}$ ^{13}C-methane. The label was recovered as ^{13}C-enriched carbon dioxide. The detected $\delta^{13}C_{CO2}$ values were $+503\pm331‰$ (station 1) and $+319\pm279‰$ (station 2) for microcosms prepared from sulfidic sediments of the Simeulue methane seep. This is an evidence for the oxidation of ^{13}C-methane to $^{13}CO_2$ at both stations. In controls with unlabelled methane, $\delta^{13}C_{CO2}$ values were -15.7‰ and -17.4‰ respectively. The corresponding $\delta^{13}C_{CH4}$ values of unlabelled methane were -36.6‰ and -34.9‰ respectively.

In 1:10 diluted subcultures of the initial microcosms, containing either sulfate, nitrate, FeOOH or MnO_2, methanotrophy was observed after 14 months incubation as well. The rates, measured by headspace analysis of methane, were similar and ranged from 0.8 µmol cm^{-3} day^{-1} (with MnO_2) at the station 1 to 1.8 µmol cm^{-3} day^{-1} (with sulfate) at station 2.

Table 6: Analyses of in situ gas and microbial AOM activity in sediments of the Simeulue seep. Errors are standard deviations from the mean of the number of replicates (n). Methane concentrations and methane isotopic ratios ($\delta^{13}C_{CH4}$) were determined in separate measurements and the number of replicates differs. Ethane concentrations were determined in the same sample with methane isotopic ratios so the number of replicates is identical. AOM rates were determined by subtracting SRR of controls without from those incubations with methane in the headspace. SRR: sulfate reduction rate, n/a = not applicable, cmbsf = centimetres below seafloor

Station	Depth [cmbsf]	Methane [pmol cm^{-3}]	Error	$\delta^{13}C$ [‰ VPDB]	Error	n	Ethane [‰$_{v/v}$]	Error	Ratio C1/C2	n	AOM rate [µmol cm^{-3} d^{-1}]	Error	n
Station 1	surface	8.5	±0.4	-70.9	±5.3	2	0.048	±0.030	2889	3	0.57	±0.10	3
Station 2	surface	10.1	±0.5	-74.8	±2.0	2	0.019	±0.003	5406	6	0.35	±0.09	3
	11	<1		n/a			n/a		n/a	n/a	n/a		
	67	<1		n/a			n/a		n/a	n/a	n/a		
Station 4	167	1.4		-39.6		1	0		n/a	1	n/a		
	267	1.4		-43.6		1	0		n/a	1	n/a		
	367	<1		n/a			n/a		n/a	n/a	n/a		

Methanogenesis from hydrocarbons, trimethylamine (TMA) and methanol

After addition of the higher hydrocarbons butane, hexadecane and ethylbenzene, a small increase of methanogenesis compared to controls was observed after seven months in 27 microcosms out of 280 initial microcosms. To exclude false positive signals by means of stimulation of methanogenic TOC digesting microorganisms, first 1:10 transfers of these microcosms were prepared. Several transferred microcosms showed significant methanogenesis in the presence of hexadecane or ethylbenzene. In these transferred microcosms, the hydrocarbon-dependent methanogenesis rate at the seep station 2 was 6.5 nmol cm^{-3} d^{-1} (hexadecane and manganese dioxide) and 14.5 nmol cm^{-3} d^{-1} at station 6 (ethylbenzene and ferrihydrite). In the Nias basin, it was 17.5 nmol cm^{-3} d^{-1} at station 8 (hexadecane and sulfate) and 18.0 nmol cm^{-3} d^{-1} at station 9 (hexadecane and manganese dioxide). Methanogenesis in microcosms without added hydrocarbons was less than 1.6 nmol methane cm^{-3} day^{-1}. However, the typical methanogenic substrates TMA and methanol in the methanogenic positive controls resulted in methane formation rates at least one order of magnitude higher than hydrocarbon amended microcosms obtained from the seep sediments. At station 1, TMA dependent methanogenesis was 0.3 µmol cm^{-3} day^{-1} and for methanol 0.5 µmol cm^{-3} day^{-1}. At station 2 methanogenesis from TMA was 0.3 µmol cm^{-3} day^{-1} and from methanol 0.7 µmol cm^{-3} day^{-1}. In microcosms prepared from sediments of the Nias basin (stations 8 and 9), TMA or methanol did not stimulate methanogenesis.

Cell numbers and quantification of selected functional genes

Results of CARD-FISH and total cell counts for the stations 1, 3 and 4 are shown in *Figure 27*. At station 2, only the top and bottom layer were investigated and data for this station are therefore not depicted in *Figure 27* but described in the following.

The total cell numbers of 10^7 to 10^9 cells cm^{-3} at the Simeulue seep were quite similar to those at sites of the Sumatra forearc basins not influenced by methane seepage [44]. CARD-FISH cell counts and qPCR measurements showed the presence of *Bacteria* and *Archaea*, but only small numbers of Eukarya. This observation is in agreement with previous marine sediment studies [44, 59].

CARD-FISH analyses, assessing the active community, indicated that living *Bacteria* were present with at least two orders of magnitude more cells than *Archaea* at the station 2. At the station 1, active bacterial and archaeal cells were distributed equally. In contrast, results obtained by qPCR, targeting also inactive microorganisms, indicate a dominance of *Bacteria* over *Archaea* by one order of magnitude. At the station 2, total cell numbers of 1×10^9 cells cm^{-3} at the top (0 cmbsf) and 4×10^9 cells cm^{-3} at the bottom (8 cmbsf) were

counted. CARD-FISH cell counts of active cells revealed cell numbers of 2×10^8 cells cm^{-3} for *Bacteria* and 4×10^7 cm^{-3} for *Archaea* at the station 2. At the stations 3 and 4, CARD-FISH indicated no living archaeal cells (*Figure 27*).
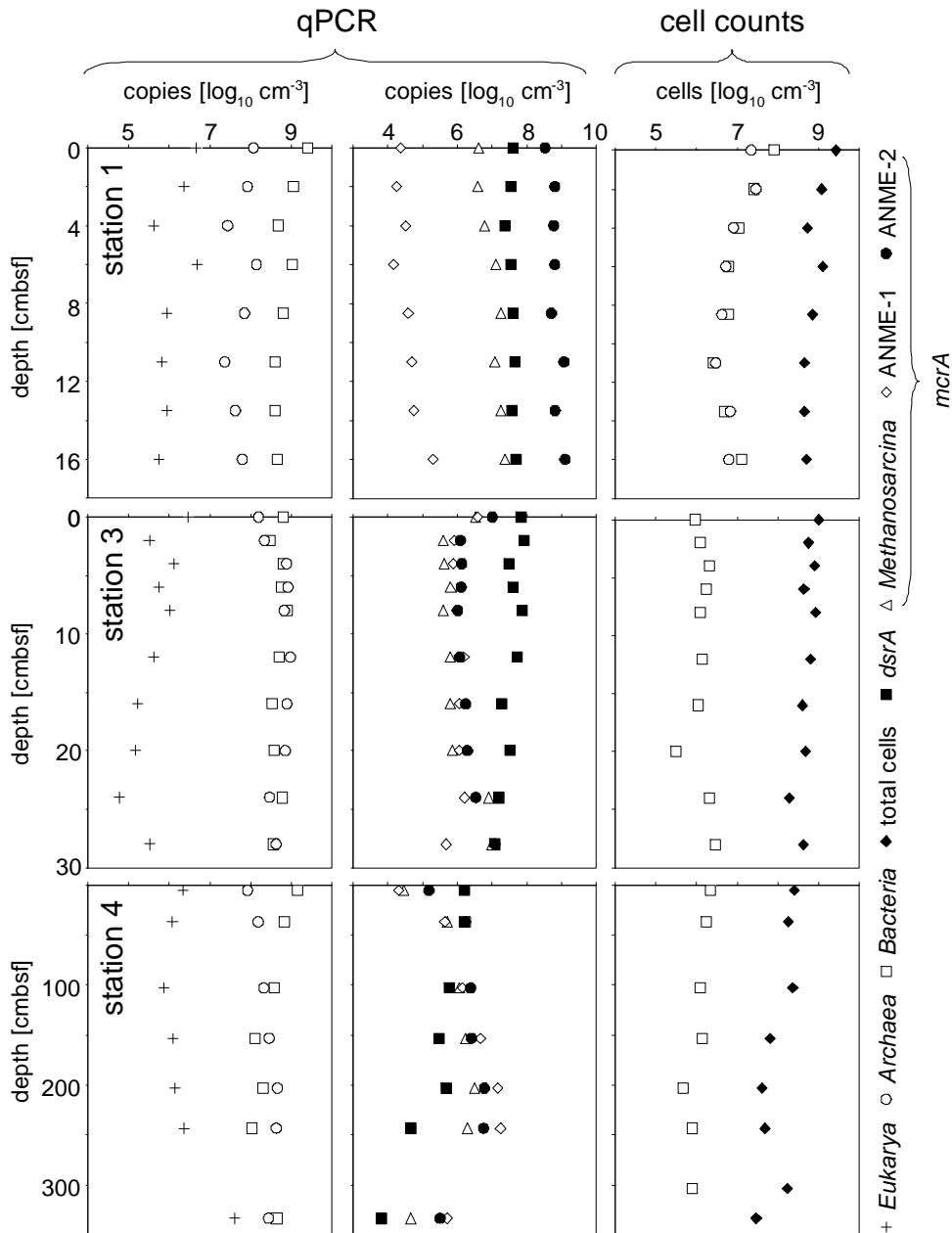

Figure 27: Depth trend of quantitative community composition of three different stations from the Simeulue seep. The left panel illustrates the composition of the three domains Bacteria, Archaea and Eukarya according to qPCR quantification of 16S or 18S rRNA genes, respectively. The middle panel displays the distribution of the functional gene numbers. In the right panel, total cell counts are compared to CARD-FISH cell counts for Bacteria and Archaea detecting active cells.

Domain specific 16S rRNA gene copies, obtained from qPCR measurements, and selected functional genes at three different stations are displayed in *Figure 27*. A clear trend was observed only for Eukarya and only at the station 4 (*Figure 27*). The copy numbers increased with depth (*Figure 27*). For functional genes, a trend with depth was observed only at the deeper sampled station 4. Its most prominent feature was the increase of all *mcrA* gene copy numbers, beginning at 103 cmbsf and dropping to the surface values below 267 cmbsf. An opposite tendency was observed for *dsrA* gene copy numbers as a clear decrease with depth. At the station 2, ANME-2 *mcrA* gene copies increased from 6×10^6 copies cm^{-3} in the top layer to 2×10^8 copies cm^{-3} at the bottom (8 cmbsf). An opposite trend appeared for the ANME-1 *mcrA* gene with copy numbers of 2×10^8 copies cm^{-3} at the surface layer and 7×10^7 copies cm^{-3} at the bottom. No change with depth was observed for the *Methanosarcina mcrA* group where copy numbers of 5×10^8 copies cm^{-3} were detected. The *dsrA* gene measurement resulted in copy numbers of 3×10^6 copies cm^{-3} at the top and 6×10^7 copies cm^{-3} at the bottom of this core.

Microbial diversity

The composition of the archaeal and bacterial microbial communities was analysed by DGGE of DNA extracted from Simeulue sediments (*Figure 28*). PCR products of the station 3 were run on a separate gel without reference to the stations 1 and 2. Therefore, band patterns were not comparable and a DGGE gel photograph is not shown. The band patterns indicate substantial differences in the microbial communities between stations 1, 2 and 4, as well as smaller changes with increasing sediment depths (*Figure 28*).

Parsimony trees of 16S rRNA gene sequences obtained from the DGGE separation are depicted in *Figure 29* and *Figure 30*. Three major bacterial phylogenetic groups (δ-*Proteobacteria*, candidate division OP9 and *Anaerolineaceae*) were abundant across the seep. According to their band thickness in the DGGE gel, OP9 bacteria and relatives of *Desulfobacteraceae* seemed to become increasingly important with depth at the station 4 (*Figure 28* and *Figure 29*). Nonetheless, since band thickness is an imprecise measure for abundance, this result indicates only a trend even when the total amount of amplified DNA products was equal for each layer. Besides δ-*Proteobacteria*, other *Proteobacteria* sequences were not recovered from the DGGE gels. Sequences affiliated to the clusters *Desulfobacteraceae*, *Desulfarculaceae* and Sh765B-TzT-29 dominated the δ-*Proteobacteria* (*Figure 28*). One a deeply branching sequence of the station 2 was more closely related to sequences obtained from municipal wastewater sludge [74] than to the genus *Leptolinea* (*Figure 29*). Another deeply branching sequence of the station 3 was closely related to the genus *Rhodococcus* (*Figure 29*). Two bands found at stations 2, 3 and 4 were relatively close relatives of the genus *Spirochaeta*.
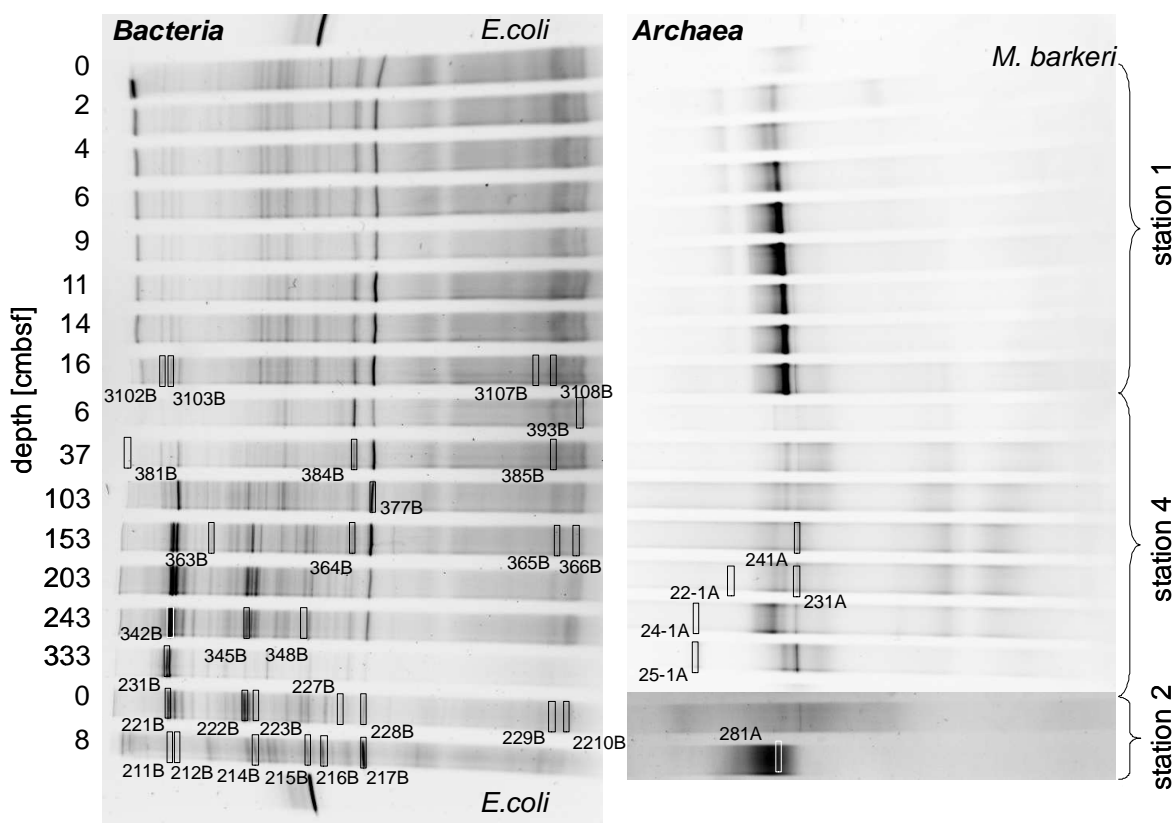
Figure 28: DGGE photographs showing the 16S rRNA gene sequence diversity of Bacteria (left) and Archaea (right) of the stations 1, 2 and 4 of the Simeulue seep. Escherichia coli and Methanosarcina barkeri served as positive controls. Excised bands used for 16S rRNA gene sequencing are high-lighted by open rectangles. The numbers enumerate gels, lanes and bands and refer to the phyloge-netic trees in Figure 29 *and* Figure 30*. Multiple gels were prepared and bands excised from different gels could be relocated in the shown photographs. Bands resulting in unsuccessful PCR re-amplifications or sequencing reactions are not shown.*

Simeulue seep sequences of all stations were related to three prominent archaeal groups (ANME-1, ANME-2 and *Figure 30*one sequence of the station 3 was assigned into the Deep Hydrothermal Vent Euryarchaeotal Group 6 (DHVEG6). The remaining sequences (stations 3 and 4) belonged to not further specified *Crenarchaeota*. Except for the *Crenarchaeota*, members of all other clusters were identified in stations 1 to 4. In summary, the bacterial di-versity was greater than the archaeal one, with most sequences related to organisms typi-cally found at hydrocarbon seeps and mud volcanoes.
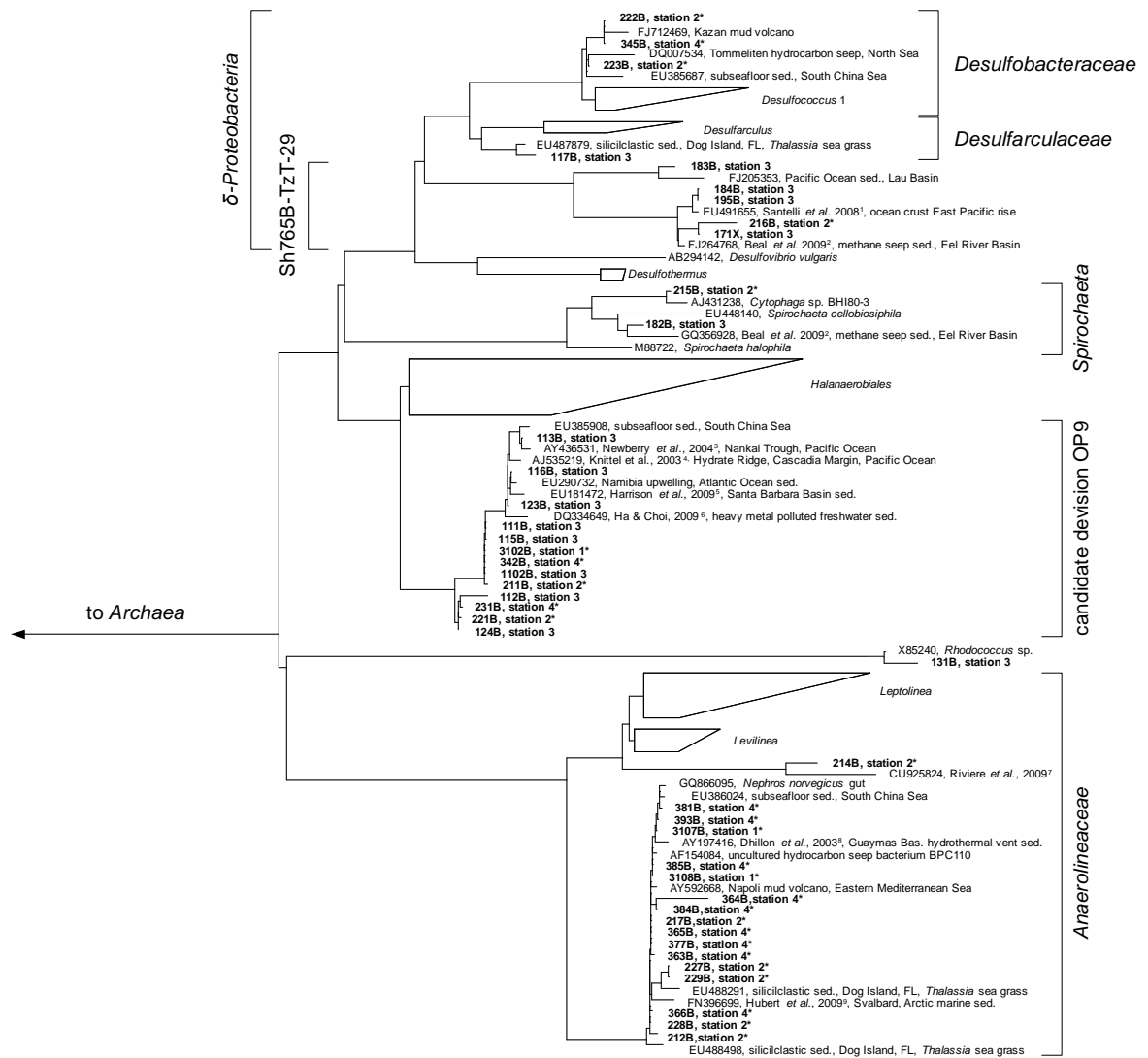
Figure 29: Parsimony tree of bacterial 16S rRNA gene sequences summarising all sampled stations. The tree is based on the SILVA tree version 102 [66]. Sequences obtained from the Simeulue seep are in bold letters. Bold numbers describe bands which were excised and used for 16S rRNA gene sequencing from three different DGGE gels. On the right, the deepest branching affiliations are shown. References are indicated in upper case: [1] [75], [2] [76], [3] [77], [4] [78], [5] [79], [6] [80], [7] [74], [8] [81], [9] [82]. Asterisks (*) indicate bands from DGGE gels in Figure 28. *"sed." = sediment.*
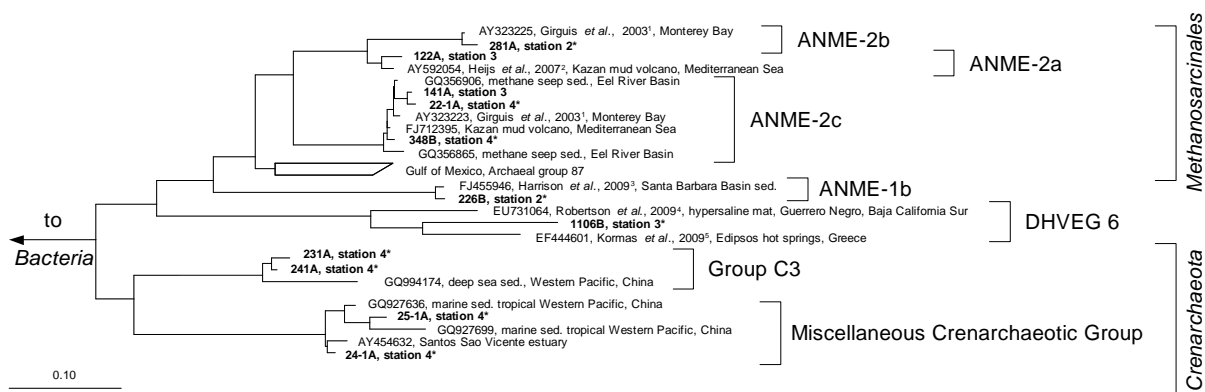
Figure 30: Parsimony tree of archaeal 16S rRNA gene sequences summarising all sampled stations [66]. Sequences obtained from the Simeulue seep are in bold letters. Numbers describe bands which were excised and used for 16S rRNA gene sequencing from three different DGGE gels with identical patterns. On the right, the deepest branching affiliations are shown. DHVEG6 = "Deep Hydrothermal Vent Euryarchaeotal Group 6"; MHVG = Marine Hydrothermal Vent Group References are indicated in upper case: [1] [83], [2] [84], [3] [79], [4] [85], [5] [86]. Asterisks (*) indicate bands from DGGE gels in Figure 28. *"sed." = sediment.*

Free gases and their isotopic composition

Free methane concentrations in the water column ranged from 10-200 nmol l^{-1} at the seep location. In the southeast boundary of the seep, methane concentration never reached values above 5 nmol l^{-1}. At the sediment surface of the station 1 and 2, methane accounted for a total of >99.9% of all free gases, with an average δ^{13}C-value of -70‰ (*Table 6*).

Porewater composition and stable carbon isotopes

All geochemical porewater data of the Simeulue seep are summarised in *Table 7*. At stations 1 and 2, δ^{13}C$_{DIC}$ values were mainly below -40‰. At the station 3, δ^{13}C$_{DIC}$ values were always above -8‰. At station 4, δ^{13}C$_{DIC}$ values ranged from -2‰ at 6 cmbsf to -24‰ at 293 cmbsf, showing a decreasing trend with depth (*Table 7*). Such clear trends were missing in case of the solid phase δ^{13}C$_{TOC}$ values. However, there was a slight decrease from -22.3‰ at 6 cmbsf to -27.6‰ at 153 cmbsf of the station 4. The values remained stable below -27.0‰ up to a depth of 293 cmbsf (*Table 7*). At the stations 1 and 2, sulfate concentrations decreased with depth while sulfide concentrations increased. At stations 3 and 4, no decline of porewater sulfate concentrations nor sulfide were detected. Elevated concentrations of reduced manganese were found at the station 2 as well as at the surface of the station 4 (*Table 7*).

Table 7: Geochemical analysis of porewater and total organic carbon (TOC) and carbon isotopic composition of TOC and dissolved inorganic carbon (DIC). n.d. = not determined, [% dw] = [% dry weight]

Depth [cmbsf]	SO_4^{2+} [mM]	HS^- [mM]	Mn^{2+} [µM]	NH_4^+ [mM]	TOC [% dw]	$\delta^{13}C_{TOC}$ [‰ VPDB]	$\delta^{13}C_{DIC}$ [‰ VPDB]
Station 1							
0	27.8	0.0	1.9	0.4	1.6	-23.8	-11.8
2	26.1	1.7	1.6	1.7	1.5	-23.4	-25.5
4	16.4	15.7	2.1	3.2	1.4	-23.0	-48.8
6	10.3	20.3	1.1	2.5	1.4	-22.9	-47.3
9	8.4	18.4	0.7	2.6	1.4	-22.8	-46.8
11	5.8	15.7	1.2	2.9	1.4	-22.6	-45.0
14	8.0	18.0	0.9	4.8	1.3	-22.7	-44.4
16	4.5	19.4	1.0	6.0	1.3	-23.2	-43.4
Station 2							
0	7.6	18.7	14.8	2.9	1.6	-23.2	-41.1
2	2.6	24.7	14.1	2.4	1.6	-22.8	-42.8
4	0.6	20.5	13.2	2.3	1.6	-22.9	-42.3
6	0.8	25.3	12.3	2.2	1.6	-24.5	-42.3
Station 3							
0	27.0	0.2	0.3	0.2			-0.9
2	27.5	< 0.1	14.7	0.4			-1.5
4	27.4	< 0.1	15.1	0.2			-2.0
6	26.9	< 0.1	11.7	0.3			-2.5
8	27.5	< 0.1	8.3	0.4	not determined	not determined	n.d.
12	27.0	< 0.1	5.5	0.3			-2.9
16	26.6	0.1	2.7	0.2			-3.3
20	27.2	< 0.1	2.0	0.2			-2.8
24	27.6	< 0.1	1.5	0.3			-3.5
28	27.4	< 0.1	1.3	0.3			-7.8
Station 4							
6	28.4	< 0.1	16.4	0.2	1.4	-22.3	-2.2
37	28.2	< 0.1	16.4	0.3	1.3	-23.1	-3.5
103	28.4	< 0.1	6.4	0.3	1.3	-24.5	-4.8
153	27.4	< 0.1	5.5	0.3	1.2	-27.6	-16.8
203	27.3	< 0.1	4.5	0.2	1.2	-27.0	-19.2
243	26.5	< 0.1	3.4	0.4	1.4	-27.2	-23.7
293	27.0	< 0.1	2.7	0.4	1.4	-27.1	-24.3
333	27.2	< 0.1	3.6	0.3	1.4	-26.9	-19.6

4.1.4. Discussion

The main objective of this study was to find active methane seeps in the Sumatra forarc as potential indicators for deeply buried hydrocarbon reservoirs. As a result, an active methane seep was for the first time discovered in the Indian Ocean. The discovered methane seep comprised highly active (stations 1 and 2) and less active or inactive (stations 3 and 4) AOM-influenced areas (*Table 4* and *Figure 27*). Stations 1 and 2 were characterised by black sulfidic surface sediments,depleted sulfate and high sulfide concentrations and light $\delta^{13}C_{DIC}$ values of the porewater, the presence of ANME-1 and ANME-2 representatives, as well as high cell and high copy numbers of 16S rRNA and functional genes related to AOM, methanogenesis and sulfate reduction. A defined seep centre of activity, like in mud volcanoes, was not discovered. The seep area was characterized by a patchy distribution of active spots. Carbonate- or sulfide-rich spots were randomly distributed over the surface. A reason for the patchiness might be tectonic activity. While some gas conduits might have been shut, other could have opened over time. An apparent feature of the active parts at the seep was the strong depletion of ^{13}C in porewater DIC, which was also observed for TOC of the guts of the seep's macro fauna. This confirms the importance of methane as carbon source for the benthos at this location. In addition, methanogenic activity was confirmed in sediment microcosms of the Simeulue seep area as well as in the Nias basin, where AOM activity was absent.

Methanotrophy and sulfate reduction activities at the seep stations

Methane is an indirect electron source for dissimilatory microbial sulfate reducers in the syntrophic process of AOM [3]. The terminal reaction products are carbonate and sulfide [3]. Sulfide in turn may be oxidised at the oxic/anoxic interface near the sediment surface. White, sometimes filamentous bacteria are usually indicators for this interface [8]. Areas covered with such white-coloured microbial mats were discovered and sampled in the Simeulue Basin using a TV-guided grab (station 2; *Figure 25*). In contrast, microbial mats were absent near the station 1. Most likely, the white colour of such mats is a result of intracellular sulfur inclusions as observed in *Thioploca*, *Beggiatoa* or *Thiomargarita* aggregates, regularly found on the surface of sulfide-rich marine sediments [87-89].

At the Simeulue seep, methane was also an important carbon source for higher biota. Methanotrophic microorganisms were important nutritional resources for crabs and bivalves as indicated by their ^{13}C depleted, presumably methane derived, carbon signatures. Such type of symbiosis between methanotrophic bacteria and macrofauna was already reported for several hot and cold deep marine vents [90-92]. In addition, it has previously been shown that symbiotic CO_2-fixing microorganisms play a vital role in the metabolism of the gutless

worm *Olavius* [93]. That this was the case in the AOM seep fauna seems possible because their ^{13}C depleted carbon signature resembled ^{13}C depleted DIC found in the porewater (*Table 7*). Symbiosis of higher benthos and methanotrophic microorganisms is also often associated with aerobic methanotrophy [8, 90-92]. However, our DGGE 16S rRNA gene analyses did not reveal aerobic methane oxidisers (*Figure 28* and *Figure 29*).

The anoxic nature of the sediment was confirmed by porewater data, showing in particular high sulfide concentrations, reduced iron and manganese as well as ammonia to be present. While sulfide concentrations increased downwards into the sediment, sulfate decreased to micromolar concentrations (*Table 7*). This and the fact that methane was detected in the surface layers (*Table 6*) indicated a narrow sulfate-methane transition zone (SMTZ) near the surface at the stations 1 and 2 with high fluxes of methane as electron donor.

Indeed, high amounts of dissolved gas with strong sulfidic odour evaporated from the sediment during sampling of the stations 1 and 2. A number of in vitro experiments could confirm AOM as an important process at the discovered methane seep. AOM supported a vital microbial community demonstrated by high cell numbers and the presence of AOM related microbial groups. Clear evidence for ongoing AOM at stations 1 and 2 were the low $\delta^{13}C_{DIC}$ values in the porewater apparently derived from ^{13}C-depleted methane (*Table 5* and *Table 6*). These were values comparable to other methane influenced seeps, as in the Gulf of Mexico [94] or at the Hydrate Ridge [42]. Since ocean water $\delta^{13}C_{DIC}$ values are usually between 0 and -10‰ [95], DIC at the Simeulue seep was obviously derived from the anaerobic oxidation of upward migrating methane (*Table 7*). $\delta^{13}C_{CH4}$ values were below -70‰ at the stations 1 and 2 (*Table 6*). It is commonly agreed that biogenic methane exhibits $\delta^{13}C_{CH4}$ values below -70‰ [96].

That methane rather than TOC was the carbon source for microorganisms is supported by low $\delta^{13}C_{TOC}$ values at station 1 and 2. These values were in a narrow range between -22.7 and -24.5‰ which are typical for marine cellular carbon [95]. These values contrast $\delta^{13}C_{DIC}$ values between -11.8 and -48.8‰ at the stations 1 and 2, most of them below -40.0‰ (*Table 7*). Since the carbon isotopic composition of methane at both sites was below -70.0‰ (*Table 6*), it is obvious that AOM contributed to the carbon budget at these active AOM sites. Moreover, the seep sediments were highly methane laden, as indicated by intensive gas emission during sampling. Huge discrepancies between sulfate reduction and AOM rates are usually observed only when methane plays a minor role in the investigated system [8], which is not the case here.

However, one may expect that there would have been a greater contribution of AOM derived carbon to TOC as observed since methane was apparently a carbon source for the dominant

AOM performing microorganisms. Wegener *et al.* [97] reported the assimilation of methane derived carbon into AOM performing microbial consortia of various geographic origins via CO_2 fixation. Furthermore, they could show that methane mostly serves microbial catabolism and to little extent microbial anabolism. This is also reflected in carbon stable isotopic signatures of DIC and TOC of the Simeulue seep, where stronger methane signals were detected in DIC. The slightly higher $\delta^{13}C_{TOC}$ values did not support a strong impact of methane derived carbon on TOC (*Table 7*). On the other hand, ammonium concentrations decrease between 6 and 11 cmbsf at station 1. An increased ammonium uptake in succession of higher methane driven metabolic rates indicates that either TOC degradation was rather slow or that biomass was built up. That AOM in this zone was presumably the reason for the decrease of ammonium concentrations is supported by high sulfide concentration, most likely a result of sulfate dependent AOM (*Table 7*).

Since at station 4 AOM was not reflected in the porewater chemistry we believe in a former, recently ceased AOM activity, which has left its imprint in the carbon isotope signatures and extractable DNA. Consequently, the $\delta^{13}C_{TOC}$ values below -27‰ are suggestive for a greater contribution of methane to TOC compared to DIC than observed for the stations 1 and 2 (*Table 7*). AOM driven microbial activity, as indicated by an increase of ANME members with sediment depth (*Figure 27*), could have caused a stronger methane signal in TOC when methane was the prevailing carbon and energy source. Moreover, the impact of TOC of the water column is presumably much lower at a depth of 150-300 cmbsf than closer to the sediment surface. Methane was relatively enriched in ^{13}C at this station, which could also be well explained by AOM activity. Extremely low methane concentrations could have led to a less pronounced isotopic fractionation effect [98] – caused by rate limiting methane concentrations (*Table 6*).

Anaerobic methanotrophy was observed in initial and in transferred microcosms, as indicated by labelling experiments as well as by methane dependent sulfate reduction rates (*Table 6*). The AOM rates observed for the Simeulue seep area were slightly lower than maximum rates reported for other methane seeps, but higher than rates observed for mud volcanoes or sediments from various marine sulfate-methane transition zones [3]. That sulfate reduction was mainly driven by methane was further supported by the observation of comparable TOC values in the sediments of both, stations 1 and 2 as well as station 4 (*Table 7*). If TOC degraders significantly accounted for sulfate reduction, depleted sulfate and high sulfide concentration would have been measured for station 4 as well, and not only for the stations 1 and 2 for which sulfate reduction via active AOM could be demonstrated. The higher rates in the first transferred microcosms indicated an enrichment of methanotrophs in these assays

after incubation for more than one year as indicated by labelling experiments using ^{13}C-methane.

Moreover, relatively high concentrations of reduced manganese and iron (data not shown) were detected at station 2 (*Table 7*). The presence of reduced manganese may be an indication for sulfide dependent or direct microbial manganese reduction. Sulfide dependent or direct microbial manganese reduction might also be a result of AOM activity at the Simeulue seep as suggested for the Eel river basin by Beal *et al.* [76]. Additionally, one sequence of station 2 and four sequences of the station 3 were assigned to the Sh765B-TzT-29 cluster, a cluster that was initially believed to belong to the family *Geobacteraceae* and was first described by Geißler [99]. This cluster contains heavy metal associated *Bacteria* which where originally found in uranium mill tailings at Shiprock (NM, USA) as described in her thesis [99]. A recent study described metal associated AOM consortia [76]. Members of the Sh765B-TzT-29 cluster may also be metal associated at the Simeulue seep. Additionally, our culturing experiments with reduced iron or manganese as electron acceptor instaed of sulfate showed anaerobic oxidation of methane, possibly associated to the Sh765B-TzT-29 cluster. Moreover, 16S rRNA gene sequences reported by Beal et al. [76] were found in a close phylogenetic neighbourhood of OTUs identified in the Simeulue seep (*Figure 29*). In conjunction with the presence of reduced iron and manganese in the porewater (*Table 7*), it seems possible that metal reduction played a role as electron acceptor, besides sulfate, for AOM.

Microbial community composition at the seep stations

Many archaeal sequences obtained from the Simeulue seep stations 1 to 4, were distributed over the ANME-1 and -2 clusters (*Figure 30*). Operational taxonomic units (OTUs) from the stations 1 and 2 were assigned to ANME-1b and ANME-2b clusters. Also at the station 3, ANME-2a/c members were identified. The detection of different ANME clusters at the seep site is consistent with isotopic analyses, culturing experiments and qPCR results, confirming the presence of an active AOM-community. Furthermore, members of the *Crenarchaeota* were frequently detected in the DGGE analysis at both AOM-stations and the station 3. The occurrence of *Crenarchaeota* at a methane seep is not unusual and has been reported from other sites [3].

Most bacterial groups belonged to the family *Anaerolineaceae* (phylum *Chloroflexi*), the candidate devision OP9 [100] and the class δ-*Proteobacteria*. These groups have been described to be dominant in marine sediments [101]. Sequences affiliated to the family *Anaerolineaceae* were derived from stations 1 to 4. The nearest cultured genus *Leptolinea* (distance matrix: 84.5% identity with the nearest *Leptolinea* member) has been described as saccharolytic, including pectin and cellulose degrading species [102, 103]. In these studies,

members of the genus *Leptolinea* were not able to reduce sulfate or other sulfur species [103]. *Leptolinea* and *Levilinea* species largely comprise taxa discovered in anaerobic waste water sludge [74], indicating active heterotrophic processes at the AOM seep. However, sequences from the Simeulue seep were closer related to sequences which could not be assigned to these genera (*Figure 29*). Three sequences of the stations 1 and 2 were closely related to the genus *Desulfococcus* of the family *Desulfobacteraceae*, which is in good agreement with previously described AOM sites [3].

At the stations 1 and 2 (only data for station 1 are shown in *Figure 27*), *mcrA* genes encoding for the enzyme methyl-CoM-reductase of the anaerobic methanotrophic ANME-2 group dominated over ANME-1. ANME-1 *mcrA* genes prevailed only at the surface of the station 2. The *Methanosarcina* ("methanogenic") type of the *mcrA* gene was detected throughout the whole seep area, while it was completely absent in other sediments of the Sumatra forearc [44]. The simultaneous occurrence of both, methane production and oxidation in the seep area, underscores the important role of the methane cycle for this system. The *dsrA* gene, an indicator for the presence of sulfate reducers, was found in slightly higher gene copy numbers at the station 1 compared to 3 (*Figure 27*).

Methanogenesis as a concomitant process

Another goal of this research was to demonstrate methanogenic hydrocarbon degradation [28, 31]. From a geological point of view, the Sumatra forearc seems a promising location for hydrocarbon generation in the deep subsurface, a potential source for upward migrating of complex hydrocarbons. Hence, a total of 14 stations in deep and shallow water were screened for such processes. That the microbial community of the Simeulue seep was able to generate methane was confirmed by the detection of *Methanosarcina* related *mcrA* genes (*Figure 27*) and CH_4 production in sediment incubations with TMA or methanol.

Hydrocarbon dependent methanogenesis was observed in microcosms of both, the Simeulue seep and the Nias basin. After a first transfer of sediment microcosms of eleven stations, three stations showed sustained methanogenesis in the presence of higher hydrocarbons. Only one of these stations was located in the seep area (station 6), the other two in the Nias basin. Moreover, the rates estimated in the initial setups as well as in the first transfers, were in the same order of magnitude compared to those of a clearly hydrocarbon adapted community of contaminated harbour mud in the North Sea [104]. Methanogenesis was absent in microcosms without added substrates. Possibly, the presence of 28 mM sulfate and other electron acceptors inhibited methanogenesis from TOC, but not from higher hydrocarbons. In contrast, it seems likely that the addition of higher hydrocarbons stimulated growth and activity of TOC and hydrocarbon utilising microorganisms.

Desulfobacteraceae species may be indicative for AOM consortia [3]. Nonetheless, one member of this family is the hexadecane degrader *Desulfococcus oleaovorans* strain Hxd3 [105, 106]. Hence, the occurrence of this family may also be suggestive for the presence of consortia capable of anaerobic degradation of higher hydrocarbons. The finding of other closely related hydrocarbon seep associated sequences, e.g. from mud volcanoes or contaminated sites, suggest that potentially hydrocarbon degrading microorganisms were present at the Simeulue seep as well (*Figure 29*). However, hydrocarbons are abundant substances in nature and our culturing experiments show that the presence of hydrocarbon degraders does not necessarily depend on the presence of hydrocarbons in higher concentrations. Additionally, a larger petroleum reservoir in the Sumatra forearc was not predicted in a sediment basin modelling study [107]. In conclusion, hydrocarbon utilising methanogenic communities were present in the Sumatra forearc sediments irrespective of methane seepage, and their presence does not infer that higher hydrocarbons played a significant role in the carbon cycle. Nonetheless, this is the first report of stable microcosms of hydrocarbon-dependent methanogenic microbial communities from the deep ocean.

Conclusions

The first-time discovery of an AOM-influenced methane seep in the Indian Ocean was confirmed by the presence of dissolved methane as well as methane-dependent pro- and eukaryotic communities. Methane $\delta^{13}C$ signatures indicate a microbial origin of methane. The released methane was oxidised by an active microbial community, sharing features with other seep communities. Besides sulfate, also iron or manganese seemed to serve as electron acceptor for AOM, indicating a broader diversity of the respective microbial community. Albeit negligible *in situ*, higher hydrocarbons were converted to methane in vitro in sediments from seep and control sites, demonstrating the widespread occurrence of the respective microorganisms in marine systems.

Acknowledgements

4.2.   Linking carbon, sulfur and nitrogen cycles in anaerobic methanotrophic mats of a marine cold vent in the Black Sea by stable isotope probing

Michael Siegert[1], Martin Taubert[2], Felipe Bastida[3*], Mirko Basen[4], Martin von Bergen[2], Matthias Gehre[3], Hans-Hermann Richnow[3], Jana Seifert[2], Martin Krüger[1]

Manuscript in preparation

[1]Bundesanstalt für Geowissenschaften und Rohstoffe, Stilleweg 2, 30655 Hannover, Germany

[2]Helmholtz Centre for Environmental Research – UFZ, Department of Proteomics, Permoserstraße 15, 04318 Leipzig, Germany

[3]Helmholtz Centre for Environmental Research – UFZ, Department of Isotope Biogeochemistry, Permoserstraße 15, 04318 Leipzig, Germany

[4]Max-Planck-Institut für Marine Mikrobiologie, Celsiusstraße 1, 28359 Bremen, Germany

[*]present affiliation: Department of Soil and Water Conservation, CEBAS-CSIC, Campus Universitario de Espinardo, 30100, Murcia, Spain

Running title: Nitrogen cycle in Black Sea chimneys

Keywords: anaerobic oxidation of methane / nitrate reduction / anammox / methyl coenzyme M reductase / (di-)nitrogen fixation / stable isotope probing

Corresponding address: Martin Krüger, martin.krueger@bgr.de, Tel +495116433102, Bundesanstalt für Geowissenschaften und Rohstoffe Hannover, Stilleweg 2, 30655 Hannover, Germany

Abstract

Anaerobic methanotrophic mats host a variety of different microorganisms. This is suggestive of various nutrient and energy pathways. Fuelled by methane as energy source and maintained by sulfate reduction, these mats presumably metabolise a broad variety of nutrients. Here, we used stable isotope probing (SIP) to link carbon, sulfur and nitrogen cycles. We could show that the anaerobic oxidation of methane (AOM) coupled to sulfate reduction drives the nitrogen cycle in anaerobic methanotrophic mats of the Black Sea. To trace the fate of nitrogen, we used four different ^{15}N labelled sources of nitrogen: dinitrogen, nitrate, nitrite and ammonium and provide evidence for their use in the mat's energy metabolism as well as catabolism. For the latter, we traced nitrogen incorporation into bulk biomass, proteins and amino acids. Nitrogen uptake was tested under conditions with and without methane or sulfate. While dinitrogen plays an insignificant role as source of nitrogen, nitrate was used for assimilatory and dissimilatory denitrification. Nitrate reduction was dependent on methane and sulfate, suggesting that denitrification is achieved by oxidation of reduced sulfur intermediates. Ammonium was used for biomass build-up as well with high incorporation rates when the mats conducted AOM coupled sulfate reduction. High metabolic rates, in turn, were dependent on ammonium supply. The methyl coenzyme M reductase is the key enzyme in anaerobic methanotrophy coupled to sulfate reduction. This enzyme was actively synthesised from all nitrogen sources except dinitrogen as demonstrated by ^{15}N-label incorporation. This emphasises the central role of MCR enzymes in anaerobic methane oxidation. In summary, methane as the predominating energy source fuelled the nitrogen cycle in the anaerobic methanotrophic mats of the Black Sea.

4.2.1. Introduction

Between 70-100 m water depth, the Black Sea becomes completely anoxic, providing ideal conditions for studying anaerobic marine nutrient cycles [108, 109]. Furthermore, the depletion of other electron acceptors like nitrate or oxidised metals makes biological energy harvesting processes challenging. Nevertheless, the Black Sea is often energy rich which is reflected in high concentrations of methane, sulfide and ammonium. Previous studies showed that AOM performed by ANME (anaerobic methane oxidising) consortia contributes significantly to carbon and sulfur turnover in marine environments worldwide [3, 5].

First evidence for a direct link to the nitrogen cycle came from Raghoebarsing *et al.* [26]. They could show that AOM was directly coupled to denitrification. In a more recent report, the intriguing capability to produce intrinsic oxygen by cleaving two moles nitric oxide to one mole dinitrogen and molecular oxygen each was shown to by responsible "anaerobic" methanotrophy [110]. This imposes the question whether AOM coupled to nitrate reduction is

in fact an aerobic (NO cleavage) or anaerobic process. The latter may be a sequential electron transfer from methane to sulfate and nitrate as terminal electron acceptor. The anaerobic oxidation of sulfide by nitrate is an example for such a possibility [111, 112]. This seems possible for AOM performing microbial consortia because sulfide is the terminal reaction product of sulfate reduction coupled to AOM [3].

A second route of nitrate reduction is dissimilatory nitrate reduction to ammonium (DNRA). This is a well known electron sink especially under reduced marine conditions [113-115]. While the benefits of dissimilatory nitrate reduction to dinitrogen (denitrification) are exclusively derived from respiratory phosphorylation, DNRA was attributed to a fermentative lifestyle [113]. However, a number of sulfate reducers are capable of DNRA, among them *Desulfovibrio* and *Desulfobulbus* species [113]. The latter were frequently detected in AOM influenced environments [3].

A reason for the frequent occurrence of DNRA in deep marine environments may be the elevated dinitrogen partial pressure opposing slow diazotrophic activity. Diazotrophy in AOM consortia was previously demonstrated by Orphan *et al* [116]. The authors could show that the uptake of ^{15}N-ammonium in labelling experiments coincided with ^{13}C depletion in biomass of methane oxidising ANME consortia. Nitrogen uptake into biomass is often linked directly to protein synthesis. Since protein extraction from sediments is challenging, the naturally occurring, methane oxidising mats of the Black Sea seem a useful study object to address this issue [6]. These large carbonated reefs are regarded as living microbial fossils similar to cemented structures of the lower Meocene which are preserved near the coast of the Black Sea in Bulgaria [117, 118]. These mats are distinguished in two different phenotypes and phylotypes. While the archaeal community of the inner pink mats comprised mainly ANME-1, the outer ring of black mats hosted also ANME-2 *Archaea* [119]. However, precise information about the relation of ANME-1 to ANME-2 archaea is scarce. *In situ*, the outer black mats were in permanent contact with sea water sulfate, while the inner pink mats inhabited a sulfate depleted environment [6]. In the living mats, MCR enzymes are the predominant fraction of total proteins [23]. These proteins were shown to conduct anaerobic methanotrophy as reverse methanogenesis [24]. Hence, these enzymes are essential for the AOM mats and a primary target of investigation.

Besides ammonium assimilation, anaerobic ammonium oxidation (anammox) might contribute to the nitrogen cycle of the Black Sea mats. Anammox is the major sink for nitrogen in the Black Sea [108]. However, it depends on the availability of nitrite which is oxidant of ammonium in this process. Nitrite is virtually absent in the water column of the Black Sea below 100 m [108]. Therefore, anammox should be restricted to the oxygen minimum zone in the Black Sea's chemocline. Hence, sulfate seems to be a possible candidate for anaerobic

ammonium oxidation at 230 m water depth – where the Black Sea chimneys naturally occur. Anaerobic ammonium oxidation by sulfate is a thermodynamically possible reaction [120], albeit never demonstrated so far. It is interesting to examine this possible pathway in the Black Sea methanotrophic mats.

For the first time, this research reports quantitative nitrogen fluxes in anaerobic methanotrophic communities in dependence on methane or sulfate amendment. We distinguish four important sources of nitrogen for energy metabolism and catabolism. For catabolism, we traced nitrogen incorporation into bulk biomass, proteins and amino acids by stable isotope probing. Additionally, we demonstrate nitrogen incorporation and thereby the *de novo* synthesis of the mat specific MCR enzyme which is a key enzyme in anaerobic methanotrophy and major constituent of bulk mat proteins.

4.2.2. Materials and Methods

Anaerobic incubations

Sample collection

Samples were collected from carbonate chimneys in the Black Sea on R/V *Poseidon* cruise 317 leg 2 in 2004 and R/V *Meteor* cruise M72/1 in 2007 [6]. Microbial mat material was separated into black and pink mats under nitrogen atmosphere on board. Subsequently, these were transferred into sterile glass bottles, sealed with butyl rubber stopper and filled up with anaerobic bottom water. Headspaces were flushed with methane and mat material was shipped at 4°C to our home lab. In our home lab, mats were incubated in batch cultures in artificial sea water and methane atmosphere as previously described [121].

Medium and slurry preparation

To exclude oxygen, all manipulations were performed under nitrogen atmosphere. Media were prepared as described in Nauhaus *et al.* [121]. Dissolved air was removed from the medium by gassing the medium with helium until air concentrations were less than 1% in the headspace. Headspace air concentrations were determined using an SRI 6810C gas chromatograph equipped with a thermal conductivity detector (TCD) and 6 foot Hayesep D column (both SRI Instruments, USA). Remaining oxygen was reduced by adding 1 mM sulfide. For sulfate reduction experiments, 20 mM $MgSO_4$ was added. In incubations without sulfate, sulfate was replaced by chloride as $MgCl_2$. Un-inoculated and inoculated but autoclaved controls were set up for helium flushed incubations. After flushing the headspace with helium, approximately 25% dinitrogen remained. Except the controls, all incubations were set up in quadruplets. If not indicated otherwise, incubations were inoculated with a 1/1 slurry mix of

black mats of two research cruises. The slurry was prepared using artificial sea water as described in Nauhaus *et al.* [121]. Ammonium was omitted for slurry preparation. 20 ml medium contained 2 ml mat material.

Isotopically labelled nitrogen compounds are frequently used to study nitrogen cycling in various habitats [122]. Three ^{15}N-nitrogen sources were tested: $^{15}N_2$ (17%$_{v/v}$), K$^{15}NO_3$ (5 mM) or $^{15}NH_4Cl$ (5 mM). Additionally, an anammox test was performed with Na$^{15}NO_2$ and $^{14}NH_4Cl$ or vice versa in equimolar concentrations of either 0.1 mM or 5 mM [123]. To maintain salinity, the missing molar amount of salt was replaced by NaCl. The headspace was either filled with helium or ^{12}C-methane. The experiment was terminated after one year of incubation but bulk biomass, ammonium and gas analyses were conducted before re-feeding the batch reactors. Re-feeding (out-dilution of ^{14}N) was required because protein incorporation rates were very slow.

To demonstrate methane oxidation, a second experiment with 10%$_{v/v}$ ^{13}C-labelled and unlabelled methane was set up. Additionally, ^{15}N-nitrate was added in concentrations of 5 mM either with 20 mM sulfate or without. $^{13}CO_2$ and ^{15}N-dinitrogen were analysed after 79 days of incubation.

For analysing ^{15}N-nitrate incorporation into amino acids, in a separate experiment with black and pink mats of the cruise R/V *Poseidon* cruise 317 leg 2 were investigated under the same incubating conditions. The only exception was that pre-incubations were nitrogen deficient. Incubation time before harvesting the mat material for amino acid extraction was four months [124]. Since nitrate uptake proceeds via reduction to ammonium, incubations to show amino acid synthesis were conducted only with ^{15}N-nitrate. Nonetheless, we reported ^{15}N-ammonium incorporation into amino acids previously and used modified methods described therein [124]. In our previous report we could also demonstrate errors below 10% using the same samples and method, which justified single measurements in the presented experiment studying the same mats.

Analyses of inorganics

Sulfide concentrations were determined spectrophotometrically by the formation of copper sulfide which was measured biweekly [49]. Reduced iron and manganese as well as ammonium, nitrate and nitrite were detected using Merckoquant analytical tests (Merck, Germany; order numbers are for Fe: 1.10004, Mn: 1.10080, NH$_4^+$: 1.14752, NO$_3^-$: 11020, NO$_2^-$: 1.10007). Iron and manganese were measured after two weeks and then again after six months of incubation. Nitrate and nitrite were measured weekly during the first month of incubation but reduction rates were determined by measuring ^{15}N-dinitrogen and ^{15}N-

ammonium after 5 days. For ^{15}N-ammonium in the supernatants, 2 ml culture broths were centrifuged, the supernatants filtered through 0.45 µm PTFE filters (Sartorius, Germany) and evaporated at 60°C over night in vacuum. The remainders were diluted using a known amount ^{14}N-ammonium sulfate, weighed in tin foil and analysed for their ^{15}N-content in a Euro EA Elemental Analyser (Eurovector) coupled to an IRMS (MAT 253, Thermo Fisher Scientific). The absence of nitrate was verified using Merckoquant tests.

^{14}N + ^{15}N-dinitrogen concentrations in the headspace were determined using an SRI 8610C gas chromatograph equipped with a helium induced detector (HID) and a 6 foot silica gel column (all SRI Instruments, USA). Isotopic dinitrogen compositions were determined using a Finnigan MAT252 GC-IRMS system (Thermo Fisher Scientific, USA), equipped with a Poraplot Q column (Agilent Technologies, USA). The gas flow was cooled after injection by passing a capillary fixed in a liquid nitrogen container to remove carbon monoxide.

Nitrogen isotopic ratios are expressed as ^{15}N‰ versus air. Rates are given in µmol cm^{-3} d^{-1} or nmol cm^{-3} d^{-1} mat. Mean values and deviations thereof were calculated from samples within 95% confidence intervals unless stated otherwise. A label recovery was defined as a greater $^{15/15}$N$_2$ area than the corresponding $^{15/14}$N$_2$ area in isotope ratio mass spectrometer chromatograms (elemental analyser, GC-IRMS). Rates were estimated as described in *Supporting Information*.

Protein and amino acid analyses

Proteins were extracted from 2 g wet mat material by triplicate sonication on ice for 10 min each, after suspension of mat material in 50 mM 3-(N-morpholino)propanesulfonic acid (MOPS) / KOH buffer (pH 7). The obtained homogenate was centrifuged for 15 min at 10,000 x *g* and 4°C. The supernatant was again centrifuged for 1 h at 120,000 x *g* and 4°C. Protein concentrations were determined as described elsewhere [126]. Protein fractions were obtained by fast protein liquid chromatography (FPLC) separation in an ÄKTA purifier 10 (GE Healthcare, USA) using a HiTrap$^®$ Q HP 5 ml column (GE Healthcare, USA). The instrument was run using a 50 mM buffer MOPS/KOH at pH 7 and the NaCl gradient was increased over 84 min from 0.2 to 0.6 M NaCl.

Identifiaction of target proteins by ultra performance liquid chromatography (UPLC) coupled LTQ™ Orbitrap mass spectrometry (MS)

10 µl of each FPLC fraction were chromatographed in denaturing SDS / acrylamid gels [127]. Protein bands of interest were excised from SDS-gel lanes, and in-gel tryptic cleavage was performed as previously described [128]. Peptides were reconstituted in 0.1% formic acid. So obtained proteins solutions were concentrated on a trapping column (nanoAcquity UPLC col-

umn, C18, 180 µm x 2 cm, 5 µm, Waters, Germany) with water containing 0.1% formic acid at flow rates of 15 µl x min^{-1}. After 4 min, peptides were eluted onto a separation column (nanoAcquity UPLC column, C18, 75 µm x 250 mm, 1.7 µm, Waters). Chromatography was performed by using 0.1% formic acid in solvents A (100% water) and B (100% acetonitrile), with peptides eluted over 30 min with a 8–40% solvent B gradient using a nano-HPLC system (nanoAcquity, Waters) coupled to an LTQ™ Orbitrap mass spectrometer (Thermo Fisher Scientific, USA). Continuous scanning of eluted peptide ions was carried out between 150 and 2000 m/z, automatically switching to MS/MS CID mode on ions exceeding an intensity of 3000.

Raw data were processed for database search using Thermo® Proteome Discoverer software (v. 1.0 build 43, Thermo Fisher Scientific). Search was performed by tandem mass spectrometry ion search algorithms from the Mascot in-house server version 2.2.1 [129]. The following parameters were selected: *Bacteria* of NCBInr (National Center for Biotechnology Information, USA) as criterion for taxonomy, tryptic cleavage, max. two missed cleavage sites. A peptide tolerance threshold of ±10 ppm and an MS/MS tolerance threshold of ±0.2 Da was chosen. Carbamidomethylation at cysteines was given as static and oxidation of methionines as variable modification. Peptides were considered to be identified by Mascot when a false positive probability <0.05 (probability based ion scores threshold >40) was achieved.

Anlaysis of isotope incorporation into proteins

Analyses of isotope incorporation into proteins by matrix assisted laser desorption / ionisation – time of flight (MALDI-TOF) mass spectrometry [130, 131] or similar methods were impossible due to low ^{15}N incorporation rates of the mats. Here we propose an alternative method to determine isotope incorporation into proteins. This method is based on elemental analyser (EA) isotopic measurements of precipitated nearly pure proteins.

FPLC fractions (2 ml each) and total soluble protein extracts (500 µg) were precipitated using 20%$_{v/v}$ trichloro acetic acid by incubation at 4°C overnight. After centrifugation (13,000 x *g*, 4°C and 15 min), pellets were dissolved with 200 µl molecular grade water and the 5-fold volume (1 ml) of 100% cold acetone was added. After incubation during 15 min, protein pellets were obtained by centrifugation as described above. Acetone was removed and the remainders were dried for 1 h at 37°C. Protein pellets were gently dissolved in 40 µl of molecular grade water and transferred into tin capsules. Then, 10 µl of pure acetone were added and the liquids were evaporated for 3 h at 60°C.

Dry protein pellets were analysed in an EA as described above. For identification of MCR dominated FPLC fractions, all fractions were separated in SDS gels and Coomassie Blue stained. Incorporation rates into MCR dominated FPLC fractions were calculated using $\delta^{15}N$ values vs. air instead of dead controls. Total protein incorporation rates, were calculated using $\delta^{15}N$ values vs. total proteins of dead controls. In case of MCR proteins, rates were not calculated in moles as the exact proportion of type-1-MCR of the total soluble proteins was unknown. However, the proportion of newly synthesised type-1-MCR relative to all extracted type-1-MCR proteins per day could be estimated. This value is expressed in % d^{-1}. Two models served the calculation of relative synthesis rates. In the first model we assumed that the ^{15}N-nitrogen source was directly derived from the supplemented ^{15}N-nutrient, meaning that each *de novo* type-1-MCR contained 100% ^{15}N. As this may underestimate the relative synthesis rate, the biomass was assumed to be the nitrogen source. In this case, the biomass isotopic composition served on the day of protein extraction was calculated using ^{15}N assimilation rates. Every *de novo* type-1-MCR molecule was assumed to contain half of this isotopic composition. Based on a linear protein synthesis rate, the half isotopic composition was chosen because at the beginning of the experiment no label could be incorporated while at the end the full biomass label was available. Hence, type-1-MCR relative synthesis rates are estimations. Absolute rates expressed in ng cm^{-3} d^{-1} were estimated as described in the *Supporting Information*.

Total amino acids were determined according to the method of Macko *et al.* [132] and Silfer *et al.* [133]. Hydrolysis of the samples was performed with 6 M HCl (0.5 ml, 110℃, 22 h). Hydrolysates were evaporated to dryness under nitrogen atmosphere and then cooled in a bath with ice for 5 min. After drying, samples were incubated in a mix of 1 ml isopropanol and 0.25 ml of acetylchlorid overnight at 60℃. Then, the trifluoroacetylation of the amino residues was performed after total evaporation of the sample under nitrogen atmosphere, adding 500 µl methylene chloride and 500 µl trifluoro acetic anhydride. The reaction mixture was incubated for 2 h at 60℃. Finally, samples were dried under nitrogen atmosphere and dissolved in 100 µl methylene chloride.

The amino acids derivatives were identified using a 7890A gas chromatograph coupled to a 5975C mass spectrometer (Agilent Technologies, Germany) was used. The carboxylic acid fractions were separated on a HP-5MS column (30 m x 0.25 mm x 0.25 µm) by injection of 3 µl sample. For identification, an external standard (50 µl) containing 50 mg ml^{-1} of each detectable amino acid was treated in parallel with the samples and was injected for comparison with each series of analyses. The individual amino acids were identified by comparison of retention times and mass spectra with those of the standard mixture. The temperature programme was: 50℃ (1 min) to 100℃ (5 min) at 30° C min^{-1}, to 175℃ (5 min) at 10℃ min^{-1},

to 250°C (5 min) at 10°C min $^{-1}$, to 300°C (12 min) at 30°C min $^{-1}$. The injector was set to 280°C and samples were injected with a split ratio of 15:1. The transfer line was held at 250°C and the helium flow was set to 2 ml min $^{-1}$.

Quantification of *mcrA*-genes

To quantify *mcrA*-genes in the black and pink mats, DNA was extracted from 0.1 g mat material using the Fast DNA for Soil Kit, according to the manufacturer's protocol except the addition of 10 µl 1% poly adenine (polyA) in the initial step [55]. An StepOne real-time PCR thermocycler (Applied Biosystems, USA) was employed to enumerate copies *mcrA*-genes belonging to ANME-1 and ANME-2 clusters [56].

4.2.3. Results

Sulfate reduction and methane oxidation
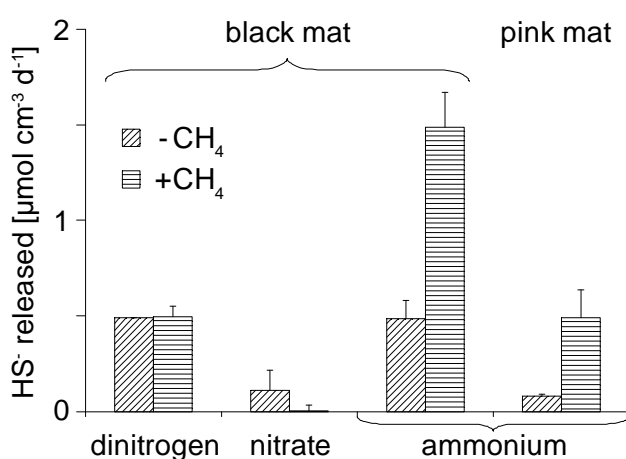
Figure 31: Sulfate reduction rates under when ^{15}N dintrogen, ^{15}N nitrate or ^{15}N ammonium were added to the black mats (left) or the pink mats (right).

Sulfate was reduced to sulfide with and without methane in the headspace (*Figure 31*). While sulfate reduction occurred to some extent in incubations with ^{15}N-dinitrogen and helium or methane in their headspace, in ammonium incubations, sulfate reduction was three times higher with methane compared to incubation with helium (1.49±0.18 µmol cm^{-3} d^{-1}; *Figure 31*). Nitrate inhibited sulfate reduction (*Figure 31*). When all nitrate was depleted, sulfate reduction remained suppressed until the experiment was terminated (more than four months after last measurement).

Moreover, ^{13}C-methane was oxidised to ^{13}CO$_2$. After 78 days of incubation, the $\delta^{13}C_{CO2}$ was +275.2±17.2‰ when sulfate and nitrate were added. Without sulfate but with nitrate, the $\delta^{13}C_{CO2}$ was -12.7±7.3‰. With ^{12}C-methane, the $\delta^{13}C_{CO2}$ was -18.2‰ with sulfate and nitrate and -21.7‰ with without sulfate but with nitrate.

<u>Distribution of ANME-1 and ANME-2 *mcrA*-genes</u>

Copy numbers of ANME-1 *mcrA*-genes were $5 \times 10^7 \pm 6 \times 10^6$ cm^{-3} in the pink mats and $2 \times 10^6 \pm 2 \times 10^5$ cm^{-3} in the black mats. ANME-2 *mcrA*-genes were present with copy numbers of $1 \times 10^4 \pm 9 \times 10^2$ cm^{-3} in the pink mats and $6 \times 10^5 \pm 6 \times 10^4$ cm^{-3} in the black mats. Errors are standard deviations of three parallel measurements.

<u>Nitrogen turnover</u>

Nitrogen uptake of three different nitrogen sources – ammonium, nitrate and dinitrogen – was investigated. Compared to ammonium and nitrate, dinitrogen fixation into biomass was approximately three orders of magnitude lower (*Figure 32B*, *Figure 33B* and *Figure 34*). Besides incorporation into biomass, dinitrogen was also channelled into dissolved ammonium to a greater extent (*Figure 32*). Of the total biomass, total soluble proteins did not incorporate the nitrogen label with final δ^{15}N values between -5.6‰ and 2.8‰ (*Table 8*) which overlapped with unlabelled controls.

Nitrate was assimilated into biomass and reduced to dinitrogen as well as dissolved ammonium (*Figure 33*). However, less than 10% of ^{15}N-nitrate was attributed to assimilatory nitrate reduction (*Figure 33*). 36% of nitrate was channelled into denitrification while DNRA made up 53% of nitrate reduction (*Figure 33A*). Assimilatory nitrate reduction was effected by methane and sulfate supply (*Figure 33B*). While there was increased assimilatory nitrate reduction when methane was present but no sulfate, dissimilatory nitrate reduction rates (denitrification and DNRA) increased only when both – nitrate and methane – were amended (*Figure 33B*). When sulfate and methane were present, nitrate was incorporated with 123 ± 8 nmol N cm^{-3} d^{-1}. Additionally, the label was incorporated into total proteins in rates of 5 nmol cm^{-3} d^{-1} in the same experiment (*Table 8* and *Figure 33B*).
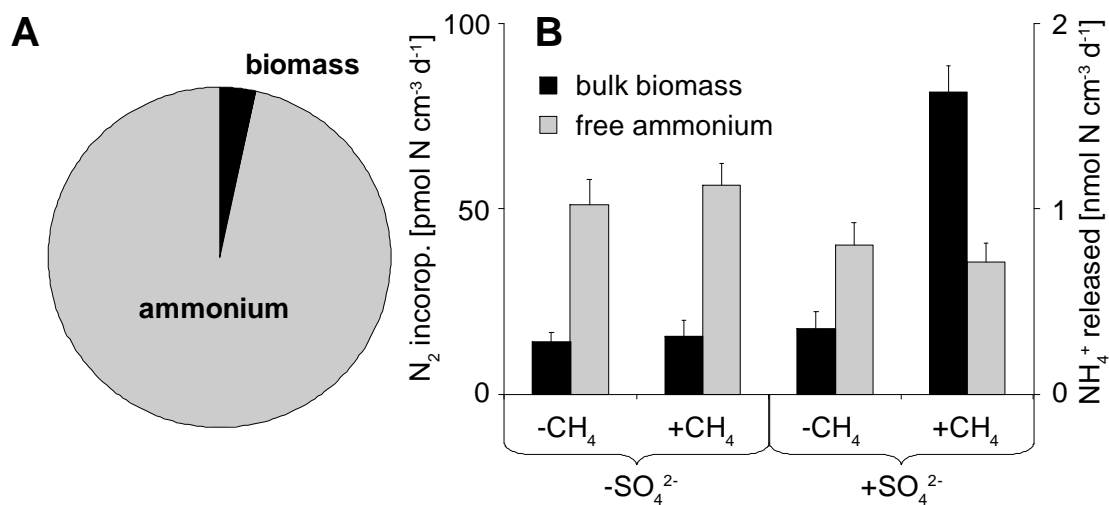
*Figure 32: Dinitrogen fixation into biomass and corresponding release of ammonium into the medium. (**A**) The pie chart depicts the the destination of dinitrogen derived N as parts. It was averaged over all incubation conditions, as indicated on the x-axis of (**B**). Errors in (**B**) indicate standard deviations of the mean of incubations within 95% confidence intervals. Further explanations are given in Materials and Methods.*
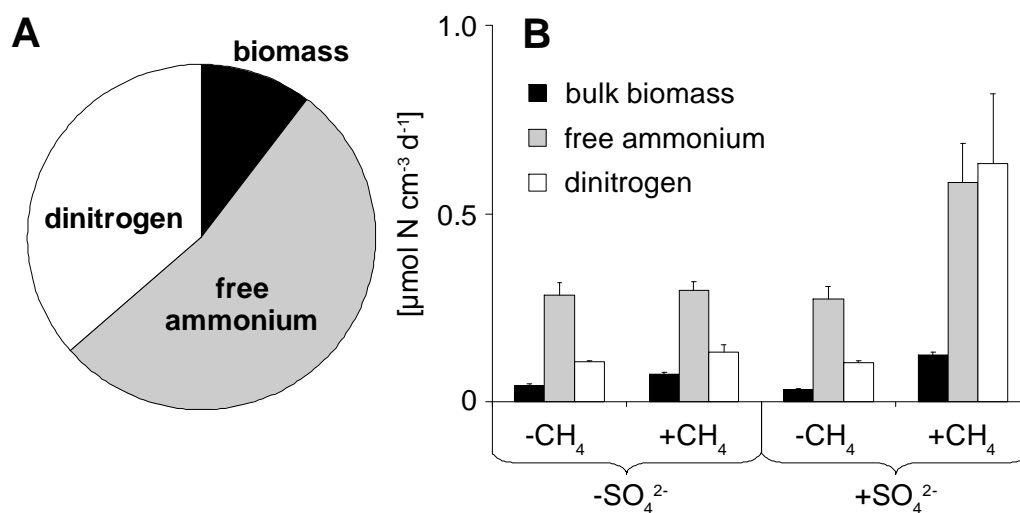
*Figure 33: Comparison of assimilatory and dissimilatory nitrate reduction. For the pie chart (**A**), the average over all incubation conditions was taken. It shows the destination of nitrate derived N as parts. **B**: Rates of biomass incorporation, DNRA (free ammonium release) and dinitrification (dinitrogen).*
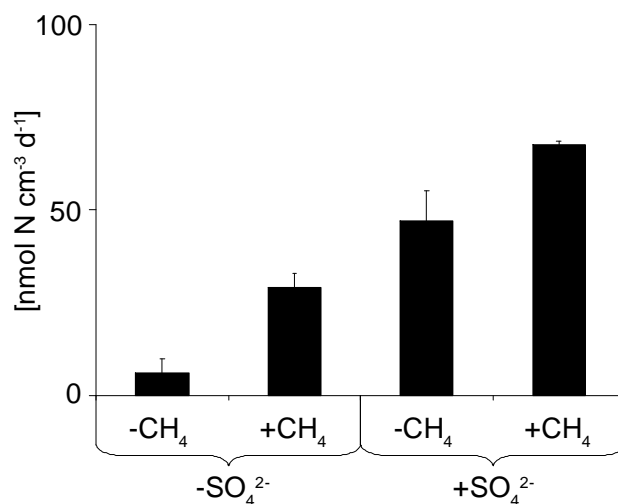
Figure 34: Assimilation of free ammonium into bio-mass. Errors in (B) indicate standard deviations of the mean of incubations within 95% confidence intervals. Further explanations are given in Materials and Methods.

Table 8: Incorporation of the ^{15}N labelled substrates dinitrogen, nitrate and ammonium into total soluble proteins. Dinitrogen was added as a mix of $17\%_{V/V}$ ^{15}N-dinitrogen to ^{14}N-dinitrogen. Nitrate and ammonium were added as 100% ^{15}N-substrates. Dead controls were killed using 8% formaldehyde and subtracted from the estimated rates. $\delta^{15}N$ values against dead controls were obtained from a single killed incubation which was extracted at the same time with the dead control incubation. The technical error of triplicate air measurements was not higher than 2‰. Rates of dinitrogen fixation and "n/a" incubations were not calculated because $\delta^{15}N$ values were too low.

Medium	Headspace	$\delta^{15}N$ vs. dead control [‰ vs. air]			corresponding rate [nmol N cm^{-3} d^{-1}]	
		Dinitrogen	Nitrate	Ammonium	Nitrate	Ammonium
-SO$_4^{2-}$	Helium	2.8	2354	624	7	1
	Methane	2.3	1770	83	5	0
+SO$_4^{2-}$	Helium	-3.9	1153	3045	2	5
	Methane	-5.6	2908	-67	5	n/a
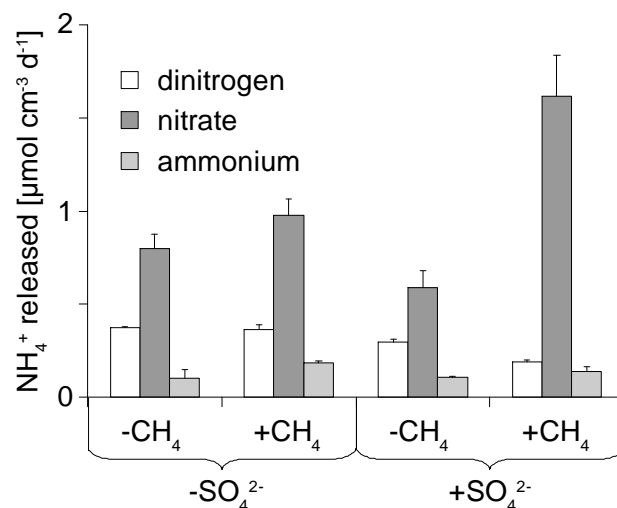
Figure 35: Net ammonium release under different incubation conditions (diazotrophic, nitrate reducing and ammonium assimilating). Ammonium released was a mix of ^{14}N and ^{15}N ammonium. Error bar calculations are described in the Materials and Methods section.

Ammonium incorporation into biomass was at least 6 times higher than into total soluble proteins (*Figure 34* and *Table 8*). In case of sulfate and methane amended microcosms, ammonium was incorporated into proteins while the rate of bulk biomass incorporation was 67.6 nmol cm^{-3} d^{-1}. Ammonium was also released from the mats (*Figure 35*). An oxidation of ammonium to dinitrogen as proposed by Schrum *et al.* [120] was not observed with neither sulfate, ferrihydrite nor manganese dioxide as electron acceptor.

While nitrite reduction to dinitrogen occurred, anammox was not observed. ^{15}N-nitrite label was always recovered as $^{15/15}N_2$. The addidition of 5 mM nitrite was not toxic. However, rates for nitrite reduction were not calculated.

Protein and amino acid synthesis

Nitrate and ammonium were channelled into protein and amino acid synthesis (*Table 8*). As major functional proteins of the methane oxidising mats, several types of MCR were investigated. MCR dominated FPLC fractions were investigated regarding their nitrogen isotopic composition after four months batch reactor incubation. The amount of MCR proteins in the cell extracts was previously reported to be 7%$_{w/w}$ [23]. Three different types of MCR were identified (Supporting Information *Figure S7*). For the following MCR investigating experiments, the fraction containing the MCR type 1 was selected (Supporting Information *Figure S7*). ^{15}N-ammonium derived label incorporation into type-1-MCR proteins was found exclusively in the black mats ($\delta^{15}N$ 1759‰, pink mats: 9.0‰). In conclusion, black mats were em-

ployed for further experiments. $\delta^{15}N$ values for the ^{14}N-ammonium controls were 3.8‰ and 3.6‰ respectively.
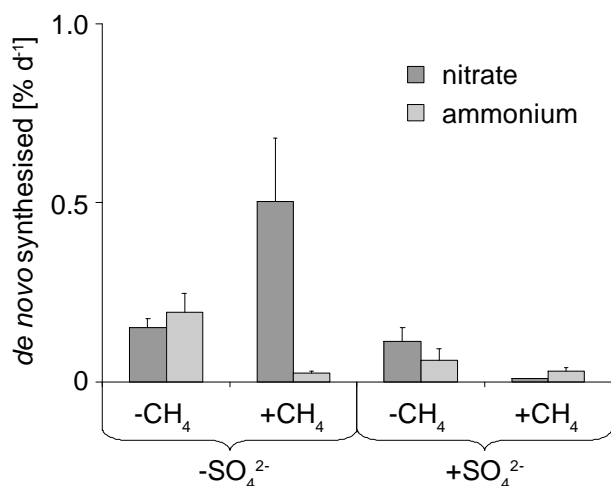
Figure 36: Relative synthesis rates of type-1-MCR enzymes. Rate calculations are described in the Supporting Information.

To test nitrogen incorporation of different nitrogen sources into the type-1-MCR under distinct incubation conditions, set-ups with and without methane or sulfate were incubated. Nitrogen sources were ^{15}N-dinitrogen, ^{15}N-nitrate or ^{15}N-ammonium. While the ^{15}N-dinitrogen label was found in the bulk biomass, it was neither detected in total soluble proteins nor in type-1-MCR enzymes. ^{15}N-nitrate as well as ^{15}N-ammonium were utilised for type-1-MCR synthesis in comparable rates (*Figure 36*). The only exceptions were incubations with ^{15}N-nitrate and methane

but without sulfate (*Figure 36*). Type-1-MCR synthesis rates were five times higher compared to corresponding ^{15}N-ammonium incubations (*Figure 36*). This effect was the same when ^{15}N-substrates were considered to be the direct nitrogen source, rather than built-up biomass (*Supporting Information Figure S8* and *Figure S9*). In all other cases, nitrate and ammonium incorporation were comparable (*Figure 36*).
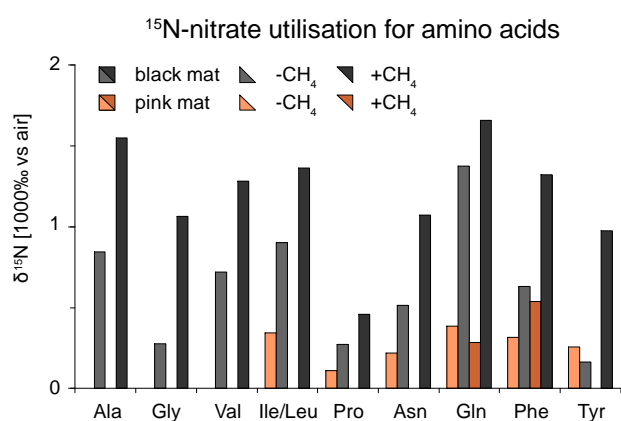
Figure 37: Assimilation of ^{15}N nitrate in selected amino acids of pink and black mats incubated under sulfate reducing conditions with or without methane.

^{15}N-nitrate was incorporated into amino acids in black and pink mats (*Figure 37*). While all investigated amino acids (Ala, Gly, Val, Leu/Ile, Pro, Asn, Gln, Phe, Tyr) of the black mats incorporated ^{15}N, some amino acids of the pink mats did not contain the label (Ala, Gly, Val). The ANME-2 dominated black mats incorporated the ^{15}N-nitrate label into amino acids to much greater extent than the ANME-1 dominated pink mats (*Figure 37*). Based on this result, the black mats were selected to demonstrate the coupling of AOM de-

pendent nitrogen metabolism. The incorporation of label was dependent on methane (*Figure 37*). In black mats, methane amendment resulted in a stronger incorporation of label. Except for phenylalanine, this trend was inverted in pink mats.

4.2.4. Discussion

While previous efforts focused to clarify carbon fluxes in AOM driven systems [97], nitrogen – an essential nutrient – received less attention. Two publications reported the incorporation of nitrogen compounds into AOM associated cells using a combined CARD-FISH and nanoSIMS approach [116, 134]. However, in both reports a quantitative evaluation was missing. Moreover, the involvement of key enzymes in nitrogen turnover is poorly understood. Aim of the presented research was to reveal major nitrogen channels and their interdependency with AOM coupled sulfate reduction.

<u>Nitrogen cycle</u>

Of all three investigated ^{15}N-nitrogen sources, dinitrogen fixation was negligible (0.05%), while ammonium accounted for approx. 35% and nitrate 65% of bulk biomass build-up in the black mats (*Figure 38*). Bulk biomass incorporation of ^{15}N-dinitrogen was clearly dependent on AOM driven sulfate reduction (*Figure 32*). On the other hand, it was independent from methane alone (*Figure 32*). This is consistent with the observation of sulfate reduction rates on the level of methane-free ammonium incubations (*Figure 31*). Most likely, dinitrogen fixation rates are rate-limiting for protein synthesis, hindering the energy flow within in the consortium and hence sulfate reduction rates. Dekas *et al.* [134] speculated on whether dinitrogen fixation is required in ammonium rich environments. For example, the authors argued that in deep marine environments so far unknown mechanisms evolved to overcome the high energetic investment of 16 ATP to fix one molecule N_2. In the Black Sea mats, however, dinitrogen fixation was negligible. Nonetheless, diazotrophic activity might have been increased in parts of the community where such capabilities were present, as it was shown in the same report [134].

Nitrate was reduced to ammonium and dinitrogen and assimilated into biomass (*Figure 33*). Nitrite, as an intermediate of nitrate reduction, was also reduced. Nitrate reduction in deep Black Sea anoxic mats seems surprising at first because a complete depletion of nitrate was reported below 70 m or 100 m water depth [108, 109]. The mat material was sampled at 230 m water depth [6]. Additionally, pre-incubations were never amended with nitrate over years. However, nitrate reducing microorganisms are frequently found in various deep marine environments. For example, *Caldithrix* – a genus containing reported nitrate reducers – was detected in clone libraries of the pink and the black mats [135]. Nevertheless, it is un-

known whether nitrate penetrated the water body of the Black Sea deep enough to sustain growth of nitrate reducing microorganisms and the discovery of such activity in this environment is quite surprising. However, unknown in-fluxes of nitrate or temporal changes of the oxygen minimum zone seem possible. That a massive built-up of living biomass like the Black Sea methanotrophic mats is accompanied by fast decay of non-functional cells seems likely as well., Additionally, active nitrate reducing capabilities were apparently preserved. This implies that nitrate reduction was required for the methanotrophic cell aggregates.
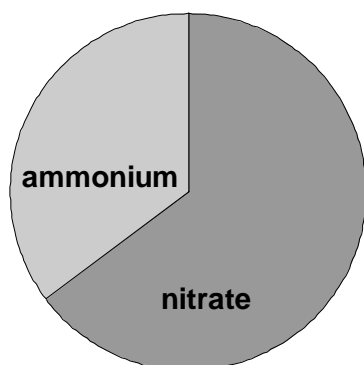
Figure 38: Overall assimilation of ^{15}N nitrate or ^{15}N ammonium into biomass.

Anammox, however, did not occur in the Black Sea methanotrophic mats, while nitrite – an intermediate of nitrate reduction – was reduced to dinitrogen. This suggests that the mat's energy metabolism was predominantly fuelled by methane rather than by ammonium. That methane was the driving force is reflected in the dependence of nitrate reduction on methane supply (*Figure 33*). Sulfate was necessary as well, which indicates that nitrate reduction was vastly de-coupled from methane oxidation alone. It presumably required the presence of reduced sulfur compounds, e.g. sulfides [111, 112]. Since sulfide was never detected in nitrate reduction experiments, not even after all nitrate was depleted, the dependence on the oxidation of sulfides remains speculative. One explanation is the re-oxidation of sulfide to elemental sulfur rather than sulfate [111] which microorganisms of the mats were possibly unable to utilise. In conclusion, lithotrophic nitrate reduction was obviously dependent on the supply of reduced sulfur compounds from AOM driven sulfate. Heterotrophic nitrate reduction without sulfate, methane or both, coupled to degradation of organic mat material, seems to be a secondary pathway when no other electron sources were provided (*Figure 33*).

It is noteworthy that DNRA may be attributed to decay of nitrogen containing matter. Net ammonium was released even when it was amended with the medium but nitrate was absent (*Figure 35*). This would imply that DNRA was in fact rather assimilatory. One may argue that the increase of ammonium release under AOM coupled sulfate reducing conditions is indicative for higher metabolic turnover rates. This is contrasted by the observation of decreasing net ammonium release under AOM coupled sulfate reducing conditions (*Figure 35* and *Figure 38*) when dinitrogen but no additional ammonium was provided. When additional ammonium was available, ammonium release rates were comparable under all incubation conditions (*Figure* 35). A clear increase of ammonium release rates was only observed when methane and nitrate were added and was the greatest when sulfate was also present. In conclusion, nitrate reduction was in favour for energy metabolism and hence dissimilatory

nitrate reduction. This is in good agreement with the observation that only 10% of ^{15}N-nitrate were assimilated into biomass (*Figure 33*) and consistent with the fact that methane was almost completely utilised for energy metabolism rather than assimilated into biomass [97].

An elevated dependence on methane supply was apparent for assimilatory nitrate reduction but not for ammonium assimilation (*Figure 34* and *Figure 33*). Ammonium incorporation was significantly dependent on sulfate presence (*Figure 34*) while it was not oxidised to dinitrogen as suggested by Schrum *et al.* [120]. This sulfate dependence may be a result of overall increased biomass synthesis, most likely driven by growth of sulfate reducers. On the other hand, AOM coupled sulfate reduction was clearly dependent on ammonium supply (*Figure 31*). This observation may mislead to the conclusion that sulfate reduction was coupled to ammonium oxidation – which was not the case. Presumably, increased metabolic rates as a result of AOM lead to higher ammonium uptake (*Figure 34* and *Figure 38*).

Synthesis of type-1-MCR enzymes

It is commonly accepted that consortia of ANME cells and bacteria of the Desulfosarcina / Desulfococcus cluster perform AOM [3]. The incorporation of nitrogen in such cells alone could be attributed to secondary metabolism like heterotrophy or CO_2 fixation [97]. Hence, we used a functional approach to provide evidence for the coupling of AOM to nitrogen assimilating cell activity and growth. MCR enzymes are the only enzymes reported to directly catalyse AOM [23, 24, 136]. Therefore, it is plausible to test nitrogen incorporation in this protein to provide evidence for AOM coupled nitrogen uptake. To show that label incorporation was attributed to *de novo* synthesis rather than to non-covalent ligation of labelled molecules, we extracted amino acids from nitrate incubations. The incorporation of ammonium into amino acids of Black Sea methanotrophic mats was reported elsewhere [124]. ^{15}N-nitrate label incorporation into amino acids was elevated in ANME-2 populated black mats compared to ANME-1 dominated pink mats (*Figure 37*). This may be a result of overall higher activity of methanotrophs of the black mats than of the pink mats (*Figure 31*). The relation of ANME-2 : ANME-1 *mcrA*-genes was 1:3500 in the pink mats while it was 1:3 in the black mats.

^{15}N-dinitrogen derived N was neither utilised for bulk protein synthesis nor for type-1-MCR synthesis. This type of MCR was previously described for Black Sea methane oxidising mats as the major fraction of all proteins by Krüger et al [23]. Corresponding GI numbers were: 40217436 for the αα'-subunit, 40217434 for the β-subunit and 40217435 for the γ-subunit. The MCR type 2 belonged to the *Methanosarcina/Methanosaeta* MCR cluster with GI numbers 34223964, 116753885 and 10946205 respectively. Type 3 MCR subunits were affiliated to uncultured *Archaea* (GI numbers 52549158, 34305112, 52549157, respectively; [136]).

The fact that ^{15}N-dinitrogen was incorporated into bulk biomass but not bulk proteins, nor type-1-MCR enzymes, suggests two spatially distinct processes. The part of the consortium fixing dinitrogen might have incorporated N before it was delivered to AOM performing *Archaea*. While Dekas *et al.* [134] showed that diazotrophic activity occurred within the same consortium with methane oxidisers, our results suggest that dinitrogen fixation and AOM was at least not performed within the same cells.

Assimilatory ^{15}N-Nitrate nitrate reduction accounted for the highest biomass incorporation rates, which is in good agreement with the observed rates for bulk proteins (*Table 8*). Relative incorporation rates into type-1-MCR enzymes – a proxy for *de novo* synthesis of this protein – were the highest when methane was added without sulfate (*Figure 36*). This may be explained by three models. (i) Since nitrate is a commonly known inhibitor of sulfate reduction [137, 138], it is not surprising that the relative type-1-MCR synthesis ceased when AOM coupled sulfate reduction was blocked in sulfate incubations. (ii) In contrast, AOM coupled sulfate reduction could have been the sulfide supplying process for nitrate reduction. As this would not require a *de novo* synthesis of type-1-MCR enzymes, incorporation rates (i.e. *de novo* synthesis rates) were low in case of sulfate amendment. (iii) When sulfate was not provided to the mats, another part of the community, also using MCR enzymes for AOM, may have been activated which resulted in an increased synthesis rate of MCR enzymes. All three models explain low ^{15}N-nitrate synthesis rates in sulfate incubations compared with the high synthesis rate without sulfate but with methane quite well. However, nitrate reduction was dependent on sulfate reduction coupled to AOM (*Figure 33*) which is in favour for model (ii). Regarding model (iii), assimilatory and dissimilatory nitrate reduction was observed when sulfate was absent but when methane was present (*Figure 33*). This is indicative for direct coupling of AOM to nitrate reduction in this case (*Figure 36*). Furthermore, this observation suggests that classic AOM catalysed by type-1-MCR enzymes is the dominating process. In conclusion, a novel kind of "anaerobic" methane oxidation involving the intrinsic production of molecular oxygen may not account for methane oxidation [110].

[15]N-ammonium assimilation into biomass was also reflected by ammonium incorporation into bulk proteins and type-1-MCR enzymes (*Table 8*; *Figure 34* and *Figure 37*). While the qualitative assimilation of ammonium into biomass and amino acids of methanotrophic consortia was reported previously [116, 124, 134], an active incorporation into a *de novo* synthesised essential catalytic enzyme is new. Moreover, the rate of *de novo* synthesised type-1-MCR enzymes was dependent on the nitrogen source and incubation conditions. Compared to killed controls, ammonia incorporation into proteins was the highest when methane was absent (*Table 8*). The relative type-1-MCR incorporation rates of ^{15}N-ammonium increased significantly when neither sulfate nor methane was supplied (*Figure 36*) while the highest bulk

protein incorporation rates were observed with sulfate but without methane amendment (*Table 8*). This is surprising because one could expect *de novo* protein synthesis under optimal growth conditions. However, when microbial communities are already adapted to certain growth conditions, only little *de novo* protein synthesis is required. Hence a change of growth conditions possible triggers the stress adaption mechanisms. Since MCR enzymes catalyse bidirectional reactions [23, 24, 136] increased MCR synthesis may be a result of induced methanogenesis and not methanotrophy in the absence of methane. This may require structural changes in the enzymatic machinery and hence *de novo* protein assemblage and synthesis. This effect was observed less pronounced in the presence of sulfate but the absence of methane (*Figure 36*) – possibly as a result of increased heterotrophic sulfate reduction: sulfate reducers often out-compete methanogens for substrate utilisation, which is consistent with the observed effect on the potentially methanogenic type-1-MCR protein synthesis.

Conclusions

AOM coupled sulfate reduction was the overall driving force for nitrogen incorporation into biomass (*Figure 39*). Nitrate reduction inhibited sulfide release but sulfate reduction was most likely the intermediate process for nitrate reduction. Nitrate reduction could be assigned mostly to energy metabolism. Moreover, we could show that dinitrogen fixation plays an insignificant role in the Black Sea mats. The synthesis of MCR proteins was strongly dependent on pre-incubation conditions but this enzyme was presumably responsible for AOM even when nitrate was the terminal electron acceptor. This was supported by the dependence of nitrate reduction on AOM coupled sulfate reduction as well as by the stimulation of *de novo* synthesis of type-1-MCR enzymes under methane oxidising conditions.
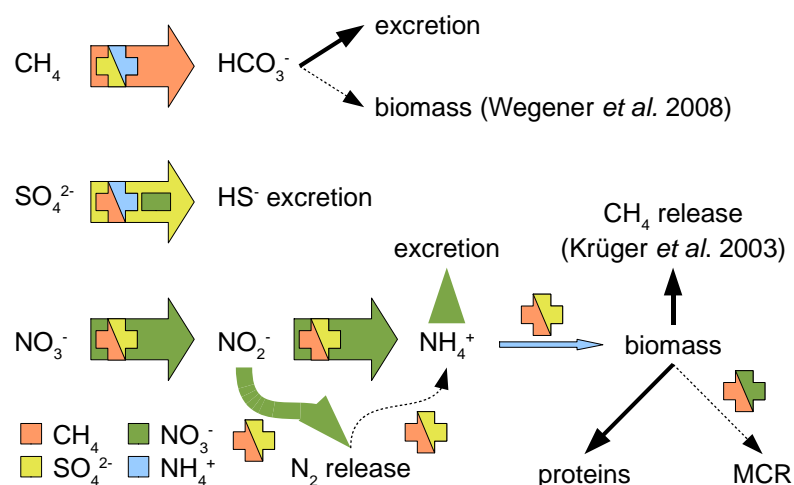
Figure 39: Chart showing the major metabolic known routes of carbon (red), sulphur (yellow) and nitrogen (green and blue) in anaerobic methanotrophic mats of the Black Sea. The thickness of arrows indicates the importance of the process in the investigated batch incubations. + indicates a stimulation and − and inhibition. **Wegener et al., 2008, [97] and Krüger et al., 2003, [23]**

4.2.5. Supporting Information

Rate Calculations

Ratios and contents are given as parts.

Ammonia formation rate:

Equation (2) $rate_{ammonium} = \dfrac{(R \times c_{ammonium})_{dayX} - (R \times c_{ammonium})_{day0}}{n_{days}}$

R is ratio of $^{15}N/^{14}N$ at day X or day 0.

$c_{ammonium}$ is the concentration of $^{14/15}N$-ammonium at day X or day 0;

n_{days} is the number of days

Bulk biomass incorporation

Equation (3) $rate_{N_{biomass}} = \dfrac{(R_{dayX} - R_{dead}) \times content_N}{M_N} \times \dfrac{1}{n_{days}} \times \dfrac{V_{^{14}N_2} + V_{^{15}N_2}}{V_{^{15}N_2}}$

R_{dayX} is the ratios of $^{15}N/^{14}N$ at day X, after n days.

R_{dead} is the ratio of $^{15}N/^{14}N$ of killed controls at day X, after n days.

$content_N$ is the nitrogen content of the mats taken from [23] (0.008).

$M_N = 15$, the atomic mass of ^{15}N-nitrogen

n_{days} is the number of days

V_{14N2} and V_{15N2} are the volumes of respective N_2 gases in the headspace. There was a mix of $^{14}N_2$ and $^{15}N_2$ in the headspace. This factor applies only for the ^{15}N-dinitrogen gas experiments.

Bulk protein incorporation

Equation (4) $rate_{N_{proteins}} = \dfrac{(R_{dayX} - R_{dead}) \times content_{protein} \times content_N}{M_N} \times \dfrac{1}{n_{days}}$

R_{dayX} is the ratios of $^{15}N/^{14}N$ at day X, after n days.

R_{dead} is the ratio of $^{15}N/^{14}N$ of killed controls at day X, after n days.

$content_{protein}$ is the protein content in the crude extracts. This was approximately 15 mg protein / g mat.

$content_N$ is the nitrogen content of proteins, approximately 0.165.

$M_N = 15$, the atomic mass of ^{15}N-nitrogen

n_{days} is the number of days

As there was no label in bulk proteins in $^{15}N_2$ incubations, rates were not calculated.

MCR calculations

Equation (5) is based on the assumption that N atoms in a *de novo* synthesised protein are of the same isotopic ratio as the bulk biomass at the time of synthesis. MCR proteins were divided into exclusively ^{14}N-proteins and exclusively ^{15}N-proteins ($part_{14NMCR}$ + $part_{15NMCR}$ = 1).

$$\text{Equation (5)} \quad rate_{MCR} = \frac{part_{15\,N_{MCR}} + part_{14\,N_{MCR}}}{n_{days}}$$

$$\text{Equation (6)} \quad part_{15\,N_{biomass}} = \frac{rate_{N_{biomass}} \times M_N \times \dfrac{n_{days}}{2}}{content_N} + R_{air}$$

At day 0, the isotopic ratio of MCR proteins was approximately the isotopic ratio of air.

$$\text{Equation (7)} \quad part_{15\,N_{MCR}} = R_{MCR} - R_{air}$$

$$\text{Equation (8)} \quad part_{14\,N_{MCR}} = \frac{(1 - part_{15\,N_{biomass}}) \times part_{15\,N_{MCR}}}{part_{15\,N_{biomass}}}$$

n_{days} is the number of days. This was divided by 2 in *Equation (6)* because:

(i) One can assume that in the beginning there is less ^{15}N than in the end.

(ii) The middle of the linear increase of a ^{15}N saturation slope represents the average ^{15}N saturation of novel proteins.

(iii) A linear ^{15}N saturation slope was assumed due to slow incorporation rates.

$M_N = 15$, the atomic mass of ^{15}N-nitrogen

rate$_{Nbiomass}$ is the rate of N incorporation into biomass.

content$_N$ is the nitrogen content of proteins, approximately 0.165.

R$_{air}$ is the ratio of ^{15}N/^{14}N in air (0.00366).

R$_{MCR}$ is the ratio of ^{15}N/^{14}N in an MCR protein that was measured after n days versus air.

Equation (9) is based on the assumption that *de novo* MCR proteins were always synthe-sised of the ^{15}N-substrate.

$$\text{Equation (9)} \quad rate_{MCR} = \frac{part_{15MCR}}{n_{days}}$$

From *Equation (5),* one can deduce the estimated absolute *de novo* MCR synthesis rate:

$$\text{Equation (10)} \quad rate_{MCR} = \frac{m_{MCR1} \times (part_{14MCR} + part_{15MCR})}{n_{days}}$$

m$_{MCR}$ is the one third of 7% MCR nickel proteins in the crude protein extract [23]. One third was assumed because the exact distribution of the three different MCR proteins is unknown. The protein content in crude extracts was approximately 15 mg protein / g mat.
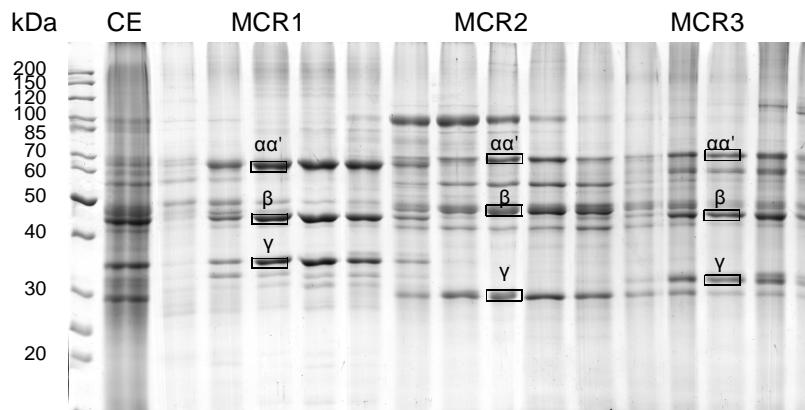

Figure S7: Typical 1D SDS-page gel of FPLC fractions from protein extracts of methanotrophic black mats. MCR containing bands are highlighted. The subunits are indicated as Greek letters. CE = crude extract before FPLC separation.
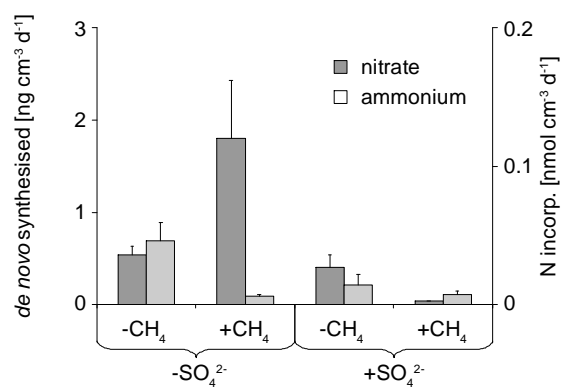
Figure S8: Absolute synthesis rate of type 1 MCR proteins. Bulk biomass, synthesised from ^{15}N-nitrate or ^{15}N-ammonium was assumed to be the direct nitrogen source. The right scale indicates incorporated moles N.
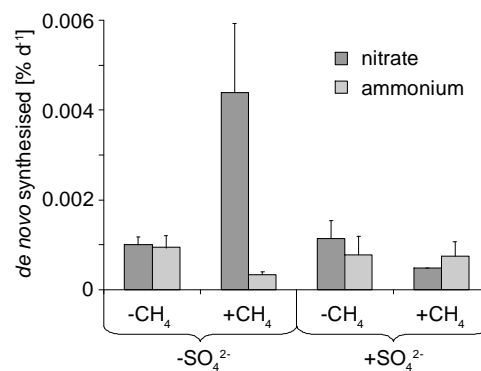

Figure S9 Relative synthesis rate of type 1 MCR proteins. ^{15}N-nitrate or ^{15}N-ammonium was assumed to be the exclusive nitrogen source.

4.3. The Trolls – novel anaerobic methanotrophic microbial mats near the methane gas hydrate stability zone of the Black Sea

Richard Seifert[1][*], Michael Siegert[2], Martin Blumenberg[3], Birte Oppermann[1], Michael Friedrich[4], Martin Krüger[2]

[1]Universität Hamburg, Institut für Biogeochemie und Meereschemie, Bundesstrasse 55, 20146 Hamburg, Germany

[2]Bundesanstalt für Geowissenschaften und Rohstoffe, Stilleweg 2, 30655 Hannover, Germany

[3]Georg-August-Univerität Göttingen, Fakultät für Geowissenschaften und Geographie, Abteilung Geobiologie, Goldschmidtstr. 3, 37077 Göttingen, Germany

[4]Universität Bremen, Leobener Straße, NW2, 28359 Bremen, Germany

*Corresponding author: Dr. Richard Seifert

Abstract

The anaerobic oxidation of methane (AOM) through microorganisms is the main sink for methane in the ocean and appears to be a common process in anoxic marine habitats wherever sulfate and methane are sufficiently available. Recent studies have shown associations of specific *Archaea* and *Bacteria* to be capable of AOM. Here we report on microbial reef structures occurring at the lower edge of the stability zone of methane gas hydrates on the sea floor of the northwestern Black Sea. Unlike all other yet reported AOM-reef structures they are ANME-2 dominated. This discovery shows for the first time, that ANME-2 dominated microbial communities are capable of massive microbial mat build up. The structures, named "Trolls" after their appearance, are up to 40 cm high and consist of microbial mats supported by internal carbonate globules. They are located at a water depth of 725 to 735 m in vicinity of active gas seeps. The release of gas bubbles during sampling indicates the hollow center to be filled with gas saturated fluids. A major part of the released gas was methane. The investigation of their community composition by lipid biomarkers and molecular microbiology showed that the structures are assembled by a microbial community performing sulfate-dependent AOM with almost only ANME-2c present within *Archaea*. The bacterial diversity was geater, dominated by d-Proteobatceria as known from other sites. High pressure incubations of the Troll mats revealed significantly higher AOM rates at increesased methane partial pressures. This newly discovered AOM-structure type is well adapted to the water depth and methane concentrations found at the sampling site.

4.3.1. Introduction

The metabolic process of AOM is proposed to be a reversed methanogenesis [23, 24, 136] coupled to the reduction of sulfate, with methanotrophic *Archaea* (ANME *Archaea*) and sulfate-reducing bacteria (SRB) interacting syntrophically [25, 139, 140]. Among the ANME-*Archaea*, three clades (ANME-1, ANME-2, and ANME-3) are reported [40, 119]. ANME-1 *Archaea* are present in methane rich sediments [12, 119, 141] with or without associated sulfate reducing bacterial partners of the *Desulfosarcina-Desulfococcus* (DSS) branch [34, 142]. Mat-type consortia dominated by ANME-1 are so far only described from the Black Sea [6, 119, 143-145]. ANME-2 *Archaea* with subgroups ANME-2a, -2b and -2c belong to the order *Methanosarcinales*. They usually occur associated with SRB forming structured ANME-2/DSS aggregates [3]. Neither members of any ANME group nor the respective sulfate-reducing bacterial partners have so far been obtained in pure culture.

Hot spots in the occurrence and preferred study sites of AOM-consortia are locations at extraordinary methane enrichments, like gas hydrates, gas seeps and mud volcanoes. There, often dense populations of AOM-consortia are found in the marine sediments. However, re-

cent occurrences of massive microbial mats performing AOM have so far been exclusively discovered in the Black Sea [6, 145]. The Black Sea offers a unique habitat favoring the growth of AOM communities. It comprises permanently anoxic methane rich deep waters for several thousand years and, moreover, methane seepage from the sediments is a common phenomenon in the shelf areas [146]. The recovery of active AOM-performing microbial mats intruding from the sea floor into the anoxic deep waters of the Black Sea in 2001 and their successful cultivation in laboratories has enabled numerous studies significantly contributing to current knowledge about AOM and the involved microorganisms (for review: [3]). These samples obtained from water depths between 180 and 240 m revealed ANME-1 consortia to be dominating over ANME-2 [119, 147].

4.3.2. Materials and Methods

Sampling

Using the manipulator of the submersible *QUEST* (marum, Germany), whole sediment push-cores as well as pieces of the Troll mats were taken between 725 and 735 m water depth (44°42,043'N, 032°03,771'E) under video control and stored in closable PVC barrels. The latter allowed transportation of the samples on deck and into the laboratory within the anoxic bottom water. Sampling barrels were opened in the ship laboratory under continuous dinitrogen flow through an inverted funnel. The samples were transferred into sampling vials filled with anoxic sea water and a methane atmosphere. Those were frozen at -20°C. Transport from the ship into the home laboratory was conducted within two days keeping the samples frozen at -20°C.

Anoxic incubations

On board, samples were manipulated under anoxic conditions in a N_2-flooded tent and transported to the home lab at 4-8°C. Incubation experiments were carried out on-shore in glass tubes (10 ml) sealed with butyl-rubber stoppers and screw caps. Pieces of mat material were homogenised through a sieve in an anoxic chamber, flooded with dinitrogen, Aliquots of 1 ml 1:1 medium-mat suspension were incubated in a total of 5 ml artificial seawater medium [46] as described by Nauhaus *et al.* [47]. Subsequently, the headspace was flushed with dinitrogen or methane. For high pressure incubation, the sea water medium was added to half filled Hungate tubes using sterile syringes by applying 30 bar on an autoclave at 4°C. Background methanogenesis was estimated by incubating inner and outer Troll mats as in AOM experiments at atmospheric pressure but without methane in the headspace. Methane formation was measured once a week and the regression slope over 45 days was used for rate estimations. Triplicate (duplicate for sedimemts) tubes were incubated horizontally at 4°C. Sulfate

reduction was measured as described by [49]. Methane evolution was monitored using an FID equipped SRI 8610 C gas chromatograph.

Gene quantification using quantitative PCR

The DNA extraction was carried out using the Fast DNA for Soil Kit, according to the manufacturer's protocol except the addition of 10 µl 1% polyadenylic acid (polyA) in the initial step [55]. 0.5 g thawed wet sediment or mat was used for extraction and 750 µl binding buffer was added instead of 1000 µl. We used qPCR analysis to quantify copies of 16S rRNA genes of *Bacteria*, *Archaea* and *Geobacteraceae* as well as for *mcrA* of ANME1, ANME2 and *Methanosarcina* and *dsrA* [56, 57, 59, 60, 148, 149].

Terminal Restriction Fragment Length Polymorphism (TRFLP) analyses

16S rRNA was amplified using a primer set targeting archaeal SSU ribosome (Ar109f: ACKGCTCAGTAACACGT and Ar912r: CTCCCCCGCCAATTCCTTTA) and the bacterial SSU ribosome (27f AGAGTTTGATCCTGGCTCAG and 907r CCATCAATTCCTTTRAGTTT) [150]. 40 ng of RNA-extracts were used. DNA contamination was eliminated using a DNase I digest prior to the PCR. Reverse transcription and subsequent PCR were performed using the Promega Access RT-PCR system. TRFLP was carried out as described previously [151, 152], using the primer 912r or 27f respectively with a 6-carboxy-fluorescein (FAM) labelled 50 end. In brief, the fluorescently labelled PCR products (75 ng) were digested with *Taq*I for Archaea and *Msp*I for Bacteria, and subsequently analysed using an automated sequencer (Model 373A, Applied Biosystems, Weiterstadt, Germany). TRFLP patterns were analysed with GeneScan analysis software (version 2.1, Applied Biosystems) by peak area integration of the different TRF. The percentage fluorescence intensity represented by single TRF was calculated relative to the total fluorescence intensity of all TRF.

Cloning and phylogenetic analyses

To prepare 16S rRNA gene clone libraries, PCR products of TRFLP analyses were used without reverse transcription prior to amplification. PCR products were cloned using the Promega pGEM vector system according to the manufacturer's instructions. *E. coli* cells were lysed at 98℃ for 3 min and the supernatant wa s used for the following PCR and sequencing. Sequencing reactions were performed at Seqlab GmbH Göttingen (Germany). All sequences were corrected manually and checked for next relatives by BLAST search in the recent RDP gene bank library (http://rdp.cme.msu.edu/). *In silico* TRFLP digestions with the obtained sequences were performed using the TRiFLE software [153]. The resulting fragments lengths were used to affiliate *in vitro* fragments. The phylogenetic tree was created by

incorporating 16S rRNA gene sequence fragments of a clone library into an existing Maximum-Parsimony tree (version 102) provided by Pruesse *et al.* [66].

Biomarker analyses

Lyophilised and homogenised samples were hydrolysed using 6% KOH in methanol (pH 14) in excess (2 h at 80℃ in ultrasonification bath) to release ester-bound lipids. The resulting alkaline reaction solution was extracted with *n*-hexane (5x) yielding the neutral lipids fraction. The neutral lipid fraction was further separated by column chromatography (Merck silica gel 60) and eluents of increasing polarity (*n*-hexane, dichloromethane, MeOH) providing a hydrocarbon and alkenone fraction, an alcohol and ketone fraction and a polar fraction, respectively. The alcohol and ketone fraction was treated with *N,O*-bis(trimethylsilyl)trifluoroacetamide for 2 h at 80℃ to silylate alcohols. To analyse the alkyl moiety of ether bond lipids, the polar fraction of neutral lipids was subjected to ether cleavage through HI treatment (HI 57% and CH_3COOH 1:1, v:v; 4 h at 110℃) and reduction of the resulting iodides by using LiAlH4 in dry tetrahydrofurane under an argon atmosphere modified after [154].

Fatty acids (FA) were obtained by acidification of the residue of the alkaline reaction solution to a pH of 1-2 and subsequently extracted using *n*-hexane (1x) and dichlormethane (5x). Prior to analysis, fatty acids were converted to their methylesters (trimethylchlorosilane in methanol 1:9; v:v; 2 h, 80℃) derivatives. Double bond positions of fatty acid methyl esters were determined using the method described by [155]. Lipids are labelled by their number of carbon atoms (e.g. C_{16}) the number of unsaturations (e.g. two unsaturations: $C_{16:2}$). If the position of double bonds is known, it is given as the number of carbon atoms from the terminal methyl carbon (ω, e.g. $C_{16\omega5}$). Positions of methyl branches are abbreviated with *i*-, a*i*-, XMe- and *m*- for, iso-, anteiso-, X-position from the functional group and position unknown, respectively. The above mentioned fractions were analysed by GC-MS using a Fisons MD 800 spectrometer (EI, 70 eV) coupled to a Fisons 8060 GC equipped with a fused silica capillary column (DB5-MS, 30 m, 0.32 mm inner diameter, 0.25 µm film thickness). Carrier gas was Helium. Temperature program: 3 min at 80℃; from 80 ℃ to 310℃ at 6℃ min $^{-1}$; 20 min at 310℃. Lipids were identified by comparison of GC-retention times, published mass spectra and checked with reference compounds if necessary, software used for this propose was MassLynx NT v3.2 (Micromass, UK). Concentration of lipids was calculated relative to an authentic standard (Squalane, Fluka, Switzerland) using GC-FID signals processed with the ChromStar 6.3 (Chromatography Software, Germany).

<u>Stable isotope analysis</u>

Stable carbon isotope analyses of bulk carbon were determined using a Finnigan MAT 252 mass spectrometer after high-temperature flash combustion in a Carlo Erba NA-2500 elemental analyser (Erba Science, Italy) at 1020 °C. The $\delta^{13}C$ value of the methane was analysed from the headspace of the fluid sampled from below the mat as described previously [156].

$\delta^{13}C$ values of methane and lipid biomarkers were analysed using a coupled gas chromatography-combustion-isotope ratio mass spectrometry (GC-C-IRMS) and were analysed according to [6]. In short, gas chromatograph (HP 6890), column and temperature program as above for lipids and a CP Plot molsieve 5 Å capillary column (25 m, 0,32 mm i.d., 30 µm film thickness) for methane, carrier gas He for methane and lipids. Combustion furnace CuO/Ni/Pt was operated at 940°C (lipid-biomarkers) or 1010°C (methane). Mass spectrometer was a Finnigan DeltaPlusXL. Samples were measured with a minimum of three replicates. GC-C-IRMS precision was checked daily using a standard alkane mix (n-C_{15} to n-C_{29}) for lipid-biomarker assembly and a methane standard, both with known isotopic composition. The stable carbon isotope compositions are reported in the delta notation ($\delta^{13}C$) *vs.* the V-PDB Standard. $\delta^{13}C$-values of derivatised components were corrected by a method modified after [157].

H/D ratios of lipids were determined using the same GC set up as for $\delta^{13}C_{lipids}$ but with a reduced column flow. Samples were injected in splitless mode. Lipids were converted to hydrogen using online high temperature conversion (tube held at 1470°C). MS set up and data processing was the similar to the above. GC-C-IRMS precision of δ^2H-analyses was checked daily using a standard alkane mix (n-C_{15} to n-C_{29}) for lipid-biomarker assembly. The H_3-factor for this instrument was measured daily by injecting pulses of H_2 gas with constant D and peak heights varying over a 10-fold range, and was typically <6 ppm mV^{-1}.

4.3.3. Results and Discussion

Microbial build-ups were discovered in the Northwestern Black Sea (44°42.08'N, 032°03,862'E) at water depths around 725 m in vicinity of active gas seeps, sometimes as close as 3 m. The structures were up to 40 cm high and consisted of microbial mats supported by carbonate globules. Although we could not observe gas escaping from the structures nor found any orifices, the release of gas during sampling indicated the hollow center to be filled with gas saturated fluids. A major part of this gas was methane (*Figure 40*). Due to their shape they were named "Trolls". Their total biomass was strongly ^{13}C-depleted demonstrating methane to be their major carbon source ($\delta^{13}C$-C_{Corg} = -81.07; $\delta^{13}C$-CH_4 = -63.2‰).

Water depth of the sampling location corresponds to pressures from 73.2 to 73.7 bar with bottom water temperatures of 8.9°C and a salinity of 22.2‰. At these conditions, methane gas hydrates (structure I) should be stable at temperatures up to 9.2 °C [158]. Solubility of methane in the bottom water at the Troll site in the presence of methane gas is 97.0 mmol kg.

High-Mg-calcite made up the majority of carbonates in the Troll-field mats with only 4% aragonite. Such facies were frequently discovered in ANME-2 affected environments [159]. An explanation is that sulfate is rapidly removed in those mats due to high turnover rates, while low turnover rates in ANME-1 associations are generally associated to aragonite [160].

In incubation experiments the Troll mats reduced sulfate to sulfide in presence or absence of methane. However, when methane was added to the headspace, sulfate reduction rates (SRR) were always significantly higher than without methane, indicative for sulfate dependent anaerobic oxidation of methane. Additionally, experiments under high partial pressure of methane (30 bar) yielded considerably higher AOM rates compared to experiments at low methane

Figure 40: Location of the Troll field in the Northwestern Black Sea and an image of a typical microbial build-up.

pressure of 1 bar (*Table 9*).

Methanogenesis rates in the Troll mats were approximately three orders of magnitude lower than AOM dependent sulfate reduction rates suggesting methanogenesis to play an insignificant role in the Troll mats. There were no significant differences between the outer and the inner part of a Troll tube (2.6 ± 1.0 and 2.8 ± 1.1 nmol cm^{-3} d^{-1}).

Table 9: Sulfate reduction rates (SRR) with and without methane in the headspace. Errors are mean values within 95% confidence intervals. Errors are standard deviations from these mean values

condition	1 bar SRR [µmol cm^{-3} d^{-1}]	error	30 bar SRR [µmol cm^{-3} d^{-1}]	error
-CH$_4$	0.51	±0.07	0.27	±0.11
+CH$_4$	0.73	±0.02	2.33	±0.98

The investigation of the microbial community composition by quantitative real-time PCR for prokaryotes revealed a total 16S rRNA gene copy numbers of 7×10^7 cm^{-3} while eukaryotes were not detectable (*Figure 41*). *Bacteria* and *Archaea* were detected in almost equal numbers of 3 and 4×10^7 copies cm^{-3} respectively (*Figure 41*).

The diversity of the active archaeal communities in Troll samples was relatively low and dominated almost exclusively by ANME-2 *Archaea*. The 16S rRNA gene clone libraries and TRFLP data showed that more than 99% of the archaeal community was comprised of ANME-2c *Archaea* (n = 77). One sequence was found to belong to the Marine Hydrothermal Vent Group. The functional gene *mcrA* of the methanotrophic ANME-2 *Archaea* is involved in the first enzymatic step of AOM [23, 24]. These genes were present in the Trolls (*Figure 41*) with four orders of magnitude more (5×10^7) copies cm^{-3} than the *mcrA* of ANME-1 (2×10^5 copies cm^{-3}). This strong dominance of ANME-2c contrasts previous observations of mats discovered at water depth of 180-240 m [6].

Further strong support for the dominance of ANME-2 in the Troll microbial mats comes from biomarker studies (*Figure 42*) where highest concentrations were found for archaeol and *sn*2-hydroxyarchaeol, both strongly depleted in ^{13}C (-115‰ vs. VPDB). A suite of polyunsaturated isoprenoid hydrocarbons (2,6,10,15,19-pentamethylicosene [PMI]) and crocetane was also found to have similar δ^{13}C-values. The high occurrence of ^{13}C-depleted *sn*2-hydroxyarchaeol and crocetane and low amounts of biphytanes strongly hint at AOM-consortia dominated by ANME-2 *Archaea* [144]. Small amounts of ^{13}C-depleted C$_{40}$ isoprenoidal hydrocarbons (biphytanes) in an ANME-1 specific distribution [144] were also released

from glycerol dialkyl glycerol tetraethers (GDGT). The presence of ANME-1 was also indi-
cated by the finding of the respective *mcrA* genes with quantitative PCR (*Figure 41*).
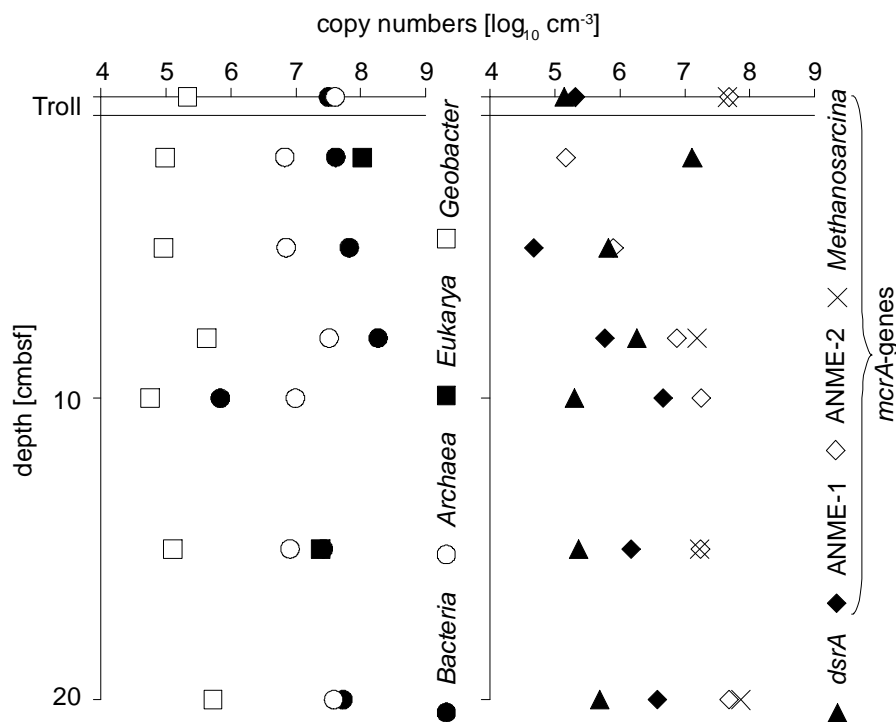

*Figure 41: Gene specific copy numbers of extracted DNA. cmbsf indicate
centimetres below seafloor. Instead of depth zero, the Troll mat's qPCR re-
sults are inserted. In the left profile, 16S rRNA genes are depicted. The right
profile shows the functional genes dsrA and mcrA.*

 The occurrence and stable carbon isotope composition of certain biomarkers also suggest
the presence of other *Archaea* in the mats from the Troll-field (*Figure 42*). Particularly
squalenes with up to four double bonds, but also specific PMI derivatives are less depleted in
^{13}C (about -90 to -100‰) than ANME-2 derived lipids (-110 to -125‰). Squalenes and PMI
derivatives are well known lipid biomarkers of methanogenic *Archaea* [161]. In the Troll-field
they may originate from methanogenic *Archaea*, which use CO_2 or other AOM-derived ^{13}C-
depleted substrates. Also qPCR analyses revealed the presence of *mcrA* genes of methano-
genic *Methanosarcina* relatives (*Figure 41*) and *in vitro* incubations demonstrated methane
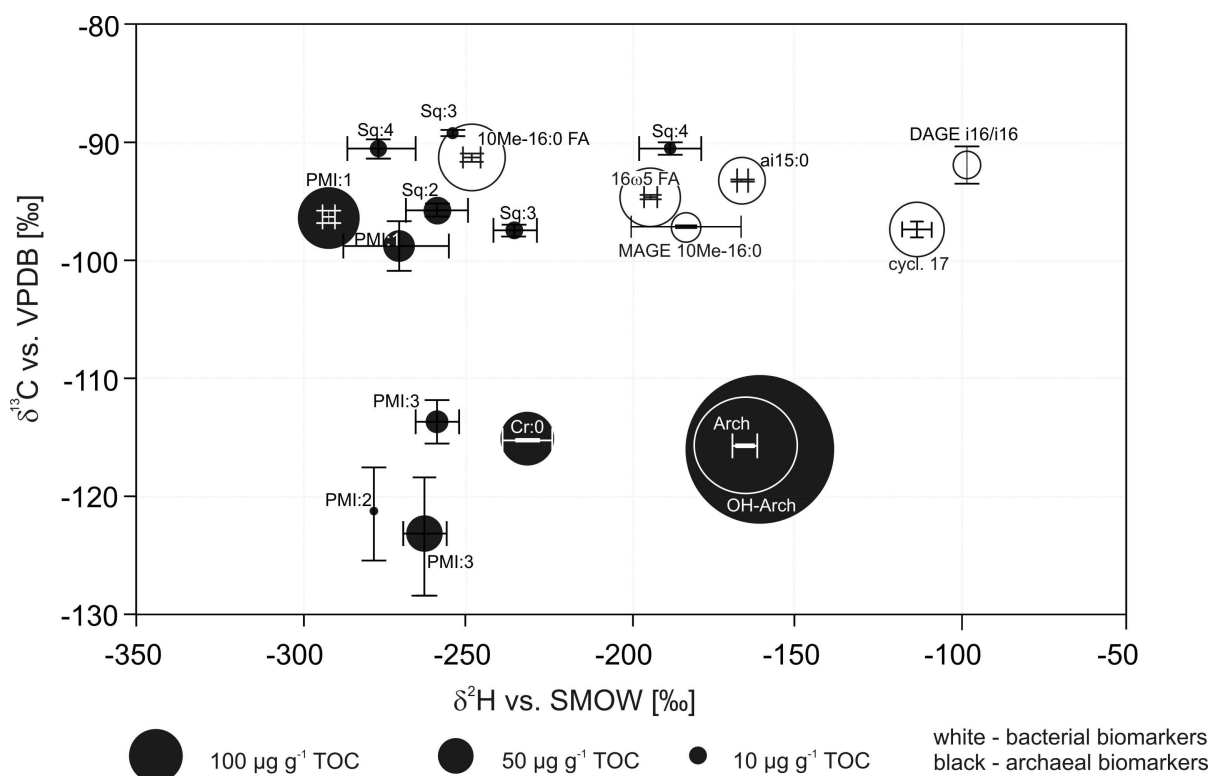production.

Figure 42: Concentrations and stable isotope signatures (δ^{13}C and δ^{2}H) of selected biomarkers from the Troll microbial mats.

Hydrogen might play a central role in coupling the syntrophic partners of AOM (SRB and ANME; [162]) and might therefore also affect lipid hydrogen isotope ratios. Factors like the isotopic composition of biosynthetic precursors, the fractionation and exchange accompanying biosynthesis, and the hydrogenation during biosynthesis also control the final δ^{2}H values of lipids. In the Troll-field mat the ^{2}H/H-ratios of lipids vary between -100 and -300‰ vs. VSMOW (*Figure 42*), consistent with lipid δ^{2}H values known from non-AOM related organisms [163]. Sessions *et al.* [164] demonstrated that δ^{2}H values of lipids of the aerobic methanotrophic bacterium *Methylococcus capsulatus* are mainly controlled by the δ^{2}H of the water with only about 30% of lipid hydrogen originating from methane. Accordingly, in the Troll-field, a minor role of methane-bound hydrogen must be assumed because methane from the vicinity exhibits a δ^{2}H value of about –245 to -255‰ vs. SMOW [165]. Among archaeal lipids, δ^{2}H differences were observed between archaeol and *sn*2-hydroxyarchaeol (about -170‰ vs. SMOW) and almost all isoprenoidal hydrocarbons (-230 to -290‰ vs. SMOW; squalenes, PMI-derivatives, crocetane, *Figure 42*). Different archaeal groups with distinct lipid metabolisms are unlikely as explanation in this ANME-2 dominated system. More likely are differences in the amount of exchangeable hydrogen, which is higher in functionalised compounds, between glycerol diethers and isoprenoid hydrocarbons.
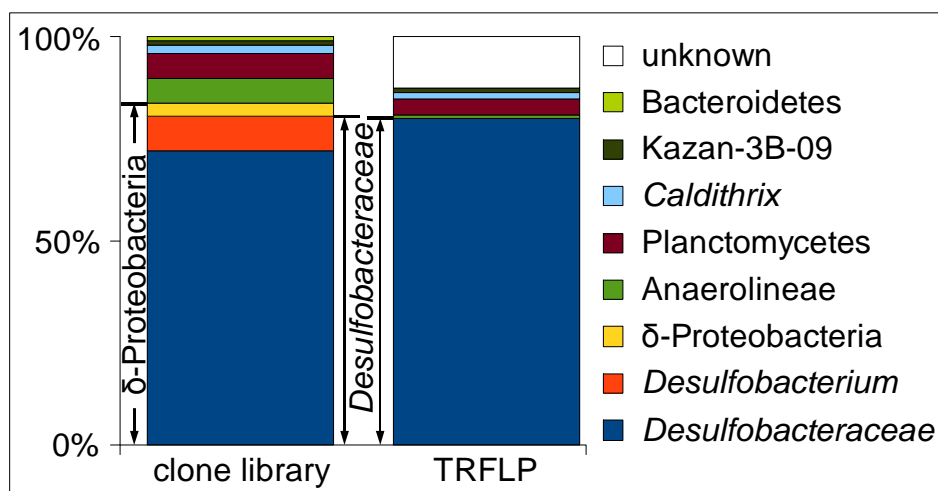
Figure 43: Bacterial 16S rRNA genes (left) and 16s rRNA (right, TRFLP) of nucleic acid extracts of the Troll mats. The "unknown" rRNA fraction represents fragments which could not clearly be assigned using clone library data (n = 96).

For the active bacterial community in the Troll mats, 16S rRNA clone libraries and TRFLP analyses revealed a typical seep community, comprising δ-*Proteobacteria* as prevailing bacterial group (*Figure 43* and *Figure 44*). Four new clusters of δ-*Proteobacteria* comprising exclusively Troll 16S rRNA gene sequences were indicated. The genera *Desulfococcus* and *Desulfobacterium* formed major bacterial sequencegroups among the *Desulfobacteraceae* (*Figure 44*). The diversity outside the *Proteobacteria* was greater and deeply branching into *Bacteroidetes*, *Planctomycetes* and *Chloroflexi* clades (*Figure 44*). Two sequences could be affiliated to the genus *Caldithrix*, known for hosting the nitrate reducing thermophile *Caldithrix abyssi* [166].

Bacterial biomarkers were also found in high amounts (*Figure 42*). These include lipid fatty acids and, in lower concentrations but in similar distributions, mono alkyl and dialkyl glycerol ethers (MAGE and DAGE). All bacterial lipids exhibit $\delta^{13}C$ values of about -90 to -100‰, slightly less depleted than the ANME-2 specific lipids. High amounts were found for the 16:1ω5 and a 17:1 with a cylopropylic group (*Figure 42*). Both fatty acids are suggested to be indicative for sulphate-reducing δ-*Proteobacteria* of the *Desulfosarcina*/*Desulfococcus* cluster associated to ANME-2 archaea [144, 167]. The bacterial 10Me-16 fatty acid and the corresponding MAGE were also high in abundance as well as depleted in ^{13}C (*Figure 42*). 10Me-16 FA was found as important fatty acid of cultivated *Desulfobacter* sp., a group of bacteria also been found by 16S rRNA extraction (*Figure 43*). Furthermore, *dsrA* genes encoding the dissimilatory sulfite reductase enzyme (DSR) of sulfate reducers was detected in copy numbers of 10^5 copies cm^{-3} in the Trolls. This relatively low number is surprising because sulfate reduction occurred with and without methane in the headspace in microcosm experiments indicating a vital SRB community (*Table 9*).

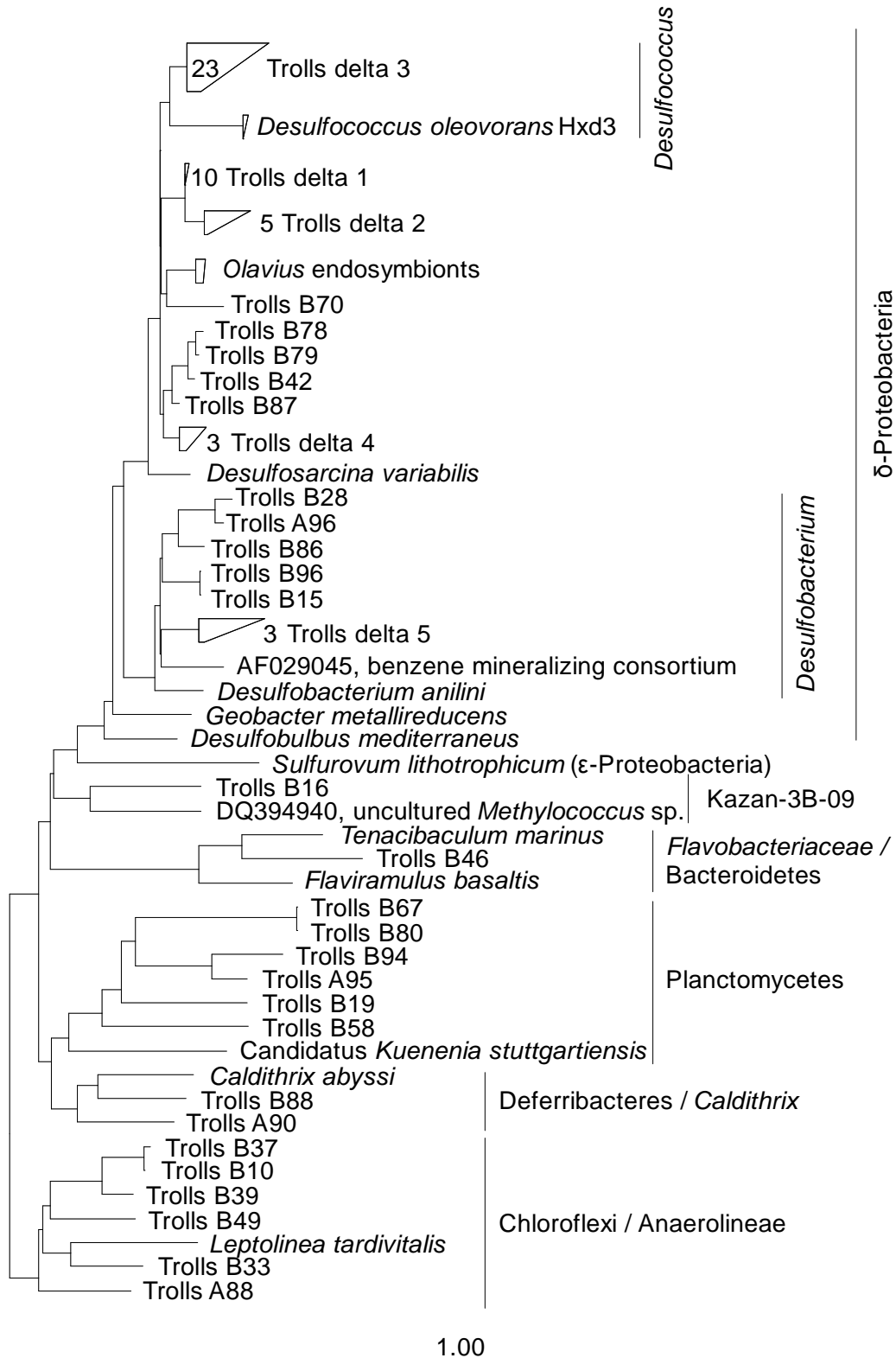*Figure 44: Parsimony tree created by integrating bacterial Troll sequences into an existing ARB-SILVA tree (version 102, [66]).*

Additionally, low numbers of *Geobacteraceae* 16S rRNA genes were found. The presence of *Geobacteraceae* might be indicative for active metal reduction coupled to AOM, as it was suggested by Beal *et al.* [76]. Nonetheless, oxidised metals at this depth were never reported

before and an involvement of *Geobacteraceae* species in metal redox cycles at the discovered methane seep seems unlikely. Probably, *Geobacteraceae* species participated in the sulfur cycle, perhaps reducing elemental sulfur as shown for *Geobacter sulfurreducens* [168].

Stable hydrogen isotopic compositions of bacterial lipids were less clear distributed than archaeal lipids and comprise a range of -110 to -250‰ vs. SMOW. Although complicated by many factors, Sessions [169] demonstrated that water is the sole hydrogen source for lipids of the SRB studied during autotrophic growth ($\Delta\delta^2H_{water\text{-}fatty\ acids}$ between -219 to -254‰). Assuming major SRB in the Troll-field being autotrophic, as been demonstrated for other AOM-sites [97, 143], the large range of δ^2H may be explained by variances in compound-group specific fractionations among individual bacteria. However, as demonstrated by cloning and terminal restriction fragment polymorphism analyses (TRFLP), the bacterial diversity was high within Troll-field mats (*Figure 43*). This complexity further complicates an explanation of δ^2H-values of bacterial lipids (fatty acids, MAGE, DAGE).

In conclusion, this is the first time that methane oxidising mats were discovered near the methane hydrate formation zone. While the discovered microbial mats of the Troll field shared some feature with previously described mats, especially the composition of the (bacterial community, the Trolls had a signifiantly different archaeal community. Unlike previously described mats, the archaeal community consisted exclusively of ANME-2c methanotrophs, and was well adapted to the prevailing environmental conditions, especially the high pressure. Another apparent difference was the much smaller dimension of the chimneys of only up to 40 cm height compared to 100-200 cm of the mats at 180-240 m water depth [6]. One reason for this may be the late onset of methane seepage in the Troll field compared to the previously discovered mats [6]. However, nothing is known about the age of the adjacent methane seep and the Trolls.

4.4. Different types of methane monooxygenases produce similar carbon and hydrogen isotope fractionation patterns during methane oxidation

Stefan Feisthauer[1], Carsten Vogt[1,*], Jakub Modrzynski[1], Maurycy Szlenkier[1], Martin Krüger[2], Michael Siegert[2], Hans-Hermann Richnow[1]

[1]Department of Isotope Biogeochemistry, Helmholtz Centre for Environmental Research - UFZ , Permoserstr. 15, D-04318 Leipzig, Germany

[2]Bundesanstalt für Geowissenschaften und Rohstoffe (BGR), Stilleweg 2, 30655 Hannover, Germany

*Corresponding author; Tel.: +493412351357; fax: +493412351443 email address: carsten.vogt@ufz.de

Abstract

We determined the stable carbon and hydrogen isotope fractionation factors for methane oxidation under oxic conditions using strains with known degradation pathways. The aerobic oxidation of methane can be initiated by two different forms of enzymes known as methane monooxygenases (MMO). The expression of these enzymes is type-specific and dependent on adjusted copper concentration in the medium (or environment). In this study, the expression of either the soluble MMO or the particulate MMO was supported by adjusting the copper concentrations in the growth medium. Taxonomically different aerobic methanotrophic strains, mainly belonging to the alpha- and gamma- classes of *Proteobacteria*, produced methane isotope enrichment factors (ε_{bulk}) ranging from -14.8 to -27.9 for carbon, and from -110.0 to -231.5 for hydrogen. The ratios of hydrogen versus carbon discrimination were similar for all tested cultures and are also identical with values calculated from previously published enrichment factors of aerobic and anaerobic methane degradation. In contrast, Λ-values for the abiotic oxidation of methane with OH radicals (this process is considered as the main removal process for methane from the atmosphere) were significantly higher than values derived from biotic oxidation. Due to the low variability of microbial methane isotope fractionation patterns, we propose that combined carbon and hydrogen isotope fractionation analyses can be used to monitor and assess the occurrence of microbial methane oxidation in marine or terrestrial environments. However, it is not possible to distinguish distinct aerobic or anaerobic methane-oxidation pathways by this approach.

4.4.1. Introduction

Methane is an important and persistent greenhouse gas, and one molecule of methane has 20 times the greenhouse effect of carbon dioxide [170]. Compared to pre-industrial levels, the concentration of methane in the atmosphere has increased from 715 ppb to 1770 ppb within the last 200 years. Approximately 69% of all methane is of microbial origin [171], mainly produced during organic matter decomposition in environments such as natural wetlands or rice paddies [171-173]. Although methane is the most inert hydrocarbon with bond energies of 104 kcal mol^{-1} [174], the microbial oxidation of methane occurs in both oxic and anoxic environments, and represents the most important process in which methane is removed from the environment, e.g. [3, 5, 25, 171, 175-178].

Under aerobic conditions, methanotrophic bacteria oxidise methane to methanol using molecular oxygen as an oxidant. Two groups of methanotrophs are distinguished according to their carbon assimilation pathways: Type I methanotrophs assimilate formaldehyde via the ribulose-monophosphate pathway, whereas type II methanotrophs use the serine pathway.

The first step in both pathways, the oxidation of methane to methanol, can be catalysed by two different forms of the methane monooxygenase (MMO). The particulate (p) or membrane-bound form of the enzyme (pMMO) is expressed at high copper concentrations by all aerobic methanotrophs except those of the genus *Methylocella* [179]. The pMMO was shown to consist of a hydroxylase and an additional component that is thought to be a methanol dehydrogenase catalyzing the second step in the methane oxidation pathway, the oxidation of methanol to formaldehyde [180-182]. In contrast, the ability to express the iron-containing soluble (s) form of the enzyme, sMMO, is mainly a feature of type II methanotrophs under copper-limited conditions [179, 183-186]. sMMO is comprised of an NADH-coupled reductase, a regulatory component, and a hydroxylase component that activates oxygen at a non-heme diiron containing reactive site, e.g. [184, 187-191]. In methanotrophs that can express both forms of MMOs, a copper concentration below 0.8 µM induces the expression of the soluble enzyme, however the activity of sMMO disappears at copper concentration above 4 µM, and the particulate form is the active enzyme complex under these conditions [185, 186, 192]. The biochemistry of methane oxidation and the corresponding genetic regulatory mechanisms of both MMOs have been studied in detail (for a review see [193]).

The assessment and quantification of microbial methane oxidation rates is of general interest in order to estimate the factors effecting the cycling of methane, which in turn is required to understand the role of atmospheric methane in global warming. Compound specific isotope analysis (CSIA) is a non-invasive method for monitoring environmental biotransformation reactions (for reviews see [194, 195]), and has also been applied for the monitoring of atmospheric methane [196]. CSIA is based on the kinetic isotope discrimination as a result of higher activation energies needed to cleave chemical bonds of heavier isotopes compared to lighter ones. This leads to an enrichment of the heavier isotope in the residual substrate compared to the original isotope composition, and is expressed by an enrichment factor (ε; [194]). For aerobic methane oxidation, several isotope fractionation factors for carbon, e.g. [197-207] and hydrogen, e.g. [198-201, 205-207] have been published in laboratory and environmental studies. The enrichment factors previously described show a broad range of values, and therefore hamper its use as a tool to describe the microbial *in situ* degradation of methane.

Generally, a kinetic isotope effect (KIE) is characteristic for the bond cleavage mechanism. However, the apparent kinetic isotope effect (AKIE) of a biochemical reaction, e.g., reactions catalysed by whole cells, can be significantly lower than its underlying KIE due to slow rate-determining steps (e.g., transport into the cell and/or binding to the enzyme) that precede the isotopically sensitive bond cleavage step. These slow steps are thought to be non-fractionating and therefore the overall fractionation pattern for a given microbial process may

become 'masked' [194, 208]. However, highly variable AKIE values have been recently observed for several compounds and degradation pathways in experiments using microbial reference strains [209-214], and indicate that masking effects frequently occur.

As a consequence, the elucidation of biotransformation mechanisms using AKIEs of single elements is problematic, and it has been suggested that the use of two-dimensional compound specific isotope analysis (2D-CSIA) can overcome these difficulties [194]. Since two (or more) different elements participating in an isotope-sensitive chemical reaction are equally influenced by masking steps, the slope of the linear regression for isotope discrimination of these elements is suitable for characterising a distinct (bio)chemical reaction [209, 214-216]. The slope value has been recently defined by Elsner *et al.* [209] as lambda $(\Lambda) = (\alpha_H^{-1} - 1) / (\alpha_C^{-1} - 1) \approx \Delta(\delta^2 H) / \Delta(\delta^{13}C)$ for hydrocarbons.

The objective of this study was to determine the Λ values for taxonomically different aerobic methanotrophic strains. In order to elucidate the range of two-dimensional aerobic methane isotope fractionation factors that may be observed in natural systems, we investigated cultures expressing either sMMO or pMMO.

4.4.2. Materials and methods

<u>Cultures and Growth Conditions</u>

Methane degradation experiments were performed with *Methylococcus capsulatus* strain Bath (NCIMB 11132), *Methylosinus sporium* strain 5 (NCIMB 11126), *Methylocystis parvus* strain OBBP (NCIMB 11129), *Methylomonas methanica* strain S1 (NCIMB 11130), and *Methylocaldum gracile* strain 14L (NCIMB 11912). All strains were ordered from The National Collection of Industrial, Marine and Food Bacteria Ltd. (NCIMB), Aberdeen, Scotland. The organisms were cultivated in mineral salt medium (according to NCIMB medium 131) and a headspace containing methane (5%) and air (95%). Bottles were shaken at 30℃ or at 45℃ (*M. capsulatus*). Different copper concentrations (0.8 µM or 8 µM) were adjusted by addition of appropriate volumes of a $CuSO_4$ stock solution (4 mM) to medium prepared without copper. For experiments under copper limitation, the medium was prepared copper-free. The isotope fractionation experiments for each culture were carried out as follows: a set of 20 serum flasks (118 ml) each filled with 20 ml of mineral salt medium containing different copper concentrations (see above) was inoculated with 5 ml of fresh inoculum grown at the designated copper concentration (0 µM, 0.8 µM or 8 µM) for at least two batch cycles. Subsequently, the serum flasks were sealed gastight with butyl rubber stoppers and crimp caps. 5 ml of methane (Air Liquide, Düsseldorf, Germany, technical grade) were injected into the headspace of each culture with a syringe resulting in molar oxygen / methane ratios of higher

than four, which are levels expected to guarantee complete methane degradation. Single culture bottles were sacrificed at different time points during methane biodegradation (0 – 99%) by addition of 1 ml of concentrated hydrochloric acid and stored at 4°C until further investigation. In each fractionation experiment, at least 10 data points were used to compile the Rayleigh plots.

Analytical Methods

The concentration of Cu^{2+} ions in the medium was determined by atomic absorption spectroscopy. Methane concentrations were measured from the headspace using a Varian 3800 gas chromatograph (Varian, Palo Alto, USA) equipped with a CP SIL 5 CB capillary column (film thickness, 0.12 μm; inside diameter, 0.25 mm; length, 25 m) and a flame ionization detector. The chromatographic conditions were as follows: injector temperature, 250°C (split 1:5); detector temperature, 260°C; oven temperature , 50°C. Helium (1 ml min $^{-1}$) was used as a carrier gas. Depending on the methane concentration in the sacrificed culture bottles, 100 to 1000 μl of headspace sample was manually injected in triplicates.

MMO Activity Assay

A naphthalene oxidation assay according to Brusseau *et al*. [217] was used to detect the activity of sMMO in the cultures. sMMOs oxidise naphthalene to 1- and 2-naphthols which can be detected in a reaction with tetrazotised-*o*-dianisidine (CAS-No: 20282-70-6; Sigma Aldrich, Germany), and produces a violet diazo dye. pMMO is not reactive in this assay [218]. The assay was conducted in duplicate for each strain and respective copper condition. Heat-killed and sterile controls were applied as negative controls. The positive control was performed with a saturated 2-naphthol (Merck, Darmstadt, Germany) aqueous solution.

Stable isotope Analyses and Calculations

Stable Isotope Analysis of Methane

Methane isotopic compositions were determined from 100 to 1000 μl headspace samples (depending on the methane concentrations) by gas chromatography isotopic ratio mass spectrometry (Finnigan MAT 253, Thermo Finnigan Bremen, Germany) coupled to a gas chromatograph (HP 6890 Series, Agilent Technology, Santa Clara, USA), either via a combustion device (for carbon analysis; [219]) or via a pyrolyis unit (for hydrogen analysis; [220]). The GC was equipped with a CP-Porabond Q column (50 m x 0.32 mm x 0.5 μm, Varian, Palo Alto, USA) and held at a constant temperature of 40°C and constant flow of helium (2 ml min $^{-1}$ for carbon and 1.6 ml min $^{-1}$ for hydrogen).

Each sample was measured at least three times. The total analytical uncertainty with respect to both accuracy and reproducibility was always better then ±0.5‰ for $\delta^{13}C$ and ±10‰ for $\delta^{2}H$, respectively.

Calculation of isotope enrichment factors

The isotopic values were expressed in delta notation ($\delta^{13}C$, $\delta^{2}H$) per mill (‰) in relation to the international standards V-PDB for carbon and SMOW for hydrogen, respectively *Equation (11)*.

Equation (11) $$\delta^{13}C \text{ or } \delta^{2}H\ [‰] = \frac{(R_{sample} - R_{Std})}{R_{Std}} \bullet 1000$$

R_{sample} and R_{Std} are the $^{13}C/^{12}C$- or $^{2}H/^{1}H$-ratios of the sample and the international standard, respectively.

For determining the isotopic enrichment factor ε, the Rayleigh equation has been used according to [194]:

Equation (12) $$\frac{R_t}{R_0} = \frac{C_t}{C_0}^{\frac{\varepsilon}{1000}}$$

with R_t, C_t and R_0, C_0 as the stable isotope ratios and concentrations of methane at the beginning (0) and after a certain time (t) of the degradation experiment, respectively. By using the delta notation according to *Equation (11)*, *Equation (12)* transforms to:

Equation (13) $$\frac{\delta_t + 1000}{\delta_0 + 1000} = \frac{C_t}{C_0}^{\frac{\varepsilon}{1000}}$$

By plotting $\ln((\delta_t+1000)/(\delta_0+1000))$ versus $\ln(C_t/C_0)$, the enrichment factor ε can be obtained from the slope of the linear regression. δ_t and δ_0 are the isotope values (expressed in the ‰-notation) at time point t and 0, respectively. The fractionation factor α is then simply related to the enrichment factor ε by:

Equation (14) $$\varepsilon = (\alpha - 1) \bullet 1000$$

Calculation of Lambda (Λ) and the Apparent Kinetic Isotope Effect (AKIE)

The factor Λ is approximated via the slope of the linear expression when plotting $\Delta\delta^2H$ versus $\Delta\delta^{13}C$ as

Equation (15)
$$\Lambda \approx \frac{\Delta(\delta^2 H)}{\Delta(\delta^{13}C)} = \frac{(\delta_t^2 H - \delta_0^2 H)}{(\delta_t^{13}C - \delta_0^{13}C)}$$

In the case of high isotope fractionation, which is often observed with hydrogen isotopes, this approximation should be regarded with suspicion. Especially if $\varepsilon_H >> -100‰$, the calculation of Λ by

Equation (16)
$$\Lambda = \frac{(\alpha_H^{-1} - 1)}{(\alpha_C^{-1} - 1)}$$

is more reliable [194]. The errors of α and ε are given as a 95% confidence interval (CI) calculated according to Elsner *et al.* [209].

For a mechanistic interpretation of isotope discrimination per reacting position, the enrichment factors have to be converted to apparent kinetic isotope effect values (AKIE) for the independent bond cleavage reactions. Since methane is a symmetrical molecule, all C-H bonds are considered as potentially reactive. Thus,

Equation (17)
$$\varepsilon_{bulk} = \varepsilon_{reactive\ position}$$

However, it is still necessary to perform a correction for intramolecular competition to obtain the AKIE for hydrogen according to

Equation (18)
$$AKIE = \frac{1}{1 + z \bullet \varepsilon_{reactive\ position} / 1000}$$

where z is the number of atoms of an element in identical reactive positions [194]. In case of methane, z is 4 for hydrogen and 1 for carbon. Note, for AKIEs with $\varepsilon \approx -1000/z$ large errors must be assumed, since the equation is mathematically not defined at this point and converges towards infinity.

4.4.3. Results and discussion

Methane Oxidation Kinetics and Induction of pMMO and sMMO by the Presence and Absence of Copper

Fractionation experiments were conducted using a variety of taxonomically distinct, well-characterised methanotrophic reference organisms [221-229]. *M. capsulatus* and *M. sporium*

were cultivated in the presence of different amounts of copper to induce the expression of pMMO or sMMO, respectively. More than 97% of methane was consumed in almost all experimental treatments (*Figure 45*). Methane was oxidised within 28 hours by *M. methanica* (copper rich conditions; *Figure 45*) and within 87 hours by *M. sporium* (copper free conditions; *Figure 45*). Under copper limitation, decreased methane oxidation rates were observed in the experiment with *M. sporium* (*Figure 45*). In each experiment, methane oxidation started without a detectable lag-phase.

The adjusted copper concentrations were adequately detected by absorption spectroscopy (*Table 10*). Additionally, the activity of sMMO was examined using a naphthalene oxidation test according to Brusseau *et al.* [217]. After adding tetrazotised-*o*-dianisidine to cultures grown in the presence of naphthalene, a color shift in the medium from a milky-transparent to deep violet color clearly indicated that naphthalene was oxidised to 1- or 2-naphthol [218]. sMMO but not pMMO can catalyse this reaction [217]. Thus, the production of the violet diazo dye provided clear evidence that the sMMO was expressed in *M. capsulatus* and *M. sporium* under copper-limited conditions (*Table 10*). As expected, no activity of sMMO was detected in both strains when cultivated in the presence of 8 µM copper. Similarly, sMMO activity was absent in all other tested strains (*Table 10*). Thus, the copper-dependent cultivation enabled us to determine fractionation factors for methane degradation catalysed by sMMO or pMMO.

Isotope Enrichment Factors (ϵ) and Apparent Kinetic Isotope Effects (AKIEs) for Methane Oxidation

A trend toward isotopic enrichment with increasing degradation of methane was observed in the residual methane of all degradation experiments. Starting with isotope signatures of $\delta^{13}C$ and δ^2H of -43‰ and -255‰, these enriched to maximal values of +86‰ ($\delta^{13}C$) and +706‰ (δ^2H), after more than 95% of the methane was consumed. Such a progressive stable isotope enrichment correlated with decreasing methane concentrations in closed isotopic systems is typical for biological processes and can be evaluated with the Rayleigh equation [200]. The linear regression of the Rayleigh plot *Equation (13)* resulted in enrichment factors (ϵ) ranging from -14.8±0.9‰ to -27.9±1.7‰ for carbon (ϵ_C) and from -110.0±11.5‰ to -231.5±30.3‰ for hydrogen (ϵ_H), respectively (*Table 11*). *Figure 45* shows the Rayleigh plots for the methane degradation experiments with *M. sporium* under copper free and copper rich conditions for carbon and hydrogen isotope fractionation. The respective graphs of all remaining fractionation experiments are shown in the supporting material section (*Figure 45*). The correlation factor (R^2) of the linear regression of each plot was always higher than 0.94.

The resulting AKIEs varied between 1.015±0.001 and 1.029±0.001 for carbon, and 1.8 and 13.5 for hydrogen (*Table 11*).

Table 10: Taxonomy and physiology of the selected aerobic methane-oxidising strains and conditions applied in the isotope fractionation experiments. [a] pMMO = particulate methane monooxygenase, [b] sMMO = soluble methane monooxygenase, [c] according to [217]; +, clearly visible production of the violet diazo dye; –, no color shift

	Methylococcus capsulatus strain Bath		*Methylosinus sporium* strain 5		*Methylocystis parvus* strain OBBP	*Methylomonas methanica* strain S1	*Methylocaldum gracile* strain 14L
Proteobacterial group	gamma		alpha		alpha	gamma	gamma
Assimilation pathway	RuMP		serine		serine	RuMP	RuMP
Type of methane MMO (a, b)	sMMO, pMMO		sMMO, pMMO		pMMO	pMMO	pMMO
Cultivation temperature [°C]	45		30		30	30	30
Copper condition:	rich	free	rich	free	rich	rich	regular
set point (µM Cu2+):	8	0	8	0	8	8	0.8
determined (µM Cu2+):	8.9	0.3	8.4	0.2	6.7	7.1	1.1
naphthol assayc / MMO expresseda, b	- / pMMO	+ / sMMO	- / pMMO	+ / sMMO	- / pMMO	- / pMMO	- / pMMO
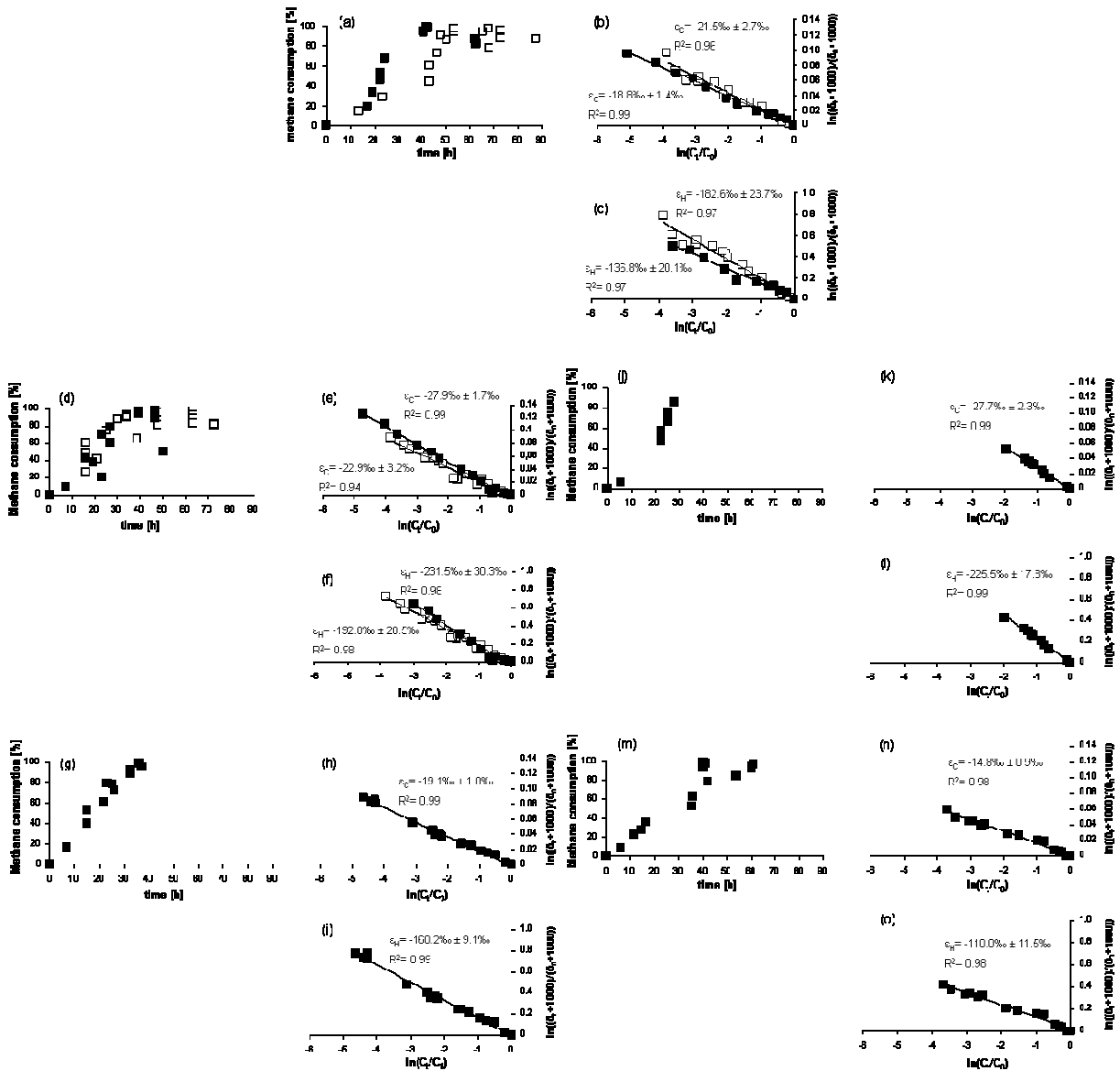
Figure 45: Methane degradation experiment with M. sporium (a-c) and M. capsulatus (d-f) under copper limited (□) and copper rich conditions (■); M. parvus (g-i), M. methanica (j-l) and M. gracile (m-o) under copper rich conditions (■). (a, d, g, j, m) Methane consumption [%] over time [h]; only time points with detectable methane concentrations (methane consumption <97.9%) are depicted. (b, e, h, k, n) Rayleigh plot for stable carbon isotope fractionation. (c, f, i, l, o) Rayleigh plot for stable hydrogen isotope fractionation. Enrichment factors ε are given within 95% confidence limits.

182

Table 11: Enrichment factors for carbon (ε_C) and hydrogen (ε_H), apparent kinetic isotope effects (AKIE) for carbon (AKIE$_C$) and hydrogen (AKIE$_H$), and lambda (Λ) values for aerobic methane-oxidising bacteria investigated in this study. Λ values were calculated using the raw data of isotope discrimination ($\Delta\delta^2H/\Delta\delta^{13}C$) or the isotope fractionation factors ($(\alpha_H^{-1}-1)/(\alpha_C^{-1}-1)$), respectively. [a] confidence interval (95%) [b] calculated according to [194][f] after error propagation

Strain	Cu condition	Carbon			Hydrogen			$\Delta\delta^2H/\Delta\delta^{13}C$[b]		$(\alpha_H^{-1}-1)/(\alpha_C^{-1}-1)$
		$\varepsilon C\pm CI$[a]	R^2	AKIEC±error[c]	$\varepsilon H\pm CI$[a]	R^2	AKIEH	$\Lambda\pm CI$[a]	R^2	$\Lambda\pm error$[c]
Methylococcus capsulatus	rich	-27.9±1.7	0.99	1.029±0.002	-231.5±30.3	0.98	13.5	8.7±0.8	0.99	10.5±2.4
Methylosinus sporium	rich	-18.8±1.4	0.99	1.019±0.001	-136.8±20.1	0.97	2.2	7.7±0.4	0.99	8.3±2.0
Methylocystis parvus	rich	-19.1±1.0	0.99	1.019±0.001	-168.2±9.1	0.99	3.1	10.5±0.5	0.99	10.4±1.2
Methylomonas methanica	rich	-27.7±2.3	0.99	1.028±0.002	-225.5±17.8	0.99	10.2	8.0±0.3	1.00	10.2±1.9
Methylocaldum gracile	regular	-14.8±0.9	0.98	1.015±0.001	-110.0±11.5	0.98	1.8	7.3±0.3	0.99	8.2±1.5
Methylococcus capsulatus	free	-22.9±3.2	0.94	1.023±0.003	-192.0±28.5	0.98	4.3	9.3±0.5	0.99	10.1±3.3
Methylosinus sporium	Free	-21.5±2.7	0.96	1.022±0.003	-182.6±23.7	0.97	3.7	9.5±0.7	0.98	10.2±2.9

The enrichment factors determined in our study are within the range of previously observed laboratory and field enrichment factors for the aerobic oxidation of methane, ranging from -4.0‰ to -26.6‰ for carbon, e.g. [197-207] (see also *Table 12* and *Table 13*) and -38‰ to -320‰ for hydrogen (*Table 12* and *Table 13*; [198-203, 205]). A similar variability of carbon and hydrogen enrichment factors has also been observed for gas samples obtained from anoxic marine sediments (*Table 13*; [230-232]), and for anaerobic methane-oxidising enrichment cultures (*Table 12*; [98]).

Generally, the AKIEs calculated in our study (*Table 11*) are in the upper range or even above the Streitwieser semi-classical limits for primary kinetic isotope effects (KIE) during C-H bond cleavages (1.021 for carbon; 6.4 for hydrogen; [194]). The Streitwieser limits are defined by the mass of the atoms forming the chemical bond and their vibration frequency. The relative mass difference between two isotopes determines the maximal value of the KIE: the greater the difference, the greater the possible KIE. Thus, the KIEs for hydrogen are expected to be much higher than those for carbon, which is reflected in the results of our study. However, particularly for hydrogen, KIE values can be greater than their Streitwieser limit for different reasons (summarised in [208]), explaining the high $AKIE_H$ values observed in our study (especially for *M. capsulatus* [$\varepsilon_H = -231.5$]) and *M. methanica* [$\varepsilon_H = -225.5$]), and by others (*Table 12*). Our determined AKIE values indicate that the observed isotope effects are mainly due to bond breaking reactions, and that the effects of preceding rate-limiting steps associated with uptake, transport, or binding of methane to the enzyme, are of minor importance.

Two-Dimensional Compound Specific Isotope Analysis

For a two-dimensional isotope analysis, we calculated the Λ factor by plotting $\Delta\delta^2H$ versus $\Delta\delta^{13}C$ (*Figure 46*; *Equation (15))*. The Λ values ranged from 7.3±0.3 to 10.5±0.5, and showed strong linear correlation coefficients ($R^2 > 0.98$). However, carbon and hydrogen discrimination ($\Delta\delta^2H$ and $\Delta\delta^{13}C$) plots are expected to be slightly curved because the hydrogen enrichment factors were always greater than -100‰ [194]. Therefore, we additionally calculated the Λ values according to *Equation (16)* to attenuate the impact associated with higher hydrogen fractionation, (*Table 11*). The latter calculation yielded Λ values ranging from 8.2±1.5 to 10.5±2.4. The most prominent differences between the two different calculation approaches using the same experimental data set coincided with the highest hydrogen enrichment factors, and support the observations of Elsner *et al.* [209].

Table 12: Enrichment factors (ε), apparent kinetic isotope effects (AKIE) and lambda (Λ) values for carbon and hydrogen of aerobic and anaerobic methanotrophic enrichment cultures reported so far. Λ values were calculated using the isotope fractionation factors $α_C$ and $α_H$ reported in the espective references. [a] ae=aerobic; an=anaerobic [b]Confidence interval (95%) [c]error after error propagation [d]not calculable after Equation (18)

Inoculum taken from	Cultivation temperature [°C] and conditions[a]	Carbon		Hydrogen		$(α_H^{-1}-1)/(α_C^{-1}-1)$	Reference
		$ε_C±CI$[b]	$AKIE_C±error$[c]	$ε_H±CI$[b]	$AKIE_H$	$Λ±error$[c]	
Drip try of ice machine	26 (ae)	-24.6±0.7	1.025±0.001	-245.3±14.2	53.0	12.9±1.4	[200]
water sample	11.5 (ae)	-12.8±0.2	1.013±0.000	-93.4±4.9	1.6	7.9±0.6	[200]
water sample until 27% of degradation	26 (ae)	-23.8±1.4	1.024±0.002	-229.0±1.2	11.9	12.2±0.8	[200]
water sample after 27% of degradation	26 (ae)	-15.4±0.3	1.016±0.000	-229.0±1.2	11.9	19.0±0.5	[200]
shane seep (California)	15 (ae)	-26.6±1.6	1.027±0.002	-156.4±n.d.	2.7	6.8±n.d.	[202]
Brian seep (California)	15 (ae)	-24.9±1.2	1.026±0.001	-319.9±n.d.	n.c.[d]	18.4±n.d.	[202]
compost + sand biofilter, 6-8% CH_4	22 (ae)	-17.7±0.5	1.018±0.001	-138.5±8.5	2.2	8.9±0.9	[203]
compost + sand biofilter, 23-24% CH_4	22 (ae)	-23.8±0.6	1.024±0.001	-191.6±3.2	4.3	9.7±0.4	[203]
Hydrate Rich; sediment free	12 (an)	-11.9±0.0	1.012±0.000	-100.7±1.7	1.7	9.3±0.2	[98]
Amon Mud Volcano; sediment free	20 (an)	-20.6±1.3	1.021±0.001	-139.4±9.4	2.3	7.7±1.1	[98]
Black Sea; microbial mats	12 (an)	-35.7±1.3	1.037±0.001	-229.6±7.1	12.2	8.1±0.6	[98]

Table 13: Enrichment factors (ε), apparent kinetic isotope effects (AKIE) and lambda (Λ) values for carbon and hydrogen of environmental gas samples showing aerobic and anaerobic methane oxidation. Λ values were calculated using the isotope fractionation factors α_C and α_H reported in the respective references. [a] data shown for individual experiment, [b] average value of individual experiments (n=6) calculated directly by plotting $\Delta\delta^2H/\Delta\delta^{13}C$, [c] error calculated after error propagation, inc. = incalculable due to missing data, Ref, reference

Sample site	Conditions	Carbon		Hydrogen		$(\alpha H^{-1}-1)/(\alpha C^{-1}-1)$	Ref.
		εC±CI	AKIEC±error[c]	εH±CI	AKIEH	Λ±error[c]	
	oxic	-4±inc.	1.004±inc.	-47.6±inc.	1.2	12.5±inc.	
		-10.9±inc.	1.011±inc.	-114.3±inc.	1.8	11.7±inc.	
Flooded swamp forestsa		-19.6±inc.	1.02±inc.	-69.8±inc.	1.4	3.7±inc.	[201]
		-18.6±inc.	1.019±inc.	-57.5±inc.	1.3	3.2±inc.	
						9±4b	
Soil	oxic	-12±inc.	1.012±inc.	-85.9±inc.	1.5	7.8±inc.	[205]
		-18±inc.	1.018±inc.	-172.9±inc.	3.2	11.4±inc.	
Landfill site	oxic	-7.9±3.0	1.008±0.003	-42.1±18	1.2	5.5±4.6	[199]
Cover soil of landfills	oxic	-7.9±3.9	1.008±0.004	-37.5±24	1.2	4.9±5.7	[198]
Black Sea, Cariaco basin; water column	anoxic	-21±1	1.021±0.001	-167±14	3	9.5±1.4	[231]
Marine coastal sediments; pore water	anoxic	-12±1	1.012±0.001	-107±16	1.8	10±2.5	[232]
Anoxic sediments, Skan Bay, Alaska	anoxic	-9±1	1.009±0.001	-136±17	2.2	17.8±5.3	[230]

(a)

$\Lambda = 5.7 + 0.8$
$R^2 = 0.99$

$\Delta\delta^2H$ [‰]

$\Delta\delta^{13}C$ [‰]

(b)

$\Lambda = 7.7 + 0.4$
$R^2 = 0.99$

$\Delta\delta^2H$ [‰]

$\Delta\delta^{13}C$ [‰]

(c)

$\Lambda = 10.5 \pm 0.5$
$R^2 = 0.99$

$\Delta\delta^2H$ [‰]

$\Delta\delta^{13}C$ [‰]

(d)

$\Lambda = 8.0 \pm 0.2$
$R^2 = 1.00$

$\Delta\delta^2H$ [‰]

$\Delta\delta^{13}C$ [‰]

(e)

$\Lambda = 7.3 \pm 0.3$
$R^2 = 0.99$

$\Delta\delta^2H$ [‰]

$\Delta\delta^{13}C$ [‰]

(f)

$\Lambda = 9.3 \pm 0.5$
$R^2 = 0.99$

$\Delta\delta^2H$ [‰]

$\Delta\delta^{13}C$ [‰]

(g)

$\Lambda = 9.5 \pm 0.7$
$R^2 = 0.98$
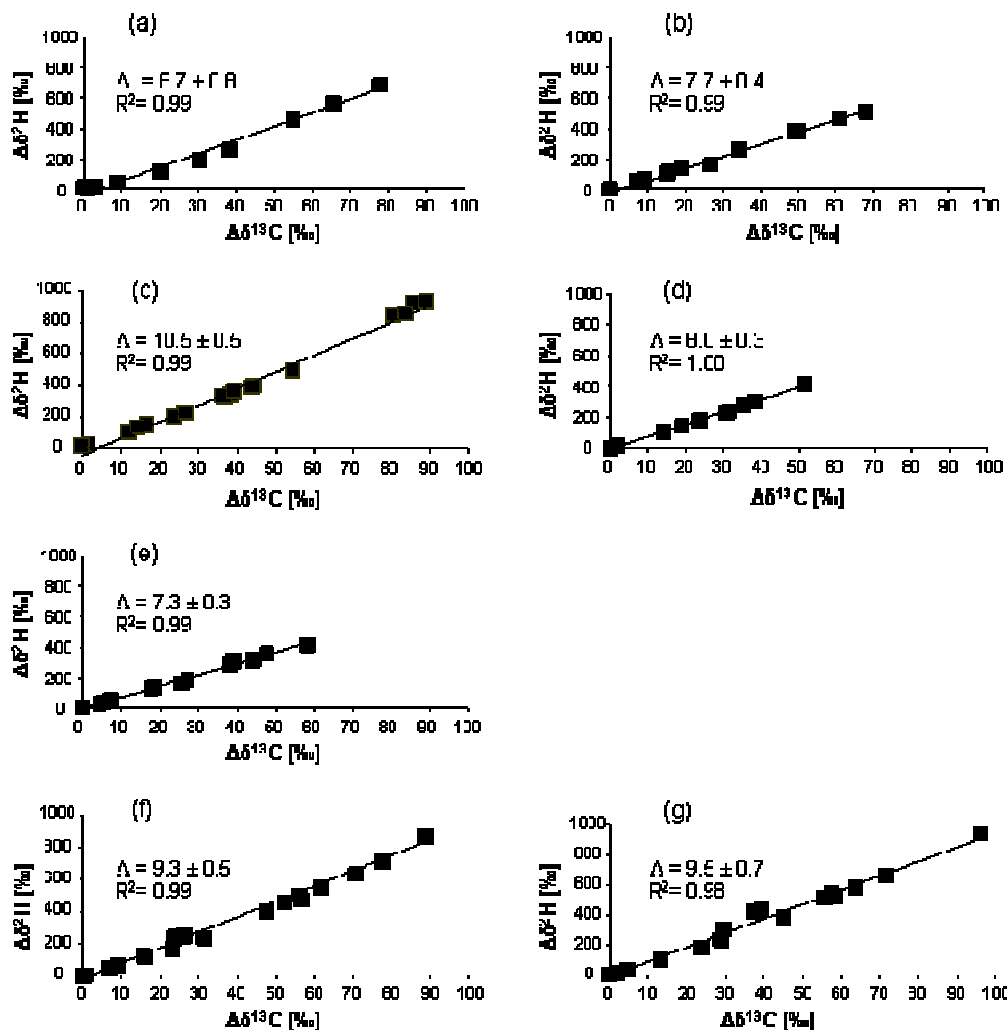
$\Delta\delta^2H$ [‰]

$\Delta\delta^{13}C$ [‰]

Figure 46: Plots of hydrogen vs. carbon stable isotope signatures for each strain and copper condition examined in this study. The slope of the regression curves gives the lambda (Λ) values for: (A) M. capsulatus, 8.9 µM Cu; (B) M. sporium, 8.4 µM Cu; (C) M. parvus, 6.7 µM Cu; (D) M. methanica, 7.1 µM Cu; (E) M. gracile, 1.1 µM Cu; (F) M. capsulatus, 0.3 µM Cu; (G) M. sporium, 0.2 µM Cu.

By grouping the Λ values, calculated by *Equation (15),* according to the expressed MMO, an average value of 9.4±0.1 for sMMO (n=2) and 8.4±1.3 for pMMO (n=5) was obtained, and therefore these two groups were statistically equal. The methanotrophic strains used in our study were selected to cover a wide taxonomic range, belonging to the alpha and gamma classes of the *Proteobacteria* [233, 234]. Since the phylogeny of 16S rRNA genes are congruent with the phylogeny of *pmoA* genes which encode a subunit of pMMO [176], we assume that the tested strains contain pMMOs with slightly varying structures and can therefore be seen as representative of the typical variability found in environmental samples. Grouped by their phylogenetic affiliation, the examined strains exhibited similar Λ values of

9.2±1.4 for the α-*Proteobacteria* (n =3) and 8.3±0.9 for the γ-*Proteobacteria* (n = 4) (calculated by *Equation (15))*. Notably, Λ values for *Methylcystis parvus* and its closest relative *Methylosinus sporium*, cultivated under similar conditions, were significantly different when calculated by *Equation (15)*, but were not significantly different when calculated by *Equation (16)*. Here, further investigations are needed to determine whether those values are statistically different or not. In summary, a clear relationship between the Λ value and the taxonomic affiliation and/or the type of MMO expressed, could not be observed. pMMO and sMMO containing strains showed similar two-dimensional fractionation patterns, indicating that the reaction mechanism for pMMO and sMMO is similar with respect to isotopic discrimination during methane oxidation.

Comparison of Λ values with literature data

Using *Equation (16)* allowed us to compare our Λ values with Λ values of methane oxidation calculated from previously published carbon and hydrogen isotope fractionation factors. For laboratory enrichment cultures (*Table 12*), Λ values are basically in the same range as we observed in our experiments. Exceptions are reported by Coleman and Risatti [200] for a water sample (Λ = 19), and by Kinnaman *et al.* [202] for a methane seep sample (Λ = 18.4; *Table 12*). Lambda values of aerobic methane-oxidising environmental gas samples showed broad variability and ranged between 3.2 and 12.5 (*Table 13*). The cited enrichment cultures and environmental samples were not further characterised. Hence, the isotope fractionation pattern cannot be related to specific methanotrophic strains and/or the type of methane-oxidising enzymes. Therefore, they should be considered as bulk enrichment factors influenced by unknown parameters, resulting in a rather high variability of enrichment factors.

Recently, carbon and hydrogen isotope fractionation factors for anaerobic methane oxidation (AOM) were provided for three microbial enrichment cultures established from three different anoxic sites (*Table 12*; [98]). The Λ values for these cultures were between 7.7 and 9.3, and thus fairly comparable to the aerobic enrichment factors obtained in our study. Also Λ values for anoxic environmental gas samples calculated from fractionation factors reported by Kessler *et al.* [231] and Martens *et al.* [232] were in this range (*Table 13*). Although the enzymes for the first isotopically sensitive oxidation step of methane are completely different, AOM is thought to proceed via reverse methanogenesis (reviewed in [3]), the anoxic C-H-bond breakage produces similar isotope effects compared to aerobic methane oxidation. Hence, within the uncertainty of our data, as well as data from the literature, the carbon and hydrogen fractionation patterns for methane do not allow to distinguish anaerobic and aerobic methane-oxidising pathways.

In contrast to the consistent Λ values observed for aerobic and anaerobic methane oxidation, highly variable Λ values were recently reported for the microbial degradation of different organic compounds. Fischer *et al.* [215] could distinguish aerobic and anaerobic benzene degradation pathways by the two-dimensional isotope fractionation approach. Elsner *et al.* [209] differentiated distinct chemical MTBE-oxidising mechanisms (S_N1, S_N2, methyl group oxidation) by plotting hydrogen against carbon isotope discrimination. Λ values for the anaerobic activation of alkylbenzenes (toluene, xylenes) were shown to be remarkably variable, although the underlying isotopically sensitive biochemical reaction was catalysed by the same enzyme (benzlysuccinate synthase) in all investigated cultures [210, 214].

Environmental implications

Among abiotic methane removal processes, the photochemical oxidation of methane in the atmosphere is the most important process [171]. Here, methane reacts either primarily with OH radicals in the troposphere, or with chlorine radicals in the stratosphere [235]. Both processes have been described to significantly affect the ^{13}C content of atmospheric methane, but the KIE of the reaction with chlorine radicals is different from the KIE associated with the hydroxyl radical reaction [235]. A KIE of 1.0039±0.0004 for carbon and of 1.294±0.018 for hydrogen, respectively, was reported for the oxidation of methane with hydroxyl radicals [236], and similar values were reported in other studies [198, 237]. For the photochemical reaction of methane with chlorine radicals, carbon and hydrogen isotope fractionation factors of 1.058 to 1.066, and of 1.47 to 1.54, respectively, were determined [235]. Whereas Λ values of 7.6-7.9 assessed for the chlorine radical reaction are similar to the lower boundary of Λ values caused by microbial oxidation, the value of 75 for the hydroxyl radical reaction differs up to an order of magnitude to all other Λ values observed to date. Thus, these Λ values might be suitable for differentiating photochemical and biotic methane oxidation processes in environmental studies.

As a practical consequence for field studies or laboratory studies using field samples, one has to consider that aerobic and anaerobic methane oxidation might be hard to distinguish by isotope fractionation methods. However, the combined application of carbon and hydrogen isotope data of methane has potential to elucidate dominant abiotic and biotic processes in the environment.

Acknowledgements

4.5. References

1.   Barnes RO & Goldberg ED (1976) Methane production and consumption in anoxic marine sediments. *Geology* **4**: 297-300.

2.   Davis JB & Yarbrough HF (1966) Anaerobic oxidation of hydrocarbons by *Desulfovibrio desulfuricans*. *Chem Geol* **1**: 137-144.

3.   Knittel K & Boetius A (2009) Anaerobic Oxidation of Methane: Progress with an Unknown Process. *Annu Rev Microbiol* **63**: 311-334.

4.   Reeburgh WS (1976) Methane consumption in Cariaco Trench waters and sediments. *Earth Planet Sci Lett* **28**: 337-344.

5.   Reeburgh WS (2007) Oceanic Methane Biogeochemistry. *Chem Rev* **107**: 486-513.

6.   Michaelis W, Seifert R, Nauhaus K*, et al.* (2002) Microbial Reefs in the Black Sea Fueled by Anaerobic Oxidation of Methane. *Science* **297**: 1013-1015.

7.   Schubert CJ, Coolen MJL, Neretin LN*, et al.* (2006) Aerobic and anaerobic methanotrophs in the Black Sea water column. *Environ Microbiol* **8**: 1844-1856.

8.   Niemann H, Duarte J, Hensen C*, et al.* (2006) Microbial methane turnover at mud volcanoes of the Gulf of Cadiz. *Geochim Cosmochim Acta* **70**: 5336-5355.

9.   Omoregie EO, Mastalerz V, de Lange G*, et al.* (2008) Biogeochemistry and Community Composition of Iron- and Sulfur-Precipitating Microbial Mats at the Chefren Mud Volcano (Nile Deep Sea Fan, Eastern Mediterranean). *Appl Environ Microbiol* **74**: 3198-3215.

10. Joye SB, Boetius A, Orcutt BN, Montoya JP, Schulz HN, Erickson MJ & Lugo SK (2004) The anaerobic oxidation of methane and sulfate reduction in sediments from Gulf of Mexico cold seeps. *Chem Geol* **205**: 219-238.

11. Knab NJ, Dale AW, Lettmann K, Fossing H & Jørgensen BB (2008) Thermodynamic and kinetic control on anaerobic oxidation of methane in marine sediments. *Geochim Cosmochim Acta* **72**: 3746-3757.

12. Niemann H, Elvert M, Hovland M*, et al.* (2005) Methane emission and consumption at a North Sea gas seep (Tommeliten area). *Biogeosciences* **2**: 335-351.

13. Treude T, Niggemann J, Kallmeyer J, Wintersteller P, Schubert CJ, Boetius A & Jørgensen BB (2005) Anaerobic oxidation of methane and sulfate reduction along the Chilean continental margin. *Geochim Cosmochim Acta* **69**: 2767-2779.

14. D'Hondt S, Jørgensen BB, Miller DJ*, et al.* (2004) Distributions of Microbial Activities in Deep Subseafloor Sediments. *Science* **306**: 2216-2221.

15. Sivan O, Schrag DP & Murray RW (2007) Rates of methanogenesis and methanotrophy in deep-sea sediments. *Geobiol* **5**: 141-151.

16. Eller G, Känel L & Krüger M (2005) Cooccurrence of Aerobic and Anaerobic Methane Oxidation in the Water Column of Lake Plußsee. *Appl Environ Microbiol* **71**: 8925–8928.

17. Froelich PN, Klinkhammer GP, Bender ML*, et al.* (1979) Early oxidation of organic matter in pelagic sediments of the eastern equatorial Atlantic: suboxic diagenesis. *Geochim Cosmochim Acta* **43**: 1075-1090.

18. Aloisi G, Pierre C, Rouchy J-M, Foucher J-P, Woodside J & Party MS (2000) Methane-related authigenic carbonates of eastern Mediterranean Sea mud volcanoes and their possible relation to gas hydrate destabilisation. *Earth Planet Sci Lett* **184**: 321-338.

19. Bohrmann G, Greinert J, Suess E & Torres M (1998) Authigenic carbonates from the Cascadia subduction zone and their relation to gas hydrate stability. *Geology* **26**: 647-650.

20. Roberts HH & Aharon P (1994) Hydrocarbon-derived carbonate buildups of the northern Gulf of Mexico continental slope: A review of submersible investigations. *Geo Mar Lett* **14**: 135-148.

21. Martens CS & Berner RA (1974) Methane Production in the Interstitial Waters of Sulfate-Depleted Marine Sediments. *Science* **185**: 1167-1169.

22. Krüger M, Treude T, Wolters H, Nauhaus K & Boetius A (2005) Microbial methane turnover in different marine habitats. *Palaeogeogr Palaeoclimatol Palaeoecol* **227**: 6-17.

23. Krüger M, Meyerdierks A, Glöckner FO*, et al.* (2003) A conspicuous nickel protein in microbial mats that oxidize methane anaerobically. *Nature* **426**: 878-818.

24. Scheller S, Goenrich M, Boecher R, Thauer RK & Jaun B (2010) The key nickel enzyme of methanogenesis catalyses the anaerobic oxidation of methane. *Nature* **465**: 606-608.

25. Boetius A, Ravenschlag K, Schubert CJ*, et al.* (2000) A marine microbial consortium apparently mediating anaerobic oxidation of methane. *Nature* **407**: 423-426.

26. Raghoebarsing AA, Arjan Pol A, van de Pas-Schoonen KT*, et al.* (2006) A microbial consortium couples anaerobic methane oxidation to denitrification. *Nature* **440**: 918-921.

27. Aharon P (1994) Geology and biology of modern and ancient submarine hydrocarbon seeps and vents: An introduction. *Geo Mar Lett* **14**: 69-73.

28. Head IM, Jones DM & Larter SR (2003) Biological activity in the deep subsurface and the origin of heavy oil. *Nature* **426**: 344-352.

29. Dolfing J, Larter SR & Head IM (2007) Thermodynamic constraints on methanogenic crude oil biodegradation. *ISME J* **2**: 442-452.

30. Gieg LM, Duncan KE & Suflita JM (2008) Bioenergy Production via Microbial Conversion of Residual Oil to Natural Gas. *Appl Environ Microbiol* **74**: 3022-3029.

31. Zengler K, Richnow HH, Rossello-Mora R, Michaelis W & Widdel F (1999) Methane formation from long-chain alkanes by anaerobic microorganisms. *Nature* **401**: 266-269.

32. Anderson RT & Lovley DR (1999) Naphthalene and benzene degradation under Fe(III)-reducing conditions in petroleum-contaminated aquifers. *Bioremediat J* **3**: 121-135.

33. Sommer S, Linke P, Pfannkuche O, Niemann H & Treude T (2010) Benthic respiration in a seep habitat dominated by dense beds of ampharetid polychaetes at the Hikurangi Margin (New Zealand). *Mar Geol* **272**: 223-232.

34. Orcutt B, Boetius A, Elvert M, Samarkin V & Joye SB (2005) Molecular biogeochemistry of sulfate reduction, methanogenesis and the anaerobic oxidation of methane at Gulf of Mexico cold seeps. *Geochim Cosmochim Acta* **96**: 4267-4281.

35. Orcutt BN, Boetius A, Lugo SK, MacDonald IR, Samarkin VA & Joye SB (2004) Life at the edge of methane ice: microbial cycling of carbon and sulfur in Gulf of Mexico gas hydrates. *Chem Geol* **205**: 239-251.

36. Inagaki F, Nunoura T, Nakagawa S*, et al.* (2006) Biogeographical distribution and diversity of microbes in methane hydrate-bearing deep marine sediments on the Pacific Ocean Margin. *Proc Natl Acad Sci U S A* **104**: 2815–2820.

37. Kormas KA, Smith DC, Edgcomb V & Teske A (2003) Molecular analysis of deep subsurface microbial communities in Nankai Trough sediments (ODP Leg 190, Site 1176). *FEMS Microbiol Ecol* **45**: 115-125.

38. Reed DW, Fujita Y, Delwiche ME, Blackwelder DB, Sheridan PP, Uchida T & Colwell FS (2002) Microbial Communities from Methane Hydrate-Bearing Deep Marine Sediments in a Forearc Basin. *Appl Environ Microbiol* **68**: 3759-3770.

39. Hinrichs K-U, Pancost RD, Summons RE, Sprott GD, Sylva SP, Sinninghe Damsté JS & Hayes JM (2000) Mass spectra of sn-2-hydroxyarchaeol, a polar lipid biomarker for anaerobic methanotrophy. *G-cubed* **1**.

40. Lösekann T, Knittel K, Nadalig T, Fuchs B, Niemann H, Boetius A & Amann R (2007) Diversity and Abundance of Aerobic and Anaerobic Methane Oxidizers at the Haakon Mosby Mud Volcano, Barents Sea. *Appl Environ Microbiol* **73**: 3348-3362.

41. MacDonald IR, Bohrmann G, Escobar E*, et al.* (2004) Asphalt Volcanism and Chemosynthetic Life in the Campeche Knolls, Gulf of Mexico. *Science* **304**: 999-1002.

42. Valentine DL, Solem RC, Kastner M*, et al.* (2005) Biogeochemical investigations of marine methane seeps, Hydrate Ridge, Oregon. *J Geophys Res* **110**: 1-17.

43. Sieh K & Natawitjaja D (2000) Neotectonics of the Sumatran Fault, Indonesia. *J Geophys Res* **105**: 28295–28326.

44. Schippers A, Köweker G, Höft C & Teichert BMA (2010) Quantification of microbial communities in three forearc sediment basins off Sumatra. *Geomicrobiol J* 1-13.

45. Martin JW & Haney TA (2005) Decapod crustaceans from hydrothermal vents and cold seeps: a review through 2005. *Zool J Linn Soc* **145**: 445-522.

46. Widdel F & Bak F (1992) Gram-negative mesophilic sulfate-reducing bacteria. *The Prokaryotes,* Vol. 4 (Dworkin M, ed.), pp. 3352-3372. Springer, New York.

47. Nauhaus K, Boetius A, Krüger M & Widdel F (2002) *In vitro* demonstration of anaerobic oxidation of methane coupled to sulphate reduction in sediments from a marine gas hydrate area. *Environ Microbiol* **4**: 296–305.

48. Treude T, Krüger M, Boetius A & Jørgensen BB (2005) Environmental control on anaerobic oxidation of methane in the gassy sediments of Eckernförde Bay (German Baltic). *Limnol Oceanogr* **50**: 1771-1786.

49. Cord-Ruwisch R (1985) A quick method for the determination of dissolved and precipitated sulfides in cultures of sulfate-reducing bacteria. *J Microbiol Methods* **4**: 33-36.

50. Lovley DR & Phillips EJP (1986) Organic Matter Mineralization with Reduction of Ferric Iron in Anaerobic Sediments. *Appl Environ Microbiol* **51**: 683-689.

51. Lovley DR & Phillips EJP (1988) Novel Mode of Microbial Energy Metabolism: Organic Carbon Oxidation Coupled to Dissimilatory Reduction of Iron or Manganese. *Appl Environ Microbiol* **54**: 1472-1480.

52.   Weinbauer MG, Beckmann C & Höfle MG (1998) Utility of Green Fluorescent Nucleic Acid Dyes and Aluminum Oxide Membrane Filters for Rapid Epifluorescence Enumeration of Soil and Sediment Bacteria. *Appl Environ Microbiol* **64**: 5000–5003.

53.   Pernthaler A, Pernthaler J & Amann R (2002) Fluorescence In Situ Hybridization and Catalyzed Reporter Deposition for the Identification of Marine Bacteria. *Appl Environ Microbiol* **68**: 3094–3101.

54.   Schippers A, Neretin LN, Kallmeyer J, Ferdelman TG, Cragg BA, Parkes JR & Jørgensen BB (2005) Prokaryotic cells of the deep sub-seafloor biosphere identified as living bacteria. *Nature* **433**: 861-864.

55.   Webster G, Newberry CJ, Fry JC & Weightman AJ (2003) Assessment of bacterial community structure in the deep sub-seafloor biosphere by 16S rDNA-based techniques: a cautionary tale. *J Microbiol Methods* **55**: 155-164.

56.   Takai K & Horikoshi K (2000) Rapid Detection and Quantification of Members of the Archaeal Community by Quantitative PCR Using Fluorogenic Probes. *Appl Environ Microbiol* **6**: 5066–5072.

57.   Nadkarni MA, Martin FE, Jacques NA & Hunter N (2002) Determination of bacterial load by real-time PCR using a broad-range (universal) probe and primers set. *Microbiology* **148**: 257–266.

58.   Applied Biosystems (2002) TaqMan® ribosomal RNA control reagents, VIC™ probe.

59.   Schippers A & Nerretin LN (2006) Quantification of microbial communities in near-surface and deeply buried marine sediments on the Peru continental margin using real-time PCR. *Environ Microbiol* **8**: 1251–1260.

60.   Nunoura T, Oida H, Toki T, Ashi J, Takai K & Horikoshi K (2006) Quantification of *mcrA* by quantitative fluorescent PCR in sediments from methane seep of the Nankai Trough. *FEMS Microbiol Ecol* **57**: 149-157.

61.   Muyzer G, Teske A, Wirsen CO & Jannasch HW (1995) Phylogenetic relationships of *Thiomicrospira* species and their identification in deep-sea hydrothermal vent samples by denaturing gradient gel electrophoresis of 16S rDNA fragments. *Arch Microbiol* **164**: 165-172.

62.   Weisburg WG, Barns SM, Pelletier DA & Lane DJ (1991) 16S ribosomal DNA amplification for phylogenetic study. *J Bacteriol* **173**: 697-703.

63.   Coolen MJL, Cypionka H, Sass AM, Sass H & Overmann J (2002) Ongoing Modification of Mediterranean Pleistocene Sapropels Mediated by Prokaryotes; Online supplementory material. *Science* **296**: 2407-2410.

64.   Øvreås L, Forney L, Daae FL & Torsvik V (1997) Distribution of Bacterioplankton in Meromictic Lake Sælenvannet, as Determined by Denaturing Gradient Gel Electrophoresis of PCR-Amplified Gene Fragments Coding for 16S rRNA. *Appl Environ Microbiol* **63**: 3367–3373.

65.   Ludwig W, Strunk O, Westram R*, et al.* (2004) ARB: a software environment for sequence data. *Nucleic Acids Res* **32**: 1363-1371.

66.   Pruesse E, Quast C, Knittel K, Fuchs B, Ludwig W, Peplies J & Glöckner FO (2007) SILVA: a comprehensive online resource for quality checked and aligned ribosomal RNA sequence data compatible with ARB. *Nucleic Acids Res* **35**: 7188-7196.

67. Zühlsdorff L, Spieß V, Hübscher C & Breitzke M (1999) Seismic reflectivity anomalies in sediments at the eastern flank of the Juan de Fuca Ridge: Evidence for fluid migration? *J Geophys Res* **104**: 15351-15364.

68. Berndt C, Bünz S, Clayton T, Mienert J & Saunders M (2004) Seismic character of bottom simulating reflectors: examples from the mid-Norwegian margin. *Mar Petrol Geol* **21**: 723-733.

69. Hyndman RD & Spence GD (1992) A Seismic Study of Methane Hydrate Marine Bottom Simulating Reflectors. *J Geophys Res* **97**: 6683-6698.

70. Dekov VM, Kamenov GD, Savelli C, Stummeyer J & Marchig V (2006) Origin of basal dolomitic claystone in the Marsili Basin, Tyrrhenian Sea. *Mar Geol* **236**: 121-141.

71. Cline JD (1969) Spectrophotometric determination of hydrogen sulfide in natural waters. *Limnol Oceanogr* **14**: 454-458.

72. Wachter EA & Hayes JM (1985) Exchange of oxygen in carbon dioxide-phosphoric acid systems. *Chem Geol* **52**: 365-374.

73. Faber E & Stahl W (1983) Analytic Procedure and Results of an Isotope Geochemical Surface Survey in an Area of the British North Sea. *Geological Society, London, Special Publications* **12**: 51-63.

74. Rivière D, Desvignes V, Pelletier E*, et al.* (2009) Towards the definition of a core of microorganisms involved in anaerobic digestion of sludge. *ISME J* **3**: 700–714.

75. Santelli CM, Orcutt BN, Banning E*, et al.* (2008) Abundance and diversity of microbial life in ocean crust *Nature* **253**: 653-656.

76. Beal EJ, House CH & Orphan VJ (2009) Manganese- and Iron-dependent marine methane oxidation. *Science* **325**: 184-187.

77. Newberry CJ, Webster G, Cragg BA, Parkes RJ, Weightman AJ & Fry JC (2004) Diversity of prokaryotes and methanogenesis in deep subsurface sediments from the Nankai Trough, Ocean Drilling Program Leg 190. *Environ Microbiol* **6**: 274-287.

78. Knittel K, Boetius A, Lemke A*, et al.* (2003) Activity, Distribution, and Diversity of Sulfate Reducers and Other Bacteria in Sediments above Gas Hydrate (Cascadia Margin, Oregon). *Geomicrobiol J* **20**: 269 - 294.

79. Harrison BK, Zhang H, Berelson W & Orphan VJ (2009) Variations in Archaeal and Bacterial Diversity Associated with the Sulfate-Methane Transition Zone in Continental Margin Sediments (Santa Barbara Basin, California). *Appl Environ Microbiol* **75**: 1487-1499.

80. Ha M-H & Choi J (2009) Effects of Environmental Contaminants on Hemoglobin Gene Expression in *Daphnia magna*: A Potential Biomarker for Freshwater Quality Monitoring. *Arch Environ Contam Toxicol* **57**: 330-337.

81. Dhillon A, Teske A, Dillon J, Stahl DA & Sogin ML (2003) Molecular Characterization of Sulfate-Reducing Bacteria in the Guaymas Basin. *Appl Environ Microbiol* **69**: 2765-2772.

82. Hubert C, Loy A, Nickel M*, et al.* (2009) A Constant Flux of Diverse Thermophilic Bacteria into the Cold Arctic Seabed. *Science* **325**: 1541-1544.

83. Girguis PR, Orphan VJ, Hallam SJ & DeLong EF (2003) Growth and Methane Oxidation Rates of Anaerobic Methanotrophic Archaea in a Continuous-Flow Bioreactor. *Appl Environ Microbiol* **69**: 5472-5482.

84. Heijs SK, Haese RR, van der Wielen PWJJ, Forney LJ & van Elsas JD (2007) Use of 16S rRNA Gene Based Clone Libraries to Assess Microbial Communities Potentially Involved in Anaerobic Methane Oxidation in a Mediterranean Cold Seep. *Microb Ecol* **53**: 384-398.

85. Robertson CE, Spear JR, Harris JK & Pace NR (2009) Diversity and Stratification of Archaea in a Hypersaline Microbial Mat. *Appl Environ Microbiol* **75**: 1801-1810.

86. Kormas KA, Tamaki H, Hanada S & Kamagata Y (2009) Apparent richness and community composition of Bacteria and Archaea in geothermal springs. *Aquat Microb Ecol* **57**: 113-122.

87. Gallardo VA (1977) Large benthic microbial communities in sulphide biota under Peru-Chile Subsurface Countercurrent *Nature* **268**: 331-332.

88. Jannasch HW, Nelson DC & Wirsen CO (1989) Massive natural occurrence of unusually large bacteria (*Beggiatoa* sp.) at a hydrothermal deep-sea vent site. *Nature* **342**: 834-836.

89. Schulz HN, Brinkhoff T, Ferdelman TG, Mariné MH, Teske A & Jørgensen BB (1999) Dense Populations of a Giant Sulfur Bacterium in Namibian Shelf Sediments. *Science* **284**: 493-495.

90. Childress JJ, Fisher CR, Brooks JM, Kennicutt MC, Bidigare R & Anderson AE (1986) A Methanotrophic Marine Molluscan (Bivalvia, Mytilidae) Symbiosis: Mussels Fueled by Gas. *Science* **233**: 1306-1308.

91. Duperron S, Nadalig T, Caprais J-C, Sibuet M, Fiala-Médioni A, Amann R & Dubilier N (2005) Dual symbiosis in a *Bathymodiolus* sp. mussel from a methane seep on the Gabon continental margin (Southeast Atlantic): 16S rRNA phylogeny and distribution of the symbionts in gills. *Appl Environ Microbiol* **71**: 1694-1700.

92. Petersen JM & Dubilier N (2009) Methanotrophic symbioses in marine invertebrates. *Environ Microbiol Rep* **1**: 319-335.

93. Blazejak A, Erséus C, Amann R & Dubilier N (2005) Coexistence of Bacterial Sulfide Oxidizers, Sulfate Reducers, and Spirochetes in a Gutless Worm (Oligochaeta) from the Peru Margin. *Appl Environ Microbiol* **71**: 1553-1561.

94. Coffin R, Hamdan L, Plummer R, Smith J, Gardner J, Hagen R & Wood W (2008) Analysis of Methane and Sulfate Flux in Methane-Charged Sediments from the Mississippi Canyon, Gulf of Mexico. *Mar Petrol Geol* **25**: 977-987.

95. Deuser WG, Degens ET & Guillard RRL (1968) Carbon isotope relationships between plankton and sea water. *Geochim Cosmochim Acta* **32**: 657-660.

96. Whiticar MJ, Faber E & Schoell M (1986) Biogenic methane formation in marine and freshwater environments: CO_2 reduction vs. acetate fermentation--Isotope evidence. *Geochim Cosmochim Acta* **50**: 693-709.

97. Wegener G, Niemann H, Elvert M, Hinrichs K-U & Boetius A (2008) Assimilation of methane and inorganic carbon by microbial communities mediating the anaerobic oxidation of methane. *Environ Microbiol* **10**: 2287-2298.

98. Holler T, Wegener G, Knittel K, Boetius A, Brunner B, Kuypers MMM & Widdel F (2009) Substantial $^{13}C/^{12}C$ and D/H fractionation during anaerobic oxidation of methane by marine consortia enriched *in vitro*. *Environ Microbiol Rep* **1**: 370-376.

99. Geißler A (2003) Molekulare Analyse der bakteriellen Diversität in Uranabraumhalden. Diploma Thesis, Technische Universität Bergakademie Freiberg, Freiberg.

100. Webster G, Parkes RJ, Fry JC & Weightman AJ (2004) Widespread Occurrence of a Novel Division of Bacteria Identified by 16S rRNA Gene Sequences Originally Found in Deep Marine Sediments. *Appl Environ Microbiol* **70**: 5708–5713.

101. Teske A (2006) Microbial community composition in deep marine subsurface sediments of ODP Leg 201: Sequencing surveys and cultivations. *Proc. ODP, Sci. Results 201,* (Jørgensen BB, ed.), pp. 1-20.

102. Ishii S, Shimoyama T, Hotta Y & Watanabe K (2008) Characterization of a filamentous biofilm community established in a cellulose-fed microbial fuel cell. *BMC Microbiol* **8**.

103. Yamada T, Sekiguchi Y, Hanada S, Imachi H, Ohashi A, Harada H & Kamagata Y (2006) *Anaerolinea thermolimosa* sp. nov., *Levilinea saccharolytica* gen. nov., sp. nov. and *Leptolinea tardivitalis* gen. nov., sp. nov., novel filamentous anaerobes, and description of the new classes *Anaerolineae* classis nov. and *Caldilineae* classis nov. in the bacterial phylum Chloroflexi. *Int J Syst Evol Microbiol* **56**: 1331–1340.

104. Siegert M, Cichocka D, Herrmann S*, et al.* (in press) Accelerated methanogenesis from aliphatic and aromatic hydrocarbons under iron and sulfate reducing conditions. *FEMS Microbiol Lett.*

105. Aeckersberg F, Bak F & Widdel F (1991) Anaerobic oxidation of saturated hydrocarbons to CO_2 by a new type of sulfate-reducing bacterium. *Arch Microbiol* **156**: 5-14.

106. So CM, Phelps CD & Young LY (2003) Anaerobic Transformation of Alkanes to Fatty Acids by a Sulfate-Reducing Bacterium, Strain Hxd3. *Appl Environ Microbiol* **69**: 3892-3900.

107. Stratmann V & Schlömer S (2009) Das Kohlenwasserstoff-System im Forearc-Bereich von Sumatra: 2D-Beckenmodellierung und Gasgeochemie. (Wiedicke-Hombach M, ed.), Bundesanstalt für Geowissenschaften und Rohstoffe, Hannover.

108. Kuypers MMM, Sliekers AO, Lavik G*, et al.* (2003) Anaerobic ammonium oxidation by anammox bacteria in the Black Sea. *Nature* **422**: 608-611.

109. Lam P, Jensen MM, Lavik G*, et al.* (2007) Linking crenarchaeal and bacterial nitrification to anammox in the Black Sea. *Proc Natl Acad Sci U S A* **104**: 7104-7109.

110. Ettwig KF, Butler MK, Le Paslier D*, et al.* (2010) Nitrite-driven anaerobic methane oxidation by oxygenic bacteria. *Nature* **464**: 543-548.

111. Eisenmann E, Beuerle J, Sulger K, Kroneck P & Schumacher W (1995) Lithotrophic growth of *Sulfurospirillum deleyianum* with sulfide as electron donor coupled to respiratory reduction of nitrate to ammonia. *Arch Microbiol* **164**: 180-185.

112. Fossing H, Gallardo VA, Jorgensen BB*, et al.* (1995) Concentration and transport of nitrate by the mat-forming sulphur bacterium *Thioploca*. *Nature* **374**: 713-715.

113. Kimura M (2000) Dissimilatory Nitrate Reduction to Ammonium (DNRA). *Soil Biochem,* Vol. 10 (Bollag J-M & Stotzky G, eds.), pp. 61-62. Marcel Dekker Inc., New York.

114. Sørensen J (1978) Capacity for Denitrification and Reduction of Nitrate to Ammonia in a Coastal Marine Sediment. *Appl Environ Microbiol* **35**: 301-305.

115. Tiedje JM (1988) Ecology of denitrification and dissimilatory nitrate reduction to ammonium. *Biology of Anaerobic Microorganisms,*(Zehnder AJB, ed.), pp. 179-245. John Wiley and Sons, New York.

116. Orphan VJ, Turk KA, Green AM & House CH (2009) Patterns of ^{15}N assimilation and growth of methanotrophic ANME-2 archaea and sulfate-reducing bacteria within structured syntrophic consortia revealed by FISH-SIMS. *Environ Microbiol* **11**: 1777-1791.

117. De Boever E, Swennen R & Dimitrov L (2006) Lower Eocene carbonate cemented chimneys (Varna, NE Bulgaria): Formation mechanisms and the (a)biological mediation of chimney growth? *Sediment Geol* **185**: 159-173.

118. De Boever E, Swennen R & Dimitrov L (2006) Lower Eocene carbonate-cemented "chimney" structures (Varna, Bulgaria) -- Control of seepage rates on their formation and stable isotopic signature. *J Geochem Explor* **89**: 78-82.

119. Knittel K, Lösekann T, Boetius A, Kort R & Amann R (2005) Diversity and Distribution of Methanotrophic Archaea at Cold Seeps. *Appl Environ Microbiol* **71**: 467–479.

120. Schrum HN, Spivack AJ, Kastner M & D'Hondt S (2009) Sulfate-reducing ammonium oxidation: A thermodynamically feasible metabolic pathway in subseafloor sediment. *Geology* **37**: 939-942.

121. Nauhaus K, Treude, T., Boetius, A., Krüger, M. (2005) Environmental regulation of the anaerobic oxidation of methane: a comparison of ANME-I and ANME-II communities. *Environ Microbiol* **7**: 98-106.

122. Zehr JP & Ward BB (2002) Nitrogen Cycling in the Ocean: New Perspectives on Processes and Paradigms. *Appl Environ Microbiol* **68**: 1015-1024.

123. Meyer RL, Risgaard-Petersen N & Allen DE (2005) Correlation between Anammox Activity and Microscale Distribution of Nitrite in a Subtropical Mangrove Sediment. *Appl Environ Microbiol* **71**: 6142-6149.

124. Krüger M, Wolters H, Gehre M, Joye SB & Richnow HH (2008) Tracing the slow growth of anaerobic methane-oxidizing communities by ^{15}N-labelling techniques. *FEMS Microbiol Ecol* **63**: 401-411.

125. Tan M, Jones G, Zhu G*, et al.* (2009) Fellatio by Fruit Bats Prolongs Copulation Time. *PLoS ONE* **4**: e7595.

126. Bradford MM (1976) A rapid and sensitive method for the quantitation of microgram quantities of protein utilizing the principle of protein-dye binding. *Anal Biochem* **72**: 248-254.

127. Laemmli UK (1970) Cleavage of Structural Proteins during the Assembly of the Head of Bacteriophage T4. *Nature* **227**: 680-685.

128. Jehmlich N, Schmidt F, Taubert M, Seifert J, von Bergen M, Richnow HH & Vogt C (2009) Comparison of methods for simultaneous identification of bacterial species and determination of metabolic activity by protein-based stable isotope probing (Protein-SIP) experiments. *Rapid Commun Mass Spectrom* **23**: 1871-1878.

129. Perkins DN, Pappin DJC, Creasy DM & Cottrell JS (1999) Probability-based protein identification by searching sequence databases using mass spectrometry data. *Electrophoresis* **20**: 3551-3567.

130. Bastida F, Rosell M, Franchini AG*, et al.* (2010) Elucidating MTBE degradation in a mixed consortium using a multidisciplinary approach. *FEMS Microbiol Ecol* **73**: 370-384.

131. Jehmlich N, Schmidt F, von Bergen M, Richnow HH & Vogt C (2008) Protein-based stable isotope probing (Protein-SIP) reveals active species within anoxic mixed cultures. *ISME J* **2**: 1122-1133.

132. Macko SA, Uhle ME, Engel MH & Andrusevich V (1997) Stable Nitrogen Isotope Analysis of Amino Acid Enantiomers by Gas Chromatography/Combustion/Isotope Ratio Mass Spectrometry. *Anal Chem* **69**: 926-929.

133. Silfer JA, Engel MH, Macko SA & Jumeau EJ (1991) Stable carbon isotope analysis of amino acid enantiomers by conventional isotope ratio mass spectrometry and combined gas chromatography/isotope ratio mass spectrometry. *Anal Chem* **63**: 370-374.

134. Dekas AE, Poretsky RS & Orphan VJ (2009) Deep-Sea Archaea Fix and Share Nitrogen in Methane-Consuming Microbial Consortia. *Science* **326**: 422-426.

135. Friedrich MW, Pommerenke B, Seifert R & Krüger M (2007) Unexpected Microbial Diversity in Anaerobically Methane-oxidizing Mats of the Black Sea. San Francisco.

136. Hallam SJ, Putnam N, Preston CM, Detter JC, Rokhsar D, Richardson PM & DeLong EF (2004) Reverse Methanogenesis: Testing the Hypothesis with Environmental Genomics. *Science* **305**: 1457-1462.

137. He Q, He Z, Joyner DC*, et al.* (2010) Impact of elevated nitrate on sulfate-reducing bacteria: a comparative Study of Desulfovibrio vulgaris. *ISME J*.

138. Jenneman GE, McInerney MJ & Knapp RM (1986) Effect of Nitrate on Biogenic Sulfide Production. *Appl Environ Microbiol* **51**: 1205-1211.

139. Hinrichs K-U, Hayes JM, Sylva SP, Brewer PG & DeLong EF (1999) Methane-consuming archaebacteria in marine sediments. *Nature* **398**: 802-805.

140. Orphan VJ, House CH, Hinrichs K-U, McKeegan KD & DeLong EF (2001) Methane-Consuming Archaea Revealed by Directly Coupled Isotopic and Phylogenetic Analysis. *Science* **293**: 484-487.

141. Orphan VJ, Hinrichs K-U, Ussler III W*, et al.* (2001) Comparative Analysis of Methane-Oxidizing Archaea and Sulfate-Reducing Bacteria in Anoxic Marine Sediments. *Appl Environ Microbiol* **67**: 1922–1934.

142. Orphan VJ, House, C.H., Hinrichs. K.-H., McKeegan, K.D., DeLong, E.F. (2002) Multiple archaeal groups mediate methane oxidation in anoxic cold seep sediments. *Proc Natl Acad Sci U S A* **99**: 7663–7668.

143. Blumenberg M, Seifert R, Nauhaus K, Pape T & Michaelis W (2005) In Vitro Study of Lipid Biosynthesis in an Anaerobically Methane-Oxidizing Microbial Mat. *Appl Environ Microbiol* **71**: 4345-4351.

144. Blumenberg M, Seifert R, Reitner J, Pape T & Michaelis W (2004) Membrane lipid patterns typify distinct anaerobic methanotrophic consortia. *Proc Natl Acad Sci U S A* **101**: 11111-11116.

145. Pimenov NV, Poglazova MN, Mityushina LL, Sorokin DY & Khmelenina VN (1997) Bacterial mats on coral-like structures at methane seeps in the Black Sea. *Microbiology (Moscow, Russ Fed)* **66**: 421-428.

146.   Naudts L, Greinert J, Artemov Y, Staelens P, Poort J, Van Rensbergen P & De Batist M (2006) Geological and morphological setting of 2778 methane seeps in the Dnepr paleo-delta, northwestern Black Sea. *Mar Geol* **227**: 177-199.

147.   Meyerdierks A, Kube M, Kostadinov I, Teeling H, Glöckner FO, Reinhardt R & Amann R (2010) Metagenome and mRNA expression analyses of anaerobic methanotrophic archaea of the ANME-1 group. *Environ Microbiol* **12**: 422-439.

148.   Hales BA, Edwards C, Ritchie DA, Hall G, Pickup RW & Saunders JR (1996) Isolation and Identification of Methanogen-Specific DNA from Blanket Bog Peat by PCR Amplification and Sequence Analysis. *Appl Environ Microbiol* **62**: 668–675.

149.   Holmes DE, Finneran KT, O'Neil RA & Lovley DR (2002) Enrichment of Members of the Family *Geobacteraceae* Associated with Stimulation of Dissimilatory Metal Reduction in Uranium-Contaminated Aquifer Sediments. *Appl Environ Microbiol* **68**: 2300–2306.

150.   Liesack W & Dunfield PF (2004) T-RFLP Analysis: A Rapid Fingerprinting Method for Studying Diversity, Structure, and Dynamics of Microbial Communities. *Environmental Microbiology: Methods and Protocols,* Vol. 16 (Walker JM, Spencer JFT & Ragout de Spencer AL, eds.), pp. 23-37. Humana Press.

151.   Chin KJ, Lukow T & Conrad R (1999) Effect of temperature on structure and function of the methanogenic archaeal community in an anoxic rice field soil. *Appl Environ Microbiol* **65**: 2341–2349.

152.   Liu W-T, Marsh TL, Cheng H & Forney LJ (1997) Characterization of Microbial Diversity by Determining Terminal Restriction Fragment Length Polymorphisms of Genes Encoding 16S rRNA. *Appl Environ Microbiol* **63**: 6452–6456.

153.   Junier P, Junier T & Witzel K-P (2008) TRiFLe, a Program for In Silico Terminal Restriction Fragment Length Polymorphism Analysis with User-Defined Sequence Sets. *Appl Environ Microbiol* **74**: 6452–6456.

154.   Kohnen MEI, Sinninghe Damsté JS, Kock-van Dalen Ac & Jan WDL (1991) Di- or polysulphide-bound biomarkers in sulphur-rich geomacromolecules as revealed by selective chemolysis. *Geochim Cosmochim Acta* **55**: 1375-1394.

155.   Buser HR, Arn H, Guerin P & Rauscher S (1983) Determination of double bond position in mono-unsaturated acetates by mass spectrometry of dimethyl disulfide adducts. *Anal Chem* **55**: 818-822.

156.   Seifert R, Nauhaus K, Blumenberg M, Krüger M & Michaelis W (2006) Methane dynamics in a microbial community of the Black Sea traced by stable carbon isotopes in vitro. *Org Geochem* **37**: 1411-1419.

157.   Goñi MA & Eglinton TI (1996) Stable carbon isotopic analyses of lignin-derived CuO oxidation products by isotope ratio monitoring-gas chromatography-mass spectrometry (irm-GC-MS). *Org Geochem* **24**: 601-615.

158.   Østergaard KK, Masoudi R, Tohidi B, Danesh A & Todd AC (2005) A general correlation for predicting the suppression of hydrate dissociation temperature in the presence of thermodynamic inhibitors. *J Pet Sci Eng* **48**: 70-80.

159. Reitner J, Peckmann J, Reimer A, Schumann G & Thiel V (2005) Methane-derived carbonate build-ups and associated microbial communities at cold seeps on the lower Crimean shelf (Black Sea). *Facies* **51**: 66-79.

160. Reitner J, Peckmann J, Blumenberg M, Michaelis W, Reimer A & Thiel V (2005) Concretion-ary methane-seep carbonates and associated microbial communities in Black Sea sediments. *Palaeogeogr Palaeoclimatol Palaeoecol* **227**: 18-30.

161. Tornabene TG, Langworthy TA, Holzer G & Oró J (1979) Squalenes, phytanes and other iso-prenoids as major neutral lipids of methanogenic and thermoacidophilic "archaebacteria" *J Mol Evol* **13**: 73-83.

162. Hoehler TM, Alperin MJ, Albert DB & Martens CS (1994) Field and laboratory studies of meth-ane oxidation in an anoxic marine sediment: Evidence for a methanogen-sulfate reducer con-sortium. *Global Biogeochem Cycles* **8**: 451-463.

163. Sessions AL, Burgoyne TW, Schimmelmann A & Hayes JM (1999) Fractionation of hydrogen isotopes in lipid biosynthesis. *Org Geochem* **30**: 1193-1200.

164. Sessions AL, Jahnke LL, Schimmelmann A & Hayes JM (2002) Hydrogen isotope fractiona-tion in lipids of the methane-oxidizing bacterium Methylococcus capsulatus. *Geochim Cosmo-chim Acta* **66**: 3955-3969.

165. Pape T, Blumenberg M, Seifert R, Bohrmann G & Michaelis W (2008) Marine methane bio-geochemisty of the Black Sea: a review. *Links Between Geological Processes, Microbial Ac-tivities & Evolution of Life,*(Dilek Y, Furnes H & Muehlenbachs K, eds.), Springer Sci-ence+Business Media B.V.

166. Miroshnichenko ML, Kostrikina NA, Chernyh NA*, et al.* (2003) *Caldithrix abyssi* gen. nov., sp. nov., a nitrate-reducing, thermophilic, anaerobic bacterium isolated from a Mid-Atlantic Ridge hydrothermal vent, represents a novel bacterial lineage. *Int J Syst Evol Microbiol* **53**: 323-329.

167. Elvert M, Boetius A, Knittel K & Jørgensen BB (2003) Characterization of Specific Membrane Fatty Acids as Chemotaxonomic Markers for Sulfate-Reducing Bacteria Involved in Anaerobic Oxidation of Methane. *Geomicrobiol J* **20**: 403 - 419.

168. Caccavo F, Jr., Lonergan DJ, Lovley DR, Davis M, Stolz JF & McInerney MJ (1994) *Geobac-ter sulfurreducens* sp. nov., a hydrogen- and acetate-oxidizing dissimilatory metal-reducing microorganism. *Appl Environ Microbiol* **60**: 3752-3759.

169. Sessions AL (2001) Hydrogen isotope ratios of individual organic compounds. Thesis, Univer-sity of Indiana.

170. Badr O, Probert SD & O'Callaghan PW (1992) Methane: A greenhouse gas in the Earth's at-mosphere. *Appl Energy* **41**: 95-113.

171. Conrad R (2009) The global methane cycle: recent advances in understanding the microbial processes involved. *Environ Microbiol Rep* **1**: 285-292.

172. Lelieveld J, Crutzen PJ & Dentener FJ (1998) Changing concentration, lifetime and climate forcing of atmospheric methane. *Tellus, Series B: Chemical and Physical Meteorology* **50**: 128-150.

173.   Wang JS, Logan JA, McElroy MB, Duncan BN, Megretskaia IA & Yantosca RM (2004) A 3-D model analysis of the slowdown and interannual variability in the methane growth rate from 1988 to 1997. *Global Biogeochem Cycles* **18**: GB3011.

174.   Dalton H & Perlman D (1980) Oxidation of Hydrocarbons by Methane Monooxygenases from a Variety of Microbes. *Adv Appl Microbiol* **26**: 71-87.

175.   Lieberman R & Rosenzweig A (2004) Biological Methane Oxidation: Regulation, Biochemistry, and Active Site Structure of Particulate Methane Monooxygenase. *Crit Rev Biochem Mol Biol* **39**: 147-164.

176.   McDonald IR, Bodrossy L, Chen Y & Murrell JC (2008) Molecular Ecology Techniques for the Study of Aerobic Methanotrophs. *Appl Environ Microbiol* **74**: 1305-1315.

177.   Valentine D (2002) Biogeochemistry and microbial ecology of methane oxidation in anoxic environments: a review. *Antonie Leeuwenhoek* **81**: 271-282.

178.   Valentine DL & Reeburgh WS (2000) New perspectives on anaerobic methane oxidation. *Environ Microbiol* **2**: 477-484.

179.   Murrell JC, McDonald IR & Gilbert B (2000) Regulation of expression of methane monooxygenases by copper ions. *Trends Microbiol* **8**: 221-225.

180.   Kitmitto A, Myronova N, Basu P & Dalton H (2005) Characterization and Structural Analysis of an Active Particulate Methane Monooxygenase Trimer from Methylococcus capsulatus (Bath). *Biochemistry (Mosc)* **44**: 10954-10965.

181.   Lieberman RL & Rosenzweig AC (2005) Crystal structure of a membrane-bound metalloenzyme that catalyses the biological oxidation of methane. *Nature* **434**: 177-182.

182.   Myronova N, Kitmitto A, Collins RF, Miyaji A & Dalton H (2006) Three-Dimensional Structure Determination of a Protein Supercomplex That Oxidizes Methane to Formaldehyde in *Methylococcus capsulatus* (Bath). *Biochemistry (Mosc)* **45**: 11905-11914.

183.   Lee SK, Fox BG, Froland WA, Lipscomb JD & Munck E (1993) A transient intermediate of the methane monooxygenase catalytic cycle containing an FeIVFeIV cluster. *J Am Chem Soc* **115**: 6450-6451.

184.   Liu KE, Valentine AM, Wang D, Huynh BH, Edmondson DE, Salifoglou A & Lippard SJ (1995) Kinetic and spectroscopic characterization of intermediates and component interactions in reactions of methane monooxygenase from *Methylococcus capsulatus* (Bath). *J Am Chem Soc* **117**: 10174-10185.

185.   Prior SD & Dalton H (1985) The Effect of Copper Ions on Membrane Content and Methane Monooxygenase Activity in Methanol-grown Cells of Methylococcus capsulatus (Bath). *J Gen Microbiol* **131**: 155-163.

186.   Stanley SH, Prior SD, Leak DJ & Dalton H (1983) Copper stress underlies the fundamental change in intracellular location of methane mono-oxygenase in methane-oxidizing organisms: Studies in batch and continuous cultures. *Biotechnol Lett* **5**: 487-492.

187.   Fox BG, Afroland W, Jollie DR, Lipscomb JD & Mary EL (1990) Methane monooxygenase from *Methylosinus trichosporium* OB3b. *Methods Enzymol* **188**: 191-202.

188. Fox BG, Froland WA, Dege JE & Lipscomb JD (1989) Methane monooxygenase from *Methylosinus trichosporium* OB3b. Purification and properties of a three-component system with high specific activity from a type II methanotroph. *J Biol Chem* **264**: 10023-10033.

189. Lund J & Dalton H (1985) Further characterisation of the FAD and Fe_2S_2 redox centres of component C, the NADH: acceptor reductase of the soluble methane monooxygenase of *Methylococcus capsulatus* (Bath). *Eur J Biochem* **147**: 291-296.

190. Lund J, Woodland MP & Dalton H (1985) Electron transfer reactions in the soluble methane monooxygenase of *Methylococcus capsulatus* (Bath). *Eur J Biochem* **147**: 297-305.

191. Nesheim JC & Lipscomb JD (1996) Large Kinetic Isotope Effects in Methane Oxidation Catalyzed by Methane Monooxygenase: Evidence for C-H Bond Cleavage in a Reaction Cycle Intermediate. *Biochemistry (Mosc)* **35**: 10240-10247.

192. Choi D-W, Kunz RC, Boyd ES*, et al.* (2003) The Membrane-Associated Methane Monooxygenase (pMMO) and pMMO-NADH:Quinone Oxidoreductase Complex from *Methylococcus capsulatus* Bath. *J Bacteriol* **185**: 5755-5764.

193. Hakemian AS & Rosenzweig AC (2007) The Biochemistry of Methane Oxidation. *Annu Rev Biochem* **76**: 223-241.

194. Elsner M, Zwank L, Hunkeler D & Schwarzenbach RP (2005) A New Concept Linking Observable Stable Isotope Fractionation to Transformation Pathways of Organic Pollutants. *Environ Sci Technol* **39**: 6896-6916.

195. Meckenstock RU, Morasch B, Griebler C & Richnow HH (2004) Stable isotope fractionation analysis as a tool to monitor biodegradation in contaminated acquifers. *J Contam Hydrol* **75**: 215-255.

196. Merritt DA, Hayes JM & Marais DJD (1995) Carbon isotopic analysis of atmospheric methane by isotope-ratio-monitoring gas chromatography-mass spectrometry. *J Geophys Res* **100**: 1317-1326.

197. Barker JF & Fritz P (1981) Carbon isotope fractionation during microbial methane oxidation. *Nature* **293**: 289-291.

198. Bergamaschi P, Lubina C, Königstedt R, Fischer H, Veltkamp AC & Zwaagstra O (1998) Stable isotopic signatures ($\delta^{13}C$, δD) of methane from European landfill sites. *J Geophys Res* **103**: 8251-8265.

199. Bergamaschi P & Harris GW (1995) Measurements of stable isotope ratios ($^{13}CH_4/^{12}CH_4$; $^{12}CH_3D/^{12}CH_4$) in landfill methane using a Tunable Diode Laser Absorption Spectrometer. *Global Biogeochem Cycles* **9**: 439-447.

200. Coleman DD, Risatti JB & Schoell M (1981) Fractionation of carbon and hydrogen isotopes by methane-oxidizing bacteria. *Geochim Cosmochim Acta* **45**: 1033-1037.

201. Happell JD, Chanton JP & Showers WS (1994) The influence of methane oxidation on the stable isotopic composition of methane emitted from Florida swamp forests. *Geochim Cosmochim Acta* **58**: 4377-4388.

202. Kinnaman FS, Valentine DL & Tyler SC (2007) Carbon and hydrogen isotope fractionation associated with the aerobic microbial oxidation of methane, ethane, propane and butane. *Geochim Cosmochim Acta* **71**: 271-283.

203.   Powelson DK, Chanton JP & Abichou T (2006) Methane Oxidation in Biofilters Measured by Mass-Balance and Stable Isotope Methods. *Environ Sci Technol* **41**: 620-625.

204.   Reeburgh WS, Hirsch AI, Sansone FJ, Popp BN & Rust TM (1997) Carbon kinetic isotope effect accompanying microbial oxidation of methane in boreal forest soils. *Geochim Cosmochim Acta* **61**: 4761-4767.

205.   Snover AK & Quay PD (2000) Hydrogen and carbon kinetic isotope effects during soil uptake of atmospheric methane. *Global Biogeochem Cycles* **14**: 25-39.

206.   Templeton AS, Chu K-H, Alvarez-Cohen L & Conrad ME (2006) Variable carbon isotope fractionation expressed by aerobic CH_4-oxidizing bacteria. *Geochim Cosmochim Acta* **70**: 1739-1752.

207.   Zyakun AM & Zakharchenko VN (1998) Carbon isotope discrimination by methanotrophic bacteria: Practical use in biotechnologial research. *Applied Biochemistry and Microbiology (Translation of Прикладная биохимия и микробиология)* **34**: 207-219.

208.   Hunkeler D & Elsner M (2010) Principles and mechanisms of isotope fractionation. *Environmental Isotopes in Biodegradation and Bioremediation,*(Aelion CM, Höhener P, Hunkeler H & Aravena R, eds.), CRC Press, Taylor & Francis Group, Boca Raton.

209.   Elsner M, McKelvie J, Lacrampe Couloume G & Sherwood Lollar B (2007) Insight into Methyl tert-Butyl Ether (MTBE) Stable Isotope Fractionation from Abiotic Reference Experiments. *Environ Sci Technol* **41**: 5693-5700.

210.   Herrmann S, Vogt C, Fischer A, Kuppardt A & Richnow H-H (2009) Characterization of anaerobic xylene biodegradation by two-dimensional isotope fractionation analysis. *Environ Microbiol Rep* **1**: 535-544.

211.   Mancini SA, Hirschorn SK, Elsner M, Lacrampe-Couloume G, Sleep BE, Edwards EA & Sherwood Lollar B (2006) Effects of Trace Element Concentration on Enzyme Controlled Stable Isotope Fractionation during Aerobic Biodegradation of Toluene. *Environ Sci Technol* **40**: 7675-7681.

212.   Nijenhuis I, Andert J, Beck K, Kastner M, Diekert G & Richnow H-H (2005) Stable Isotope Fractionation of Tetrachloroethene during Reductive Dechlorination by *Sulfurospirillum multivorans* and *Desulfitobacterium* sp. Strain PCE-S and Abiotic Reactions with Cyanocobalamin. *Appl Environ Microbiol* **71**: 3413-3419.

213.   Rosell M, Barceló D, Rohwerder T, Breuer U, Gehre M & Richnow HH (2007) Variations in $^{13}C/^{12}C$ and D/H Enrichment Factors of Aerobic Bacterial Fuel Oxygenate Degradation. *Environ Sci Technol* **41**: 2036-2043.

214.   Vogt C, Cyrus E, Herklotz I*, et al.* (2008) Evaluation of Toluene Degradation Pathways by Two-Dimensional Stable Isotope Fractionation. *Environ Sci Technol* **42**: 7793-7800.

215.   Fischer A, Herklotz I, Herrmann S*, et al.* (2008) Combined Carbon and Hydrogen Isotope Fractionation Investigations for Elucidating Benzene Biodegradation Pathways. *Environ Sci Technol* **42**: 4356-4363.

216.   Meyer AH, Penning H & Elsner M (2009) C and N Isotope Fractionation Suggests Similar Mechanisms of Microbial Atrazine Transformation Despite Involvement of Different Enzymes (AtzA and TrzN). *Environ Sci Technol* **43**: 8079-8085.

217. Brusseau GA, Tsien H-C, Hanson RS & Wackett LP (1990) Optimization of trichloroethylene oxidation by methanotrophs and the use of a colorimetric assay to detect soluble methane monooxygenase activity. *Biodegradation* **1**: 19-29.

218. Wackett LP & Gibson DT (1983) Rapid Method for Detection and Quantitation of Hydroxylated Aromatic Intermediates Produced by Microorganisms. *Appl Environ Microbiol* **45**: 1144-1147.

219. Richnow HH, Meckenstock RU, Ask Reitzel L, Baun A, Ledin A & Christensen TH (2003) In situ biodegradation determined by carbon isotope fractionation of aromatic hydrocarbons in an anaerobic landfill leachate plume (Vejen, Denmark). *J Contam Hydrol* **64**: 59-72.

220. Fischer A, Theuerkorn K, Stelzer N, Gehre M, Thullner M & Richnow HH (2007) Applicability of Stable Isotope Fractionation Analysis for the Characterization of Benzene Biodegradation in a BTEX-contaminated Aquifer. *Environ Sci Technol* **41**: 3689-3696.

221. Anonymous (1998) Validation of publication of new names and new combinations previously effectively published outside the IJSB. *Int J Syst Bacteriol* **48**: 631-632.

222. Bodrossy L, Holmes EM, Holmes AJ, Kovács KL & Murrell JC (1997) Analysis of 16S rRNA and methane monooxygenase gene sequences reveals a novel group of thermotolerant and thermophilic methanotrophs, *Methylocaldum* gen. nov. *Arch Microbiol* **168**: 493-503.

223. Bowman JP, Sly LI, Nichols PD & Hayward AC (1993) Revised Taxonomy of the Methanotrophs: Description of *Methylobacter* gen. nov., Emendation of *Methylococcus*, Validation of *Methylosinus* and *Methylocystis* Species, and a Proposal that the Family *Methylococcaceae* Includes Only the Group I Methanotrophs. *Int J Syst Bacteriol* **43**: 735-753.

224. Dedysh SN, Berestovskaya YY, Vasylieva LV, *et al.* (2004) *Methylocella tundrae* sp. nov., a novel methanotrophic bacterium from acidic tundra peatlands. *Int J Syst Evol Microbiol* **54**: 151-156.

225. Dunfield PF, Khmelenina VN, Suzina NE, Trotsenko YA & Dedysh SN (2003) *Methylocella silvestris* sp. nov., a novel methanotroph isolated from an acidic forest cambisol. *Int J Syst Evol Microbiol* **53**: 1231-1239.

226. Lindner AS, Pacheco A, Aldrich HC, Costello Staniec A, Uz I & Hodson DJ (2007) *Methylocystis hirsuta* sp. nov., a novel methanotroph isolated from a groundwater aquifer. *Int J Syst Evol Microbiol* **57**: 1891-1900.

227. Romanovskaia VA, Iu RM & Bogachenko VN (1978) Refinement of the diagnosis of the genera and species of methane-using bacteria. *Mikrobiologiia* **47**: 120-130.

228. Wartiainen I, Hestnes AG, McDonald IR & Svenning MM (2006) *Methylocystis rosea* sp. nov., a novel methanotrophic bacterium from Arctic wetland soil, Svalbard, Norway (78° N). *Int J Syst Evol Microbiol* **56**: 541-547.

229. Whittenbury R, Phillips KC & Wilkinson JF (1970) Enrichment, Isolation and Some Properties of Methane-utilizing Bacteria. *J Gen Microbiol* **61**: 205-218.

230. Alperin MJ, Reeburgh WS & Whiticar MJ (1988) Carbon and hydrogen isotope fractionation resulting from anaerobic methane oxidation. *Global Biogeochem Cycles* **2**: 279-288.

231. Kessler JD, Reeburgh WS & Tyler SC (2006) Controls on methane concentration and stable isotope (δ^2H-CH$_4$ and δ^{13}C-CH$_4$) distributions in the water columns of the Black Sea and Cariaco Basin. *Global Biogeochem Cycles* **20**: GB4004.

232.   Martens CS, Albert DB & Alperin MJ (1999) Stable isotope tracing of anaerobic methane oxi-
        dation in the gassy sediments of Eckernförde Bay, German Baltic Sea. *Am J Sci* **299**: 589-
        610.

233.   Hanson RS & Hanson TE (1996) Methanotrophic bacteria. *Microbiol Rev* **60**: 439-471.

234.   Op den Camp HJM, Islam T, Stott MB*, et al.* (2009) Environmental, genomic and taxonomic
        perspectives on methanotrophic Verrucomicrobia. *Environ Microbiol Rep* **1**: 293-306.

235.   Feilberg KL, Griffith DWT, Johnson MS & Nielsen CJ (2005) The ^{13}C and D kinetic isotope
        effects in the reaction of CH_4 with Cl. *Int J Chem Kinet* **37**: 110-118.

236.   Saueressig G, Crowley JN, Bergamaschi P, Brühl C, Brenninkmeijer CAM & Fischer H (2001)
        Carbon 13 and D kinetic isotope effects in the reactions of CH_4 with O(^{1}D) and OH: New labo-
        ratory measurements and their implications for the isotopic composition of stratospheric meth-
        ane. *J Geophys Res* **106**: 23127-23138.

237.   Tyler S, C. (1992) Kinetic Isotope Effects and Their Use in Studying Atmospheric Trace Spe-
        cies. *Isotope Effects in Gas-Phase Chemistry* **502**: 390-408.

Acknowledgements

Erklärung zur Dissertation

Gemäß §6(1) der Promotionsordnung der Naturwissenschaftlichen Fakultät der Gottfried Wilhelm Leibniz Universität Hannover

für die Promotion zum Dr. rer. nat.

Hierdurch erkläre ich, daß ich meine Dissertation mit dem Titel

„Methanogenic hydrocarbon degradation and methane oxidation in benthic microbial communities"

selbständig verfaßt und die benutzten Hilfsmittel und Quellen gegebenenfalls die zu Hilfeleistung herangezogenen Institutionen vollständig angegeben habe.

Die Dissertation wurde nicht schon als Masterarbeit, Diplomarbeit oder andere Prüfungsarbeit verwendet.

Curriculum Vitae

Since 2011

Postdoc at the Université de Pau et des Pays de l'Adour, Pau (France)

Subject is microbially enhanced oil recovery (MEOR)

Supervisors are Dr. Regis Grimaud and Pr. Michel Magot

2006 – 2010

Doctoral thesis at the Federal Institute for Geosciences and Natural Resources (BGR) in Hannover (Germany); graduated: 5 May 2011

Subject is "Methanogenic hydrocarbon degradation and methane oxidation in benthic microbial communities"

Supervisors were Dr. Martin Krüger and Prof. Dr. Axel Schippers

2005 – 2006

Diploma thesis at the Centre for Environmental Research („Umweltforschungszentrum", UFZ) in Leipzig (Germany)

Subject was "Stable carbon isotope fractionation of tetrachloroethylene and trichloroethylene by crude extracts from Sulfurospirillum spp. and enrichment cultures from Bitterfeld (Germany)"

Supervisors were Ivonne Nijenhuis, Ph.D., Dr. Hans-Hermann Richnow and Prof. Gabriele Diekert

2003 – 2005

Studied biology at the university „Friedrich-Schiller-Universität" in Jena (Germany)

Exams in microbiology (major subject), biochemistry and genetics as minor subjects

Courses in microbiology and genetics of fungi, anaerobic bacteria and molecular immunology

1998 – 2003

Studied biology at the university „Westfälische Wilhelms Universität" in Münster (Germany)

Focus was microbiology and the minor subjects were biochemistry and genetics.

Courses in general microbiology, general biochemistry and molecular genetics,

Course in fermenting technologies which mainly focused on the biotechnological production of bio-polymers such as poly hydroxy butyrate and cyanophycin; the latter by fermenting the cyanobacterium *Synechococcus* sp. in an especially constructed photo tubing fermenter

Expeditions:

2008, R/V Meteor cruise M76/1 (Cape Town – Walvis Bay): "Process studies in the South-East Atlantic, PROSA"

2007, R/V Meteor cruise M72/1 (Istanbul – Istanbul): "Biogeochemistry, fluids, gas hydrates and paleo climate of the Black Sea"

Etc.

Two months NASA PBI in summer 2009 on "Anaerobic oxidation of arsenite by the phototroph *Chloroflexus aurantiacus*" at the Duquesne University in Pittsburgh (USA)